



Viability analysis of the natural population of Atlantic salmon (*Salmo salar* L.) in the Allier catchment

Analyse de la viabilité d'une population naturelle de saumon atlantique (*Salmo salar* L.) dans le bassin de l'Allier

Guillaume Dauphin & Etienne Prévost

INRA, UMR ECOBIOP, Station d'hydrobiologie, Quartier Ibaron, 64310 Saint Pée sur Nivelles



Mai 2013

Contents

Résumé opérationnel

1. Mécanismes de renouvellement de la population de l'Allier
2. Analyse rétrospective
3. Viabilité de la population de l'Allier
4. Conditions nécessaires au rétablissement de la population de l'Allier

Executive summary

1. Renewal mechanisms of the Allier population
2. Retrospective analysis
3. Viability of the Allier population
4. Conditions necessary for the recovery of the Allier population

1. Background and objective of the study

2. Summary of data available

- 2.1 Professional and rod catches
- 2.2 Adult counts
- 2.3 Redd counts
- 2.4 Stocking
- 2.5 Electric fishing

3. Getting hands dirty: modelling

3.1 General framework

- 3.1.1 Hierarchical Bayesian models
- 3.1.2 State-space models
- 3.1.3 Bayesian inference

3.2 Observation models

- 3.2.1 0+ Juvenile densities

3.2.2 Potential spawners to redd counts relationship

3.3 Full lifecycle model

3.3.1 Adult returns

3.3.2 spatial distribution of potential spawners

3.3.3 0+ juvenile densities

4. Results

4.1 Retrospective analysis

4.1.1 Adult returns

4.1.2 Repartition in the different spatial units

4.1.3 Potential spawners to redd counts relationship

4.1.4 0+ juvenile production

4.1.5 0+ juvenile and stocked smolts to adult return rate

4.1.6 Simulation without stocking

4.2 Retrospective simulation and 20 years forecast without stocking

4.2.1 Retrospective simulation without stocking

4.2.2 20 years forecast without stocking

4.2.2a Under the same environmental conditions

4.2.2b Improvement of migration transparency at Langeac only

4.2.2c Improvement of migration transparency at Poutès only

4.2.2d Improvement of migration transparency at Langeac and Poutès

4.2.2e Improvement of average adult return rate from juvenile/smolts to 50% percent of initial adult return rate

4.2.2f Improvement of average adult return rate from juvenile/smolts to 100% percent of initial adult return rate

4.2.2g Improvement of average adult return rate from juvenile/smolts to 50% percent of initial adult return rate and improvement of migration transparency at Langeac and Poutès

5. Conclusions and perspectives

5.1 Modelling

5.2 Retrospective analysis

5.3 Retrospective simulation without socking

5.4 Viability of the Atlantic salmon population in the Allier catchment

Tables

Figures

Appendix A.1: Electric fishing calibration relationship

Appendix A.2: 0+ juvenile densities model

Appendix A.3: Egg stocking in the Allier catchment

Appendix A.4: Potential spawners to redd counts relationship

Appendix A.5: Full lifecycle model

Appendix A.6 : OpenBUGs code for the full lifecycle model

Résumé opérationnel

Les objectifs de ce projet étaient:

- 1) Améliorer la compréhension et quantifier les mécanismes de renouvellement de la population de saumon de l'Allier
- 2) Fournir une analyse rétrospective de la dynamique de population du saumon de l'allier des années 70 à nos jours
- 3) Évaluer la capacité de la population de l'Allier à se maintenir de façon autonome (sans repeuplement)
- 4) Identifier les conditions requises (d'ordre naturel ou anthropique) pour assurer la viabilité de la population « sauvage » de saumon atlantique dans le bassin de l'Allier.

Pour atteindre ces objectifs un effort conséquent a été entrepris pour collecter, réviser et centraliser les jeux de données en rapport avec la population de saumon de l'Allier. Une des sorties principales de ce travail est la mise à disposition de fichiers récapitulatifs de ces données au format numérique (disponibles sur demande ; contact : tableau-salt-loire@logrami.fr). Ces fichiers contiennent les données brutes concernant la population de saumon atlantique de l'Allier telles que la cartographie des habitats fluviaux, les séries de captures par pêche professionnelle et amateur (Fig. 2.2), les pêches électriques de juvéniles (Fig. 2.7), les comptages d'adultes et de frayères (Fig. 2.3 et 2.4) ainsi que les effectifs de poissons déversés à des fins de repeuplement (stade œuf, juvénile 0+ et "smolt", Fig. 2.5).

1. Mécanismes de renouvellement de la population de l'Allier

1.1 Le modèle développé dans cette étude s'intéresse à la dynamique de population du saumon à l'amont de Vichy. Il prend en compte les principales caractéristiques et processus écologiques gouvernant la dynamique de population, en particulier :

- i. une division spatiale du bassin versant en trois zones définies pour répondre aux objectifs de gestion et aux caractéristiques de l'habitat : de Vichy à Langeac, de Langeac à Poutès et à l'amont de Poutès (Fig. 2.1). Les deux dernières zones correspondent à la zone refuge réservée à la reproduction naturelle (i.e. pas de repeuplement depuis 2009). La zone la plus en aval présente un habitat de moindre qualité pour la reproduction et le développement de juvéniles.

- ii. un mécanisme de régulation densité dépendant de la transition entre les géniteurs et les juvéniles 0+ automnaux. Le recrutement des juvéniles 0+ est supposé limité par un plafond, i.e. capacité d'accueil, quand le nombre de géniteurs augmente. En conséquence, la survie des juvéniles décroît en fonction du nombre de géniteurs.
- iii. un mécanisme de régulation densité dépendant de la survie des juvéniles 0+ de repeuplement déversés au printemps jusqu'au stade 0+ automnal gouverné à la fois par la densité de juvéniles 0+ déversés et la densité de juvéniles 0+ sauvages issus de la reproduction naturelle. Ces derniers sont supposés avoir un avantage sur les poissons déversés dû à l'antériorité de leur résidence. De cette façon la densité de juvéniles 0+ sauvages a un effet sur la survie des poissons issus du repeuplement, mais pas l'inverse.
- iv. la prise en compte de différentes histoires de vies, i.e. les retours d'adultes d'une année donnée sont principalement dépendant de 3 années de production de juvéniles 0+.
- v. un changement du niveau moyen du taux de retour du juvénile 0+ à l'adulte au cours de la période d'étude considérée.
- vi. un processus original de répartition spatiale des géniteurs sur l'axe Allier en amont de Vichy, combinant un mécanisme de distribution idéale libre (i.e. la distribution des géniteurs reflète la distribution de l'habitat disponible) et un mécanisme de « homing » (i.e. les géniteurs se distribuent en fonction de leur lieu de développement lorsqu'ils étaient juvéniles 0+). Des effets supplémentaires, rendant compte de l'impact potentiel de la construction de barrages ou d'autres activités humaines (e.g. qualité de l'eau) sur la distribution spatiale des géniteurs ont également été introduits.
- vii. la prise en compte de l'hétérogénéité spatiale des trois zones (cf. (i)) dans le mécanisme régulation densité dépendant de la survie des juvéniles 0+ sauvages et issus du repeuplement et dans la stochasticité environnementale affectant la répartition spatiale des géniteurs.

1.2. Le modèle de dynamique de population prenant en compte les éléments décrits ci-dessus est mis en relation avec les données disponibles au moyen de modèles d'observation représentant les différentes procédures d'échantillonnage et de collecte de données utilisées pour étudier la population de saumon de l'Allier.

1.3. L'ajustement du modèle aux données disponibles montre que :

- i. le recrutement naturel de juvéniles est en moyenne deux fois plus efficace dans la zone refuge (i.e. les deux zones à l'amont de Langeac) ; il en va de même pour la survie des juvéniles 0+ issus du repeuplement (Fig. 4.8).
- ii. le taux de retour du juvénile 0+ à l'adulte a sévèrement décru à la fin des années quatre-vingt et est resté à un niveau bas depuis (Fig. 4.10).
- iii. le taux de retour des smolts de repeuplement à Vichy est extrêmement faible (Fig 4.10).
- iv. les barrages et/ou les problèmes de qualité d'eau conduisent à une accumulation des géniteurs potentiels à l'aval de Langeac (i.e. la zone la moins favorable au recrutement de juvéniles), et dans une moindre mesure à l'aval de Poutès (Fig. 4.2).

2. Analyse rétrospective

Le modèle développé dans cette étude permet d'effectuer une analyse rétrospective de la dynamique de population du saumon de l'Allier au cours des 35 dernières années.

2.1. Les retours d'adultes à Vichy (i.e. les retours d'adultes totaux dans le bassin de l'Allier) ont décriés fortement entre le milieu des années 80 et le milieu des années 90. Ces retours sont restés relativement stables, autour de quelques centaines de poissons, durant les 15 dernières années (Fig. 4.1).

2.2. Au cours des 35 dernières années, la zone aval entre Vichy et Langeac a reçu la majorité des géniteurs potentiels. Avant l'ouverture de la zone à l'amont de Poutès, en moyenne 84 % des géniteurs potentiels restaient à l'aval de Langeac. Quand l'ascenseur à poisson a été installé à Poutès (en 1986), cette proportion est descendue à 68% en moyenne, i.e. la proportion de géniteurs potentiels accédant aux zones où l'habitat est plus favorable à la production de juvénile a augmenté. La proportion de géniteurs potentiels dans la zone entre Langeac et Poutès a augmenté de 16 à 22% en moyenne et la zone à l'amont de Poutès a reçu en moyenne 10% des géniteurs potentiels (Fig. 4.2).

2.3. Dans l'ensemble, la contribution du programme de repeuplement à la production de juvéniles 0+ a été substantielle à partir du milieu des années 90 et correspond à une augmentation significative du nombre de juvéniles 0+ déversés annuellement. En fonction de l'année et de la zone considérée, la contribution des juvéniles 0+ issus du repeuplement à la densité totale de juvéniles 0+ varie entre 40% et 80% durant cette période. La contribution des œufs déversés au moyen d'incubateurs de terrain est négligeable (Fig. 4.5 à 4.7)

2.4. Le recrutement des juvéniles 0+ sauvages ne montre pas de tendance claire au cours des 25 dernières années quelque soit la zone considérée. La densité totale de juvéniles 0+ (sauvages et issus du repeuplement) à l'aval de Langeac a légèrement augmentée au cours des dernières années. Ceci est principalement dû à une augmentation de l'effort de repeuplement dans cette zone en lien avec l'instauration de la zone refuge à l'amont de Langeac, et par conséquent l'arrêt des repeuplements dans cette zone (Fig. 4.5).

2.5. En moyenne, les densités de juvéniles 0+ sauvages les plus élevées sont observées dans la zone entre Langeac et Poutès (Fig. 4.6). Les densités de juvéniles 0+ plus faibles rencontrées dans la zone à l'amont de Poutès (Fig. 4.7) sont dues au faible nombre de géniteurs atteignant cette zone (en moyenne 10% des géniteurs potentiels) par rapport à l'habitat favorable disponible au développement des juvéniles 0+ (20% de l'habitat du bassin de l'Allier). La zone la moins productive en termes de densités de juvéniles 0+ sauvages se situe entre Vichy et Langeac. Malgré deux tiers des géniteurs potentiels présents sur cette zone, la zone entre Vichy et Langeac a contribué en moyenne à moins de la moitié du recrutement total de juvéniles 0+ sauvage durant les 15 dernières années (Fig. 4.9).

3. Viabilité de la population de l'Allier

3.1. L'impact du repeuplement entre 1977 et 2011 a été mesuré au travers d'une analyse rétrospective reconstruisant la dynamique de la population de l'Allier s'il n'y avait pas eu de repeuplement. Cette analyse montre que le repeuplement a contribué de façon significative aux retours d'adultes à Vichy. Bien que la population de saumon de l'Allier n'aurait pas disparu sans le repeuplement, le nombre de retours d'adultes aurait été inférieur en moyenne de 80% au cours des 10 dernières années (Fig. 4.11).

3.2. La viabilité d'une population de saumon sauvage dans l'Allier a été évaluée en simulant les retours d'adultes pour les 20 prochaines années en l'absence de repeuplement et en supposant que les conditions environnementales restent les mêmes qu'au cours des 15 dernières années. Sous ces conditions, les retours d'adultes à Vichy décroîtraient de façon constante pour atteindre en moyenne 260 poissons dans 20 ans avec une probabilité non-négligeable de voir moins de 100 adultes revenir à Vichy (i.e. environ 10% ; Fig. 4.12). Sous les conditions environnementales actuelles, comprenant les conditions en mer, sur l'axe Loire-Allier en aval de Vichy et dans l'Allier en amont de Vichy, la population sauvage de saumon serait sur la route d'une quasi-extinction. Cependant, atteindre cette quasi-extinction prendrait un certain temps et le risque est faible à court-terme (i.e. pour les 10 prochaines années ; Fig. 4.13).

4. Conditions nécessaires au rétablissement de la population de l'Allier

4.1. L'analyse précédente montre que, malgré un maintien du nombre de retours d'adultes au cours des 15 dernières années, le programme de repeuplement n'a pas résolu le problème du rétablissement d'une population de saumon se maintenant de façon autonome sur l'Allier à l'amont de Vichy.

4.2. La viabilité d'une population de saumon sauvage dans l'Allier à l'amont de Vichy a été analysée par simulation en fonction de différents scénarii de conditions environnementales affectant à la fois la survie du saumon au cours de son cycle biologique et la distribution spatiale des géniteurs potentiels. Une population sauvage pourrait se maintenir de façon autonome dans l'Allier, i.e. sans repeuplement, si les conditions environnementales s'amélioraient et la survie (sur l'ensemble du cycle de vie) retrouvait un niveau équivalent à la moitié du niveau observé avant le déclin intervenu à la fin des années quatre-vingt. Cela correspond à une augmentation de la survie actuelle par un facteur 1,9. Ce scénario conduirait à des retours d'adultes à Vichy fluctuant autour de 750 poissons en moyenne (Fig. 4.20 et 21). La probabilité d'observer moins de 250 poissons chaque année serait faible ($< 5\%$) et la probabilité d'observer plus de 1000 poissons serait relativement élevée (environ 30%). Dans le cas d'un retour à une survie au niveau historique (avant la moitié des années quatre-vingt, Fig. 4.22 et 23), la probabilité d'observer pour une année donnée moins de 1000 poissons à Vichy resterait non négligeable (environ 10%) alors que le niveau moyen des retours d'adultes se situerait autour de 2000 poissons.

4.3. Le principal facteur qui permettra le rétablissement d'une population sauvage de saumon autonome dans l'Allier n'est pas l'augmentation ou l'optimisation du programme de repeuplement, mais l'amélioration des conditions environnementales pour une meilleure survie de tous les stades de vie. Si l'objectif premier de la gestion est de restaurer une population sauvage autonome, l'amélioration des conditions environnementales pour une meilleure survie doit être la priorité des actions de gestion.

4.4. A court terme (dans les 10 prochaines années) la restauration de la continuité écologique, et donc la transparence migratoire, sur l'axe Loire-Allier devrait être une préoccupation majeure pour la gestion pour au moins deux raisons : (i) elle a potentiellement un impact significatif sur la survie des smolts et des adultes durant leurs migrations, (ii) elle fait partie des rares facteurs environnementaux susceptibles d'être améliorés rapidement sous l'action directe des autorités en charge de la gestion de la population de saumon. Restaurer la continuité écologique entre l'Allier et ses affluents, en supposant que ces affluents soient aussi productifs que les zones à l'amont de Langeac, est une autre option de gestion à envisager. La priorité devrait être donnée aux affluents se jetant dans la zone la moins favorable au recrutement de juvéniles (i.e. entre Vichy et Langeac). Combattre par des mesures de gestion additionnelles toute source de mortalité (braconnage et captures accessoires, prédateurs, ...) serait également une contribution précieuse.

Executive summary

The objectives of this project were:

- 1) Understand better and quantify the renewal mechanisms of this Allier river salmon population
- 2) Provide a retrospective analysis of the Allier's salmon population dynamics from the mid-seventies to present
- 3) Evaluate the ability of the Allier's population to maintain itself autonomously (i.e. without stocking)
- 4) Identify the required conditions (natural or human related) to ensure the viability of the “wild” population of Atlantic salmon in the Allier catchment

Meeting these objectives required a significant amount of time gathering, reviewing and centralising the datasets related to the Allier salmon population. One of the main outputs of this part of the project is several data summary files in digital format which are now available upon request from Logrami (contact: tableau-salt-loire@logrami.fr). These files contain raw data in relation with Atlantic salmon in the Allier catchment such as adult catches (Fig. 2.2), electric fishing of juveniles (Fig. 2.7), riverine habitat mapping, redd and adult counts (Fig 2.3 and 2.4) and stocking (eggs, 0+ juveniles and smolts, Fig 2.5).

1. Renewal mechanisms of the Allier population

1.1 The model developed in this study considers the salmon population dynamics upstream from Vichy. It takes into account the major ecological features and processes governing the population dynamics, in particular:

- i. a spatial partitioning of the watershed into three zones defined according management and habitat quality characteristics: from Vichy to Langeac, from Langeac to Poutès and upstream from Poutès (Fig. 2.1). The last two zones correspond to the refuge area where only wild reproduction is allowed (i.e. no stocking since 2009). The lowermost zone is of poorer quality for wild reproduction and juvenile rearing.
- ii. density dependent regulation in the spawner to autumnal 0+ juvenile transition. 0+ juvenile recruitment is assumed to be limited by a ceiling, i.e. carrying capacity, when the

number of spawners increases. As a consequence, juvenile survival decreases according to the number of spawners.

- iii. density dependent regulation of the survival of stocked juveniles up to the autumnal 0+ stage due both to the stocked 0+ juveniles density and to the wild 0+ juveniles density issuing from natural reproduction. The latter are further assumed to have a prior residency advantage over stocked fish, so that wild recruit density has an effect on the survival of stocked fish, but the density of stocked fish does not influence the survival of their wild counterparts.
- iv. consideration of the different life histories, i.e. adults returns of a given year being primarily dependent on 3 years of juvenile production.
- v. a change during the study period in the average level of 0+ juvenile to adult return rate.
- vi. an original spatial distribution process of the spawners along the Allier above Vichy combining ideal free distribution (i.e. reflecting the distribution of available habitat) and homing (i.e. spawners distribute according to their spatial origin as juvenile). Additional effects allowing for the potential consequences of damming or any other human activity influence (e.g. water quality) on the spawners spatial distribution were also included.
- vii. spatial heterogeneity according to three zones in the density dependent regulation of the survival of wild and hatchery reared juveniles, and in the environmental stochasticity affecting spatial distribution of spawners.

1.2. The population dynamics model encompassing the above features and processes is linked to available data by means of observation models representing the various sampling and data collection procedures used to survey the Allier salmon population.

1.3. Model fitting on available data shows that

- i. wild juvenile recruitment is on average two times more efficient in the refuge area (i.e. the two zones upstream from Langeac); so do survival of hatchery reared juveniles (Fig. 4.8).
- ii. the 0+ juvenile to adult return rate severely dropped (by a factor of 3.7) in the late eighties and has stayed at a very low level since then (Fig. 4.10).
- iii. the return rate at Vichy of hatchery reared smolts is extremely low (Fig. 4.10).
- iv. dams and/or water quality problems lead to a relative accumulation of potential spawners downstream from Langeac (i.e. in the zone less suitable for juvenile recruitment), and to a lesser extent downstream from Poutès (Fig. 4.2).

2. Retrospective analysis

The modelling developed in this study allows a retrospective analysis of the Allier population dynamics over the last 35 years.

2.1. The adult returns at Vichy (i.e. the total returns in the Allier catchment) have dramatically decreased between the mid-eighties and the mid-nineties. They have then remained fairly stable around several hundred during the last 15 years (Fig 4.1).

2.2. Over the last 35 years, the river section between Vichy and Langeac has been receiving the bulk of the potential spawners. Before the opening of the river section upstream of Poutès on average, 84% of the potential spawners would stay below Langeac. When the fish lift was installed at Poutès (from 1986), this proportion went down to 68% on average, i.e. the proportion of spawners accessing the zones where juvenile recruitment is more efficient increased. The proportion of potential spawners in the river section between Langeac and Poutès went up from 16% to 22% on average, while the river section upstream of Poutès received on average 10% of the potential spawners (Fig 4.2).

2.3. Overall, the contribution of the stocking programme to the 0+ juvenile production has been substantial from the mid-nineties, and corresponds to the dramatic increase of the number of 0+ juveniles stocked annually. Depending on the year and river section, the contribution of the stocked 0+ juvenile to the total 0+ juvenile density varied from 40% to 80%. The contribution of stocked eggs by means of field incubators to the total juvenile production is negligible (Fig 4.5-7).

2.4. Wild 0+ juvenile recruitment did not show any clear trend over the last 25 years, whatever the zone. The total 0+ juvenile (wild and stocked) density below Langeac tended to increase in recent years. This is mainly due to an increased stocking effort in this zone, in relation with the establishment of the refuge area upstream from Langeac and the cessation of stocking in this area (Fig 4.5).

2.5. On average, the highest densities of wild 0+ juvenile are observed on the Langeac to Poutès zone (Fig 4.6). The lower densities of wild 0+ juveniles observed above Poutès (Fig 4.7) are due to the too low number of spawners accessing to this area (10% of potential spawners on average) relative to juveniles rearing habitat available (20% of total nursery habitat). The lowermost zone produces the lowest wild 0+ juvenile densities. Despite receiving two thirds of the potential spawners, the Vichy to Langeac zone contributes on average to less than half of the total wild 0+ juvenile recruitment over the last 15 years (Fig. 4.9).

3. Viability of the Allier population

3.1. The impact of stocking from 1977 to 2011 was looked at through a retrospective analysis reconstructing the fate of the Allier salmon population as if no stocking had occurred. It shows that stocking has been contributing significantly to the support of the number of adult returns at Vichy. Although the Allier salmon population would have not gone extinct today, on average adult returns would have been 80 % lower in the last 10 years in the absence of stocking (Fig. 4.11).

3.2. The viability of a wild salmon population in the Allier has been assessed by forecasting population estimates over the next 20 years in the absence of any stocking and assuming the environment would stay the same as in the last 15 years. Under these conditions, the number of adult returns at Vichy would tend to constantly decrease over time to reach an average level of 260 fish 20 years ahead, with non-negligible probability of seeing less than 100 adults returning (i.e. about 10%, Fig. 4.12). Under current environment, combining conditions at sea, along the Loire-Allier migration axis and in the Allier itself above Vichy, a wild salmon population would be on the road to quasi-extinction. However, getting to (quasi-)extinction would take time, and the risk is very low in the short term (over the next 10 years, Fig.4.13).

4. Conditions necessary for the recovery of the Allier population

4.1. The previous analysis shows that, despite maintaining the numbers of returning adults over the last 15 years, the stocking programme alone did not solve the problem of the recovery of a naturally reproducing and self-sustaining population.

4.2. The fate of a wild salmon population in the Allier above Vichy has been forecasted under various scenarios of environmental conditions affecting both survival and spatial distribution of spawners. A wild population could be self-sustaining in the Allier, i.e. in the absence of any stocking, if the environmental conditions improved to allow survival (across the full life-cycle) to reach a level corresponding to half the one it used to be prior to the drop observed in the late eighties. This corresponds roughly to improving survival by a factor of 1.9 over the current level. This scenario leads to adult returns at Vichy fluctuating around an average of 750 fish (Fig. 4.20-21). The probability of getting adult returns below 250 in any year would stay low (< 5%), but returns would have a significant probability to exceed 1000 (i.e. about 30%). Even restoring survival to its historical level (i.e. prior to the mid-eighties, Fig 4.22-23) would leave non-negligible probability of getting adult returns below 1000 twenty years ahead (around 10%), although the average level of expected returns would be around 2000.

4.3. The main driver for the recovery of a wild salmon population self-sustaining in the Allier is not expanding or optimizing the stocking programme, but it is the improvement of environmental

conditions for better survival at all stages of the life cycle. Provided the restoration of a wild self-sustaining population is the primary management objective, improvement of environmental conditions for better survival should be the priority target of management actions.

4.4. In the short term (over the next 10 years) restoring ecological continuity, hence migration transparency, along the Loire-Allier axis should be of primary concern for management for at least two reasons: (i) it has potentially a significant impact on the survival of smolts and adults during their migrations; (ii) it is among the few environmental factors amenable to rapid improvement by the direct action of the authorities in charge of salmon population management. Restoring ecological continuity between the Allier and tributaries, provided they would be potentially as efficient as the Allier above Langeac for juvenile recruitment, is another and complementary management option. Priority should be given to tributaries flowing into the zone less suitable for juvenile recruitment, i.e. between Langeac and Vichy. Fighting against any source of mortality (poaching and by-catches, predators...) would be valuable management contributions too.

1. Background and objectives of the study

The idea of building a population dynamics model for Atlantic salmon in the Allier catchment is not new. The need for such a study has been identified in 2001 and then repeatedly recommended at several occasions (in 2004, following a study carried out by INRA¹ for the DIREN², in 2004 and 2005 following studies carried out by the GRISAM³ on the LIFE⁴ project “Sauvegarde du grand saumon de la Loire” and on hydroelectric plant of Poutes-Monistrol and in 2009, following advice from the scientific committee of plan Loire).

The present project has several objectives:

- 1) Provide a retrospective analysis of the Allier’s salmon population dynamics from the mid-seventies to present
- 2) Understand better and quantify the renewal mechanisms of this population
- 3) Evaluate the ability of the Allier’s population to maintain itself autonomously (i.e. without stocking)
- 4) Identify the required conditions (natural or human related) to ensure the viability of the “wild” population of Atlantic salmon in the Allier catchment

In order to evaluate if a natural population of Atlantic salmon can maintain itself autonomously it is crucial to gather and synthesize as comprehensively as possible the information, knowledge and expertise available about the Atlantic salmon in the Allier catchment. Additionally, the different stocking programs that have been occurring in the Allier catchment need to be assessed and their impact on the whole population dynamics measured.

Since the seventies, numerous dataset regarding the population dynamic of the Atlantic salmon population of the Allier catchment have been collected. However, these dataset are quite heterogeneous regarding the lifestages considered, the observation techniques, the temporal and spatial scale and often include missing data. Typical dataset are electric fishing indices of abundance, redd and adult counts, stocking events, etc.

¹ INRA: Institut National de la Recherche Agronomique / French National Institute for Agricultural Research.

² DIREN: Direction Régionale de l’ENvironnement /Regional direction for the environment .

³ GRISAM: Groupement d’Intérêt Scientifique sur les poissons Amphihalins / Scientific working group on amphihaline fishes.

⁴ LIFE: EU’s financial instrument supporting environmental and nature conservation projects throughout the EU.

2. Summary of data available

Different organizations were contacted to retrieve the the various dataset used in this study in digital format. When this was not possible, paper reports and logbooks were consulted and information contained within was entered in digital format. On several occasion, some discrepancies appeared between logbooks, technical reports or digital files. When such situation occurred, the different organisations were contacted and requested to give their advice and expertise on these misfits. The decisions taken on how to deal with these discrepancies were discussed and acknowledged during several meetings where all the partners of the project were presents in order to make sure that everyone agreed on the decisions taken. The organisations involved in the data collection and sharing information include the ONEMA⁵, LOGRAMI⁶, CNSS⁷, several angling federations and the French Ministry of Environment. In this section, the various dataset used in this study are summarily described in order to get an overall view of the quantity and quality of the information available to get a first understanding of the strength and weaknesses of the datasets. Some of the datasets are described a bit more extensively in some of the appendices. If interested in the full dataset, one should refer to Logrami (tableau-salt-loire@logrami.fr).

The time-series considered in this study runs from 1975 to 2011. The spatial scales considered divides the Allier catchment in 3 large river sections: Vichy-Langeac (including the Allagnon and the Dore), Langeac-Poutès and upstream of Poutès (Fig. 2.1). There are several reasons for such partition: 1) Poutès dam was a major obstacle to fish migration (impassable) until 1985, 2) the three adult counting structures at Vichy, Langeac and, Poutès provide information on the number of adults in the river sections above these structures and 3) in 2009, the river section upstream of Langeac counting station was designated as “refuge area” where no stocking should occur.

⁵ ONEMA: Office National de l'Eau et des Milieux Aquatiques / National Water and Aquatic Habitats Office

⁶ LOGRAMI: Association LOire GRAnds MIgrateurs / Loire Large Migratory Fish Association

⁷ CNSS: Conservatoire National du Saumon Sauvage / National Conservatoire of Wild Salmon

2.1 Professional and rod catches

The information about professional and rod catches is available from 1975 to 1993 (date of the closure of the salmon fishery). The figures come from the French Ministry of Environment. Professional catches occurred in 6 French départements (Loire Atlantique, Maine et Loire, Indre et Loire, Loire et Cher, Loiret and Nièvre). During the time-series considered they ranged between 77 and 819 salmon (mean = 371, Fig 2.2). The rod catches are assumed to have all occurred in the Allier upstream of Vichy. During the time-series considered they ranged between 72 and 1280 salmon (mean = 436, Fig 2.2).

2.2 Adult counts

Adult counts are collected by means of three counting stations located at Vichy, Langeac and Poutès. The information about adult counts is available for different period of times depending on the counting station. At Vichy, full adult counts are available from 1997 to 2011. At Langeac, partial adult counts are available from 2003 to 2008. At Poutès, full adult counts are available from 1986 to 2011 (Fig. 2.3).

2.3 Redd counts

Redd counts are collected annually since 1977 around December time. From 1977 to 1984, redds were counted by foot or by boat. From 1985, redds were counted from a helicopter. When weather and hydrological conditions are good it was possible to get counts for the 3 river sections as well as the percentage of spawning grounds sampled. When bad hydrological or weather conditions occurred, only partial counts and sometimes no counts at all were obtained. Bad conditions are quite frequent, this led to an absence of redd counts in 8 occasions. On average, 140, 100 and 70 redds are counted in the three river sections Vichy –Langeac, Langeac- Poutès and upstream Poutès respectively (Fig 2.4).

2.4 Stocking

Stocking has been occurring in the Allier catchment for a long time. During the time series considered there has not been a year without stocking. Various life stages of Atlantic salmon have been used: eggs, 0+ and “smolts” (1+ and older). The Atlantic salmon population of the river Allier has been stocked since 1970 by the salmon hatchery of the Conseil Supérieur de la Pêche (CSP) in Augerolles. In 2001, the implementation of the first step of the Plan Loire Grandeur Nature, led to a change in the stocking strategy (number of stocked salmon multiplied by 3) associated with the opening of a new salmon hatchery in Chanteuges which now produces all the salmon to be stocked in the Allier (Fig. 2.5). The stocking procedures vary depending on the lifestages: eggs are stocked using fixed incubators in small streams close to the Allier river, the 0+ juveniles are stocked homogeneously over the different river sections either by boat or by foot and the smolts are stocked from the bank of the river only at a handful number of places which are usually chosen for their ease of access. Additionally, in 2009, the area upstream of Langeac has been classified as refuge area and since then no fish are stocked in this part of the Allier catchment. In order to support the broodstock, every year, up to a hundred adults are captured in the river section between Vichy and Langeac (Fig. 2.6).

2.5 Electric fishing

Two types of electric fishing sampling have been used in the Allier catchment during the time-series considered. During the first part of the time-series (1975 to 1990), a successive removal technique was used. In the second part of the time-series (1994 to 2011), a 5 minutes index of abundance technique was used.

The successive removal technique is very labour intensive, which leads to only a few sites sampled every year. On the contrary, the 5 minutes index of abundance technique is much less labour intensive and allows sampling much more sites annually (Fig. 2.7).

3. Getting hands dirty

In this report, the technical aspect of the modeling work is kept to its minimum. The methodology used is briefly described in section 3.1. Additionally, mathematical formulas and equations from the different models are mostly cut down from the main text to focus on the hypotheses that are made. However, all equations and more precise descriptions of the modeling exercise are available in the different appendices.

3.1 General Framework

3.1.1 Hierarchical Bayesian Models

Probability statements about a vector of unknown quantities (e.g. model parameters) θ , given a vector of observed data y , require a model providing a joint probability distribution for θ and y . This joint probability or density distribution $p(\theta, y)$ is the product of two probability distributions which combine *a priori* knowledge about the parameters $p(\theta)$ (also known as the prior distribution) and the likelihood of the parameters $p(y|\theta)$. When y is known, the likelihood $p(y|\theta)$ is a function of θ which expresses degrees of credibility of θ given the data.

$$\text{Eq. 3.1 } p(\theta, y) = p(\theta) \cdot p(y|\theta)$$

The posterior distribution $p(\theta|y)$ of the parameter θ given the observation y is obtained by using equation 3.1 :

$$\text{Eq. 3.2 } p(\theta|y) = \frac{p(\theta, y)}{p(y)} = \frac{p(\theta) \cdot p(y|\theta)}{p(y)}$$

Hierarchical Bayesian models (Congdon, 2001; Gelman et al., 2004) describe the heterogeneity across different spatial (e.g. different habitats) or temporal units (e.g. different years of a time-series). Formally this is done by supposing that the vector of parameters θ is a random quantity sampled from a prior distribution $p(\theta|\lambda)$ with λ is a vector of hyper parameters. For instance, if

y_i is an observed abundance of 0+ juvenile salmon in a river section i , θ_i would be the true abundance of 0+ juvenile salmon in this river section i . In this context, λ could be a parameter controlling spatial variation across river sections. If λ is known, equation 3.2 becomes

$$\text{Eq. 3.3 } p(\theta|y, \lambda) = \frac{p(y, \theta|\lambda)}{p(y|\lambda)} = \frac{p(y|\theta) \cdot p(\theta|\lambda)}{p(y|\lambda)}$$

However in most cases λ will not be known and a hyperprior distribution $p(\lambda)$ will be required.

$$\text{Eq. 3.4 } p(\theta, \lambda|y) = \frac{p(y|\theta) \cdot p(\theta|\lambda) \cdot p(\lambda)}{p(y)} = \frac{\int p(y|\theta) \cdot p(\theta|\lambda) \cdot p(\lambda) d\lambda}{\int p(y|\theta) \cdot p(\theta|\lambda) \cdot p(\lambda) d\theta d\lambda}$$

3.1.2 State space models

Bayesian state-space models are specific hierarchical models which are made of a dynamic (or process) component which is composed of unobserved variables and an observation component which is composed of observed variables that depends on the dynamic component. This can be summarized in two equations (Carlin et al., 1992; Calder et al., 2003). The first one is called the process equation and summarizes the links between the different states of the model.

$$\text{Eq. 3.5 } X_t = F(X_{t-1}, \theta_1, \varepsilon_t)$$

Where the function F accounts for all the equations describing the dynamics of the system studied (e.g. survival, density dependence, etc. for population dynamics) and reflects the dependence of the different hidden states at a given time on the hidden states at another time conditionally on the transition parameters θ_1 and a stochastic component ε_t . The second equation is called the observation equation:

$$\text{Eq. 3.6 } y_t = G(X_t, \theta_2, \omega_t)$$

Where the function G describes the link between the observed datasets y_t and the hidden states X_t conditionally on the observation model parameters θ_2 and the stochastic component of the observation models ω_t . The Bayesian statistical inference calculates the joint posterior probability density functions (pdf) of all the model parameters $\theta = (\theta_1, \theta_2)$ and the hidden states series X conditionally on the observations series y .

$$\text{Eq. 3.7 } p(\theta, X|y) \propto p(\theta) \cdot p(X|\theta) \cdot p(y|X, \theta)$$

A basic state space model is described in Figure 3.1.

3.1.3 Bayesian inference

Markov chain Monte Carlo (MCMC) methods are today the most popular computing tools in Bayesian practice. This is due to their ability to enable inference for joint posterior distributions of very high dimension. This is done by reducing the high-dimensional problem to treating recursively a sequence of lower dimensional (often one dimensional) problems. MCMC methods do not provide a closed form of the posterior distribution (Eq. 3.2 and 3.4) but a sample of values from this distribution. If the sample is large enough, the histogram of the sampled values is a good approximation this distribution. Other computation techniques such as sequential importance sampling (SIS) can be used, but this technique is not necessarily more efficient (see comparaisn between MCMC and SIS in Newman *et al.*, 2009)

All the models presented in this study were implemented using OpenBUGS. This software performs MCMC simulations using principally a generalised Gibbs sampling algorithm (Spiegelhalter *et al.*, 2003).

3.2 Observation models

Two observations models were developed:

a juvenile production model which allows the estimation of 0+salmon juvenile densities at two scale (i.e. electric fishing site and river section) and the decomposition of these densities in 3 components reflecting the wild production (0+ produced by the natural reproduction of the returning adults), the stocked 0+ production and the stocked egg production.

a model relating the potential spawners to the redd counts.

These observation models were first developed and tested independently and then incorporated in the full lifecycle model. Therefore, the results related to the observation models alone are not presented in sections 3.2.1 and 3.2.2. However the outputs related to these two models once incorporated in the full lifecycle model are presented and discussed in section 4.

3.2.1 0+ juvenile densities

Data used:

- Calibration data (9 electric fishing sites)
- Electric fishing samples using successive removal technique (66 sites sampled from 1975 to 1990)
- Electric fishing sites samples using 5 minutes sampling technique (546 sites sampled from 1994 to 2011)
- Number of eggs and 0+ juveniles stocked

Objectives:

This model aims to estimate average densities of 0+ juveniles in the 3 river sections of the Allier catchment considered in this study. One of the main challenges is to identify the contribution of the “wild” 0+, the stocked 0+ and the stocked eggs

Appendices to refer to: A.1; A.2; A.3

In order to measure the 0+ juvenile densities, electric fishing was carried out at various sites in the Allier catchment throughout the time-series (1977-2011). Until 1990, sites were fished using a successive removal technique. This technique provides estimates of 0+ densities but is quite time consuming and labour intensive. On average, only 5 sites over the whole catchment were fished annually. From 1991 to 1993 no sampling was carried out. Since 1994 until present, a 5 minutes index of abundance is used to sample 0+ juveniles in various sites of the Allier catchment (Fig. 2.6). This technique does not provide direct estimates of 0+ juvenile densities but it is much more cost effective than the successive removal technique.

To be able to use the two types of data collected throughout the time-series it was necessary to measure how the 5 minutes sampling was related to the 0+ juvenile densities. To do so, 9 sites were sampled in 1997, 2000 and 2001 using first the 5 minutes index of abundance and followed by the successive removal technique. The information obtained from these 9 sites was used to build a calibration relationship (Fig. 3.1). A model developed by Dauphin et al. (2009) was

modified in order to fit to the Allier data. Description of the model and its results can be found in App. A.1.

The Atlantic salmon population of the river Allier has been stocked since 1970 by the salmon hatchery of the Conseil Supérieur de la Pêche (CSP) in Augerolles. In 2001, the implementation of the first step of the Plan Loire Grandeur Nature, led to a change in the stocking strategy (number of stocked salmon multiplied by 3) associated with the opening of a new salmon hatchery in Chanteuges which now produces all the salmon to be stocked in the Allier. Additionally, in 2009, all the area upstream of Langeac was declared “refuge area” which means that no stocking is allowed in this area anymore (Fig. 2.5a and b). The Allier river has been stocked with different Atlantic salmon lifestages such as eggs (Fig. 2.5a), 0+ juveniles (Fig. 2.5b) and smolts (Fig. 2.5c). Before 1985, Atlantic salmon stocked in the Allier river came from Scotland, Iceland and Denmark strains in combination with the Allier strain (spawners captured in the Allier). Since 1985, all lifestages stocked stemmed from the Allier strain.

The electric fishing carried out in early autumn will reflect the spawners success but since the Allier is heavily stocked it will also reflect the survival of the stocked 0+ juveniles and eggs. The electric fishing data provides information regarding the 0+ juvenile densities at a local scale and the objective is to obtain density estimates at a river section scale.

Therefore, densities of 0+ juveniles ($0+/m^2$) are expressed at two spatial scales:

- 1) a macro scale corresponding at the river section scale (Vichy-Langeac, Langeac-Poutès and upstream Poutès). Densities at this scale are indicated by an upper-case *D*.
- 2) a micro scale corresponding at the electric fishing scale. Densities at this scale are indicated by a lower-case *d*.

At both scale, total 0+ densities can be broken down in 3 components:

- 1) “wild” 0+, the descendants of the returning adults which have spawned
- 2) Stocked 0+, the survivors from the stocked 0+ during spring
- 3) Stocked eggs, the survivors from the stocked eggs (in field incubators, App. A.3) during winter

Macro scale:

For the two river sections downstream of Poutès dam, there is a total average 0+ juvenile density $D_{t,i}^{tot}$ associated to every year. For the river section upstream of Poutès a density is associated only from 1987 which corresponds to the year following the installation of the fish lift at Poutès (i.e. the first year following the first possible natural spawning). There is always a “wild” component $D_{t,i}^{wild}$ to the total average density since during the time-series there has always been some adults returning in the Allier. The two other components $D_{t,i}^{juv}$ and $D_{t,i}^{egg}$ are facultative since the stocking of 0+ juveniles or eggs is not systematic in every river sections every year (Fig. 2.5a and 2.5b).

The “wild” component of the macro scale density (i.e. river section) $D_{t,i}^{wild}$ is conditioned by a density dependence relationship with a Beverton-Holt (BH) shape. This relationship depends on the number of potential spawners present in the river section, the 0+ juvenile habitat available in the river section and two parameters. The first parameter a^{wild} governs the slope of the relationship: it reflects the average maximum number of 0+ produced by one potential spawner. The second parameter $Rmax^{wild}$ governs the asymptote of the relationship (i.e. the average maximum density the river section can support). In addition, a multiplicative spatial effect is incorporated in order to reflect the differences between the river sections upstream and downstream of Langeac on their BH relationships. The relation is also associated with a variance parameter which allows accommodating for any discrepancies between the data and the model.

The stocked 0+ juvenile component of the macro scale densities $D_{t,i}^{juv}$ is also conditioned by a density dependence relationship depending on the number of 0+ juvenile stocked, the juvenile habitat available in the river section and also two density dependence parameters. The slope parameter a^{juv} is comprised between 0 and 1 since it reflects the average survival of a stocked 0+ juvenile between the moment they were released in the river and the moment the electric fishing sample is carried out (i.e. at the beginning of autumn). It is assumed that the asymptote parameter $Rmax^{juv}$ is conditioned by the success of the “wild” juveniles i.e. if the “wild” 0+ juveniles are produced in large quantities or have a good survival, this will negatively impact the success of the stocked 0+ juveniles. This reflecting the fact that stocked 0+ juveniles enter the system later than the “wild” fish and are therefore constrained by the prior occupancy of the habitat by 0+ wild juveniles. Similarly to the “wild” 0+ relationship, a variance parameter is added to account for any discrepancies between the data and the model.

The stocked eggs component of the macro scale densities $D_{t,i}^{egg}$ is modelled in a different way than the two others components. Due to the lack of data on the success of stocked eggs (no systematic electric fishing close to the field incubators sites), only a simple survival relationship between the density and the number of stocked eggs was implemented. Similarly to the two other density components, a variance parameter was added to account for all discrepancies between the model and the data.

Micro scale:

For each electric fishing site, a total local density $d_{t,i}^{tot}$ was estimated using the successive removal or 5 minutes IA data using the calibration described above and in Appendix A.1. As for the macro scale, this density is composed of three components (“wild” $d_{t,i}^{wild}$, stocked 0+ juveniles $d_{t,i}^{juv}$ and stocked eggs $d_{t,i}^{egg}$). All sites were assumed to have a “wild” component. For all years, it was possible to determine if an electric fishing site had been affected by some stocking events. The 0+ juvenile stocking events were assumed to have been done in a homogeneous manner; therefore any site located within two stocking points was assumed to have a 0+ juvenile density component. The egg stocking was assumed to have a much more local impact due to the nature of the lifestage stocked and the technique used (i.e. field incubators, App. A.3). Only sites within an area 1600m downstream of the field incubator were assumed to be impacted (Beall et al., 1994). Each micro-scale density components are dependent on the annual macro-scale density as well as an inter-site variance specific to each component.

3.2.2 Potential spawners to redd counts relationship

Data used:

- Redd counts (from 1977 to 2011 with missing years)
- Proportion of spawning areas surveyed (same years than redd counts)
- Adult counts :
 - 1) Vichy (exhaustive counts from 1997 to 2011)
 - 2) Langeac (partial counts from 2003 to 2008)
 - 3) Poutès (exhaustive counts from 1986 to 2011)

Objectives:

This model aims to provide a relationship between annual redd counts and potential spawners in each river section of the Allier catchment.

Appendices to refer to: A.4

One of the most frequent types of data available related to adult escapements is redd counts (the nest structure that salmon female dig to lay their eggs) and the Allier catchment is not an exception. Since 1977, annual redd counts have been carried out excepted when the weather conditions did not permit it. Redd counts dataset are affected by various factors related to the sampling process or the observer's experience (Dunham et al., 2001; Muhlfeld et al. 2006). This means that the information underlying these dataset is often a noised measurement of the adult escapement and it is therefore important to take this uncertainty in account when using them.

In the Allier catchment, additionally to the collection of redd counts, three fish counters were installed progressively during the time-series along the Allier river providing exhaustive or partial figures of returning adults in the different river sections considered. Years for which both dataset (i.e. redd counts and fish counts) are simultaneously available are used to build a calibration relationship relating the two types of dataset.

The model used for this relationship is based on a similar work developed by Dauphin et al. (2010) and modified to accommodate for the environmental and data specificities of the Allier catchment. In addition to the redd counts ($R_{t,i}$) and adult counts (N_t^V, N_t^L, N_t^P), the proportion of spawning area surveyed during the redd counts data collection ($p_{t,i}^R$) and the number of adults taken for broodstock for stocking purposes B_t , are incorporated in the model. The adults taken as broodstock are always captured in the river section between Vichy and Langeac.

Redd counts are carried out around December once most of the females have spawned (ref). From 1977 to 1996, the counting operations were carried out by foot or by boat. Since 1997, the counts were fulfilled by the means of a helicopter. Full adult counts are available from Vichy counting station (from 1997 to 2011) and Poutès fish lift (from 1986 to 2011). The Langeac counting station provides only a minimal number of adult migrating upstream because fish can bypass the counting facility during high flow events (from 2003 to 2008).

The time series considered can be divided in two parts: the first 9 years (1977 to 1985) during which only the area downstream of Poutès dam is available and the rest of the time-series (from 1986 to 2011) when, after the construction of a fish lift, the adults were allowed to move upstream of Poutès dam. Returning adults at Vichy are distributed in the three river sections according to a random process involving two annual probabilities of moving upstream of Langeac and Poutès counting station which is in detail in section 3.3.

It is assumed that, on average, the redd counts is the product of the potential spawners by the proportion of spawning habitat surveyed by a redd:potential spawner ratio $\kappa_{t,i}$. The redd:potential spawner varies annually and accounts for the differences in the relationship between redd counts and potential spawners upstream and downstream of Langeac. Due to the change in the counting technique in 1997 (i.e. foot and boat counting to helicopter counting), a “methodology” effect γ was incorporated into the model.

3.3 Full lifecycle model

Data used:

- All dataset used in section 3.1 and 3.2
- Professional and anglers catches (From 1975 to 1993)
- Number of stocked smolts (from 1975 to 2011)
- Adult returns of marked stocked smolts (from 1997 to 2011)

Objectives:

The aim of this model is to attempt understanding the population dynamics of the Atlantic salmon in the Allier catchment and the role that stocking had in this dynamics over a 35 years time-series while taking in account all form of uncertainties.

Appendices to refer to: A.1, A.2, A.3, A.4, A.5, A.6

The lifecycle model aims to reflect the biological processes between the different lifestages for which information is available. In this particular study, three lifestages are considered:

- 0+ juveniles
- Adult returns
- Potential spawners

As described in section 2, the Allier catchment was divided in three main river sections. Using the model described in section 3.2.1, a juvenile production can be calculated annually for each sections using the 0+ densities and the surface of favorable 0+ juvenile habitat available in each river section.

3.3.1 Adult returns

Annual adult returns at Vichy N_t^V are assumed to be conditioned on average by three years of juvenile production J_{t-3} , J_{t-4} and J_{t-5} (these 3 years account for more than 90% of the life histories encountered in the Allier catchment. Cuiat, 1988). The contribution of each year is assumed to be equal and the sum of these 3 years of juvenile production forms the juvenile cohort for a given year $J_t^{coh_tot}$.

Every year, the stocked smolts are composed of two size modes (the numbers in each mode are known); the larger smolts are assumed to leave the river system the year they are stocked while the smaller smolts are assumed to migrate the following year. The total number of smolts leaving the river system on a given year Sm_t is therefore the sum of the larger smolts stocked on year t and the smaller smolts stocked on year $t-1$. For more than 10 years (1995 and 1996 and then from 2001 to 2011), a proportion of the stocked smolts have been marked (adipose fin clipping). Data from marked adult returns show that stocked smolts return as adult two or three years after they have been stocked. Therefore the adult returns at Vichy N_t^V are related to the number of smolts stocked two and three years earlier (Sm_{t-2} and Sm_{t-3}) which forms the smolt cohort Sm_t^{coh} . Henceforth the term smolt refers to stocked smolts.

The cohorts of juvenile $J_t^{coh_tot}$ are assumed to have an average unknown (i.e. estimated) return rate μ^{s-J} . The smolt cohorts Sm_t^{coh} are assumed to have an average known (i.e. calculated from the overall number of smolts marked and the number of marked returning adults) return rate μ^{s-Sm} .

There are annual variations around these mean return rates at Vichy. They correspond to (i) annual variations in the contribution of each year of juvenile production, (ii) annual variations in the contribution of each year of stocking as well as (iii) annual variations in the return rate of the juvenile or smolt cohort. Since it is not possible to explicitly identify the contributions of these various sources of variations, they are all accounted for in one single year effect with an associated variance parameter.

In earlier versions of the model, it was found that setting only one average 0+ juvenile to adult return rate μ^{s-J} and one average stocked smolt to adult return rate μ^{s-Sm} did not provide the best fit to the data. Therefore it was assumed that both return rates may have changed during the time series. The model modified to allow for return rate levels. The year during which the switch from one level to another is unknown (i.e. estimated) and once the switch is made, it is assumed to be permanent until the end of the time-series.

Some additional information was incorporated in the model to refine the adult returns estimates. Based on historical catch records, it was assumed that having more than 15 000 adults returning in the Allier catchment during the time series was unrealistic and therefore set as a maximum annual adult returns. During the part of the time-series during which salmon fishing was authorised, it was possible to identify the catches from professional and recreational fishermen occurring downstream and upstream of Vichy. All adults caught upstream of Vichy were assumed to be potential spawners of the Allier catchment while it was assumed that only an unknown proportion (i.e. estimated) of the adults captured downstream of Vichy would have actually managed to migrate upstream of Vichy if they had not been captured. Additionally, every year, some adults were taken between Vichy and Langeac for broodstock purposes (up to 103 in 2003). These adults returned to the Allier catchment but did not participate in the natural reproduction. The sum of the annual adult catches upstream of Vichy and the proportion of adult catches downstream of Vichy that would have migrate upstream of Vichy and the number of adults taken for broodstock purposes is used as a minimum number of adult returns at Vichy min_t^{N-V} . Therefore N_t^V corresponds to the number of returning adults at Vichy without fishing exploitation downstream of Vichy. This is the actual situation for most of the time-series (1991 to 2011) but not at the beginning of the time-series since there was some fishing occurring downstream of Vichy until 1990.

3.3.2 spatial distribution of potential spawners

Returning adults at Vichy N_t^V have a probability p_t^L of moving upstream of Langeac counting station. Annual probabilities are conditioned by an average probability of migrating upstream of Langeac and an inter-annual variation parameter. The average probability of migrating upstream of Langeac is explicitly conditioned by two main components: 1) the proportion of 0+ juvenile habitat available in the river section upstream of Langeac in order to reflect the fact that adults may distribute themselves following an ideal free distribution and 2) the proportion of the cohort of 0+ juvenile production in the river section upstream of Langeac in order to reflect the fact that returning adults may be distributing themselves depending on where they grew up as juveniles (homing). The relative contribution of these two components is unknown (i.e. estimated). Note that the two proportions are calculated differently throughout the time-series to reflect the impact of the installation of the fish lift at Poutès in 1986 which opened some new habitat for the adults to migrate in and for the juveniles to grow in (App. A.5). Additionally, a discrepancy parameter is incorporated so the average probability of moving upstream of Langeac can be systematically increased or decreased to represent the facilitation or the interference occurring either during the upstream migration of the adults between Vichy and Langeac or the downstream migration of smolts between Langeac and Vichy. Langeac counting station's efficiency is influenced by

hydraulic conditions therefore it is assumed to only provide a minimum value of adults migrating upstream of Langeac (i.e. the exact number of adults is never known throughout the time-series).

In 1986, a fish lift was installed at Poutès dam allowing adults migrating upstream of Langeac N_t^L to move upstream of Poutès with a probability p_t^P . In the same way than for the probability of migrating upstream of Langeac, the annual probabilities of moving upstream of Poutès are conditioned by an average probability and an inter-annual variation parameter. The average probability of migrating upstream of Poutès is explicitly conditioned by the same two main components in order to reflect a mixture of ideal free distribution and homing processes. It is assumed that the relative contribution of these two components is the same than for the average probability of moving upstream of Langeac. A discrepancy parameter is incorporated so the average probability of moving upstream of Poutès can be systematically increased or decreased. The number of adults entering the river section upstream of Poutès is known exactly since 1986 (year of the installation of the fish lift).

With the number of adults moving upstream of each counting station it is possible to calculate the number of potential spawners $S_{t,i}$:

the number of potential spawners in the river section between Vichy and Langeac is the number of adults moving upstream of Vichy minus the number of adults moving upstream of Langeac and minus the adults taken for broodstock purposes,

the number of potential spawners in the river section between Langeac and Poutès is the number of adults moving upstream of Langeac minus the number of adults moving upstream of Poutès,

the number of potential spawners in the river section upstream of Poutès is the number of adult moving upstream of Poutès.

The potential spawners in each river sections $S_{t,i}$ are related to the redd counts in the same river sections $R_{t,i}$. This relationship is the one described in section 3.2.2 (App. A.4).

3.3.3 0+ juvenile densities

The average wild 0+ juvenile density in each river section for a given year $D_{t+1,i}^{wild}$ is related to the number of potential spawners in the same river section the year before $S_{t,i}$ using a Beverton and Holt density dependence relation.

Two other 0+ juvenile density components are calculated: one of them corresponding to the density of 0+ juveniles resulting from the stocked 0+ juveniles $D_{t+1,i}^{juv}$ and the second corresponding to the density of 0+ juveniles resulting from the stocked eggs $D_{t+1,i}^{egg}$. Details of how these densities are obtained can be found in section 3.2.1 and appendix A.2. The three components are summed to obtain a total annual density for each river section $D_{t+1,i}^{tot}$. The surface of favorable rearing habitat for 0+ juveniles in each river section is then used to calculate a juvenile production for a given year and a juvenile production cohort $J_t^{coh-tot}$ that will be related to the adults returns in Vichy as described at the beginning of this section.

4. Results

Two types of results are presented in this section:

- 1) The outputs of the full lifecycle model (sub-section 4.1) and,
- 2) the outputs of a set of simulations (sub-section 4.2) which were carried out to look at the dynamics and assess the viability of the population over the next 20 years under different scenarios

4.1 Retrospective analysis

4.1.1 Adult returns

The number of adults returning at Vichy is estimated from 1977 to 1996. From 1997, the counting station is assumed to provide exhaustive figures. The first half of the time-series has higher adult returns than the second half with a maximum of 3105 adults (median) entering the Allier catchment return in 1982. After then, the annual returns at Vichy have slowly declined and for the last 15 years the average adult returns have remained stable around 550 salmon returning at Vichy (Fig. 4.1). Every year adult returns at Vichy are estimated with a fairly high level of uncertainty with coefficients of variation (CVs, sd/mean) ranging from 28% to 63% (Fig. 4.1).

4.1.2 Repartition in the river sections

The evolution of the abundance of potential spawners in the Vichy-Langeac and Langeac-Poutès river section follow roughly the same trend as the adult returns at Vichy (Figure 4.2 a, b and c). The CVs are on the same scale than the adult returns at Vichy but are more variable: in recent years when all the data is available the CVs are around 10% and 30% for the potential spawners estimates of the Vichy-Langeac and Langeac-Poutès river section respectively. In the first part of the time series, when no information regarding the counting station and that the potential spawners estimates rely mainly on the red counts, the CVs are predominantly ranging between 50 and 85 %. All potential spawners in the river section upstream of Poutès are known and show a different pattern evolution. There is an increasing trend in the number of potential spawners

entering the river section upstream of Poutès from the year the fish lift was installed. Although low numbers were observed over the last 3 years

During the first part of the time-series (when the river section upstream of Poutès is not available) the potential spawners are distributed almost proportionally to the 0+ juvenile habitat available. After the opening of the river section upstream of Poutès, the two river sections downstream of Poutès received more potential spawners relatively to the proportion of 0+ juvenile habitat while the river section downstream of Poutès received significantly less potential spawners relatively to the proportion of 0+ juvenile habitat (Figure 4.2 d, e and f). Since the mid-1990s the river section between Langeac and Poutès has been receiving on average significantly more potential spawners relative to the ratio of 0+ juvenile habitat available: 22% of the total potential spawners versus 13% of the total favorable 0+ juvenile habitat. In the meantime, the two other river sections have been receiving a smaller proportion of potential spawners relative to the habitat available in these river sections: on average 63% of the total potential spawners versus 69% of the total favorable 0+ juvenile habitat for the river section between Vichy and Langeac and 14% of the total potential spawners versus 17% of the total favorable 0+ juvenile habitat for the river section upstream of Poutès.

4.1.3 Potential spawners to redd counts relationship

The average spawner:red ratio downstream and upstream Langeac counting station $\mu^{K_{down}}$ and $\mu^{K_{up}}$ are significantly different ($P(\mu^{K_{down}} > \mu^{K_{up}}) = 0.99$). On average, a potential spawner will produce 0.57 redds in the river section downstream of Langeac, whereas this figure is doubled for spawners settling in the river sections upstream Langeac (1.35 redds for one potential spawner, Table 41, Figure 4.3).

4.1.4 0+ juvenile production

For each year and each river section, a total 0+ juvenile density $D_{t,i}^{tot}$ is calculated. These densities are the sum of three components:

- the “wild” 0+ juveniles component $D_{t,i}^{wild}$ corresponding to the density of 0+ related to the potential spawners,
- the stocked 0+ juveniles component $D_{t,i}^{juv}$ corresponding to survivors of the 0+ stocked during spring and,
- the stocked egg component $D_{t,i}^{egg}$ corresponding to the survivors of the eggs stocked in incubators during the winter.

For each river section a summary figure is produced. It shows the annual total densities and its three components when available (Figure 4.5, 4.6 and 4.7). For instance, there is no stocked egg component for the river section upstream of Poutès because no egg incubators were used in this river section. The years during which there are no stocking events are indicated with a lighter color. For each component, the goodness of fit of the model to data is verified throughout the residuals. The relative contributions of each component are also displayed.

The annual total 0+ juvenile densities are often fairly uncertain but it is possible to see trends over the time-series and see some differences between the three river sections. For instance, the total average 0+ juvenile density tends to increase over the last five years of the time-series for the river section between Vichy and Langeac while the total 0+ juvenile density decreases for the two other river sections. The identification of three components in the total 0+ juvenile density (“wild”, stocked 0+ juveniles, stocked eggs) allows identifying the contribution of the two types of stocking. The first thing to be noted is the negligible impact of the egg incubators to the total 0+ juvenile density. The second thing is the important contribution of the stocked 0+ juvenile especially during the period starting from the mid-nineties which correspond to a dramatic increase of the number of 0+ juveniles stocked annually. Depending on the year and river section, the contribution of the stocked 0+ juvenile to the total 0+ juvenile density varied from 40% to 80%. It is important to notice that in the two river sections where some eggs were stocked, their contribution to the total juvenile density is close to being null (Fig. 4.5j and 4.6j).

Additionally, significant spatial differences were found between the river sections upstream and downstream of Langeac: the two river sections upstream of Langeac are on average two times more productive than the river section downstream of Langeac. This can be seen in Fig. 4.8a and 4.8b which display the potential spawners to wild 0+ juvenile density dependence relationship and the stocked 0+ juvenile density dependence relationship respectively. The posterior distributions of the different parameters of the average relationships are described in table 4.2. Note that the R_{max} parameters of the average stocked 0+ juvenile density dependence relationship represented in Fig 4.8b are the same than the R_{max} parameters of the potential spawners to wild 0+ juvenile density dependence relationship since the R_{max} parameter for this relationship are calculated annually and dependent on the annual “wild” density and therefore not practical to be represented (App. A.2). The main thing to retain is that the river sections upstream of Langeac are on average about two times more productive than the river section downstream of Langeac.

It is also possible to calculate the annual relative 0+ juvenile production by cohort for each river section $J_{t,i}^{coh}$ (App. 5, Figure 4.9, d and g) and relate it to the proportion of favourable 0+ juvenile rearing habitat and the relative distribution of potential spawners (Fig. 4.9b, e and h).

During the last 35 years the relative 0+ juvenile production have been quite variable and not necessarily related to the proportion of 0+ juvenile rearing habitat. For instance, in the last 20 years the river section between Vichy and Langeac has been producing a significantly smaller proportion of 0+ juvenile compared to the relative availability of favourable 0+ juvenile rearing habitat. The inverse pattern is observed for the two other river sections.

If there is a strict homing mechanism and no obstacle to the migration of fish (i.e. all the surviving 0+ juveniles of a given river section will return as adults in the same river section), one would expect the difference between the ratio of potential spawners in each river section minus the ratio of the 0+ juvenile production to be on average around 0. Figure 4.9c, f and i show that it is not what happens. Indeed, the river section between Vichy and Langeac (Fig. 4.9c) “receives” one average 14% more potential spawners in comparison to its 0+ juvenile production. The river section between Langeac and Poutès (Fig. 4.9f) “receives” on average 4% less potential spawners in comparison to its 0+ juvenile production, while the river section upstream of Poutès has on average a 13% deficit of potential spawners in comparison to its 0+ juvenile production.

4.1.5 0+ juvenile and stocked smolts to adult return rate

As described in section 3.3 and App. A.5, two levels of 0+ juvenile to adult return rate μ^{s-J} and stocked smolt to adult return rate μ^{s-Sm} were implemented. The change in the level of adult return rate is found to occur between 1985 and 1990. The historical level of adult return rate was about 3.7 times higher than the current adult return rate (i.e. 0+ juvenile to adult return rate moving from 6.457×10^{-3} to 1.777×10^{-3} and the stocked smolt to adult return rate moved from 2.02×10^{-3} to 0.545×10^{-3}).

4.2 Retrospective simulation and 20 years forecast without stocking

4.2.1 Retrospective simulation without stocking1

In order to measure the impact of stocking a simulation was carried out using the posterior distributions of parameters of the full lifecycle model but removing the stocking component (i.e. the stocked 0+ juvenile, the stocked smolts and the returning adults taken for broodstock purposes). The adults returns of both the lifecycle model (Fig. 4.11a) and the retrospective simulation (Fig. 4.11b) were compared to quantify the impact of stocking during the time series considered (Fig. 4.11c). Due to the structure of the model (i.e. juvenile cohorts depending on 3 years of juvenile production) the posterior distributions of first 6 years of adult returns at Vichy are identical (plain dots in Fig. 4.11c).

Starting from the mid-nineties, the adult returns estimates obtained in the retrospective simulation are significantly lower than the adult returns estimates from the full lifecycle model (Fig. 4.11b and c).

Stocking has been contributing significantly to the adult returns especially during the last 15 years: on average about 330 returning adults at Vichy (Fig. 4.11c) or about 67 % (Fig. 4.11d). This can be correlated to the increase of stocking (0+ juvenile and smolts, Fig 2.5) occurring at the same period. The impact of stocking on the adult returns in the first part of the time series is less obvious and should be considered carefully since the uncertainty of the adult returns estimates is much higher.

4.2.2 20 years forecast without stocking

In addition to the retrospective work allowing the understanding of the mechanisms involved in the Atlantic salmon population dynamics in the Allier catchment. A simulation exercise was also carried out to test different scenarios and their impact on the evolution of the adult returns at Vichy for the next 20 years. Five scenarios were implemented under different assumptions, however for all of them it was assumed that there was no stocking during these 20 years:

- 1) The environmental conditions stay the same as they currently are i.e. the 0+ to adult return rate stays the same.
- 2) The environmental conditions stay the same as they currently are but the migration transparency is improved at Langeac only i.e. it is assumed that the discrepancy observed between the ratio of juvenile produced in the river sections upstream of Langeac and the ratio of

adult returning in the same river sections is reduced to zero during the first 10 years of the simulation and stays at this level for the remaining 10 years.

3) The environmental conditions stay the same as they currently are but the migration transparency is improved at Poutès only i.e. it is assumed that the discrepancy observed between the ratio of juvenile produced in the river sections upstream of Poutès and the ratio of adult returning in the same river sections is reduced to zero during the first 10 years of the simulation and stays at this level for the remaining 10 years.

4) The environmental conditions stay the same as they currently are but the migration transparency is improved at Langeac and Poutès i.e. it is assumed that the discrepancy observed between the ratio of juvenile produced in the river sections upstream of Langeac and Poutès and the ratio of adult returning in the same river sections is reduced to zero during the first 10 years of the simulation and stays at this level for the remaining 10 years.

5) The environmental conditions change i.e. the 0+ to adult return rate increase from the current level to 50 % of the historic level during the first 10 years of the simulation and stays at this level for the remaining 10 years.

6) The environmental conditions change i.e. the 0+ to adult return rate increase from the current level to 100 % of the historic level during the first 10 years of the simulation and stays at this level for the remaining 10 years.

7) The migration transparency is improved in a similar way than scenario 4 and simultaneously the environmental conditions change in a similar way than scenario 5.

For each scenario, probabilities of reaching certain threshold numbers of returning adults at Vichy (i.e. 10, 50, 100, 250 and 500 adults) were calculated as a measure of the population's viability. The values of the thresholds were determined based on the average number of returning adults in the last 15 years (i.e. a bit more than 500). If high probabilities of not reaching a low thresholds are observed then the population is not likely to be viable.

It would have been possible to extend these projections for more than 20 years but longer projections make less sense since more changes (either environmental or anthropic changes) are likely to occur in the Allier catchment and it's difficult to predict these changes and how they will affect the model.

4.2.2a Under the same environmental conditions

In this simulation scenario, the adult returns at Vichy projections slowly decline to reach on average 260 returning adults (Fig. 4.12) with non-negligible probabilities of observing less than 100 adults returning at Vichy (about 10%, Fig. 4.13) and high probabilities of not observing the average number of adults that have been returning at Vichy in the last 15years (about 80% at the end of the projection period, Fig. 4.13).

4.2.2b Improvement of migration transparency at Langeac only

In this simulation scenario, the adult returns at Vichy projections slowly decline in a very similar way than in scenario 1. Only improving the migration transparency at Langeac (as implemented in the model) does not allow for higher adult returns (Fig. 4.14) or lower probabilities of not reaching small threshold (Fig. 4.15).

4.2.2c Improvement of migration transparency at Poutès only

In this simulation scenario, the adult returns at Vichy projections slowly decline in a very similar way than in scenario 1. Only improving the migration transparency at Poutès (as implemented in the model) does not allow for higher adult returns (Fig. 4.16) or lower probabilities of not reaching small threshold (Fig. 4.17).

4.2.2d Improvement of migration transparency at Langeac and Poutès

In this simulation scenario, the adult returns at Vichy projections slowly decline in a very similar way than in scenario 1. Improving the migration transparency at Langeac and Poutès (as implemented in the model) allow for higher adult returns (Fig. 4.18) and lower probabilities of not reaching small threshold (Fig. 4.19).

4.2.2e Improvement of average adult return rate from 0+ juvenile/ stocked smolts to 50% of initial adult return rate level

In this simulation scenario, the adult returns at Vichy projections stay stable with on average 750 adults returning at Vichy every year (Fig. 4.20) and lower probabilities of not reaching the average number of returning adults at Vichy in the last 15 years (20% probability of observing less than 500 adults at Vichy, Fig. 4.21). This is very similar to the results obtained in the scenario where an improvement of the migration transparency at Langeac and Poutès is simulated (scenario 4).

4.2.2f Improvement of average adult return rate from 0+ juvenile/ stocked smolts to 100% of initial adult return rate

In this simulation scenario, the adult returns at Vichy projections increase over the projection period to reach over several thousand adult returns (Fig. 4.22) and almost null probabilities to be under the average number of returning adults at Vichy in the last 15 years (Fig. 4.23).

4.2.2g Improvement of average adult return rate from juvenile/smolts to 50% percent of initial adult return rate and improvement of migration transparency at Langeac and Poutès

In this simulation scenario, the adult returns at Vichy projections and probabilities of reaching a certain number adults are very similar to the one obtained with scenario 3 (Fig. 4.24 and 4.25).

5. Conclusions and perspectives

5.1 Modelling

The model presented in this study is quite comprehensive and detailed. It incorporates a large amount of the datasets available regarding Atlantic salmon in the Allier catchment. It also takes into account the major ecological processes governing the population dynamics: density-dependence between spawners and 0+ juveniles, density dependence between “wild” and stocked 0+ juveniles, incorporation of the different life histories (i.e. adults returns are dependent on 3 years of juvenile production), two levels of 0+ juvenile to adult return rate, an original spawners distribution process combining ideal free distribution and homing hypotheses, spatial heterogeneity according to three zones in the recruitment, and environmental stochasticity affecting all these processes. However, from autumnal 0+ juvenile stage to potential spawner, the model makes no explicit hypothesis about potential fitness differences between individuals according to their wild and hatchery origin. All the datasets used are brought together in a coherent and formal framework. This had not been done so far and can therefore be seen as a benchmark and a major achievement of the present study. The proposed model can be modified and improved from now on and solid basis has been set for this endeavour.

Like all models, it is a simplification of reality and it does not explicitly describe all the different processes and lifestages of the lifecycle of *A. salmon* in the Allier catchment. There are several reasons for this: 1) there was no or not enough data available to identify some processes we may have wished to include, 2) sometimes there was not enough time available during the study and choices had to be made to decide which process was more important to model. However, even if all the different processes are not explicitly incorporated in the model, the framework used (HBM) to implement the model allows dealing with this lack of details by accounting for the overall uncertainties and quantify them.

5.2 Retrospective analysis

Adult returns at Vichy have been severely declining between the mid 80's and the mid 90's. Previous to this decline, a few thousands of adults returned to Vichy while at present it is several hundreds. Stocking is likely to have had a significant contribution to the returning adults at Vichy especially in the last 15 years during which high number of salmon (0+ juveniles and smolts) have been released. Although the large contribution of the stocked 0+ juvenile to the total juvenile production is very clear, it is not possible to know precisely how the stocked 0+

juveniles perform compared to their wild counterparts. There is presently no data in the Allier catchment to evaluate the differences in 0+ to adult return rates between the wild and stocked 0+. A genetic study is currently undertaken in order to evaluate the adult return rate of stocked 0+ juvenile, and even if these results will only be available for a couple of years, they could provide partial information that could be incorporated in the current model.

The 0+ juvenile to adult return rate parameter is the main driver of the populations dynamics. It is quite broad however and could be split in several components in order to reflect more precisely the different events occurring this period of time: the freshwater survival (0+ juvenile to smolt transformation), survival during the smolt migration, survival at sea, survival during the upstream migration and straying before reaching Vichy. Unfortunately, it is not possible to explicitly identify each of these component with data at hand (i.e. some of required data are not available at all or are too scarce). Therefore, from this model output it is currently only possible to conclude that one or several of these components have been declining over time with a major shift located around the mid-eighties.

5.3 Retrospective simulation without stocking

The simulation exercise allowed looking at what would have been the fate of the Allier population if there had been no stocking during the 37 years of the time series considered (1975 to 2011). It is important to notice that even if stocking has had a significant impact on the number of adults returning at Vichy, these numbers have remained stable over the years and there are no signs that the population is increasing. In the absence of stocking, the population would not have gone extinct today: adult returns would however be currently at a much lower level (162 on average over the last 15 years compared to 547 with stocking).

5.4 Viability of the Atlantic salmon population in the Allier catchment

Simulations also allowed testing different scenarios and their impact on the evolution of the adult returns at Vichy for the next 20 years. All scenarios assumed that no stocking would be occurring during these 20 years in order to assess the viability of the self-reproducing population. Stationarity hypotheses were made for this exercise i.e. the different parameters and processes of the model (except for the one modified on purpose to test the different scenarios) are assumed to

stay the same during the 20 year projections. Given the restriction of our projections to only two decades this hypothesis remains reasonable.

There are two main results from this exercise:

1) Without stocking and no changes in the 0+ juvenile to adult return rate or no improvement in the migration transparency, the A. salmon population of the Allier is likely to decrease to a low level (on average a bit more than 250 adults returning at Vichy) with non-negligible probabilities of observing very low returns (10% chance to see less than 100 adults returning at Vichy).

2) The main driver for the recovery of the Atlantic salmon population of the Allier catchment is the 0+ juvenile to adult return rate: if the adult return rate increases to 50% of the historical level, the population is likely to be self-sustaining and to have returning adults levels similar to those observed over the last 15 years. If the adult return rate increases to reach its historical level, the population is likely to increase progressively over the next 20 years.

The improvement of the migration transparency as implemented in the simulation scenarios (i.e. just allowing the returning adults to move upstream of Langeac and Poutès in larger proportion without impacting the adult return rate) does not significantly improve the adult returns at Vichy. However, the improvement of the migration transparency is likely to have an impact on salmon adult return rate either when fish are migrating downstream as smolts or when migrating upstream as returning adults. Some punctual experiments have shown that different obstacles on the migration route can delay the adult migration and lead to higher mortality rate (Baisez et al., 2011). The same is true for the smolts when delayed by obstacles. Studies on these topics would allow improving the knowledge on the different processes occurring in between the different lifestages which could be incorporated in future modeling exercises. Although their contribution to the currently low return rates is not precisely known, obstacles to migration (both downstream and upstream) should be of primary concern for management for at least two reasons: (i) they have potentially a significant impact on the survival of smolts and adults during their migrations and (ii) they are among the few (if not the sole) environmental factors amenable to improvement by the direct and lone action of the authorities in charge of salmon population management.

The outputs of the model show that the potential spawners accumulate themselves in the lower part of the catchment which is also the less productive area for recruitment. The model could be used to test the influence of opening the access to tributaries of this lower part of the catchment and potentially establish some stocking strategies for these tributaries to promote potential spawners migration in these tributaries. These tributaries could increase the number of 0+ juvenile produced but also increase the overall productivity of the lower part of the catchment.

Additionally, the model represents the interactions between wild and stocked 0+ juveniles. Nevertheless, since no data is available this is done in a simple way: the wild 0+ juveniles constrain the survival of the stocked 0+ juveniles but the stocked 0+ juveniles do not influence the wild 0+ juveniles. Moreover, it is assumed that after the first autumnal stage, wild and stocked 0+ behave in a similar way (survival, migration, spawning, etc.). This is expected to be different from what happens in reality and therefore, in this study, the contribution of stocked fish is likely to be seen more optimistically than what it really is (and the renewal process of the wild component is seen more pessimistically than how it is). Consequently, it is important to gather more information on the differences between wild and stocked fish to refine these elements of the model. In the future, the model could be used to test and compare alternative management scenarios. The model offers a framework for testing the outcomes of alternative scenarios given their anticipated effects on salmon mortality rates. Alternative strategies of releases of hatchery reared juveniles can be considered too. Provided the ultimate goal is the restoration of a self-sustaining salmon population in the Allier, management action must primarily aim at reducing salmon mortality. In this respect, improving fish passage, both for juveniles migrating downstream and for adults migrating upstream, remain of highest priority. Providing or improving access of spawners to new zones or tributaries of significant size and where juvenile recruitment could be as efficient as in the upper Allier (above Langeac) should be another management priority. The anticipated outcomes of such management actions could be assessed, in conjunction or not with hatchery releases.

Tables

Table 4.1: Prior distributions of parameters related to the potential spawners to redds relationship ($\varepsilon = 0.001$) and their associated posterior distribution.

Parameter	Prior	Posterior						
		Mean	sd	2.5%	25%	50%	75%	97.5%
$\mu^{k_{down}}$	Gamma (1, ε)	0.574	0.160	0.323	0.461	0.553	0.661	0.949
$\mu^{k_{up}}$	Gamma (1, ε)	1.356	0.324	0.839	1.124	1.315	1.541	2.094
β	Gamma (0.01,0.01)	2.661	0.900	1.266	2.016	2.541	3.173	4.774

Table 4.2: Posterior distribution of the two density dependence relationship parameters.

Parameter	Posterior						
	Mean	sd	2.5%	25%	50%	75%	97.5%
$Rmax_{down}^{wild}$	0.118	0.050	0.055	0.084	0.107	0.139	0.241
a_{down}^{wild}	482	181	239	355	443	560	940
a_{down}^{juv}	0.344	0.113	0.165	0.258	0.329	0.417	0.594
$Rmax_{up}^{wild}$	0.250	0.077	0.147	0.198	0.236	0.284	0.433
a_{up}^{wild}	1045	349	549	797	985	1222	1894
a_{up}^{juv}	0.769	0.295	0.321	0.544	0.729	0.957	1.427

Figures

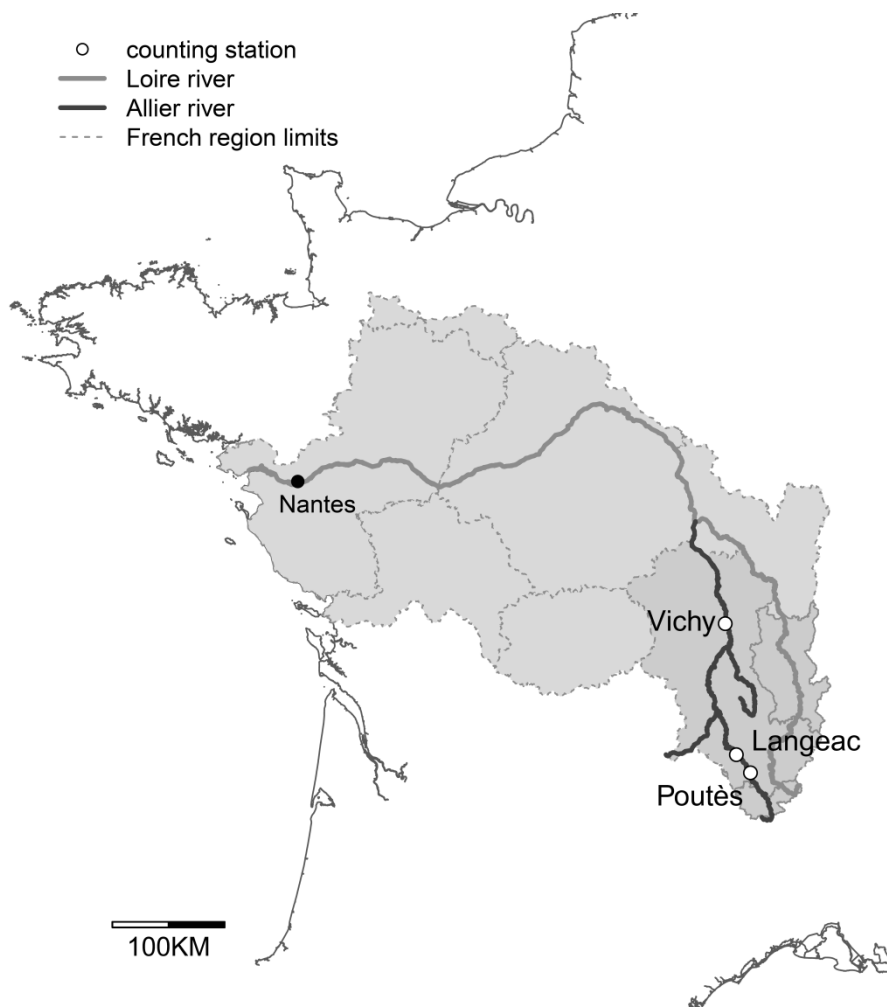


Figure 2.1: Location of the Loire river and the Allier river and the three adults counting station in Vichy, Langeac and Poutès.

Figure 2.1: Localisation de la Loire et de l'Allier ainsi que les stations de comptage d'adultes à Vichy, Langeac et Poutès.

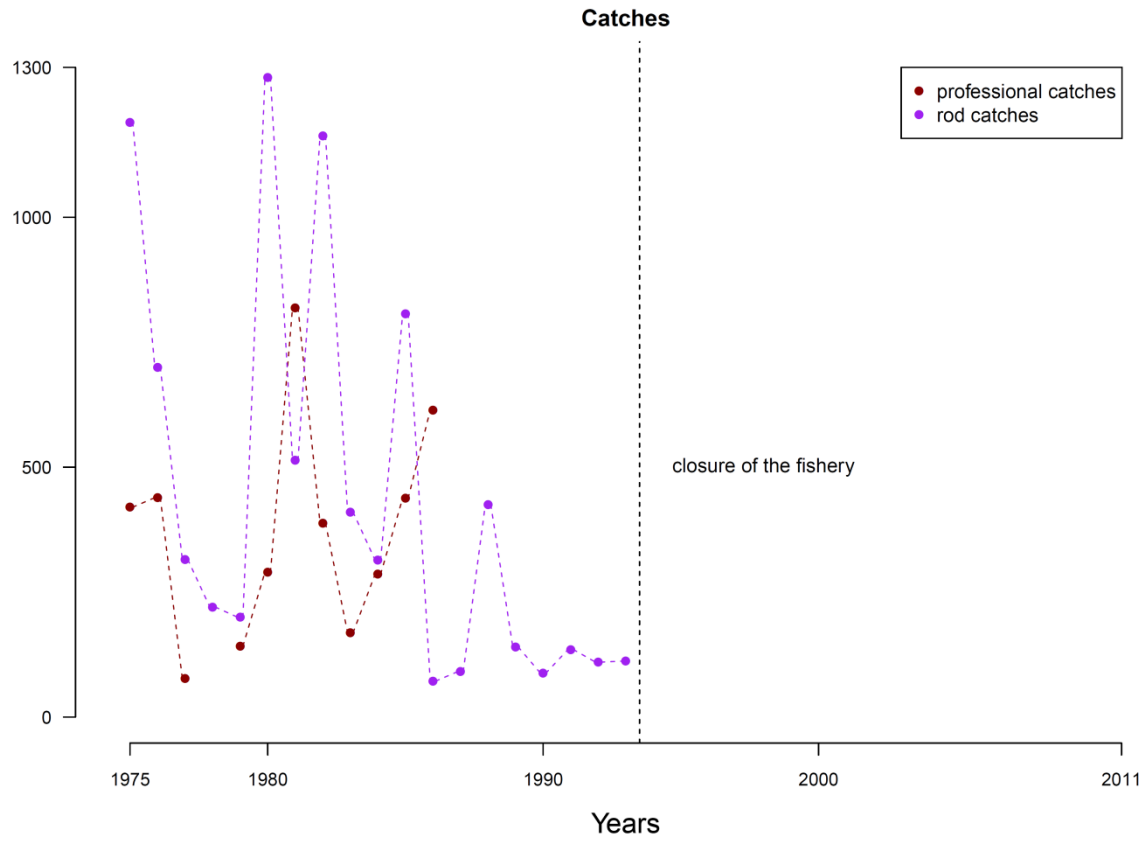


Figure 2.2: Professional and rod catches occurring on the Loire and Allier river.

Figure 2.2: Captures de pêche professionnelle et pêche à la ligne sur l'axe Loire-Allier.

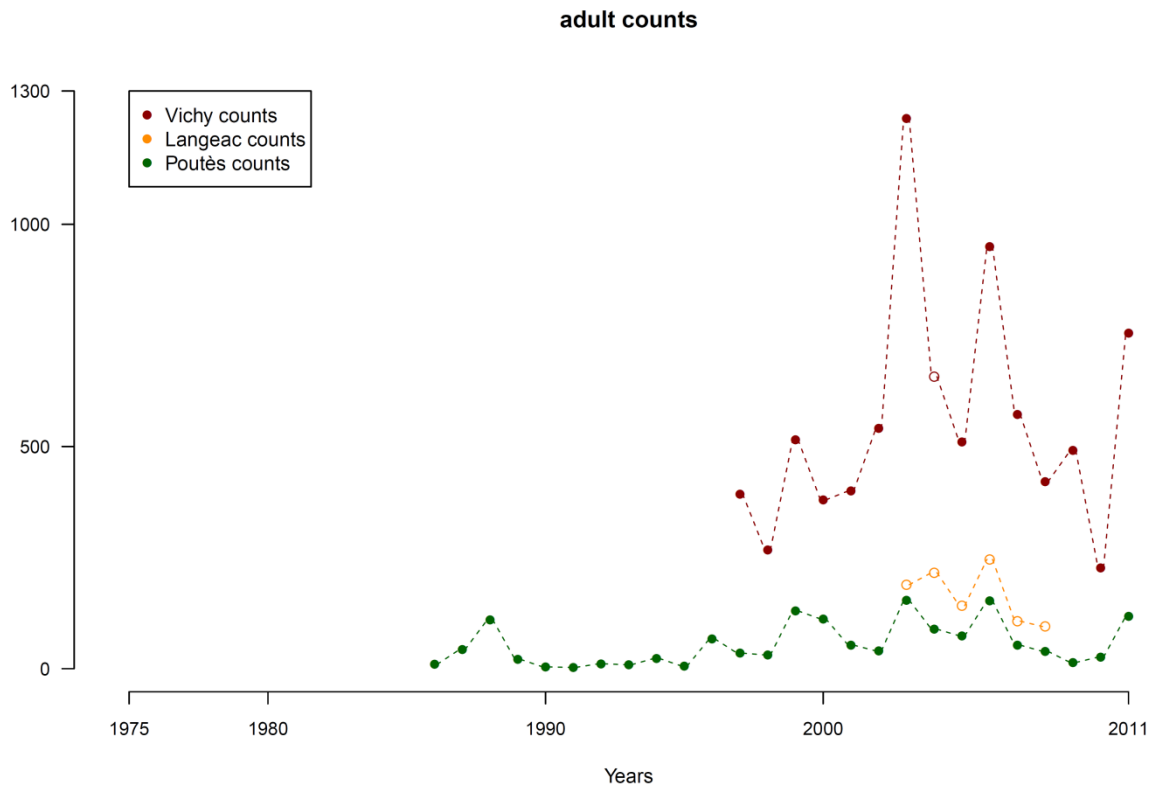


Figure 2.3: Adult counts at the 3 counting stations of Vichy, Langeac and Poutès. Filled dots indicate exhaustive counts, empty dots indicate minimum counts.

Figure 2.3: Comptages d'adultes au niveau des 3 stations de comptage à Vichy, Langeac et Poutès. Les cercles remplis indiquent les comptages exhaustifs et les cercles vides les comptages partiels.

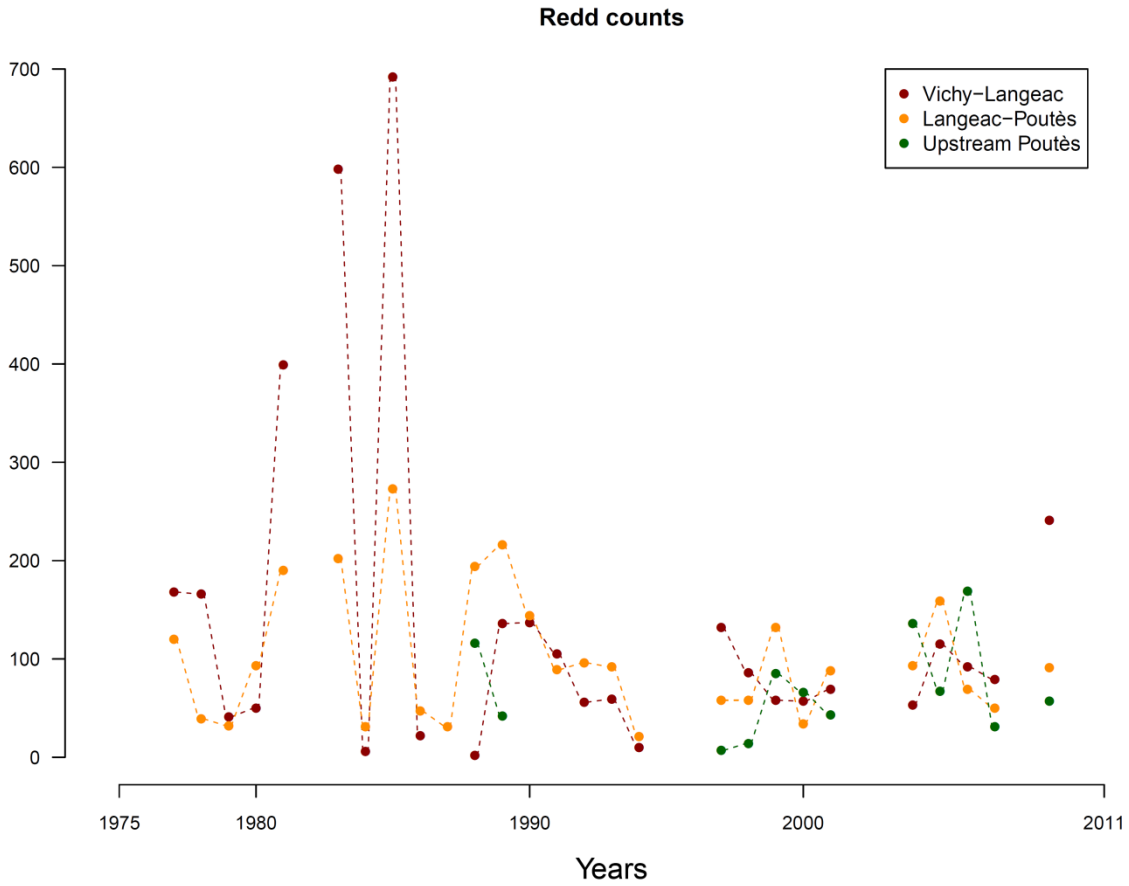


Figure 2.4: Redd counts in the three river sections of the Allier catchment (Vichy-Langeac, Langeac-Poutès and upstream Poutès).

Figure 2.4: Comptages de frayères dans les 3 zones de l'Allier (Vichy-Langeac, Langeac-Poutès et à l'amont de Poutès).

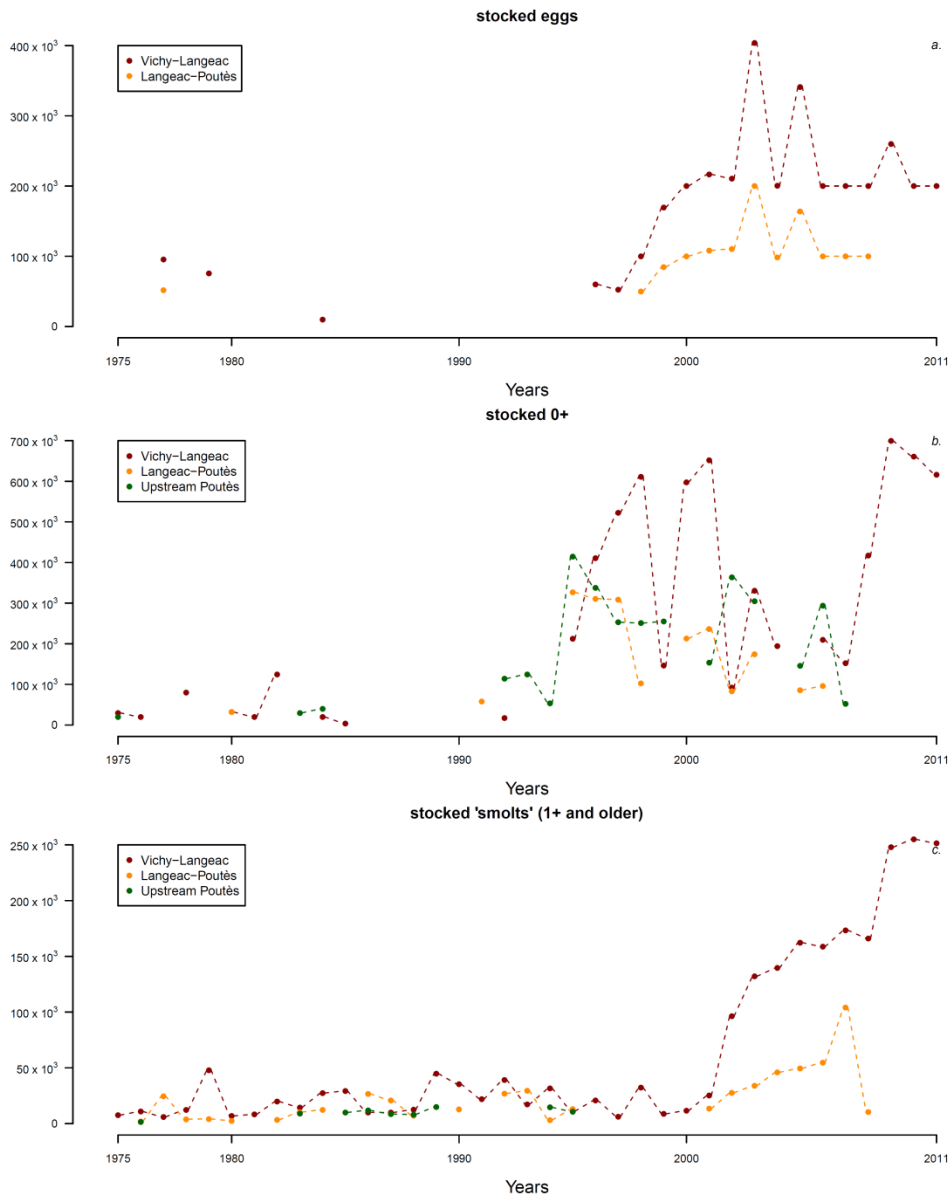


Figure 2.5: Total number of eggs (a), 0+ (b) and smolts (c) stocked annually in the three river sections of the Allier catchment (Vichy-Langeac, Langeac-Poutès and upstream Poutès).

Figure 2.5: Nombre total d'œufs (a), de 0+ (b) et de "smolts" (c) déversés annuellement dans les 3 zones du bassin de (Vichy-Langeac, Langeac-Poutès et à l'amont de Poutès).

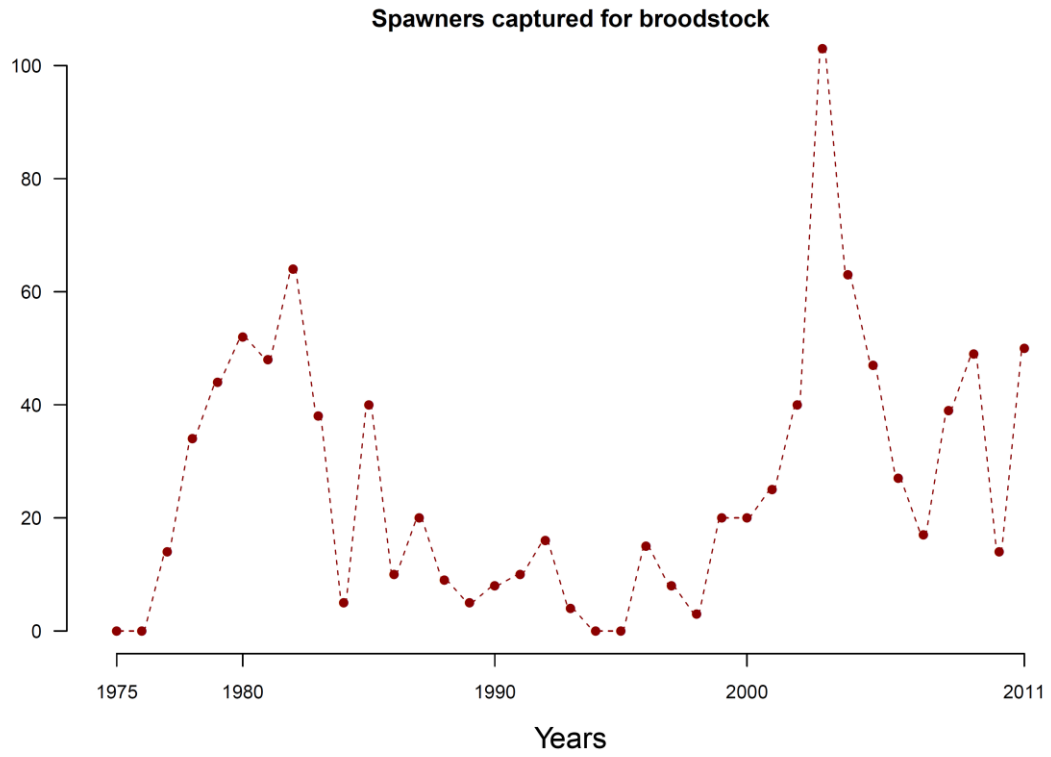


Figure 2.6: Spawners captured annually between Vichy and Langeac for broodstock purposes.

Figure 2.6: Géniteurs capturés entre Vichy et Langeac à destination de la pisciculture.

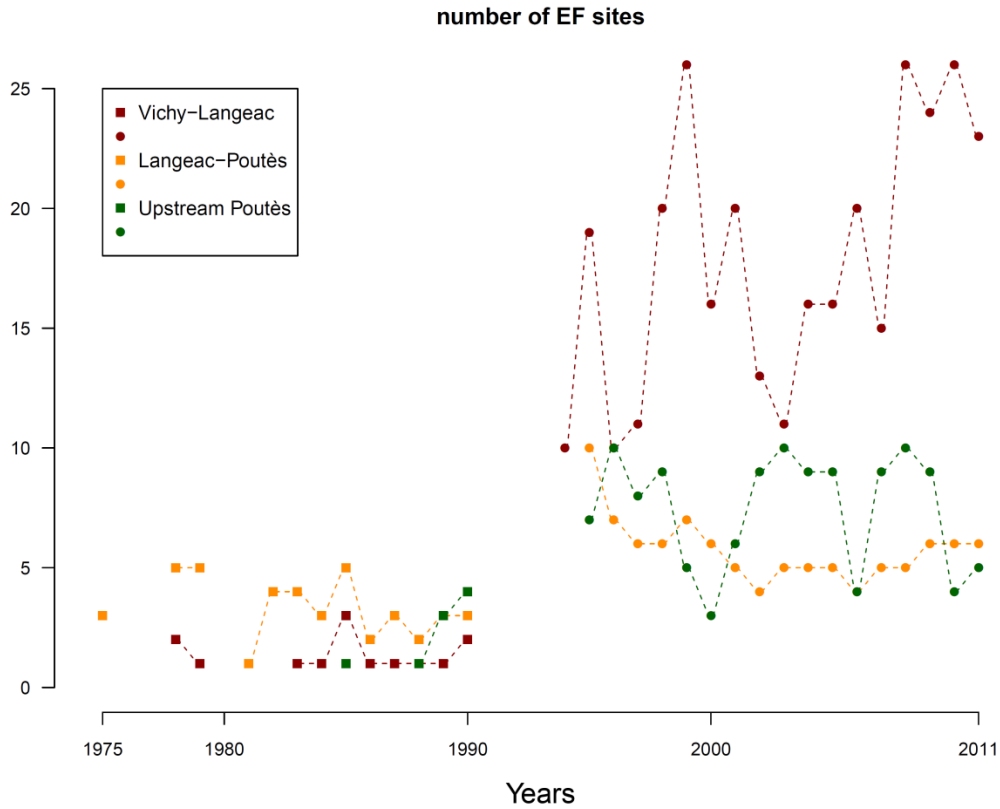


Figure 2.7: Number of sites electric fished in the three river section of the Allier catchment. Filled squares indicate years during which successive removal was used and filled dots indicate years during which 5 minutes sampling was used.

Figure 2.7: Nombre de sites de pêche électrique échantillonnés dans les 3 zones du bassin de l'Allier. Les carrés indiquent les années durant lesquelles les pêches par enlèvement successif sont utilisées et les cercles les années durant lesquelles les pêches 5 minutes sont utilisées.

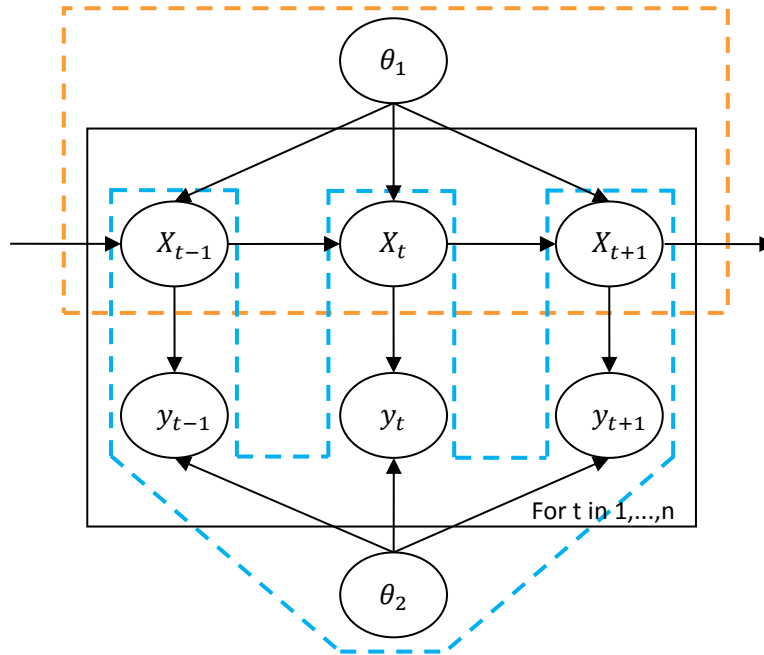


Figure 3.1: Graphical representation of a simple state-space model. The dashed orange frame represent the process model. The dashed blue frame represent the observation models. X_t is a vector of hidden states during year t . The transition from X_t to X_{t+1} is conditioned by the parameters θ_1 and forms the process equation. y_t is a vector of observations depending on one or several hidden states during year t . These observations are conditioned by θ_2 , the vector of parameters of the different observation models. The relation between X_t and y_t corresponds to the observation equation.

Figure 3.1: Représentation graphique d'un modèle d'états simple. Le cadre pointillé orange indique le modèle de processus. Le cadre bleu représente le modèle d'observation. X_t est le vecteur des états cachés pendant l'année t . La transition de X_t à X_{t+1} est conditionnée par les paramètres θ_1 et forme l'équation stochastique des processus. y_t est le vecteur des observations dépendante de un ou plusieurs états cachés pour une année donnée t . Ces observations sont conditionnées par θ_2 , le vecteur des paramètres des différents modèles d'observation. La relation entre X_t et y_t correspond à l'équation stochastique d'observation.

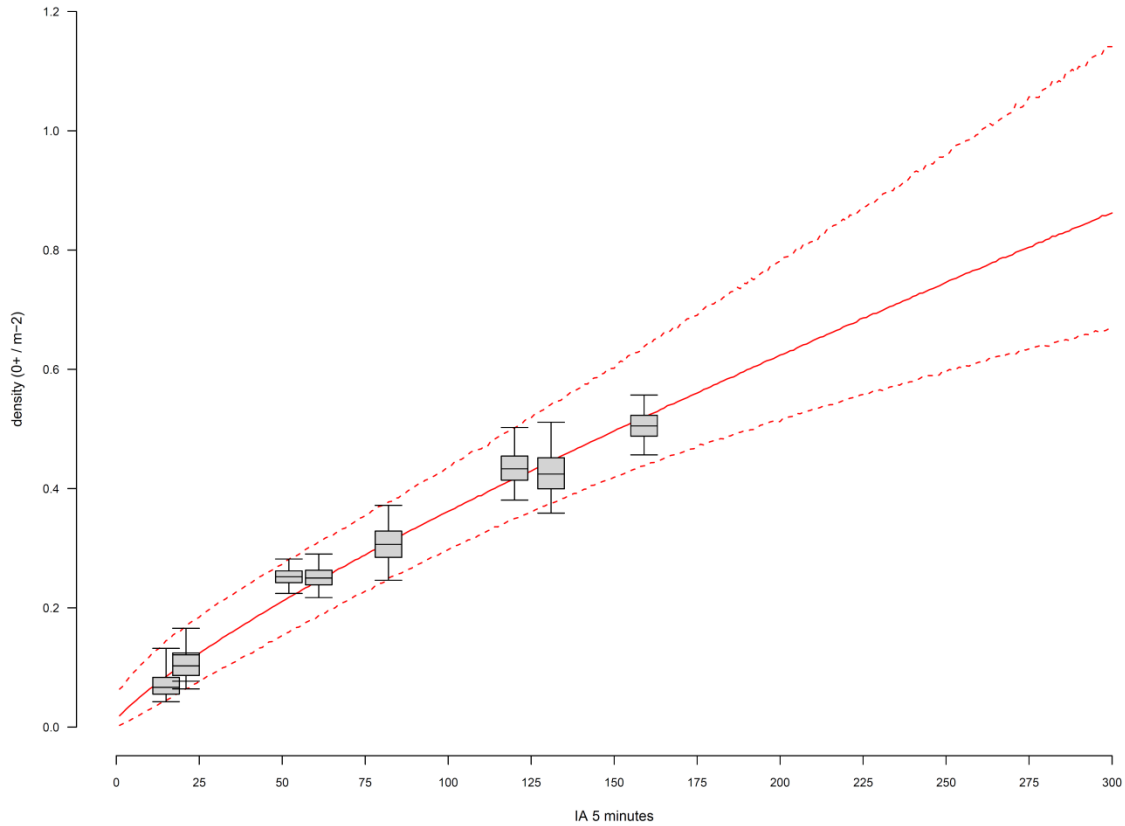


Figure 3.1: 0+ juveniles density estimates vs 5 minutes index of abundance for the 9 sites sampled with the two electric fishing techniques. Boxplots indicate 2.5th, 25th, median, 75th and 97.5th quantiles. The plain and dashed red lines indicate the 2.5th, median and 97.5th quantiles of predicted densities for 5 minutes index of abundance only ranging from 1 to 300.

Figure 3.1: Relation entre les indices d'abondances des pêches électriques 5 minutes et les densités de juvéniles 0+ pour 9 sites échantillonnés avec les deux types de méthodologies (enlèvements successifs et 5 minutes). Les boxplots indiquent les quantiles à 2.5th, 25th, médiane, 75th et 97.5th. Les lignes rouges pleines et pointillées indiquent la médiane et les quantiles à 2.5th et 97.5th des densités de juvéniles 0+ pour des valeurs d'indices d'abondance compris entre 1 et 300.

Adults returns at Vichy

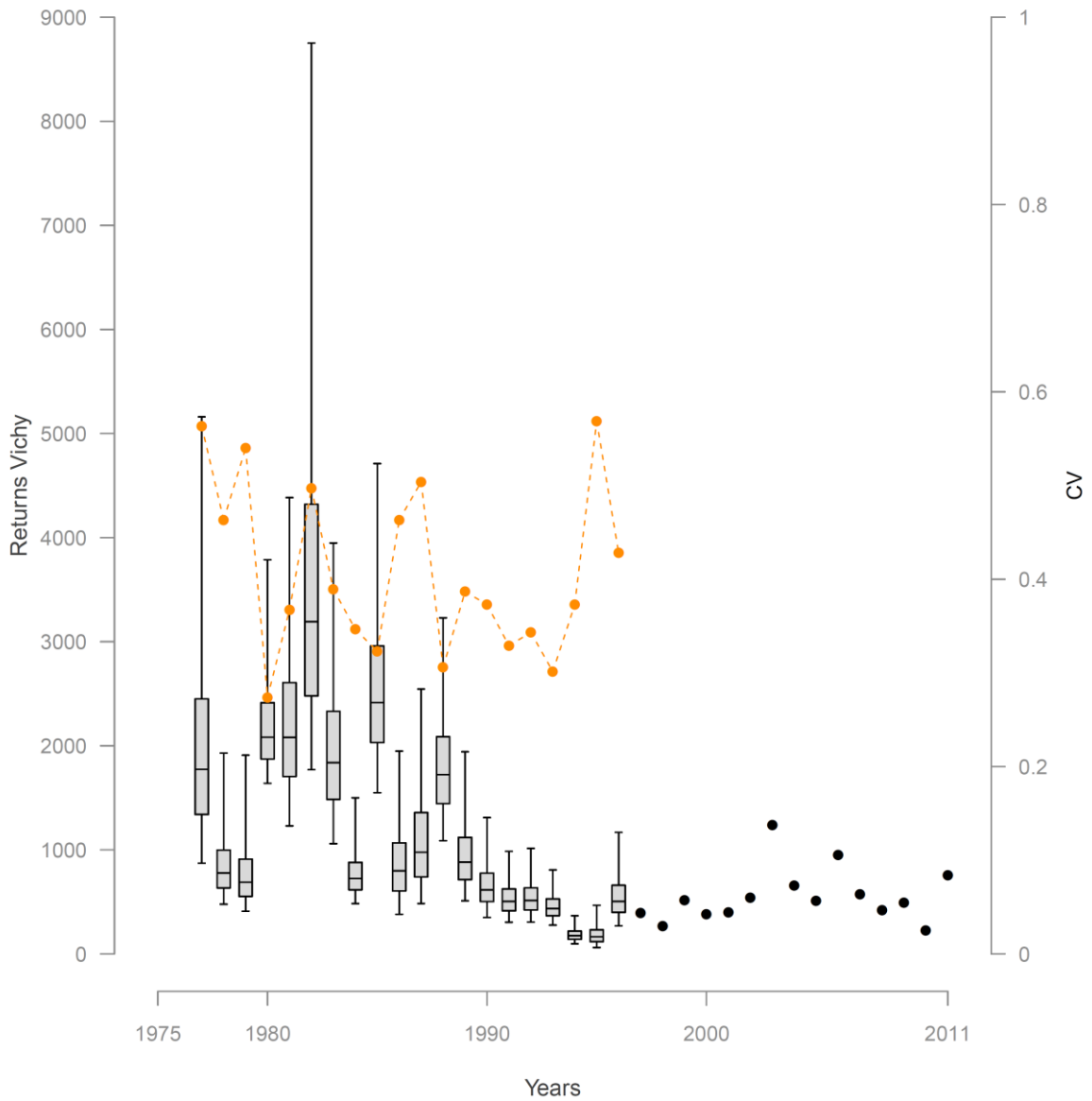


Figure 4.1: Posterior distributions of the annual adult returns at Vichy counting station. Boxplots indicate the median, 25th and 75th percentiles, whiskers indicate 2.5 and 97.5th percentiles. The plain dots indicate the years during which Vichy counting station was operational and adult returns are assumed to be known. The red dots corresponds to the coefficients of variation associated with the annual returns at Vichy

Figure 4.1: Distribution a posteriori des retours d'adultes a Vichy Les boxplots indiquent les quantiles à 2.5th, 25th, médiane, 75th et 97.5th. Les cercles pleins indiquent les années pour lesquelles la station de comptage à Vichy est opérationnelle et fournit le nombre de retours d'adultes. Les cercles orange représentent les coefficients de variation (CVs) associés aux estimations de retour d'adultes.

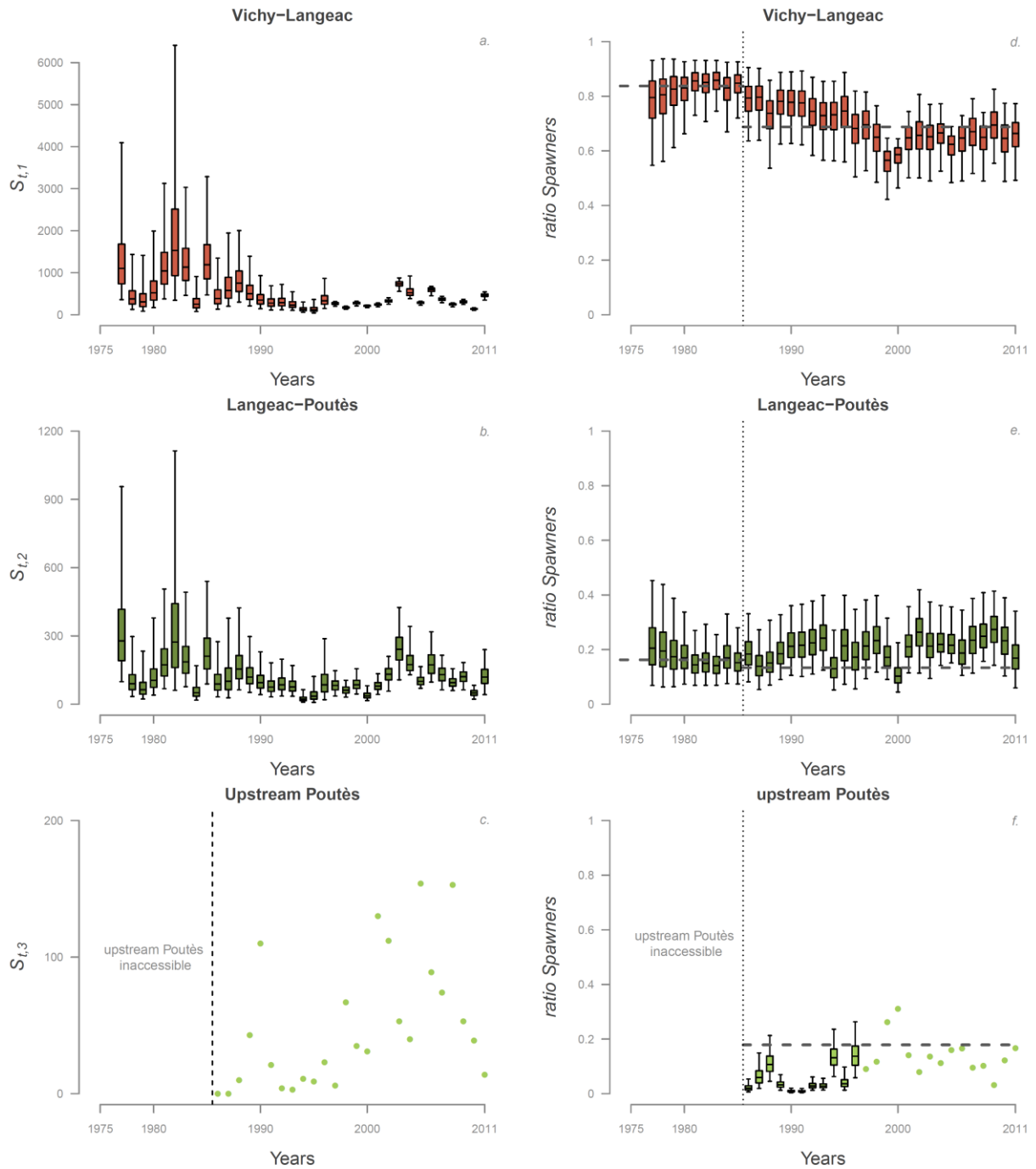


Figure 4.2: Posterior distributions of the annual absolute and relative potential spawners abundances in each river section of the Allier catchment: Vichy-Langeac (a and d), Langeac-Poutès (b and e) and upstream Poutès (c and f). Boxplots indicate the median, 25th and 75th percentiles, whiskers indicate 2.5 and 97.5th percentiles. Thick dashed grey lines d, e and f indicate relative availability of potential juvenile habitat. Note that for the river section upstream Poutès there are no estimates of absolute abundance since the exact number of potential spawners is known (c) and the relative abundance is known when Vichy counts are available (f).

Figure 4.2: Distribution a posteriori des abondances annuelles absolues et relatives de géniteurs potentiels dans chaque zones du bassin de l'Allier: Vichy-Langeac (a et d), Langeac-Poutès (b et e) et à l'amont de Poutès (c et f). Les boxplots indiquent les quantiles à 2.5th, 25th, médiane, 75th et 97.5th. Les lignes pointillées horizontales pour d, e et f indiquent la disponibilité relative de l'habitat potentiel pour les juvéniles. On notera que pour la zone à l'amont de Poutès il n'y a pas d'estimation des abondances absolues car le nombre exact de géniteurs potentiels est toujours connu (c) et l'abondance relative est connue lorsque les comptages à Vichy sont disponibles.

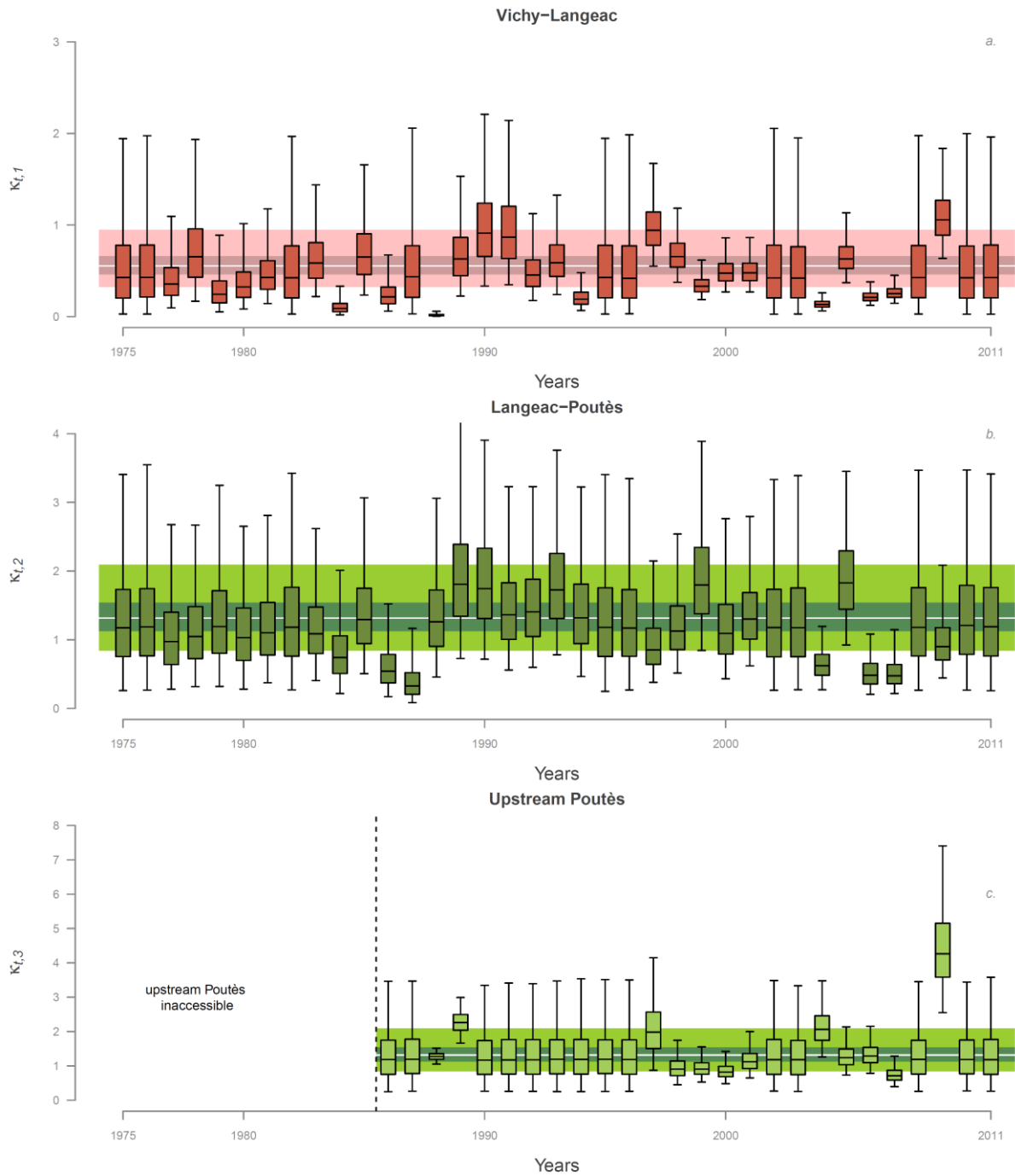


Figure 4.3: Posterior distribution of the annual potential spawner:red ratio for each section of the river Allier: a) Vichy-Langeac, b) Langeac-Poutès and c) upstream of Poutès. Boxplots indicate the median, 25th and 75th percentiles, whiskers indicate 2.5 and 97.5th percentiles. The coloured bands in the background represent the median, 2.5th, 25th, 75th and 97.5th percentiles of the hyper-parameters $\mu^{\kappa_{down}}$ (a) and $\mu^{\kappa_{up}}$ (b and c).

Figure 4.3: distribution a posteriori du ratio géniteurs potentiels:frayères pour chaque zone du bassin de l'Allier: a) Vichy-Langeac, b) Langeac-Poutès et c) à l'amont de Poutès. Les boxplots indiquent les quantiles à 2.5th, 25th, médiane, 75th et 97.5th. Les bandes colorées en arrière-plan représentent la médiane et les quantiles à 2.5th, 25th, 75th et 97.5th des hyper-paramètres $\mu^{K_{down}}$ (a) et $\mu^{K_{up}}$ (b and c).

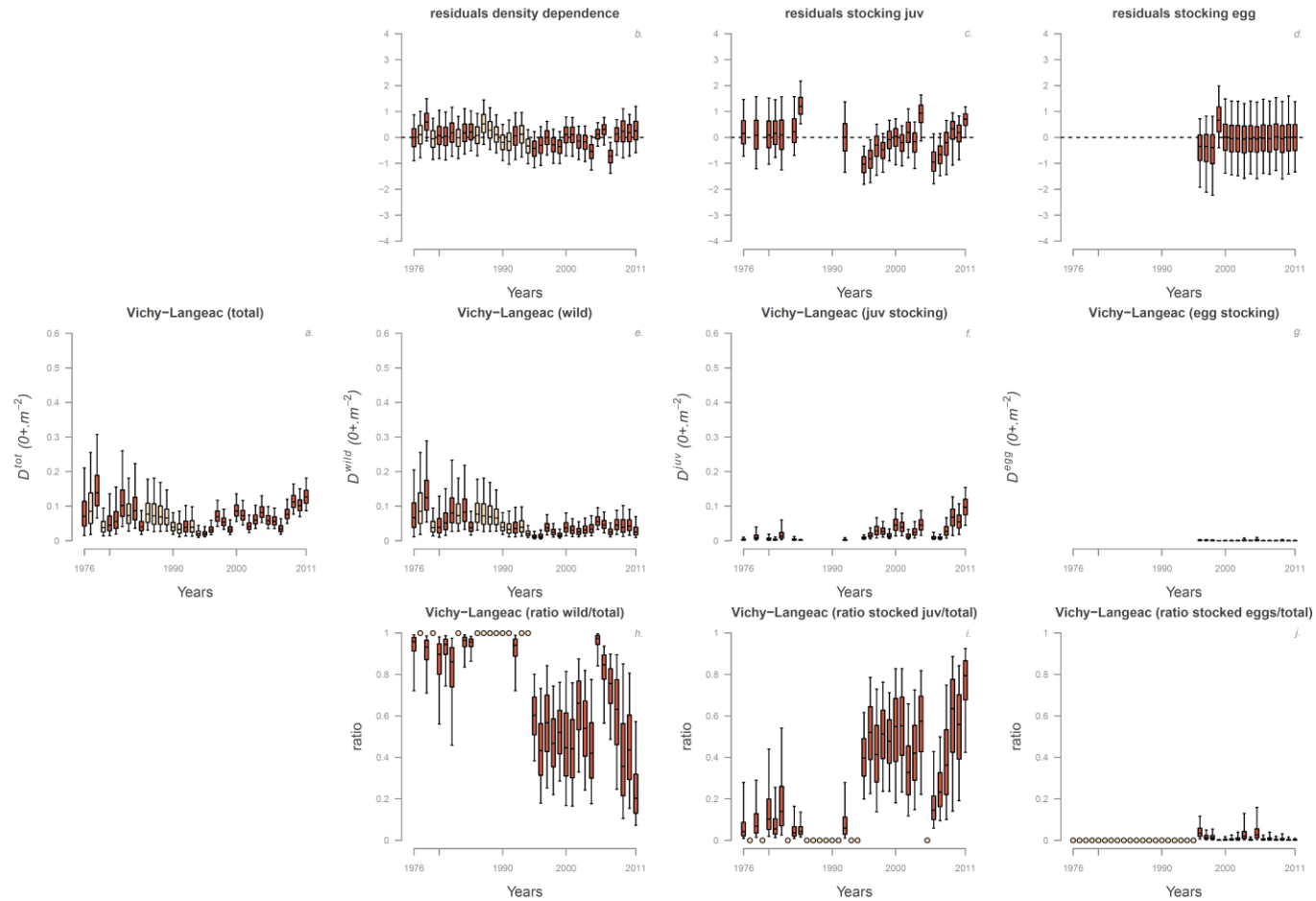


Figure 4.5: Posterior distributions of annual macro scale densities $D_{t+1,i}^{tot}$ (panel *a*) and its 3 components $D_{t+1,i}^{wild}$, $D_{t+1,i}^{juv}$ and $D_{t+1,i}^{egg}$ (panel *c*, *f* and *i*) in the Vichy-Langeac river section. Dark orange indicate years with stocking and light orange years with no stocking. Relative contributions of each components are indicated in panels *d*, *g* and *j*. (orange dots indicate years with no stocking event). Residuals of the different components are represented in panels *b*, *e* and *h*. Boxplots indicate 2.5th, 25th, median, 75th and 97.5th quantiles.

Figure 4.5: Distribution a posteriori des densités de juvéniles 0+ à l'échelle macroscopique $D_{t+1,i}^{tot}$ (panneau *a*) et ses 3 composantes : $D_{t+1,i}^{wild}$, $D_{t+1,i}^{juv}$ et $D_{t+1,i}^{egg}$ (panneau *c*, *f* et *i*) dans la zone Vichy-Langeac. Le remplissage orange foncé indique les années durant lesquelles il y a eu du repeuplement. La contribution relative de chaque composantes est indiquée dans les panneaux *d*, *g* et *j* (les cercles oranges indiquent les années sans repeuplement). Les résidus du modèle associés à chaque composantes sont indiqués dans les panneaux panels *b*, *e* and *h*. Les boxplots indiquent les quantiles à 2.5th, 25th, médiane, 75th et 97.5th.

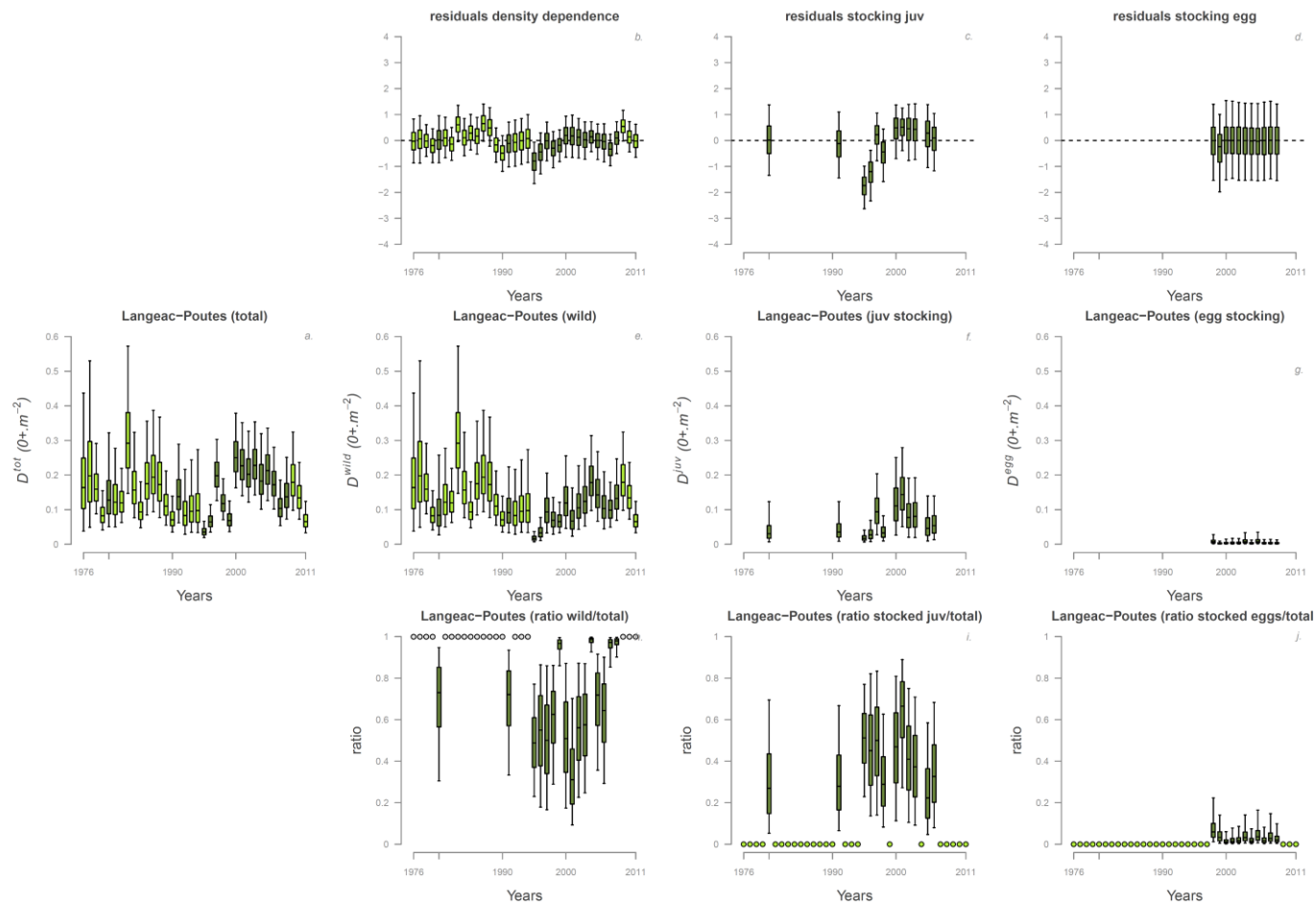


Figure 4.6: Posterior distributions of annual macro scale densities $D_{t+1,i}^{tot}$ (panel *a*) and its 3 components $D_{t+1,i}^{wild}$, $D_{t+1,i}^{juv}$ and $D_{t+1,i}^{egg}$ (panel *c*, *f* and *i*) in the Langeac-Poutès river section. Dark green indicate years with stocking and light green years with no stocking. Relative contributions of each component are indicated in panels *d*, *g* and *j*. (green dots indicate years with no stocking event). Residuals of the different components are represented in panels *b*, *e* and *h*. Boxplots indicate 2.5th, 25th, median, 75th and 97.5th quantiles.

Figure 4.6: Distribution a posteriori des densités de juvéniles 0+ à l'échelle macroscopique $D_{t+1,i}^{tot}$ (panneau *a*) et ses 3 composantes : $D_{t+1,i}^{wild}$, $D_{t+1,i}^{juv}$ et $D_{t+1,i}^{egg}$ (panneau *c, f* et *i*) dans la zone Langeac-Poutès. Le remplissage vert foncé indique les années durant lesquelles il y a eu du repeuplement. La contribution relative de chaque composantes est indiquée dans les panneaux *d, g* et *j* (les cercles verts indiquent les années sans repeuplement). Les résidus du modèle associés à chaque composantes sont indiqués dans les panneaux panels *b, e* and *h*. Les boxplots indiquent les quantiles à 2.5th, 25th, médiane, 75th et 97.5th.

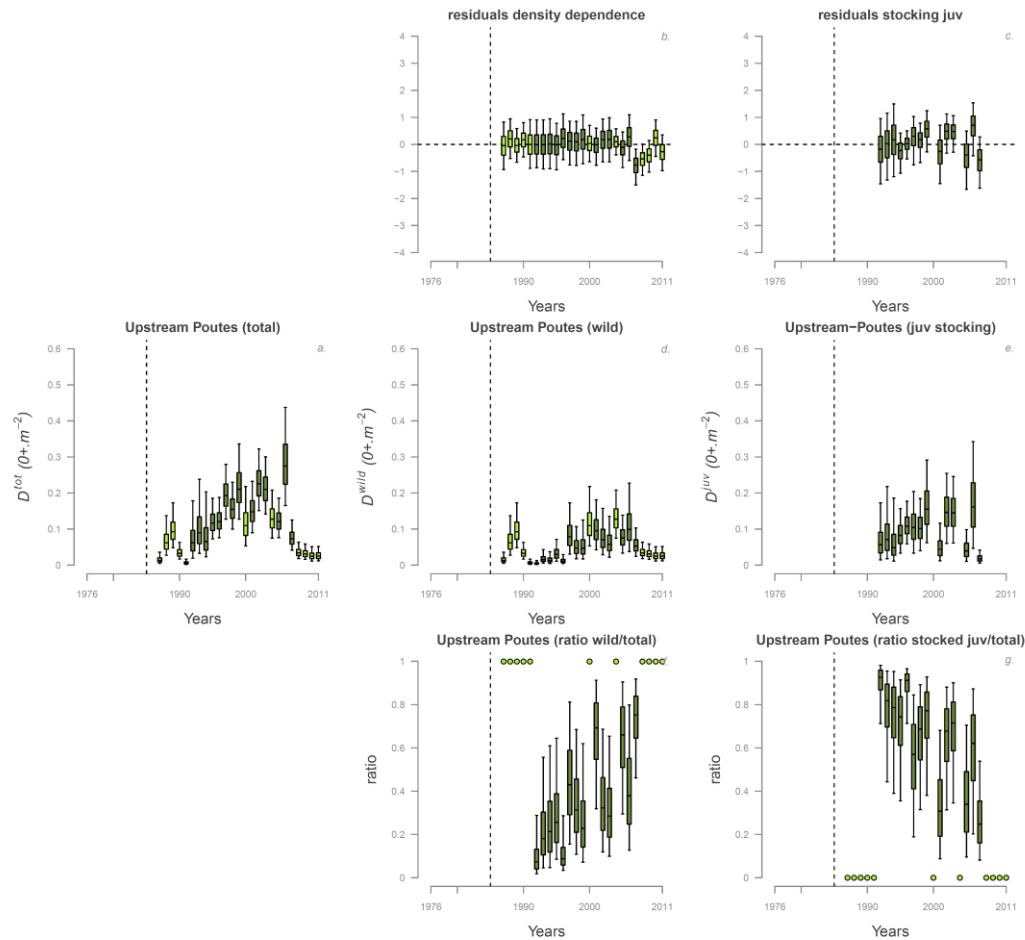


Figure 4.7: Posterior distributions of annual macro scale densities $D_{t+1,i}^{tot}$ (panel *a*) and its 2 components $D_{t+1,i}^{wild}$ and $D_{t+1,i}^{juv}$ (panel *c* and *f*) in the upstream of Poutès river section. Dark green indicate years with stocking and light green years with no stocking. Relative contributions of each components are indicated in panels *d* and *g*. (green dots indicate years with no stocking event). Residuals of the different components are represented in panels *b* and *e*. Boxplots indicate 2.5th, 25th, median, 75th and 97.5th quantiles.

Figure 4.7: Distribution a posteriori des densités de juvéniles 0+ à l'échelle macroscopique $D_{t+1,i}^{tot}$ (panneau *a*) et ses 2 composantes : $D_{t+1,i}^{wild}$, $D_{t+1,i}^{juv}$ (panneau *c*, *f*) dans la zone à l'amont de Poutès. Le remplissage vert foncé indique les années durant lesquelles il y a eu du repeuplement. La contribution relative de chaque composantes est indiquée dans les panneaux *d*, *g* (les cercles verts indiquent les années sans repeuplement). Les résidus du modèle associés à chaque composantes sont indiqués dans les panneaux panels *b*, *e*. Les boxplots indiquent les quantiles à 2.5th, 25th, médiane, 75th et 97.5th.

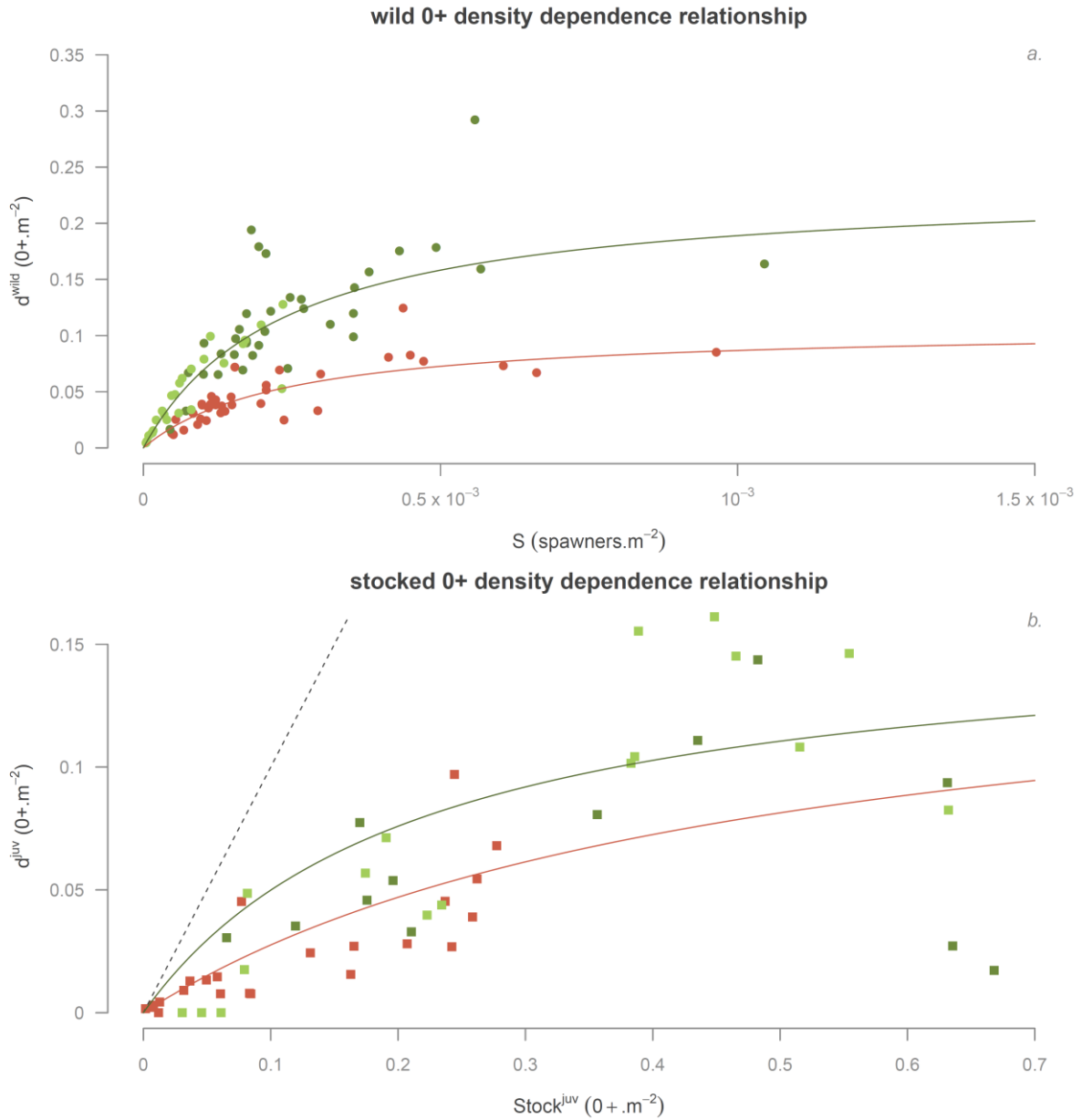


Figure 4.8: Average density dependence relationships between a) the potential spawners density of a given year t and the wild 0+ juvenile density the following year $t+1$ and between b) the number of 0+ juvenile stocked and the stocked 0+ juvenile density. Spatial differences downstream and upstream of Langeac are represented by two colored curves (orange downstream of Langeac and green upstream of Langeac). Plain colored dots and squares correspond to annual “data” for the three river sections: orange for Vichy-Langeac, dark green for Langeac-Poutès and light green for upstream of Poutès. The dashed line in panel b is the identity function.

Figure 4.8: Relation de densité dépendance moyenne entre a) les géniteurs potentiels d'une année donnée t et la densité de juvéniles 0+ sauvage l'année suivante $t+1$ et entre b) le nombre de juvéniles 0+ déversés au printemps et la densité de juvéniles issu du repeuplement à l'automne. Les différences spatiales a l'aval et l'amont de Langeac sont représentées par deux courbes de couleurs différentes (orange pour l'aval, vert pour l'amont). Les cercles et les carrés colorés représentent les « données » pour chaque zones du bassin de l'Allier : orange pour la zone Vichy-Langeac, vert foncé pour la zone Langeac-Poutès et vert clair pour la zone a l'amont de Poutès. La ligne pointillée dans le panneau b représente la fonction identité.

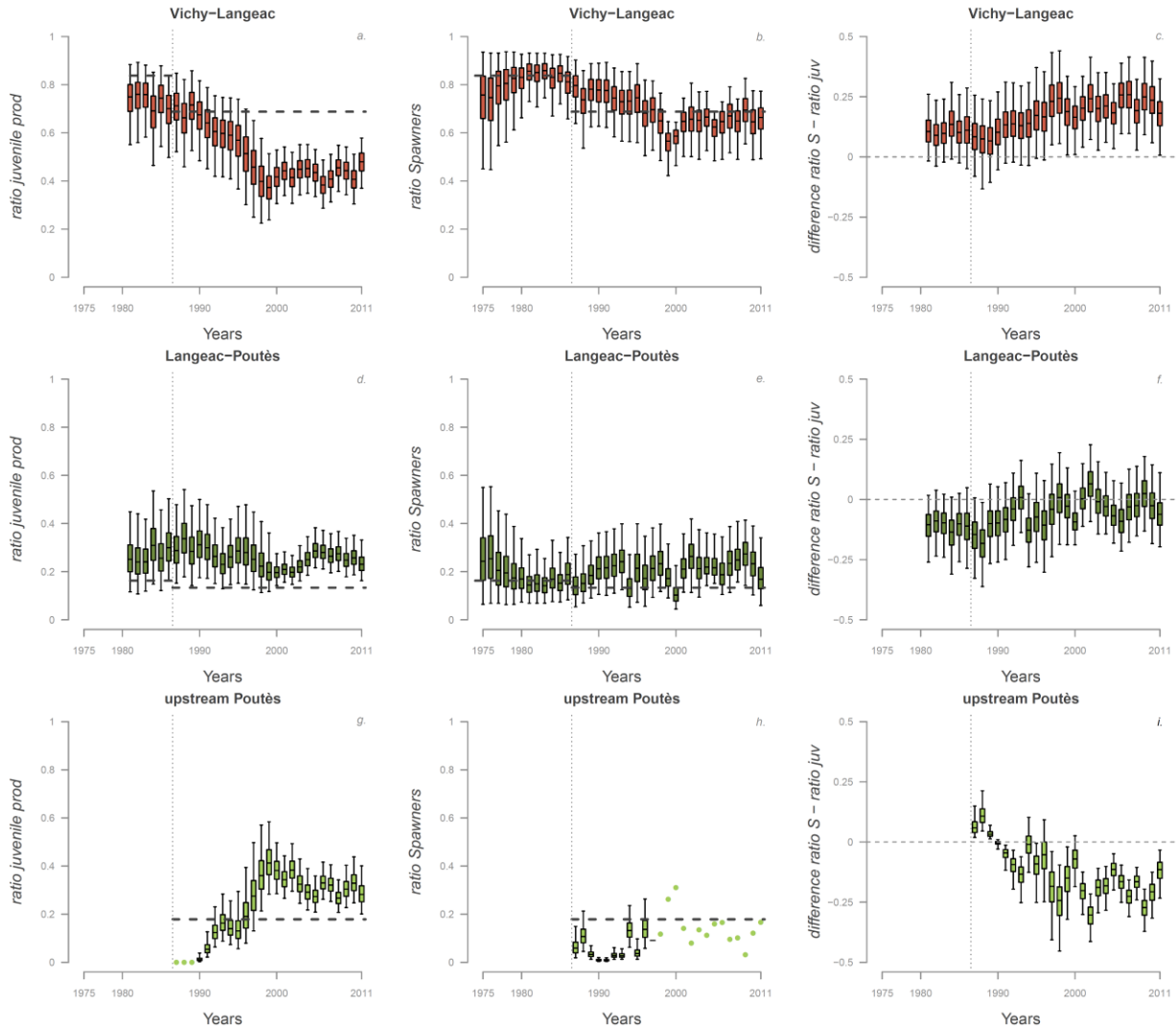


Figure 4.9: Posterior distributions of the relative juvenile production for a given year ($J_{t,i}^{coh}$) for each river section (panels a, d and g), posterior distribution of the relative potential spawner abundances (panels b, e and h) and posterior distributions of the difference between the potential spawners and the juvenile production contribution (panels c, f and i). In panels a, b, d, e, g and h, the thick dashed lines indicate relative availability of potential juvenile habitat. Boxplots indicate 2.5th, 25th, median, 75th and 97.5th quantiles

Figure 4.9: Distribution a posteriori de la production relative de juvéniles 0+ pour une année donnée ($J_{t,i}^{coh}$) pour chaque zone du bassin de l'Allier (panneaux a, d et g), distribution a posteriori des abondances relatives de géniteurs potentiels (panneaux b, e et h) et distribution a posteriori de la différence entre les abondances relatives de géniteurs potentiels et de production de juvéniles 0+ (panneaux c, f et i). Dans les panneaux a, b, d, e, g et h les lignes pointillées horizontale indiquent la disponibilité relative de l'habitat potentiel pour les juvéniles. Les boxplots indiquent les quantiles à 2.5th, 25th, médiane, 75th et 97.5th.

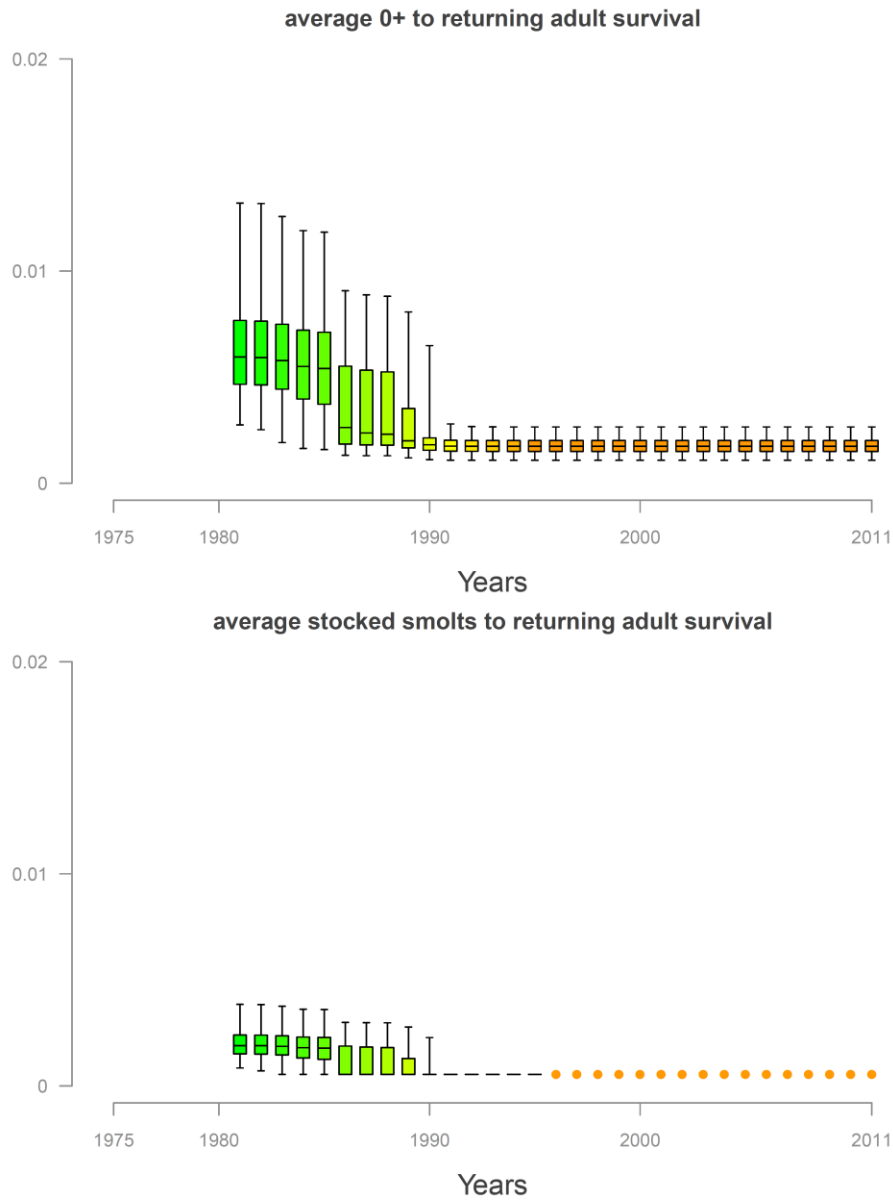


Figure 4.10: Evolution of a) 0+ juvenile to adult return rate μ^{s-J} and b) stocked smolt to adult return rate μ^{s-Sm} . The dots indicate the fixed average stocked smolt to adult return rate obtained from the marked adults returns ($\mu^{s-Sm} = 5.45 \times 10^{-4}$).

Figure 4.10: Evolution a) du taux de retour du juvénile 0+ à l'adulte μ^{s-J} et b) du taux de retour du smolt issu du repeuplement à l'adulte μ^{s-Sm} . Les points indiquent la survie moyenne du smolt issu du repeuplement à l'adulte fixée à partir des données de marquage ($\mu^{s-Sm} = 5.45 \times 10^{-4}$).

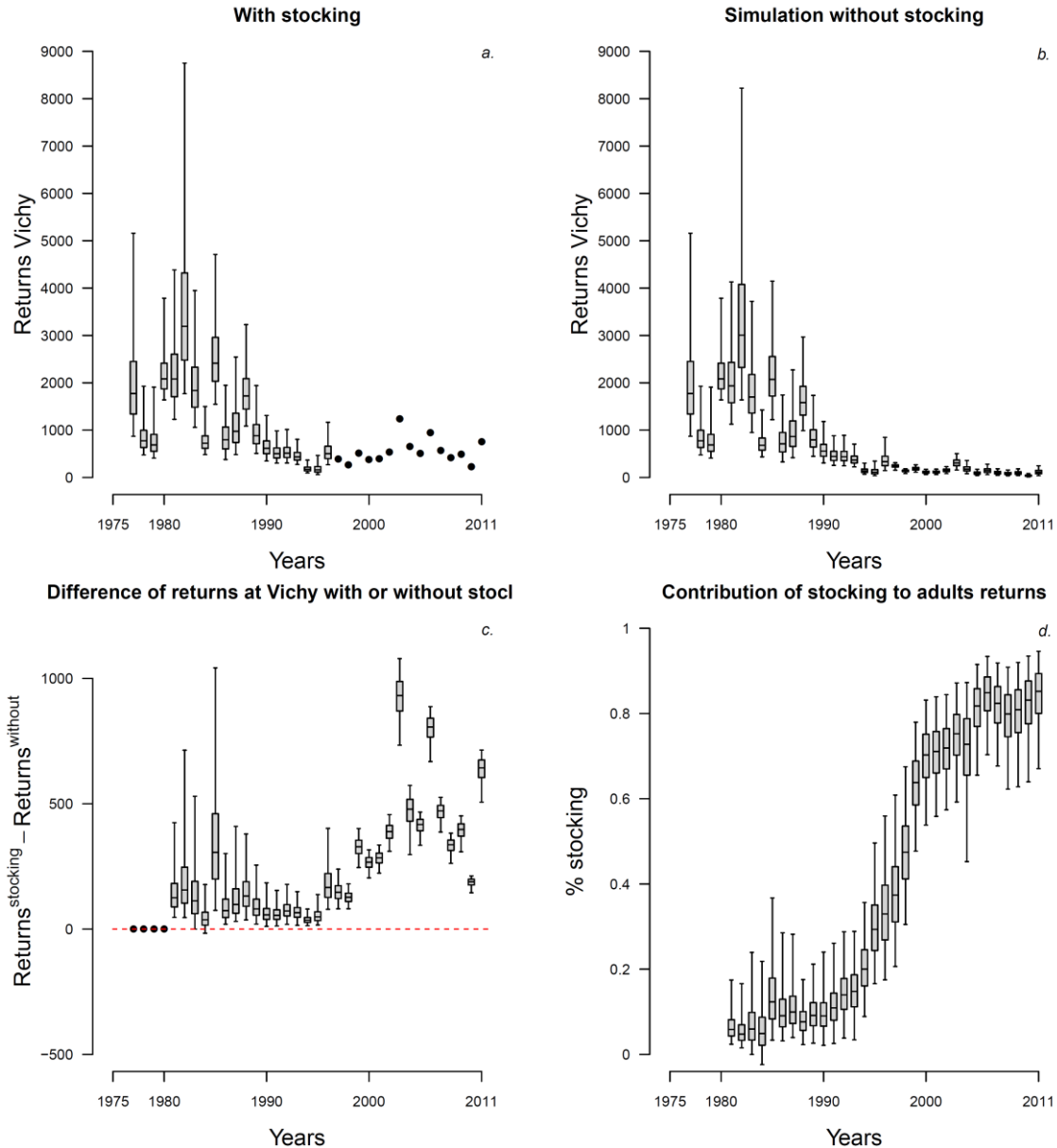


Figure 4.11: a) Posterior distributions of the annual adult returns at Vichy counting station. b) Posterior distributions of the simulated annual adult returns at Vichy counting station when removing stocking. c) Annual differences between the adult returns at Vichy with stocking and without stocking. d) Contribution of stocking to the adult returns at Vichy. Boxplots indicate the median, 25th and 75th percentiles, whiskers indicate 2.5 and 97.5th percentiles).

Figure 4.11: a) Distributions a posteriori des retours d'adultes à Vichy. b) Distributions a posteriori des retours d'adultes à Vichy simulés si il n'y avait pas eu de repeuplement. c) Différences annuelles entre les retours d'adultes avec ou sans repeuplement. d) Contribution du repeuplement aux retours d'adultes à Vichy. Les boxplots indiquent les quantiles à 2.5th, 25th, médiane, 75th et 97.5th.

Adults returns at Vichy and 20 years projection without stocking

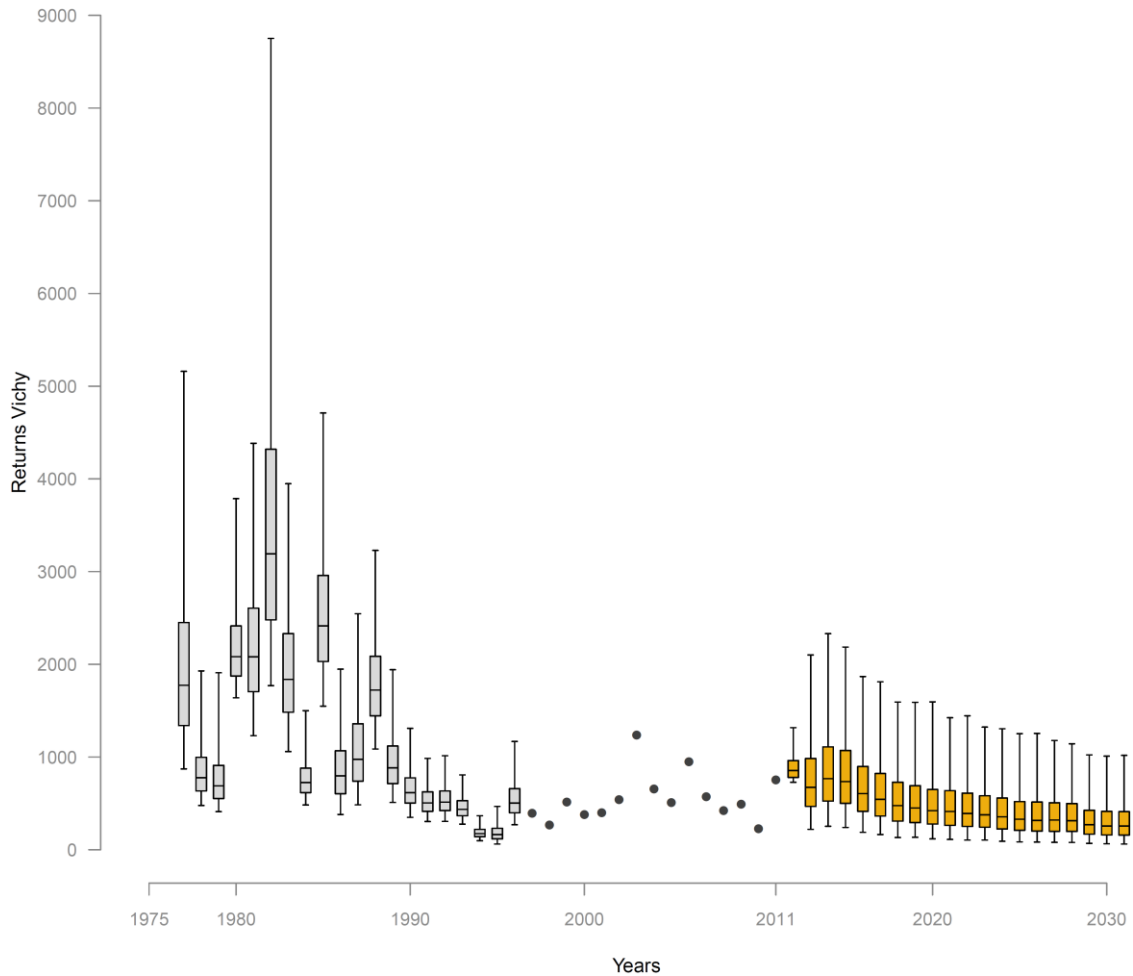


Figure 4.12: Posterior distributions of the annual adult returns at Vichy counting station. Boxplots indicate the median, 25th and 75th percentiles, whiskers indicate 2.5 and 97.5th percentiles. The plain dots indicate the years during which Vichy counting station was operational and adult returns are assumed to be known. The orange boxplot indicate the 20 years forecast under scenario 1 assumptions.

Figure 4.12: Distributions a posteriori des retours d'adultes à Vichy. Les boxplots indiquent les quantiles à 2.5th, 25th, médiane, 75th et 97.5th. Les cercles pleins indiquent les années pour lesquelles la station de comptage à Vichy est opérationnelle et fournit le nombre de retours d'adultes. Les boxplots orange correspondent aux estimations des retours d'adultes à Vichy pour les 20 prochaines années dans le cadre du scénario 1.

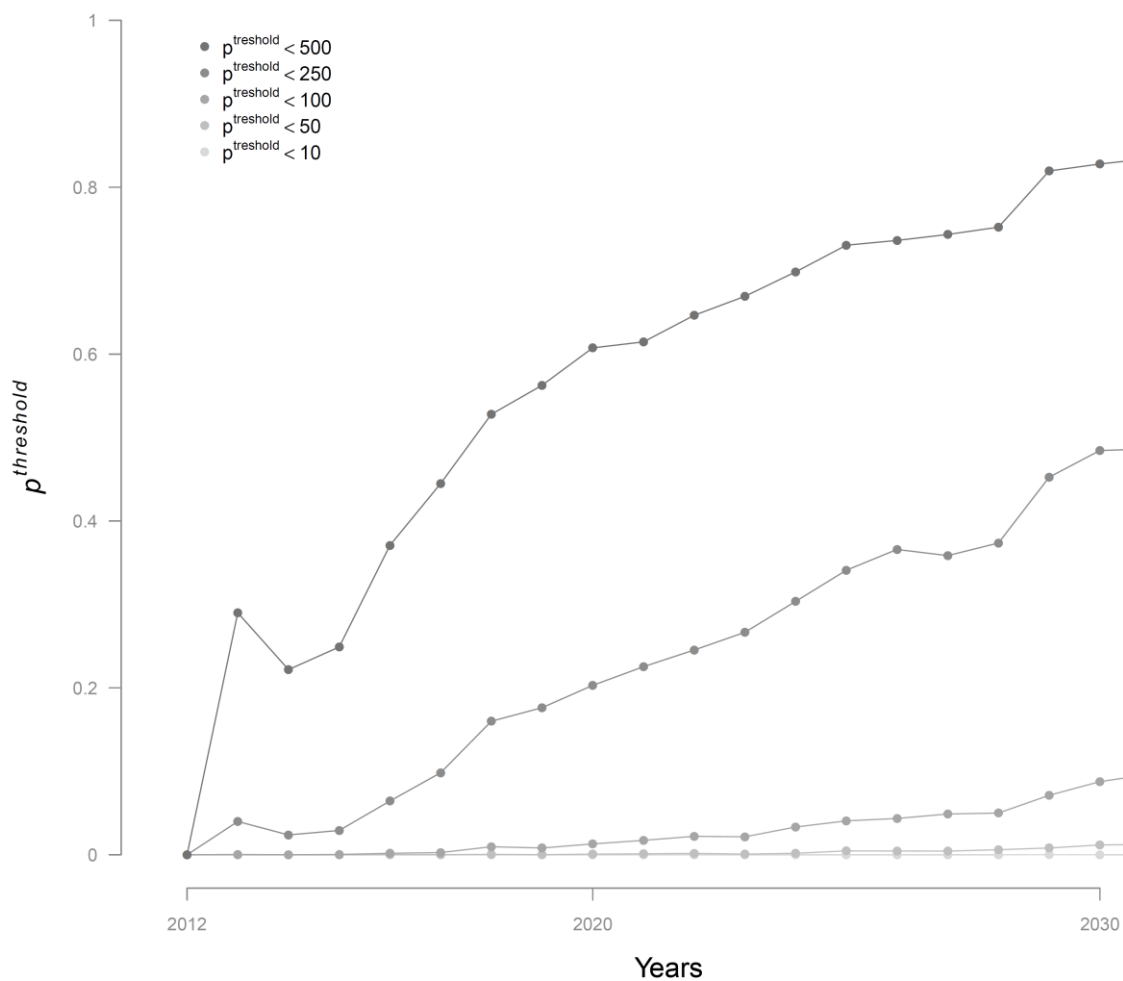


Figure 4.13: Evolution of the probabilities $p^{threshold}$ of reaching arbitrary threshold number of returning adults during the projection period (2012 to 2031) under scenario 1 assumptions.

Figure 4.13: Evolution de la probabilité $p^{threshold}$ d'atteindre certains seuils arbitraires du nombre de retours d'adultes à Vichy pendant la période 2012 à 2031 dans le cadre du scenario 1.

20 years projection – improvement of migration transparency at Langeac

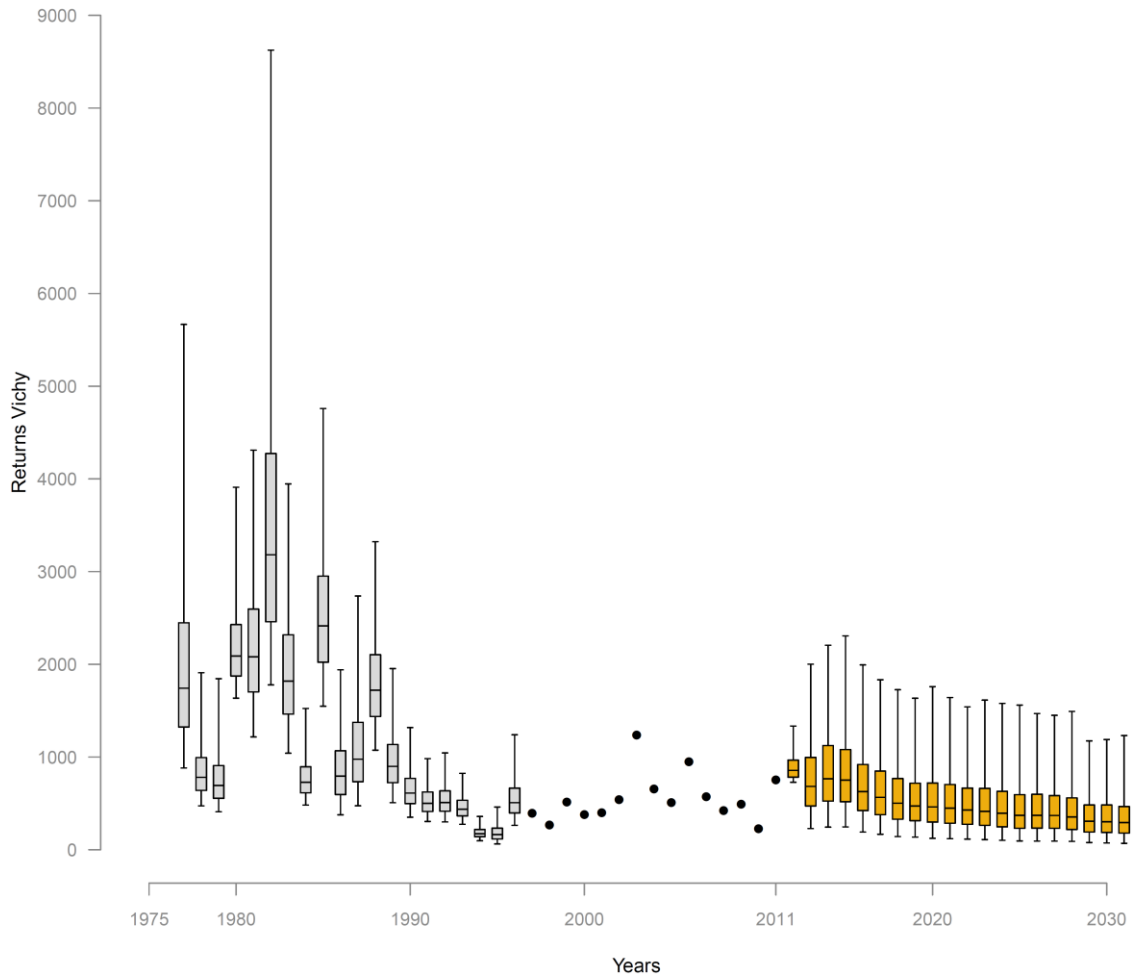


Figure 4.14: Posterior distributions of the annual adult returns at Vichy counting station. Boxplots indicate the median, 25th and 75th percentiles, whiskers indicate 2.5 and 97.5th percentiles. The plain dots indicate the years during which Vichy counting station was operational and adult returns are assumed to be known. The orange boxplot indicate the 20 years forecast under scenario 2 assumptions.

Figure 4.14: Distributions a posteriori des retours d’adultes à Vichy. Les boxplots indiquent les quantiles à 2.5th, 25th, médiane, 75th et 97.5th. Les cercles pleins indiquent les années pour lesquelles la station de comptage à Vichy est opérationnelle et fournit le nombre de retours d’adultes. Les boxplots orange correspondent aux estimations des retours d’adultes à Vichy pour les 20 prochaines années dans le cadre du scenario 2.

20 years projection – improvement of migration transparency at Langeac

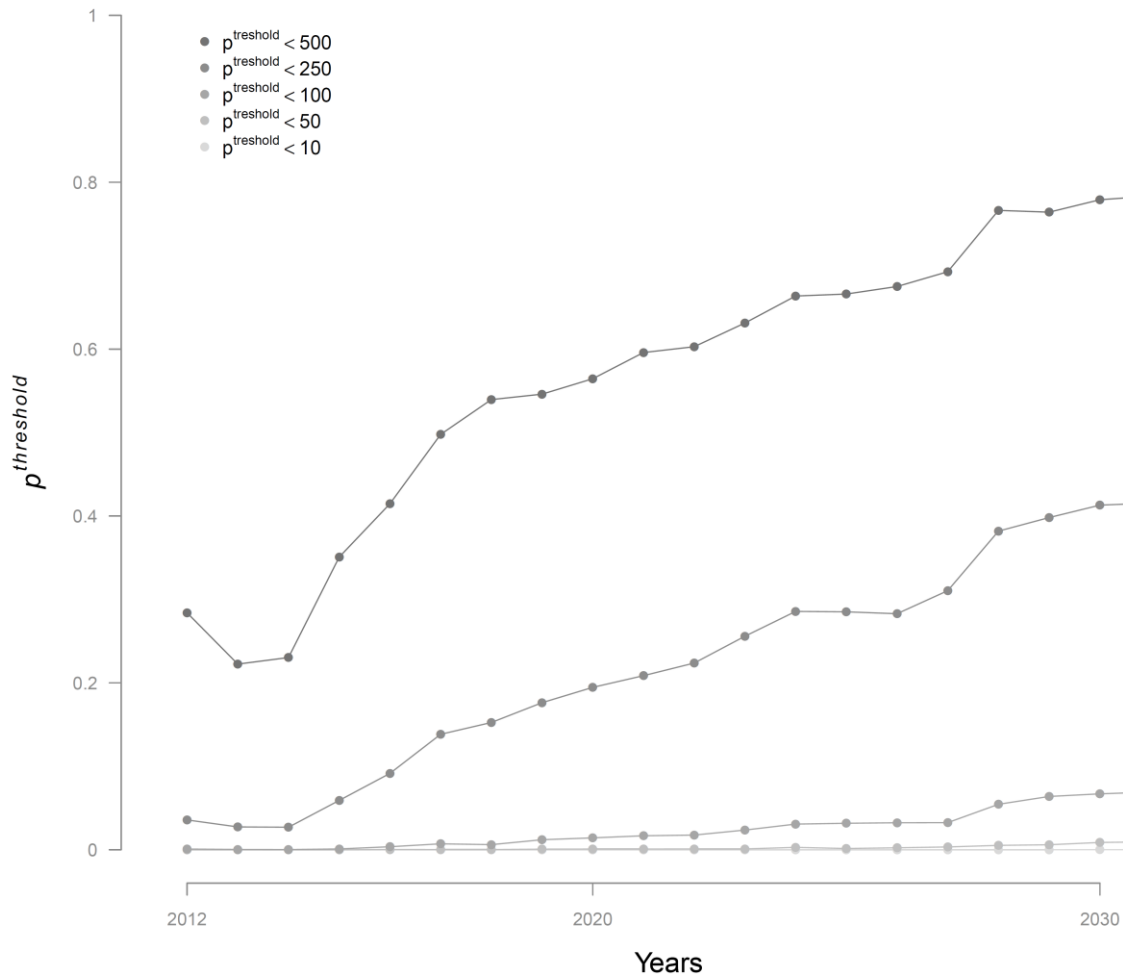


Figure 4.15: Evolution of the probabilities $p^{threshold}$ of reaching arbitrary threshold number of returning adults during the projection period (2012 to 2031) under scenario 2 assumptions.

Figure 4.15: Evolution de la probabilité $p^{threshold}$ d'atteindre certains seuils arbitraires du nombre de retours d'adultes à Vichy pendant la période 2012 à 2031 dans le cadre du scenario 2.

20 years projection – improvement of migration transparency at Poutes

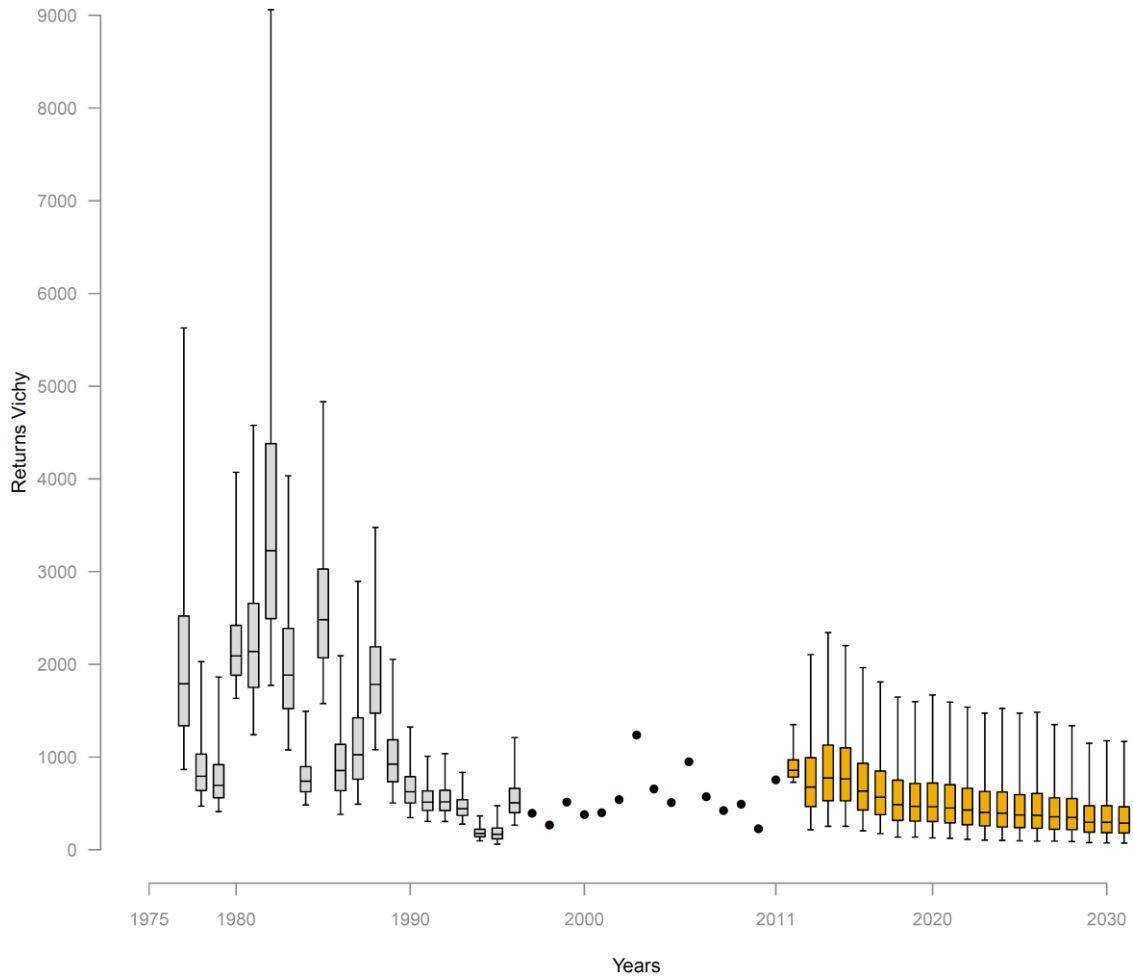


Figure 4.16: Posterior distributions of the annual adult returns at Vichy counting station. Boxplots indicate the median, 25th and 75th percentiles, whiskers indicate 2.5 and 97.5th percentiles. The plain dots indicate the years during which Vichy counting station was operational and adult returns are assumed to be known. The orange boxplot indicate the 20 years forecast under scenario 3 assumptions.

Figure 4.16: Distributions a posteriori des retours d’adultes à Vichy. Les boxplots indiquent les quantiles à 2.5th, 25th, médiane, 75th et 97.5th. Les cercles pleins indiquent les années pour lesquelles la station de comptage à Vichy est opérationnelle et fournit le nombre de retours d’adultes. Les boxplots orange correspondent aux estimations des retours d’adultes à Vichy pour les 20 prochaines années dans le cadre du scenario 3.

20 years projection – improvement of migration transparency at Poutesi

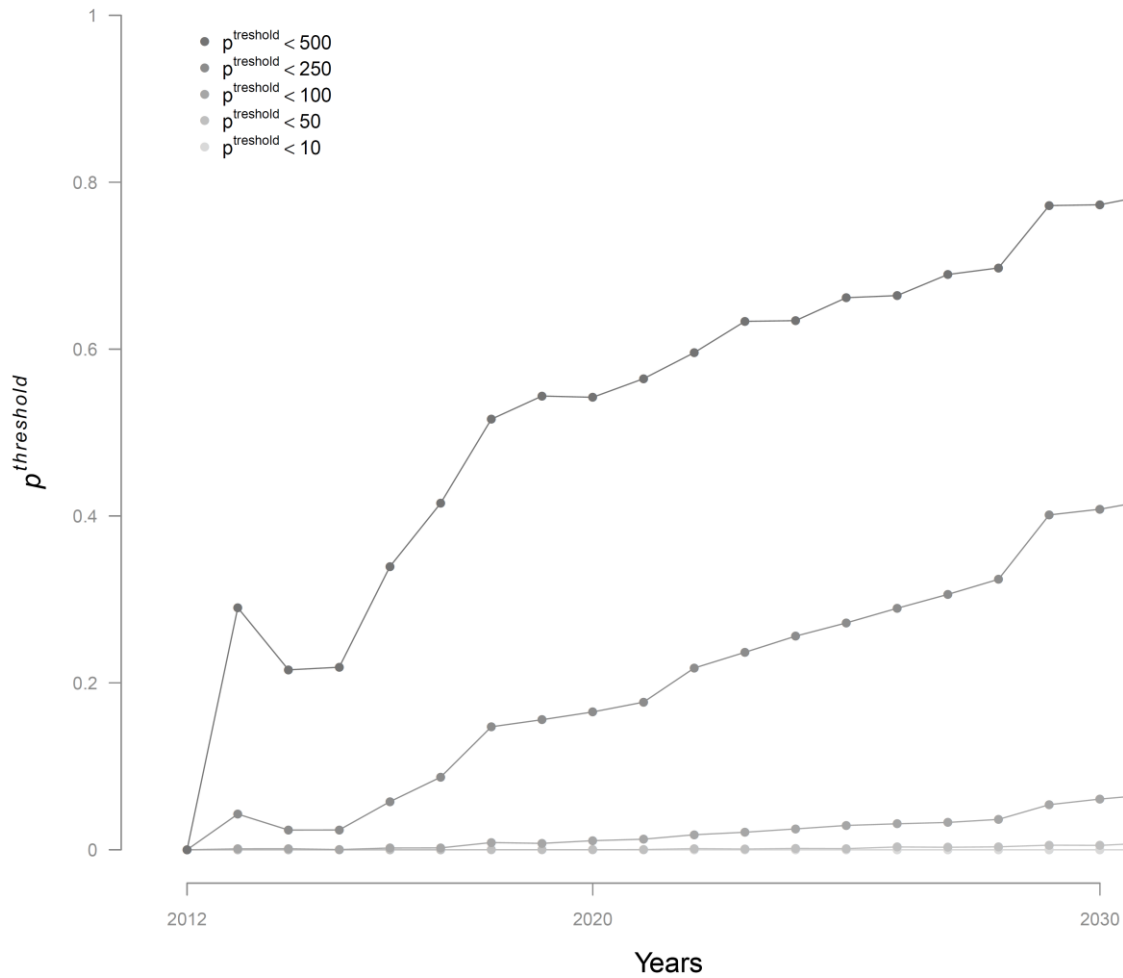


Figure 4.17: Evolution of the probabilities $p^{threshold}$ of reaching arbitrary threshold number of returning adults during the projection period (2012 to 2031) under scenario 3 assumptions.

Figure 4.17: Evolution de la probabilité $p^{threshold}$ d'atteindre certains seuils arbitraires du nombre de retours d'adultes à Vichy pendant la période 2012 à 2031 dans le cadre du scénario 3.

20 years projection – improvement of migration transparency at Langeac and Poutes

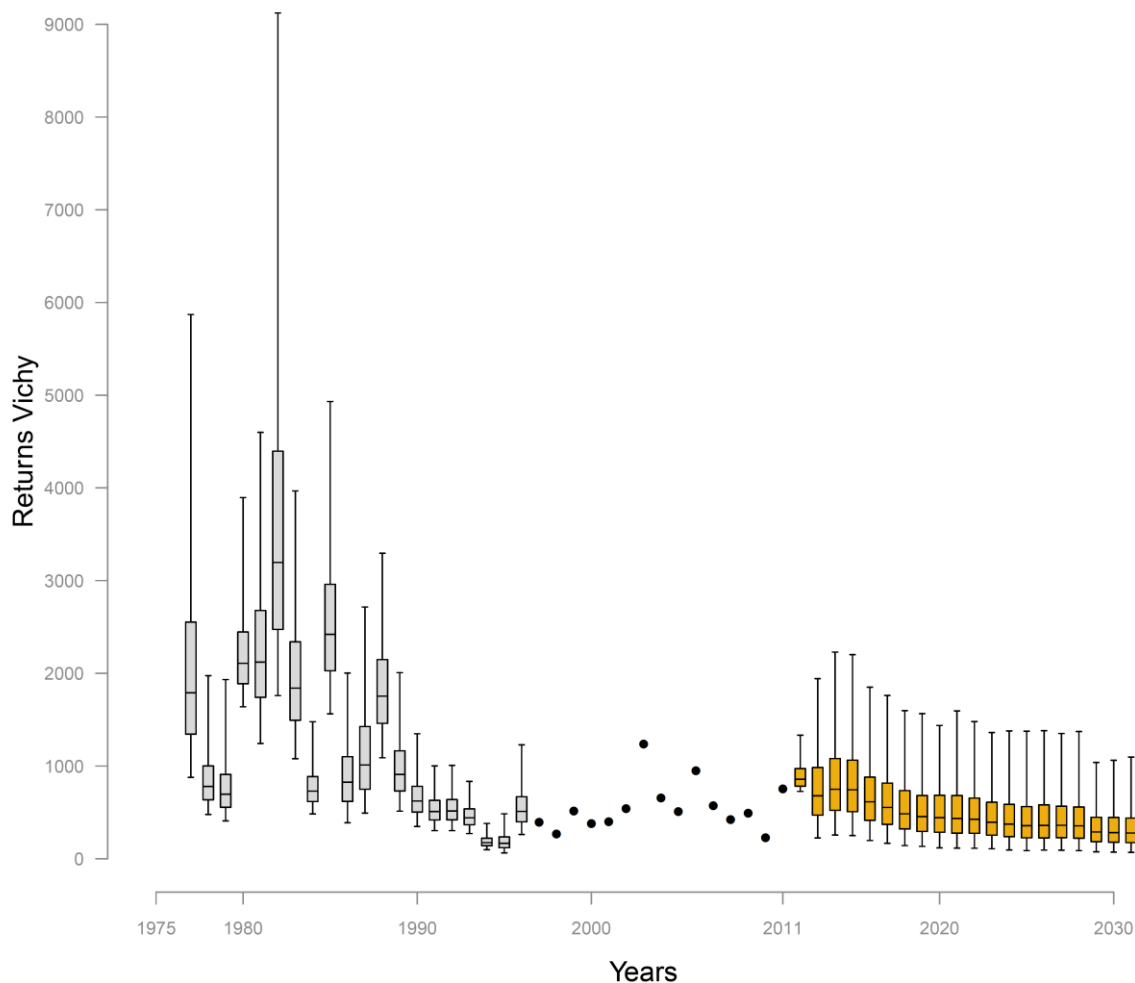


Figure 4.18: Posterior distributions of the annual adult returns at Vichy counting station. Boxplots indicate the median, 25th and 75th percentiles, whiskers indicate 2.5 and 97.5th percentiles. The plain dots indicate the years during which Vichy counting station was operational and adult returns are assumed to be known. The orange boxplot indicate the 20 years forecast under scenario 4 assumptions.

Figure 4.18: Distributions a posteriori des retours d'adultes à Vichy. Les boxplots indiquent les quantiles à 2.5th, 25th, médiane, 75th et 97.5th. Les cercles pleins indiquent les années pour lesquelles la station de comptage à Vichy est opérationnelle et fournit le nombre de retours d'adultes. Les boxplots orange correspondent aux estimations des retours d'adultes à Vichy pour les 20 prochaines années dans le cadre du scénario 4.

20 years projection – improvement of migration transparency at Langeac and Poutes

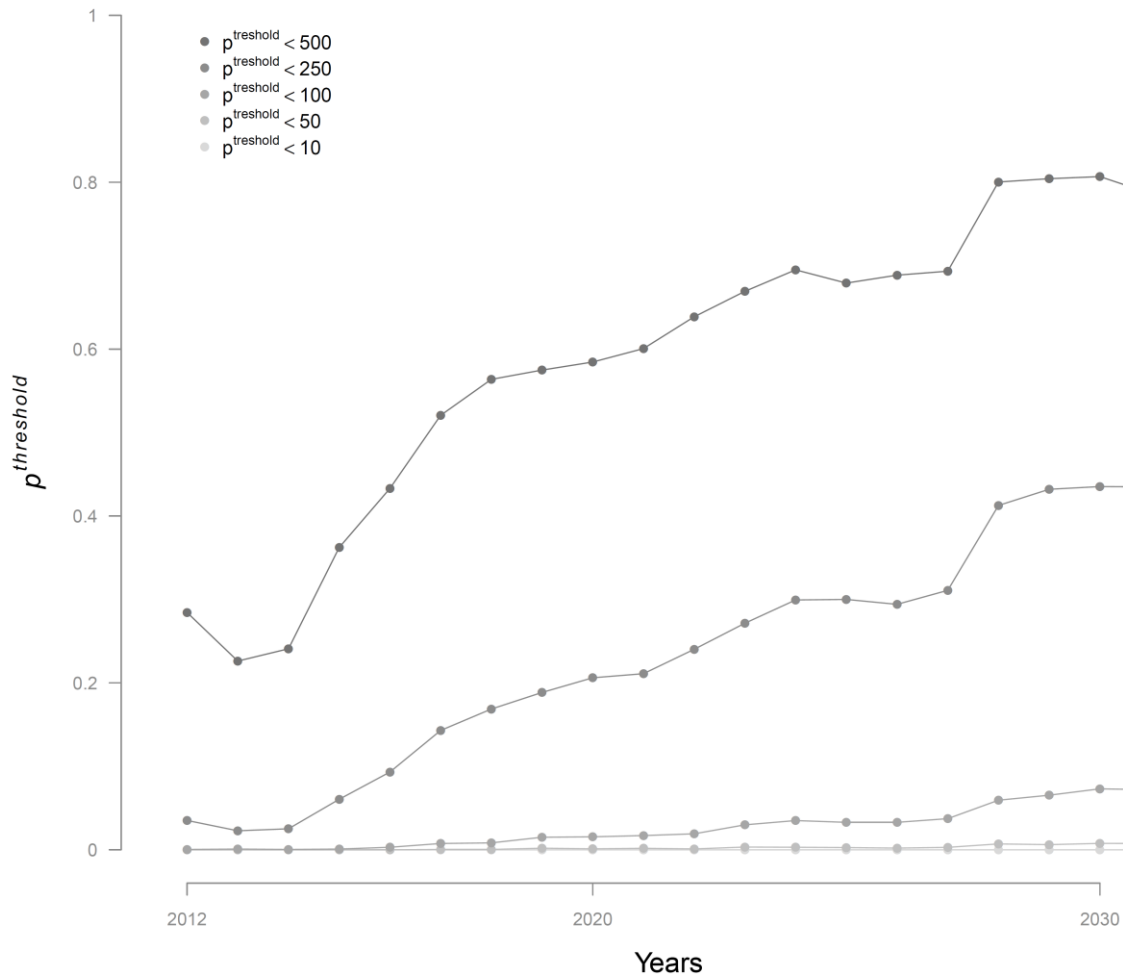


Figure 4.19: Evolution of the probabilities $p^{threshold}$ of reaching arbitrary threshold number of returning adults during the projection period (2012 to 2031) under scenario 4 assumptions.

Figure 4.19: Evolution de la probabilité $p^{threshold}$ d'atteindre certains seuils arbitraires du nombre de retours d'adultes à Vichy pendant la période 2012 à 2031 dans le cadre du scenario 4.

20 years projection – improvement 50% old level survival

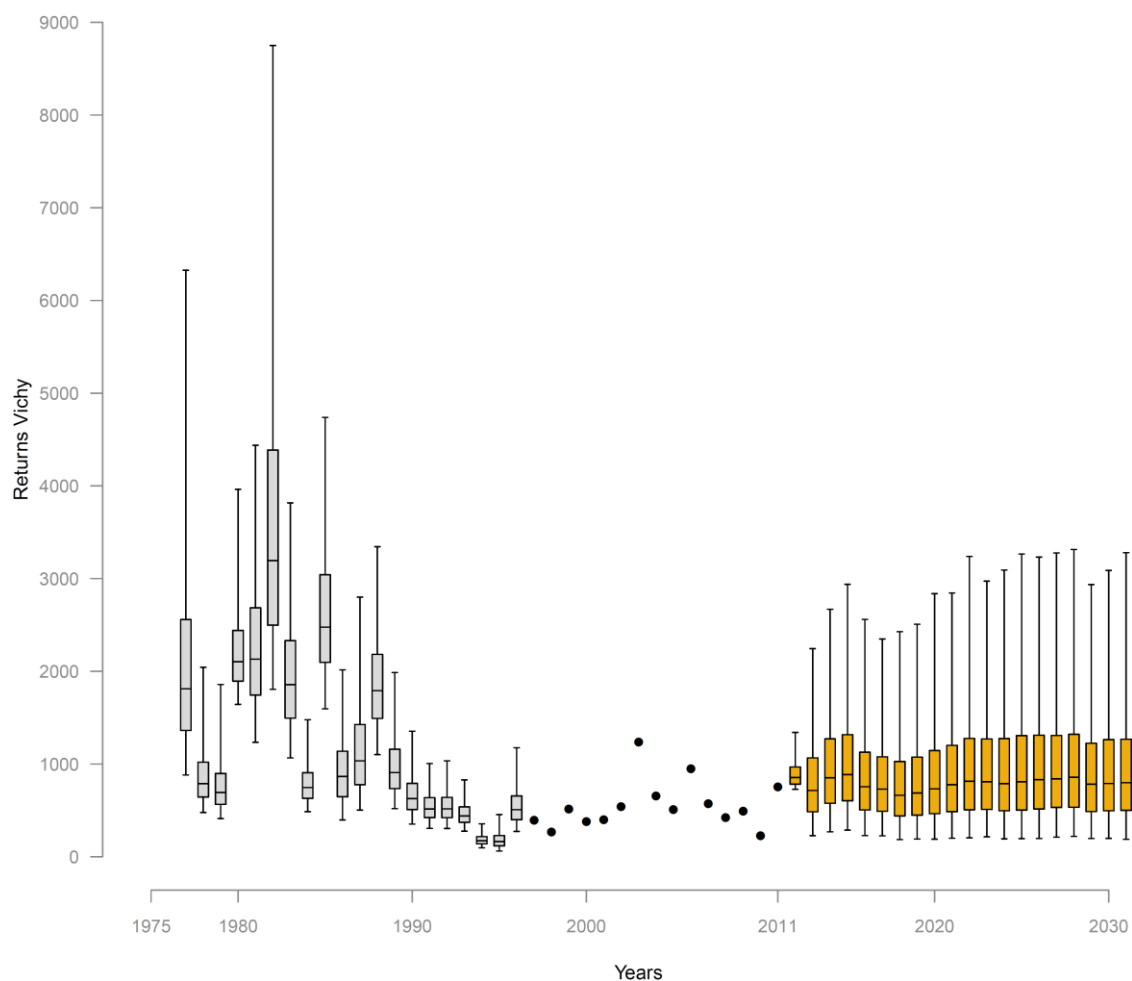


Figure 4.20: Posterior distributions of the annual adult returns at Vichy counting station. Boxplots indicate the median, 25th and 75th percentiles, whiskers indicate 2.5 and 97.5th percentiles. The plain dots indicate the years during which Vichy counting station was operational and adult returns are assumed to be known. The orange boxplot indicate the 20 years forecast under scenario 5 assumptions.

Figure 4.20: Distributions a posteriori des retours d'adultes à Vichy. Les boxplots indiquent les quantiles à 2.5th, 25th, médiane, 75th et 97.5th. Les cercles pleins indiquent les années pour lesquelles la station de comptage à Vichy est opérationnelle et fournit le nombre de retours d'adultes. Les boxplots orange correspondent aux estimations des retours d'adultes à Vichy pour les 20 prochaines années dans le cadre du scenario 5.

20 years projection – improvement 50% old level survival

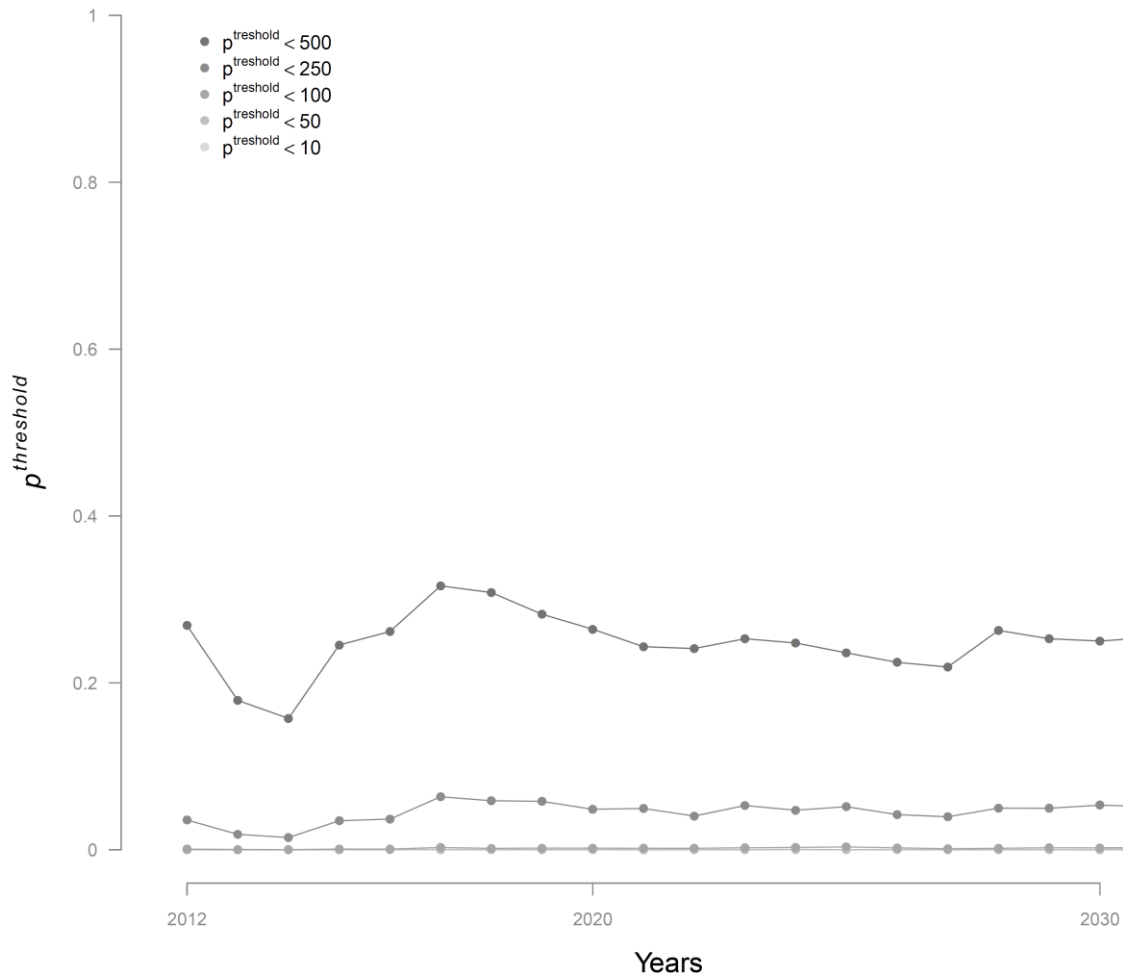


Figure 4.21: Evolution of the probabilities $p^{threshold}$ of reaching arbitrary threshold number of returning adults during the projection period (2012 to 2031) under scenario 5 assumptions.

Figure 4.21: Evolution de la probabilité $p^{threshold}$ d'atteindre certains seuils arbitraires du nombre de retours d'adultes à Vichy pendant la période 2012 à 2031 dans le cadre du scenario 5.

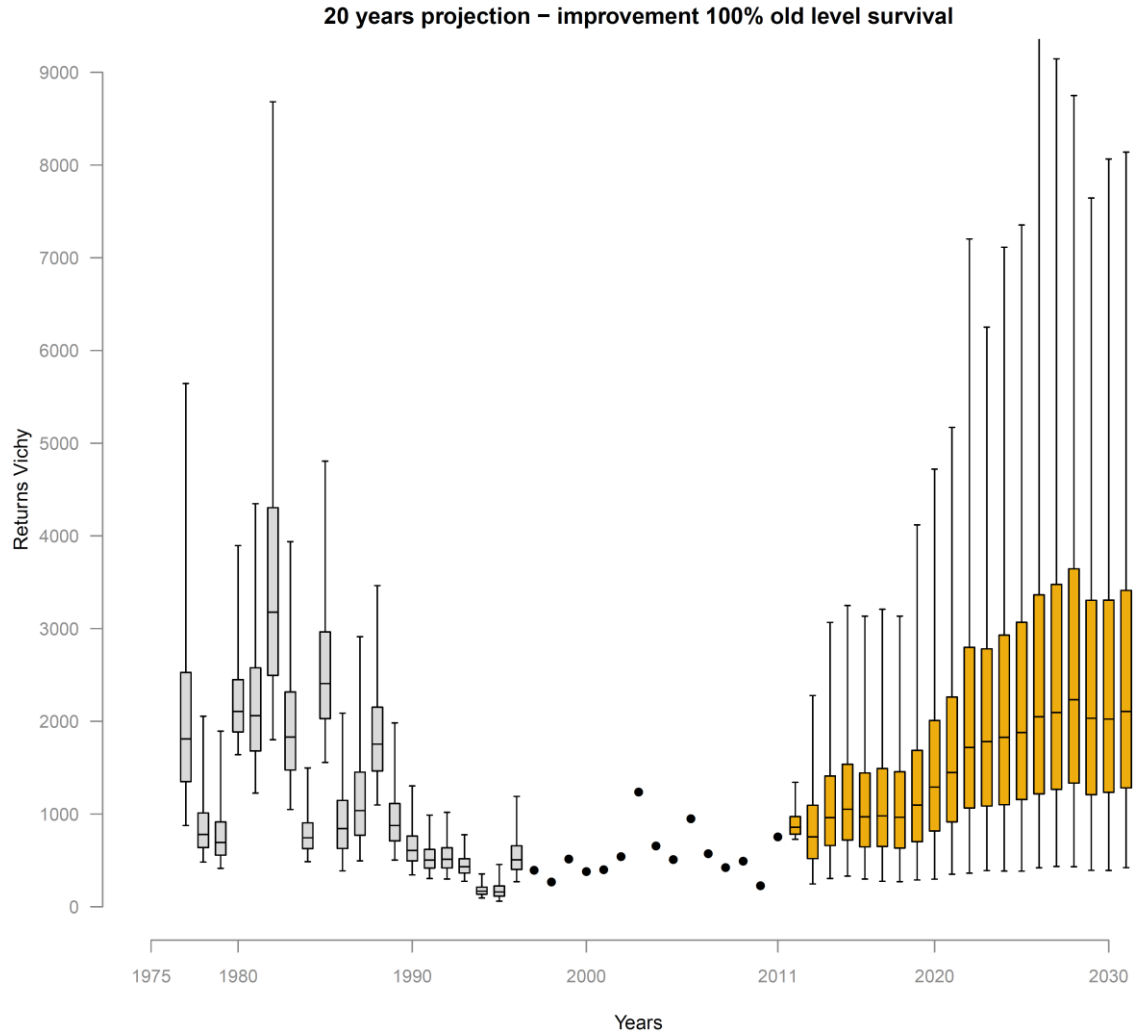


Figure 4.22: Posterior distributions of the annual adult returns at Vichy counting station. Boxplots indicate the median, 25th and 75th percentiles, whiskers indicate 2.5 and 97.5th percentiles. The plain dots indicate the years during which Vichy counting station was operational and adult returns are assumed to be known. The orange boxplot indicate the 20 years forecast under scenario 6 assumptions.

Figure 4.22: Distributions a posteriori des retours d'adultes à Vichy. Les boxplots indiquent les quantiles à 2.5th, 25th, médiane, 75th et 97.5th. Les cercles pleins indiquent les années pour lesquelles la station de comptage à Vichy est opérationnelle et fournit le nombre de retours d'adultes. Les boxplots orange correspondent aux estimations des retours d'adultes à Vichy pour les 20 prochaines années dans le cadre du scénario 6.

20 years projection – improvement 100% old level survival

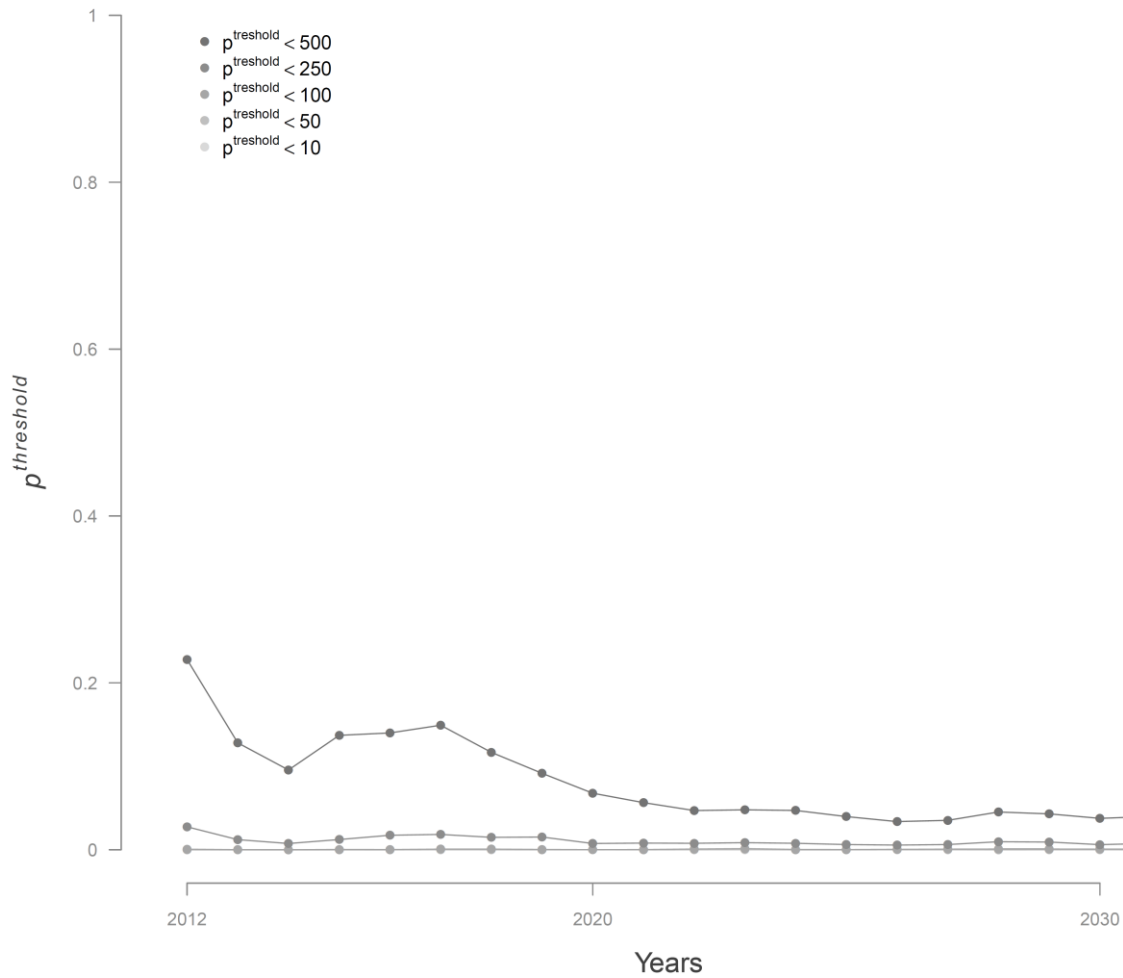


Figure 4.23: Evolution of the probabilities $p^{threshold}$ of reaching arbitrary threshold number of returning adults during the projection period (2012 to 2031) under scenario 6 assumptions.

Figure 4.23: Evolution de la probabilité $p^{threshold}$ d'atteindre certains seuils arbitraires du nombre de retours d'adultes à Vichy pendant la période 2012 à 2031 dans le cadre du scenario 6.

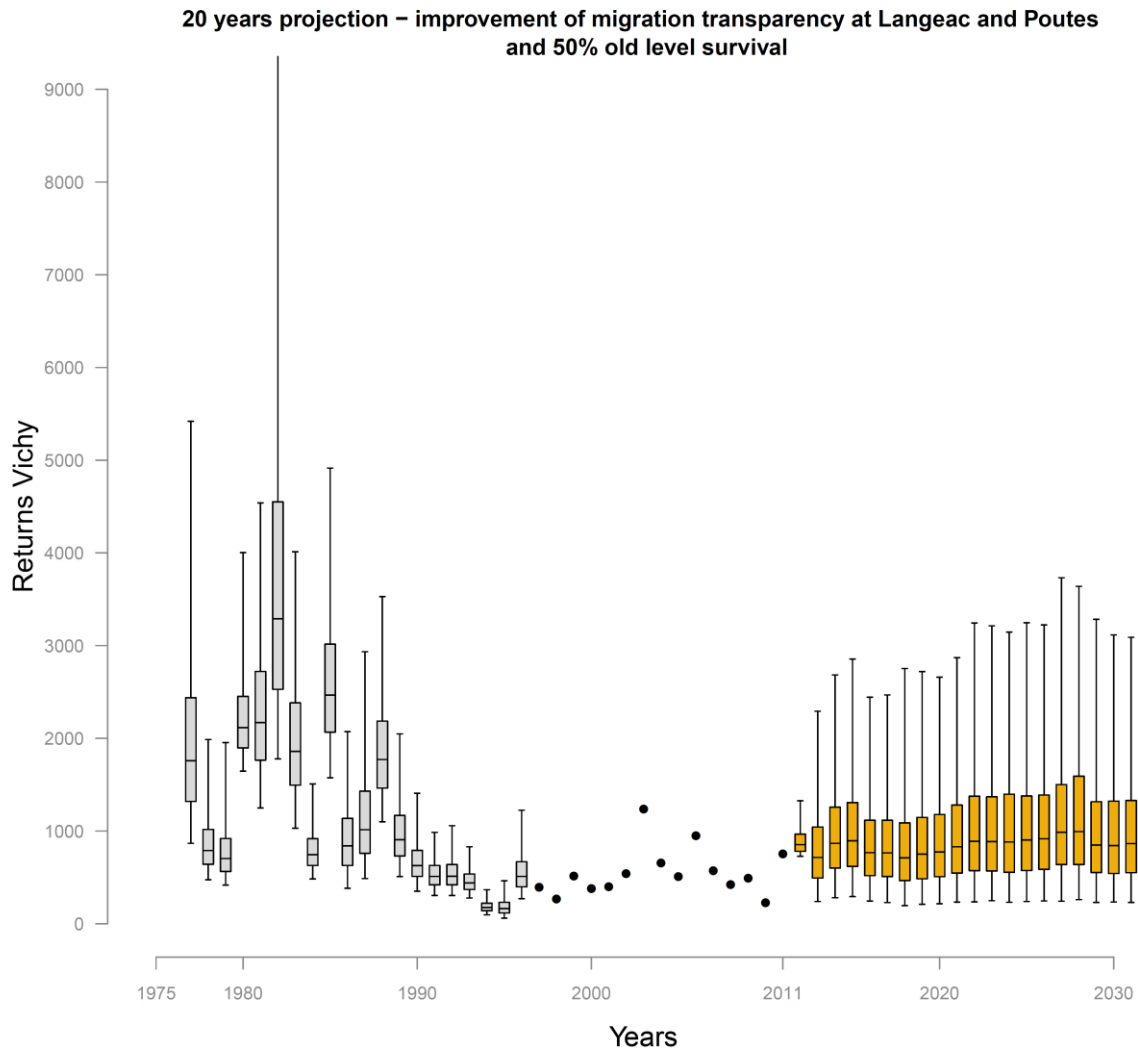


Figure 4.24: Posterior distributions of the annual adult returns at Vichy counting station. Boxplots indicate the median, 25th and 75th percentiles, whiskers indicate 2.5 and 97.5th percentiles. The plain dots indicate the years during which Vichy counting station was operational and adult returns are assumed to be known. The orange boxplot indicate the 20 years forecast under scenario 7 assumptions.

Figure 4.24: Distributions a posteriori des retours d'adultes à Vichy. Les boxplots indiquent les quantiles à 2.5th, 25th, médiane, 75th et 97.5th. Les cercles pleins indiquent les années pour lesquelles la station de comptage à Vichy est opérationnelle et fournit le nombre de retours d'adultes. Les boxplots orange correspondent aux estimations des retours d'adultes à Vichy pour les 20 prochaines années dans le cadre du scénario 7.

20 years projection – improvement of migration transparency at Langeac and Poutes
and 50% old level survival

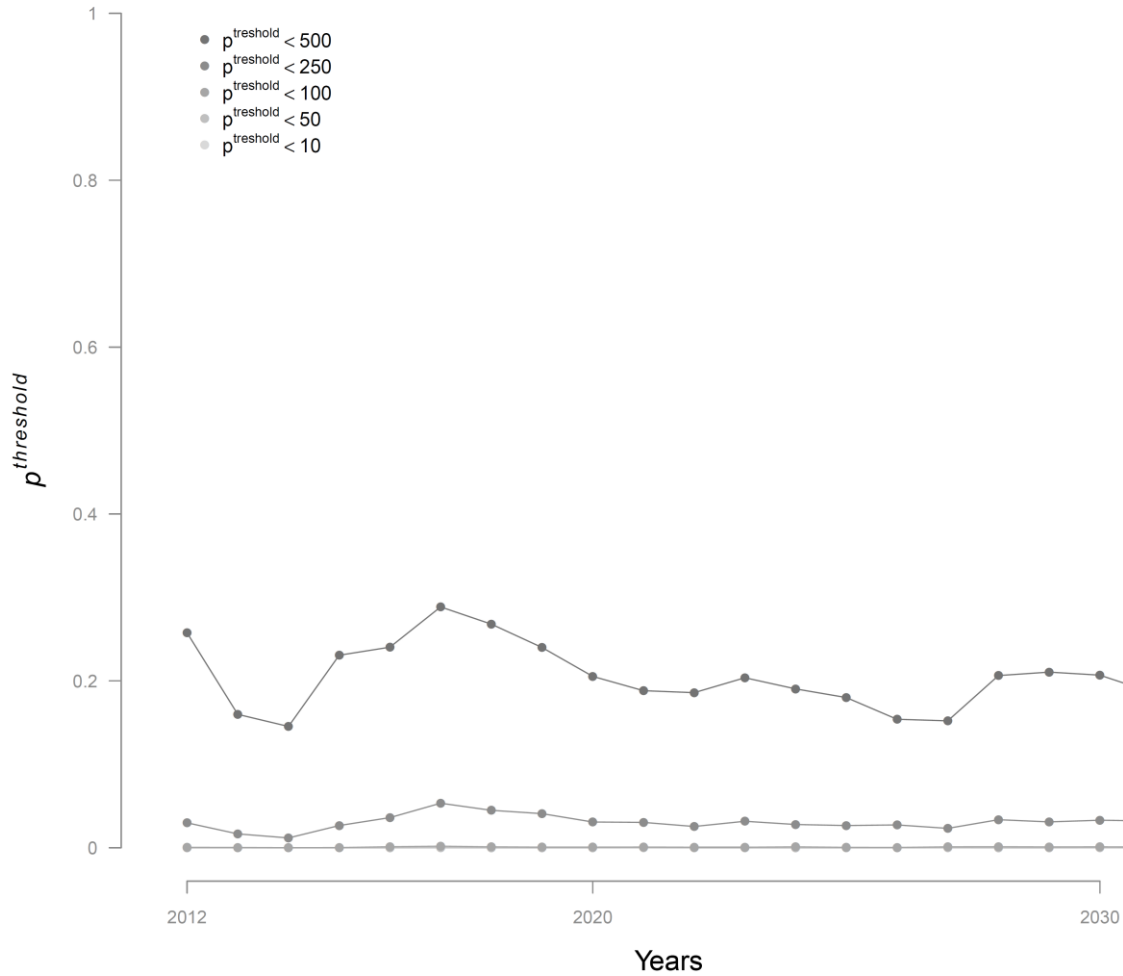


Figure 4.25: Evolution of the probabilities $p^{threshold}$ of reaching arbitrary threshold number of returning adults during the projection period (2012 to 2031) under scenario 7 assumptions.

Figure 4.25: Evolution de la probabilité $p^{threshold}$ d'atteindre certains seuils arbitraires du nombre de retours d'adultes à Vichy pendant la période 2012 à 2031 dans le cadre du scénario 7.

Appendices

Appendix A.1:

Electric fishing calibration relationship:

1. Introduction

To evaluate 0+ juvenile densities of Atlantic salmon, two different types of electric fishing techniques have been used in the Allier catchment throughout the time series considered in this project (1975 to 2011). From 1975 to 1990, a successive removal sampling technique was used. And from 1994 to 2011 the successive removal method was replaced by a timed (5 minutes) sampling technique.

In order to be able to use the two dataset together to estimate local densities throughout the time series, in 1997, 2000 and 2001, 9 sites (Figure A1.1) were sampled using both techniques in order to build a calibration relationship (Crozier and Kennedy, 1994) . A 5 minutes pass was carried out first and followed by 2 removal passes. In addition, the area of the site was measured and fish collected were measured.

To estimate the parameters of this relationship a model developed by Dauphin et al. (2009) was slightly modified to fit to the data available.

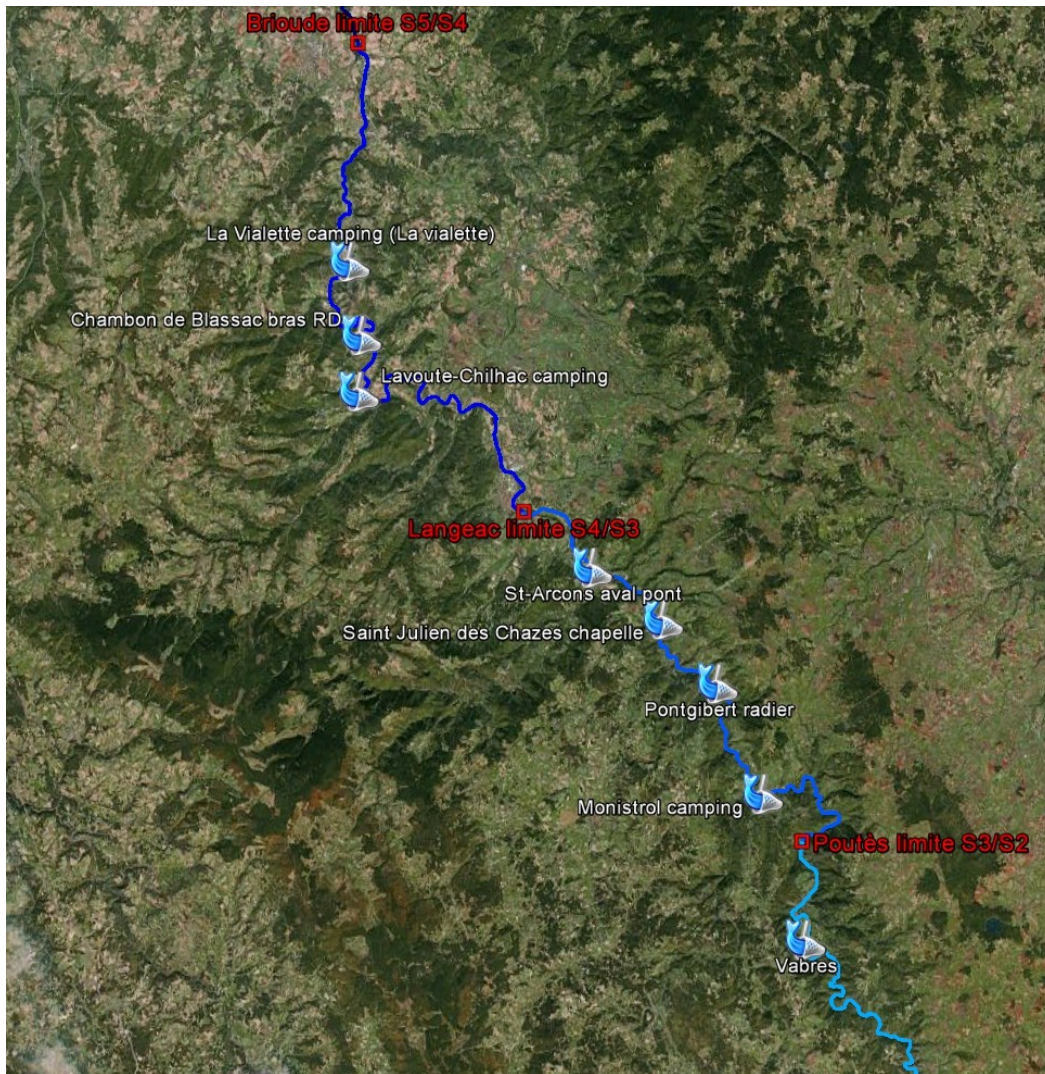


Figure A1.1: Partial map of the Allier catchment. The 9 sites sampled for the calibration relationship are indicated by a picture of a fish in a net.

2. Model

All sites were assumed to be exchangeable and for every site sampled, the 0+ juvenile density d_i was assumed to follow a Gamma distribution with a common mean d^{moy} and inverse scale parameter β^d .

$$(Eq. A1.1) \quad d_i | d^{moy}, \beta^d \sim \text{Gamma}(d^{moy} \times \beta^d, \beta^d)$$

Each site was first sampled using the 5 minutes index of abundance (IA) A_i technique. The IA A_i is assumed to follow a Negative Binomial distribution such as:

$$(Eq. A1.2) \quad A_i | a_i, \varphi \sim \text{Negative Binomial}(\lambda_i^A \times \varphi, \varphi)$$

Where φ is the inverse scale parameter and λ_i^A is the mean of the distribution which is deterministically linked to the density d_i :

$$(Eq. A1.3) \quad \lambda_i^A = \kappa \times d_i^{(\eta)}$$

Where κ is a factor of proportionality between the IA and the density d_i and, η is a power coefficient applied to the density d_i . If $\eta > 1$ the relationship will be concave up, if $\eta = 1$ the relation will be linear and if $0 < \eta < 1$ the relationship will be concave down. This power coefficient is introduced in order to deal with the possibility that operatives might fail to capture a proportion of the fish affected by the electric field and this proportion could increase/decrease with fish density. The 5 minutes sample was followed by two successive removal fishing pass, the remaining 0+ juveniles in the site is:

$$(Eq. A1.4) \quad n_i^{tot} = N_i^{tot} - A_i$$

Where N_i^{tot} is the total number of fish present in the site before any sampling occurred. The total number of fish N_i^{tot} is directly related to the 0+ juvenile density and is assumed to follow a Poisson distribution.

$$(Eq. A1.5) \quad N_i^{tot} | \lambda_i^N \sim Poisson(\lambda_i^N)$$

Where λ_i^N is calculated as the product of the site's surface S_i by the 0+ juvenile density d_i

$$(Eq. A1.6) \quad \lambda_i^N = S_i \times d_i$$

The number of 0+ juvenile caught during the first successive removal pass C_i^1 is assumed to follow a Binomial distribution

$$(Eq. A1.7) \quad C_i^1 | p_i, N_i^{tot} \sim Binomial(p_i, N_i^{tot})$$

Where p_i is the probability of capturing 0+ juveniles at site i . The number of fish remaining after the first removal pass is:

$$(Eq. A1.8) \quad N_i^1 = N_i^{tot} - C_i^1$$

Likewise the first removal pass, the number of 0+ juvenile caught during the second successive removal pass C_i^2 is assumed to follow a Binomial distribution

$$(Eq. A1.9) \quad C_i^2 | p_i, N_i^1 \sim Binomial(p_i, N_i^1)$$

In our calibration model, the probability of capturing 0+ juvenile is assumed to be the same during the two successive removal passes. The probabilities of capture each site p_i were assumed to be exchangeable and to follow a normal distribution (logit scale) such as:

$$(Eq. A1.10) \quad \text{Logit}(p_i) | \mu^p, \sigma^p \sim \text{Normal}(\text{Logit}(\mu^p), \sigma^p)$$

Where μ^p is the mean probability of capturing 0+ juveniles and σ^p the standard deviation (logit scale).

The structure of conditional dependency of the relations described in equations A1.1-10 can be graphically summarized in a Directed Acyclic Graph (DAG) (Fig. A1.2).

All parameters of the model were given little-informative and independent prior distributions (Table A1.1) in order to obtain posterior inferences reflecting the information brought by the data. The full dataset used in this calibration model can be found in Table A1.2. The joint posterior distribution of all unknowns (i.e. parameters and latent variables) conditionally on all the observed data was approximated using MCMC sampling. All computations were carried out with the OpenBUGs software (version 3.2.1). In order to test the convergence of the MCMC sampling, three chains with contrasted starting points were used. The Gelman-Rubin statistic as calculated in OpenBUGs indicated good mixing of the MCMC chains after $2 \cdot 10^6$ iterations. An additional sample of 8000 values ($8 \cdot 10^6$ iterations, but only retaining one out a hundred) was used to provide estimates of the joint posterior distributions of all parameters.

Table A1.1: Prior distributions of the main parameters of the model ($\varepsilon = 10^{-3}$) and their associated posterior distribution.

parameters	Prior distribution	Posterior distribution						
		mean	sd	2.5 th	25 th	median	50 th	97.5 th
d^{moy}	$Gamma(\varepsilon, \varepsilon)$	0.364	4.361	0.188	0.254	0.295	0.350	0.552
β^d	$Gamma(\varepsilon, \varepsilon)$	8.694	5.348	1.692	4.880	7.595	11.180	22.190
κ	$1/Gamma(\varepsilon, \varepsilon)$	371.2	81.89	263.4	316.7	354.8	404.8	575.1
η	$1/Gamma(\varepsilon, \varepsilon)$	1.278	0.192	0.991	1.144	1.249	1.377	1.740
μ^p	$Inv.Logit(Normal(0, \varepsilon))$	0.465	0.105	0.263	0.397	0.465	0.533	0.674
σ^p	$Uniform(0,10)$	1.189	0.414	0.657	0.916	1.106	1.359	2.217

Table A1.2: Summary of data available in the 9 sites used for the calibration relationship: 5minutes index of abundance, 0+ caught during the first and second removal pass and surface of the site.

Site	A_i	C_i^1	C_i^2	S_i
Vabres	52	222	68	1210
Pontgibert radier	131	83	34	464
St-Arcons aval pont	159	296	60	751.2
St-julien des Chazes chapelle	120	221	132	1134.3
La Vialette camping	61	140	45	828
Truchon	15	50	21	1854
Monistrol camping	82	136	121	2880
Chambon de Blassac RD	21	21	14	752
Lavoûte-Chilhac camping	21	46	31	1192.5

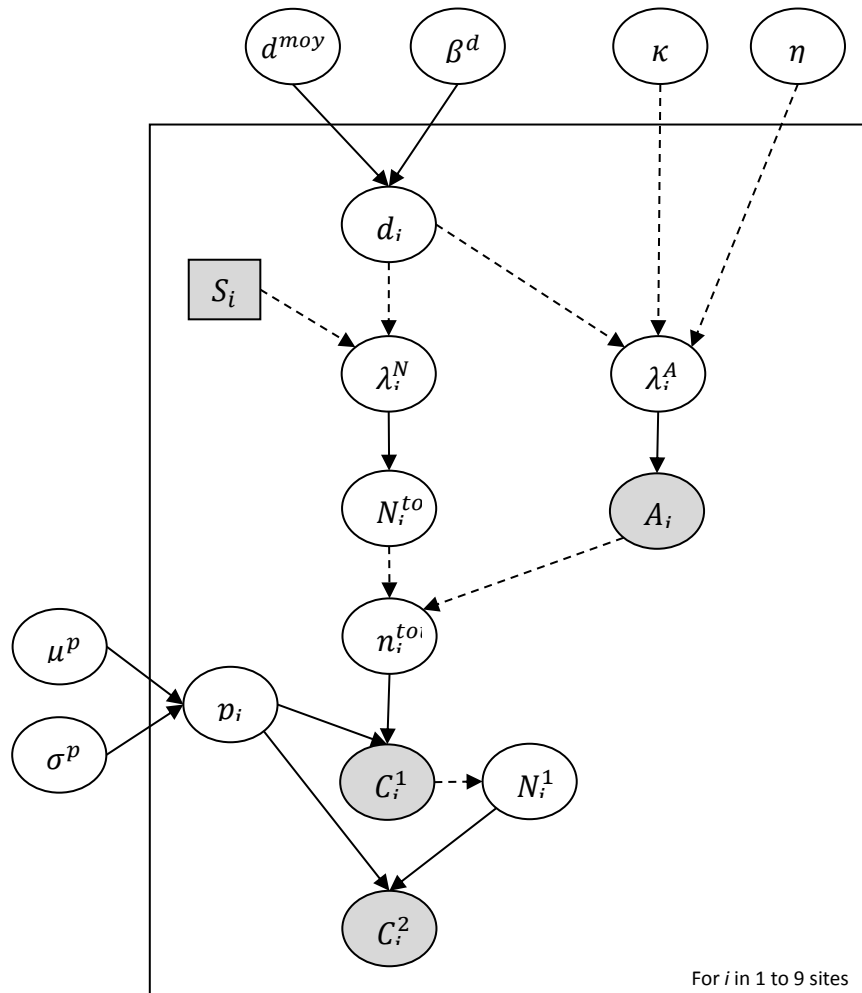


Figure A1.2: Directed Acyclic Graph (DAG) of the model used to estimate densities of the sites studied. Squares represent fixed quantities. All observed quantities are greyed. Arrows represent the parent-child dependencies between the different nodes: single arrows represent probabilistic relationship between the parent(s) and child nodes, dashed arrows indicate deterministic relationship. The frame represents a repetition of structure over sites. Nodes outside the frame are unknown parameters constant across sites.

3. Results & Discussion

All posterior distributions of the model parameters revealed a significant updating from the data (Table A1.1). The 9 sites sampled for this calibration exercise presented contrasted densities ranging from 0.06 to 0.51 0+ salmon juvenile per square meter (Fig. A1.3). The average probability of capturing a 0+ juvenile overall sites μ^p is 0.465 but with important variations across sites ($\sigma^p = 1.189$, p_i ranging from 0.16 to 0.79). The shape of the relationship between the 5 minutes IA and the density is concave up ($\eta = 1.278$), with the density increasing slower than the IA.

On Figure A1.3, the 5 minutes IA to density relationship average relationship is represented along side with the density estimates of the 9 calibration sites. The relationship is extended to IAs values up to 300 which are the maximum values observed in the Allier catchment over the last 30 years. It is important to notice that no calibration sites presented an IA higher than 159 and therefore the relationship is more speculative for IAs above this value. However, the 9 sites sampled for this calibration exercise present contrasted density over the mainly encountered range of IAs in the Allier catchment making this model a good tool to provide 0+ salmon juvenile density estimates based on the 5 minutes IAs. Additionally, Table A1.3 provides the 0+ juvenile density predictions (2.5th, 25th, median, 75th and 97.5th quantiles) for any given IA ranging from 1 to 300.

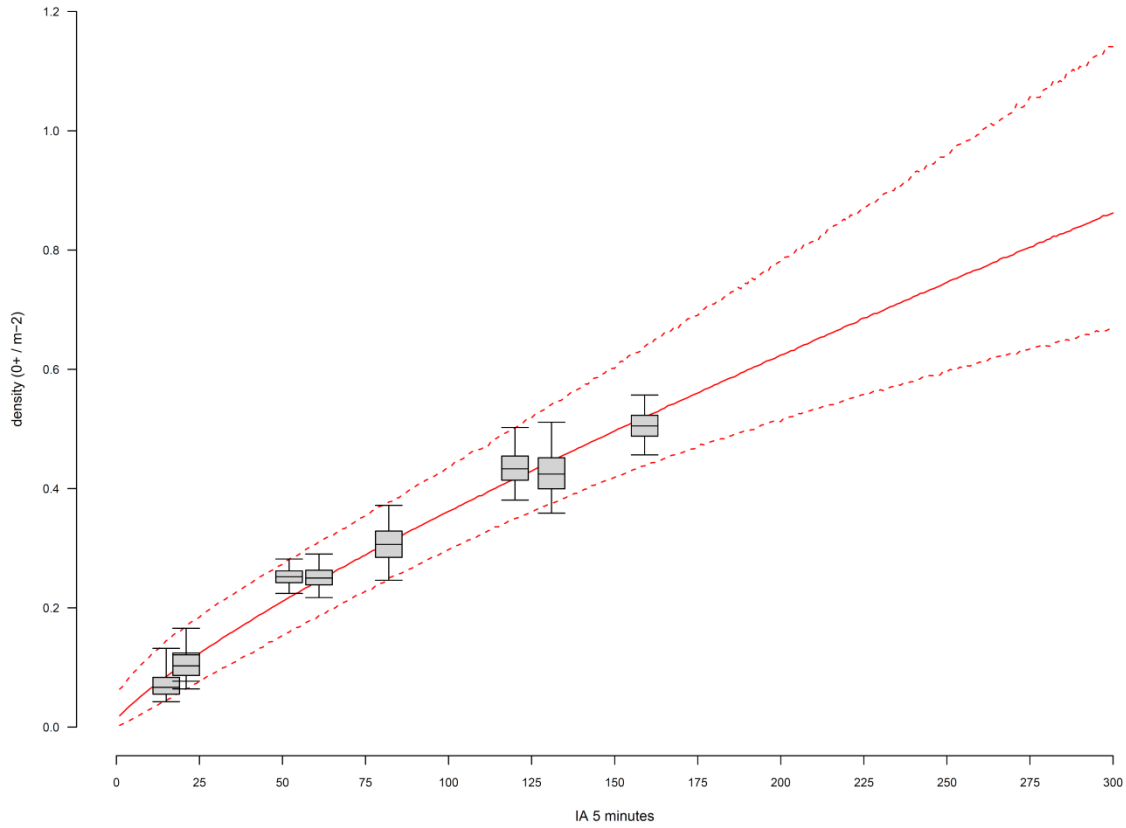


Figure A1.3: 0+ juveniles density estimates vs 5 minutes index of abundance for the 9 sites sampled with the two electric fishing techniques. Boxplots indicate 2.5th, 25th, median, 75th and 97.5th quantiles. The plain and dashed red lines indicate the 2.5th, median and 97.5th quantiles of predicted densities for 5 minutes index of abundance only ranging from 1 to 300.

Table A1.3: Predicted densities (2.5th, 25th, median, 75th and 97.5th quantiles) for a given 5 minutes samples from the calibration model.

IA 5 min	Predicted density 0+/m2 (quantiles)				
	2.5%	25%	50%	75%	97.5%
1	0.003	0.011	0.019	0.030	0.064
2	0.006	0.016	0.024	0.036	0.069
3	0.009	0.021	0.030	0.043	0.077
4	0.011	0.025	0.035	0.048	0.084
5	0.014	0.029	0.040	0.054	0.090
6	0.017	0.033	0.045	0.059	0.096
7	0.020	0.037	0.050	0.065	0.103
8	0.024	0.042	0.055	0.070	0.108
9	0.027	0.046	0.059	0.075	0.113
10	0.030	0.050	0.064	0.080	0.118
11	0.033	0.053	0.068	0.084	0.125
12	0.035	0.058	0.072	0.089	0.129
13	0.039	0.061	0.076	0.094	0.132
14	0.042	0.065	0.080	0.098	0.138
15	0.045	0.069	0.085	0.103	0.145
16	0.048	0.073	0.089	0.107	0.147
17	0.050	0.077	0.093	0.111	0.154
18	0.055	0.081	0.097	0.116	0.158
19	0.058	0.084	0.101	0.120	0.159
20	0.060	0.088	0.105	0.123	0.165
21	0.064	0.091	0.109	0.128	0.170
22	0.066	0.095	0.112	0.131	0.174
23	0.071	0.099	0.117	0.136	0.178
24	0.073	0.102	0.120	0.139	0.181
25	0.076	0.106	0.124	0.143	0.184
26	0.080	0.110	0.128	0.147	0.190
27	0.084	0.113	0.131	0.152	0.193
28	0.088	0.117	0.135	0.155	0.197
29	0.089	0.120	0.138	0.158	0.202
30	0.092	0.123	0.142	0.162	0.205
31	0.096	0.127	0.146	0.166	0.210
32	0.099	0.131	0.150	0.170	0.212
33	0.101	0.134	0.153	0.173	0.215
34	0.103	0.137	0.157	0.178	0.220
35	0.107	0.141	0.160	0.181	0.222
36	0.110	0.144	0.163	0.184	0.226

IA 5 min	Predicted density 0+/m2 (quantiles)				
	2.5%	25%	50%	75%	97.5%
37	0.114	0.147	0.167	0.188	0.230
38	0.117	0.151	0.170	0.191	0.233
39	0.120	0.155	0.174	0.195	0.237
40	0.123	0.157	0.177	0.198	0.240
41	0.124	0.161	0.181	0.201	0.243
42	0.129	0.164	0.184	0.205	0.248
43	0.132	0.168	0.188	0.209	0.251
44	0.134	0.170	0.191	0.211	0.254
45	0.139	0.174	0.194	0.216	0.259
46	0.143	0.178	0.198	0.218	0.261
47	0.143	0.181	0.201	0.222	0.263
48	0.147	0.184	0.204	0.226	0.268
49	0.150	0.187	0.208	0.229	0.270
50	0.154	0.190	0.211	0.232	0.273
51	0.157	0.193	0.214	0.236	0.278
52	0.159	0.197	0.218	0.239	0.281
53	0.164	0.200	0.220	0.242	0.285
54	0.167	0.202	0.224	0.245	0.286
55	0.168	0.206	0.226	0.248	0.290
56	0.171	0.210	0.230	0.252	0.294
57	0.175	0.213	0.234	0.255	0.298
58	0.178	0.215	0.236	0.257	0.301
59	0.180	0.219	0.240	0.261	0.304
60	0.182	0.221	0.243	0.264	0.307
61	0.187	0.225	0.246	0.268	0.311
62	0.190	0.228	0.249	0.271	0.313
63	0.191	0.231	0.253	0.274	0.317
64	0.196	0.234	0.255	0.277	0.319
65	0.198	0.237	0.258	0.280	0.321
66	0.200	0.241	0.262	0.284	0.325
67	0.205	0.245	0.266	0.287	0.329
68	0.208	0.246	0.268	0.290	0.332
69	0.210	0.249	0.270	0.292	0.334
70	0.213	0.253	0.274	0.296	0.339
71	0.216	0.255	0.277	0.299	0.341
72	0.220	0.259	0.281	0.302	0.345

IA 5 min	Predicted density 0+/m2 (quantiles)				
	2.5%	25%	50%	75%	97.5%
73	0.221	0.262	0.282	0.305	0.350
74	0.225	0.265	0.286	0.308	0.352
75	0.228	0.267	0.289	0.310	0.354
76	0.230	0.271	0.292	0.314	0.357
77	0.232	0.274	0.296	0.318	0.363
78	0.237	0.277	0.298	0.320	0.365
79	0.241	0.279	0.301	0.323	0.370
80	0.241	0.282	0.304	0.326	0.371
81	0.244	0.284	0.307	0.329	0.373
82	0.250	0.288	0.309	0.332	0.378
83	0.252	0.292	0.313	0.336	0.379
84	0.254	0.294	0.316	0.338	0.384
85	0.257	0.297	0.319	0.342	0.385
86	0.259	0.299	0.322	0.345	0.389
87	0.263	0.303	0.325	0.347	0.392
88	0.265	0.306	0.328	0.350	0.397
89	0.267	0.309	0.331	0.353	0.400
90	0.270	0.311	0.333	0.357	0.404
91	0.273	0.314	0.336	0.360	0.408
92	0.275	0.316	0.339	0.362	0.409
93	0.280	0.320	0.342	0.364	0.414
94	0.282	0.322	0.345	0.368	0.416
95	0.285	0.326	0.348	0.371	0.419
96	0.287	0.328	0.350	0.374	0.422
97	0.289	0.330	0.353	0.377	0.426
98	0.292	0.334	0.357	0.379	0.428
99	0.295	0.336	0.359	0.383	0.432
100	0.298	0.339	0.362	0.386	0.437
101	0.301	0.342	0.364	0.388	0.439
102	0.304	0.344	0.367	0.391	0.445
103	0.305	0.347	0.370	0.394	0.447
104	0.308	0.351	0.373	0.397	0.449
105	0.310	0.352	0.376	0.400	0.453
106	0.314	0.356	0.379	0.403	0.457
107	0.315	0.357	0.381	0.406	0.462
108	0.317	0.361	0.384	0.408	0.463
109	0.321	0.364	0.388	0.412	0.465
110	0.323	0.366	0.388	0.414	0.467
111	0.326	0.369	0.392	0.417	0.472
112	0.329	0.373	0.395	0.420	0.472
113	0.331	0.375	0.398	0.423	0.481

IA 5 min	Predicted density 0+/m2 (quantiles)				
	2.5%	25%	50%	75%	97.5%
114	0.336	0.378	0.400	0.426	0.483
115	0.336	0.380	0.403	0.430	0.486
116	0.340	0.382	0.406	0.432	0.490
117	0.342	0.384	0.409	0.435	0.493
118	0.345	0.388	0.412	0.438	0.496
119	0.347	0.390	0.414	0.440	0.500
120	0.350	0.393	0.417	0.443	0.502
121	0.351	0.394	0.419	0.446	0.505
122	0.354	0.398	0.422	0.449	0.508
123	0.356	0.400	0.424	0.452	0.514
124	0.358	0.402	0.427	0.455	0.518
125	0.360	0.404	0.429	0.457	0.519
126	0.364	0.408	0.432	0.460	0.524
127	0.366	0.409	0.435	0.464	0.527
128	0.370	0.413	0.438	0.467	0.530
129	0.370	0.415	0.441	0.469	0.533
130	0.374	0.419	0.444	0.473	0.538
131	0.375	0.420	0.446	0.474	0.541
132	0.377	0.423	0.448	0.478	0.546
133	0.379	0.425	0.452	0.482	0.547
134	0.383	0.428	0.455	0.485	0.548
135	0.384	0.430	0.457	0.486	0.554
136	0.387	0.433	0.460	0.489	0.557
137	0.390	0.436	0.462	0.493	0.562
138	0.392	0.438	0.465	0.494	0.563
139	0.392	0.440	0.468	0.499	0.567
140	0.396	0.443	0.470	0.501	0.570
141	0.399	0.445	0.473	0.503	0.575
142	0.399	0.447	0.476	0.507	0.575
143	0.405	0.450	0.479	0.510	0.583
144	0.406	0.452	0.481	0.513	0.586
145	0.409	0.456	0.483	0.516	0.586
146	0.411	0.458	0.486	0.518	0.591
147	0.413	0.459	0.488	0.521	0.594
148	0.414	0.462	0.491	0.524	0.600
149	0.416	0.464	0.494	0.528	0.601
150	0.419	0.467	0.497	0.529	0.602
151	0.420	0.470	0.500	0.533	0.610
152	0.423	0.473	0.502	0.536	0.614
153	0.425	0.475	0.505	0.537	0.612
154	0.428	0.477	0.507	0.540	0.622

IA 5 min	Predicted density 0+/m2 (quantiles)				
	2.5%	25%	50%	75%	97.5%
155	0.430	0.479	0.510	0.544	0.625
156	0.432	0.481	0.512	0.548	0.628
157	0.433	0.483	0.515	0.549	0.628
158	0.437	0.485	0.517	0.552	0.631
159	0.438	0.488	0.519	0.554	0.638
160	0.438	0.491	0.522	0.558	0.643
161	0.443	0.494	0.525	0.560	0.642
162	0.444	0.495	0.527	0.563	0.650
163	0.446	0.498	0.529	0.566	0.652
164	0.448	0.501	0.533	0.569	0.655
165	0.450	0.502	0.535	0.572	0.662
166	0.452	0.505	0.539	0.576	0.661
167	0.456	0.507	0.541	0.578	0.665
168	0.456	0.509	0.542	0.581	0.671
169	0.457	0.511	0.545	0.582	0.668
170	0.460	0.513	0.548	0.587	0.676
171	0.462	0.517	0.550	0.589	0.680
172	0.465	0.518	0.553	0.592	0.685
173	0.466	0.522	0.556	0.596	0.686
174	0.467	0.523	0.558	0.599	0.689
175	0.470	0.526	0.560	0.599	0.691
176	0.474	0.528	0.563	0.603	0.697
177	0.473	0.530	0.566	0.605	0.701
178	0.477	0.533	0.568	0.609	0.707
179	0.479	0.535	0.570	0.611	0.709
180	0.480	0.538	0.574	0.614	0.710
181	0.481	0.539	0.575	0.618	0.715
182	0.484	0.541	0.579	0.620	0.716
183	0.483	0.544	0.581	0.622	0.721
184	0.488	0.547	0.584	0.626	0.723
185	0.488	0.548	0.586	0.628	0.730
186	0.491	0.550	0.587	0.632	0.731
187	0.494	0.553	0.590	0.635	0.738
188	0.494	0.556	0.594	0.638	0.735
189	0.496	0.558	0.596	0.639	0.745
190	0.496	0.559	0.599	0.643	0.744
191	0.499	0.562	0.601	0.646	0.754
192	0.499	0.564	0.604	0.649	0.750
193	0.501	0.566	0.606	0.651	0.754
194	0.506	0.568	0.608	0.655	0.760
195	0.507	0.572	0.612	0.656	0.764

IA 5 min	Predicted density 0+/m2 (quantiles)				
	2.5%	25%	50%	75%	97.5%
196	0.509	0.574	0.614	0.660	0.763
197	0.512	0.575	0.616	0.662	0.773
198	0.513	0.577	0.618	0.666	0.774
199	0.511	0.579	0.621	0.668	0.778
200	0.513	0.583	0.624	0.673	0.782
201	0.518	0.584	0.626	0.674	0.788
202	0.519	0.586	0.628	0.677	0.789
203	0.520	0.589	0.631	0.679	0.790
204	0.521	0.590	0.632	0.682	0.795
205	0.526	0.592	0.636	0.685	0.803
206	0.525	0.594	0.639	0.687	0.800
207	0.528	0.598	0.641	0.691	0.809
208	0.530	0.598	0.642	0.692	0.809
209	0.531	0.601	0.645	0.695	0.813
210	0.533	0.604	0.649	0.700	0.815
211	0.534	0.604	0.651	0.701	0.814
212	0.536	0.609	0.654	0.704	0.824
213	0.538	0.610	0.655	0.708	0.824
214	0.539	0.613	0.658	0.711	0.834
215	0.541	0.614	0.660	0.712	0.836
216	0.541	0.616	0.663	0.715	0.841
217	0.544	0.619	0.665	0.719	0.843
218	0.545	0.621	0.667	0.721	0.847
219	0.548	0.623	0.671	0.723	0.852
220	0.549	0.626	0.673	0.729	0.849
221	0.551	0.627	0.675	0.731	0.859
222	0.552	0.628	0.677	0.731	0.858
223	0.553	0.631	0.679	0.735	0.861
224	0.557	0.634	0.684	0.739	0.867
225	0.558	0.635	0.686	0.740	0.871
226	0.557	0.638	0.687	0.743	0.874
227	0.560	0.640	0.690	0.744	0.878
228	0.563	0.642	0.693	0.751	0.878
229	0.563	0.645	0.694	0.752	0.883
230	0.566	0.647	0.697	0.754	0.889
231	0.564	0.648	0.699	0.758	0.894
232	0.567	0.651	0.702	0.760	0.897
233	0.570	0.653	0.705	0.763	0.900
234	0.571	0.655	0.707	0.764	0.900
235	0.574	0.657	0.710	0.769	0.909
236	0.573	0.657	0.711	0.772	0.907

IA 5 min	Predicted density 0+/m2 (quantiles)				
	2.5%	25%	50%	75%	97.5%
237	0.577	0.663	0.714	0.773	0.912
238	0.577	0.664	0.716	0.777	0.914
239	0.579	0.665	0.718	0.779	0.921
240	0.579	0.668	0.722	0.782	0.930
241	0.581	0.669	0.724	0.788	0.933
242	0.584	0.673	0.727	0.786	0.930
243	0.588	0.673	0.728	0.790	0.934
244	0.589	0.675	0.731	0.793	0.943
245	0.589	0.677	0.734	0.794	0.945
246	0.589	0.679	0.735	0.798	0.944
247	0.588	0.682	0.738	0.803	0.951
248	0.591	0.684	0.740	0.804	0.956
249	0.597	0.686	0.743	0.807	0.956
250	0.596	0.688	0.746	0.810	0.959
251	0.600	0.688	0.749	0.813	0.963
252	0.598	0.692	0.751	0.816	0.972
253	0.600	0.694	0.753	0.817	0.976
254	0.604	0.697	0.756	0.821	0.978
255	0.602	0.698	0.758	0.825	0.979
256	0.606	0.700	0.761	0.826	0.983
257	0.605	0.703	0.762	0.830	0.985
258	0.610	0.705	0.765	0.832	0.986
259	0.610	0.706	0.767	0.835	0.993
260	0.612	0.709	0.768	0.838	0.995
261	0.612	0.711	0.771	0.842	1.003
262	0.614	0.713	0.773	0.843	1.006
263	0.618	0.715	0.776	0.846	1.013
264	0.618	0.718	0.779	0.848	1.009
265	0.621	0.719	0.781	0.851	1.013
266	0.622	0.720	0.785	0.854	1.018
267	0.620	0.723	0.787	0.856	1.022
268	0.624	0.725	0.788	0.859	1.025
269	0.626	0.728	0.790	0.863	1.029
270	0.626	0.729	0.792	0.866	1.031
271	0.626	0.730	0.796	0.868	1.045
272	0.630	0.733	0.798	0.870	1.038
273	0.633	0.736	0.800	0.874	1.040
274	0.632	0.737	0.803	0.878	1.046
275	0.634	0.740	0.805	0.877	1.057
276	0.636	0.742	0.806	0.880	1.055
277	0.638	0.743	0.810	0.884	1.056

IA 5 min	Predicted density 0+/m2 (quantiles)				
	2.5%	25%	50%	75%	97.5%
278	0.639	0.746	0.813	0.889	1.056
279	0.642	0.748	0.813	0.890	1.068
280	0.639	0.749	0.817	0.891	1.071
281	0.639	0.751	0.819	0.895	1.071
282	0.644	0.753	0.823	0.899	1.083
283	0.645	0.755	0.823	0.901	1.079
284	0.647	0.758	0.827	0.906	1.084
285	0.647	0.759	0.828	0.905	1.081
286	0.650	0.761	0.830	0.909	1.096
287	0.648	0.762	0.832	0.911	1.097
288	0.652	0.765	0.836	0.913	1.103
289	0.652	0.768	0.838	0.918	1.098
290	0.656	0.770	0.839	0.919	1.108
291	0.657	0.771	0.841	0.920	1.106
292	0.659	0.772	0.844	0.924	1.108
293	0.658	0.777	0.846	0.927	1.119
294	0.661	0.778	0.849	0.931	1.123
295	0.665	0.779	0.851	0.932	1.126
296	0.663	0.781	0.853	0.935	1.125
297	0.664	0.784	0.858	0.938	1.129
298	0.665	0.786	0.857	0.939	1.141
299	0.668	0.788	0.860	0.944	1.141
300	0.671	0.790	0.862	0.948	1.141

Appendix A.2:

0+ Juvenile densities model

1. Introduction

In this section, we look at an important component of the Atlantic salmon lifecycle: the 0+ juvenile lifestage. Indeed, the 0+ juvenile densities are related to the spawners success for a given year.

In order to measure the 0+ juvenile densities, electric fishing was carried out at various sites in the Allier catchment throughout the time-series (1977-2011). Until 1990, sites were fished using a successive removal technique. This technique provides estimates of 0+ densities but is quite time consuming and labour intensive. On average, only 5 sites over the whole catchment were fished annually. From 1991 to 1993 no sampling was carried out. From 1994 until present, a 5 minutes index of abundance is used to sample 0+ juveniles in various sites of the Allier catchment. This technique does not provide direct estimates of 0+ juvenile densities but it is much more cost effective (calibration relationship between 5 minutes index of abundance and successive removal can be built, see App A.1). On average, 30 sites over the whole catchment are sampled annually.

The electric fishing carried out in early autumn will reflect the spawners success but since the Allier is heavily stocked it will also reflect the survival of the stocked 0+ juveniles and eggs. Total number of 0+ and eggs stocked in the 3 river sections considered in the study can be found in Fig. A2.1 and Fig. A2.2. Atlantic salmon stocked in the Allier river came from Scotland, Iceland and Denmark strains in combination with the Allier strain (spawners captured in the Allier). Since 1985, all lifestages stocked stemmed from the Allier strain.

The Atlantic salmon population of the river Allier has been stocked since 1970 by the salmon hatchery of the Conseil Supérieur de la Pêche (CSP) in Augerolles. In 2001, the implementation of the first step of the Plan Loire Grandeur Nature, led to a change in the stocking strategy (number of stocked salmon multiplied by 3) associated with the opening of a new salmon hatchery in Chanteuges which now produces all the salmon to be stocked in the Allier. Additionally, in 2009, all the area upstream Langeac was declared “refuge area” which means that stocking is not allowed in this area anymore.

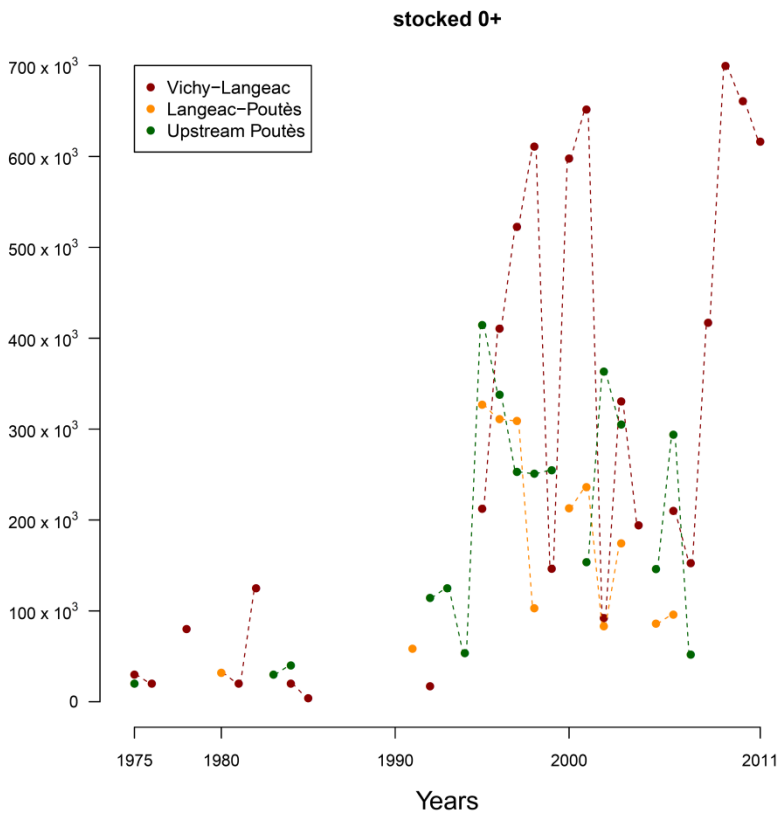


Figure A2.1: Total number of 0+ juveniles stocked annually in each of the three river sections of the allier catchment.

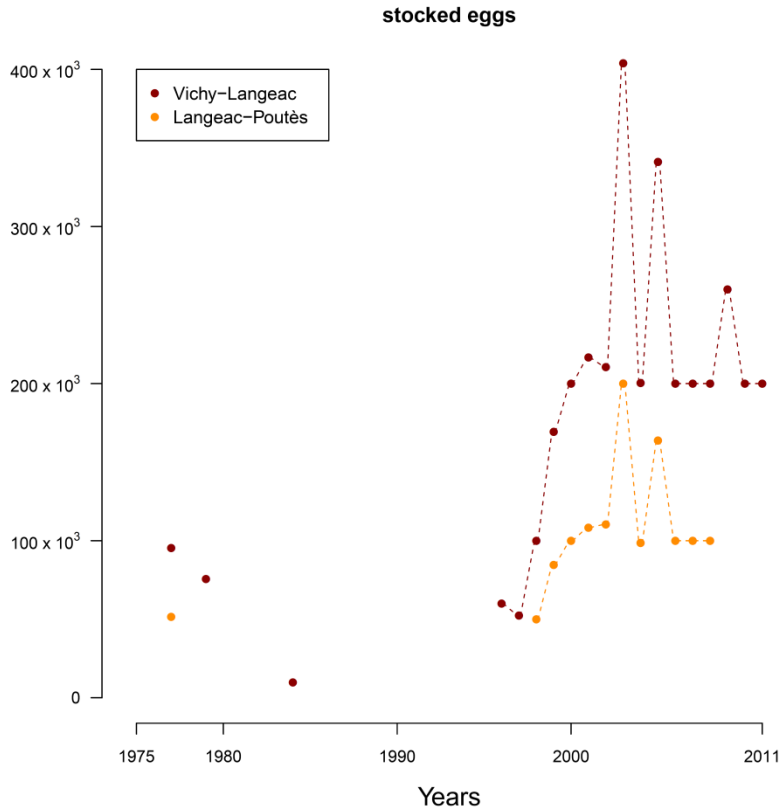


Figure A2.2: Total number of eggs stocked annually in each of the three river sections of the Allier catchment.

2. Model

The electric fishing data provides some information regarding the 0+ juvenile densities at a local scale and the objective is to obtain density estimates at a river section scale.

Therefore, densities of 0+ juveniles ($0+/\text{m}^2$) are expressed at two spatial scales:

- 1) a macro scale corresponding at the river section scale (Vichy-Langeac, Langeac-Poutès and upstream Poutès). Densities at this scale are indicated by an upper-case D .
- 2) a micro scale corresponding at the electric fishing scale. Densities at this scale are indicated by a lower-case d .

At both scale, total 0+ densities can be broken down in 3 components:

- 1) “wild” 0+, the descendants of the returning adults which have spawned

- 2) Stocked 0+, the survivors from the stocked 0+ during spring
- 3) Stocked eggs, the survivors from the stocked eggs (in field incubators, App. A.3) during winter

Macro scale:

The annual “wild” 0+ density component $D_{t+1,i}^{wild}$ is conditional on the number of spawners which were in the river section the year before. The number of potential spawners $S_{t,i}$ is obtained from an adult count to redd count relationship described in section 3.2 and appendix A.4 and brought to the same scale than the 0+ densities by dividing the number of potential spawners by the surface of habitat available for 0+ juveniles H_i . Following the literature available on this topic (Walters and Martell, 2004) we included a Beverton and Holt (1957) density dependence relationship between these two lifestages. The “wild 0+” density component $D_{t+1,i}^{wild}$ is assumed to follow a Normal distribution (log scale) Inter-annual variations around this density-dependence relationship are allowed and incorporated via the precision parameter τ^{D_wild} .

$$(Eq. A2.1) \quad \text{Log}(D_{t+1,i}^{wild}) | \mu_{t+1,i}^{D_wild}, \tau^{D_wild} \sim \text{Normal}(\text{Log}(\mu_{t+1,i}^{D_wild}), \tau^{D_wild})$$

$$(Eq. A2.2) \quad \mu_{t+1,i}^{D_wild} = \frac{S_{t,i}/H_i}{\alpha^{D_wild} + \beta^{D_wild} \times (S_{t,i}/H_i)} \times e^{\eta_i^{D_wild}}$$

A spatial effect $\eta_i^{D_wild}$ was incorporated to reflect geographical juvenile densities differences downstream and upstream of Langeac (Cuinat, 1988). The two parameters of the Beverton and Holt relationship α^{D_wild} and β^{D_wild} can be expressed in function of the slope a^{wild} and the asymptote of the relationship $Rmax^{wild}$ respectively.

$$(Eq. A2.3) \quad \alpha^{D_wild} = \frac{1}{a^{wild}}$$

$$(Eq. A2.4) \quad \beta^{D_wild} = \frac{1}{Rmax^{wild}}$$

The annual stocked 0+ juveniles density component is conditional on the number of 0+ stocked in the river section and the parameters of the Beverton and Holt relationship of the wild 0+. The stocked 0+ juveniles density component $D_{t+1,i}^{juv}$ is assumed to follow a Normal distribution (log scale). Inter-annual variations around this density-dependence relationship are allowed and incorporated via the precision parameter τ^{D-juv} .

$$(Eq. A2.5) \quad \text{Log}(D_{t+1,i}^{juv}) | \mu_{t+1,i}^{D-juv}, \tau^{D-juv} \sim \text{Normal}(\text{Log}(\mu_{t+1,i}^{D-juv}), \tau^{D-juv})$$

$$(Eq. A2.6) \quad \mu_{t+1,i}^{D-juv} = \frac{\text{Stock}_{t+1,i}^{juv}/H_i}{\frac{1}{e^{\eta_i^{D-wild}}} \times \alpha^{D-juv} + \beta_{t+1,i}^{D-juv} \times (\text{Stock}_{t+1,i}^{juv}/H_i)}$$

Where $\beta_{t+1,i}^{D-juv}$ is deterministically related the asymptote parameter $Rmax_{t+1,i}^{D-juv}$

$$(Eq. A2.7) \quad \beta_{t+1,i}^{D-juv} = \frac{1}{Rmax_{t+1,i}^{D-juv}}$$

The new asymptote parameter of the stocked 0+ juvenile can be seen as the available space left by the wild 0+ for the stocked 0+ for any given year t+1. This is calculated as the asymptote parameter of the “wild” Beverton and Holt relationship $Rmax^{wild}$ minus the average “wild” 0+ density of the year t+1 $\mu_{t+1,i}^{D-wild}$ (note that the spatial effect η_i^{D-wild} is removed)

$$(Eq. A2.8) \quad Rmax_{t+1,i}^{D-juv} = Rmax^{wild} - \left(\frac{\mu_{t+1,i}^{D-wild}}{e^{\eta_i^{D-wild}}} \right)$$

The assumption that stocked 0+ juveniles have an advantage over the stocked juveniles relies on the fact that stocked 0+ juveniles are introduced much later than the wild 0+ which will have the priority of residency over the stocked fish. This also reflects the difficulty that stocked 0+ overcome to install themselves in a new environment (fish farm vs natural river, obtain food, competition, predation).

In the model, the eggs stocked before 1996 are not considered. During this time period (1975 to 1996), there were 3 years during which eggs were stocked using different methodologies but there is not enough information available to input them in the model. Moreover, the quantity of eggs stocked is small. More information on these events can be found in annex A.3.

Every year, the number of egg incubators N^{inc} varies between 1 and 6. The stocked eggs density component is considered in a different way than the two other juvenile density components due to the very local impact of egg incubators (see App. A.3). Therefore, the average relationship between the density and the stocked eggs only involves for the each of the N^{inc} a survival parameter s^{egg} , the number of eggs stocked in the incubator $Stock^{egg}$ and the surface impacted by the egg incubator H^{inc}

The annual stocked eggs density produced by the egg incubators $D_{t+1,i}^{egg,tot}$ is assumed to follow a Normal distribution (log scale). Inter-annual variations around this survival relationship are allowed and incorporated via the precision parameter τ^{D-egg}

$$(Eq. A2.9) \quad \text{Log}(D_{t+1,i}^{egg,tot}) | \mu_{t+1,i}^{D-egg}, \tau^{D-egg} \sim \text{Normal}(\text{Log}(\mu_{t+1,i}^{D-egg}), \tau^{D-egg})$$

$$(Eq. A2.10) \quad \mu_{t+1,i}^{D-egg} = \sum_{j=1}^{N^{inc}} s^{egg} \times \frac{Stock_{t+1,i,j}^{egg}}{H_{i,j}^{inc}}$$

The annual stocked eggs density component $D_{t+1,i}^{egg}$ is then calculated as the annual stocked eggs density produced by the egg incubators $D_{t+1,i}^{egg,tot}$ rescaled relatively to the total nursing and rearing juvenile habitat H_i .

$$(Eq. A2.11) \quad D_{t+1,i}^{egg} = \frac{\sum_{j=1}^{N^{inc}} H_{i,j}^{inc}}{H_i} \times D_{t+1,i}^{egg,tot}$$

Finally the total density at a macro scale for a given year and river section $D_{t+1,i}^{tot}$ is the sum of all three density components:

$$(Eq. A2.12) \quad D_{t+1,i}^{tot} = D_{t+1,i}^{wild} + I_{t+1,i}^{D-juv} \times D_{t+1,i}^{juv} + I_{t+1,i}^{D-egg} \times D_{t+1,i}^{egg}$$

Where $I_{t+1,i}^{D-juv}$ and $I_{t+1,i}^{D-egg}$ are indicators of absence or presence of 0+ stocking or egg stocking on year t+1 in the river section i.

Micro scale:

For each electric fishing site a micro scale density can be calculated. In a similar way than the macro scale densities, it can be broken down in 3 components. Each component of the microscale density ($d_{t+1,i,k}^{wild}$, $d_{t+1,i,k}^{juv}$ and $d_{t+1,i,k}^{egg}$) are drawn from a Normal distribution (Log scale) with the mean parameter being the annual density of a given component at the macro scale ($D_{t+1,i}^{wild}$, $D_{t+1,i}^{juv}$ and $D_{t+1,i}^{egg}$) and a precision parameter ($\tau^{d.wild}$, $\tau^{d.juv}$ and $\tau^{d.egg}$) to account for inter site variations. Thus, for a given electric fishing site, the density of the wild component $d_{t+1,i,k}^{wild}$ of a local site k can be written as follow:

$$(Eq. A2.13) \quad \text{Log}(d_{t+1,i,k}^{wild}) | D_{t+1,i}^{wild}, \tau^{d.wild} \sim \text{Normal}(\text{Log}(D_{t+1,i}^{wild}), \tau^{d.wild})$$

The density of the stocked 0+ $d_{t+1,i,k}^{juv}$ component is:

$$(Eq. A2.14) \quad \text{Log}(d_{t+1,i,k}^{juv}) | D_{t+1,i}^{juv}, \tau^{d.juv} \sim \text{Normal}(\text{Log}(D_{t+1,i}^{juv}), \tau^{d.juv})$$

And the density of the stocked eggs $d_{t+1,i,k}^{egg}$ is:

$$(Eq. A2.15) \quad \text{Log}(d_{t+1,i,k}^{egg}) | D_{t+1,i}^{egg}, N_{t+1,i}^{inc}, \tau^{d.egg} \sim \text{Normal}\left(\text{Log}\left(\frac{D_{t+1,i}^{egg}}{N_{t+1,i}^{inc}}\right), \tau^{d.egg}\right)$$

Our data, show that a given electric fishing site can only be affected by one incubator, this is why the mean parameter is the density of stocked eggs at the macro scale $D_{t+1,i}^{egg}$ divided by the number of incubator which were loaded on a given year $t + 1$ in a given river section i .

Therefore for a given electric fishing site, the total 0+ juvenile micro scale density is:

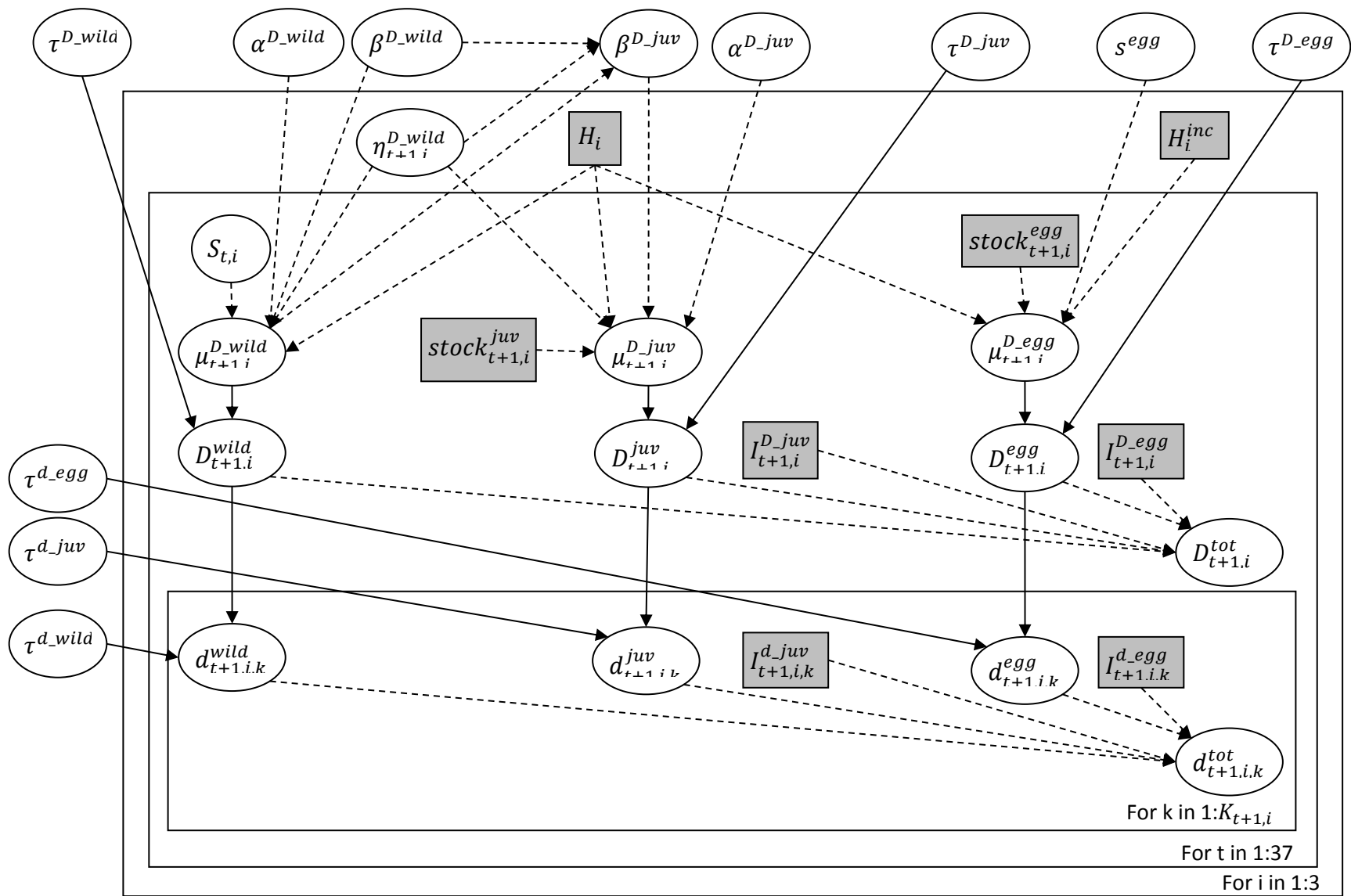
$$(Eq. A2.16) \quad d_{t+1,i,k}^{tot} = d_{t+1,i,k}^{wild} + I_{t+1,i,k}^{d_juv} \times d_{t+1,i,k}^{juv} + I_{t+1,i,k}^{d_egg} \times d_{t+1,i,k}^{egg}$$

Where $I_{t+1,i,k}^{d_juv}$ and $I_{t+1,i,k}^{d_egg}$ are indicators of absence or presence of 0+ stocking or egg stocking at the site k during year $t+1$ in the river section i .

The micro scale densities are related to electric fishing indice of abundance or successive removals the same way they are in the electric fishing calibration relationship (App. A.1)

The structure of conditional dependency of the relations described in equations A2.1-16 can be graphically summarized in a Directed Acyclic Graph (DAG) (Fig. A2.3).

Figure A2.3: Directed Acyclic Graph (DAG) of the model used to the average annual 0+ juvenile densities at macro and micro scales. Squares represent fixed quantities. All observed quantities are greyed. Arrows represent the parent-child dependencies between the different nodes: plain arrows represent probabilistic relationship between the parent(s) and child nodes, dashed arrows indicate deterministic relationship. The frames represent a repetition of structure over years t , river sections i and sites k . Nodes outside the frame are unknown parameters constant across sites.



Appendix A.3:

Egg stocking in the Allier catchment

1. Events of egg stocking from 1977 to 2011

In 1977, stocking of about 100 000 eggs in 15 streams of the Allier river(Fig. A3.1):

1. ruisseau du Pradel (Le Pradel amont st julien chazes ?)
2. ruisseau de Ste Marie desChazes
3. Ruisseau de Metou
4. ruisseau de Guissou (vereuges)
5. ruisseau le merdansson (rognac)
6. la fioule
7. ruisseau de cizieres (Morange)
8. ruisseau de Bancillon (st privat du dragon)
9. la besque
10. ruisseau de Darne (St Julien des Chazes)
11. La Desges
12. Le Ramade (ruisseau de peyrusse)
13. La Cronce
14. Le ruisseau d'Arcon
15. Le Ceroux

In 1996, egg incubator of Laprade / crouce (60 000 eggs)

In 1997, egg incubator of Laprade / crouce (52 400 eggs)

In 1998, three egg incubators (Laprade/crouce, gourdon and véreuges, 50 000 eggs each).

From 1999 to 2002, 50 000 eggs on each of the 6 egg incubators:

1. Arçon
2. Ruisseau du mas
3. Crouce
4. Ruisseau de Peyrusse/le ramade
5. Guissou
6. Ruisseau de Peyre/monistrol

In 2003, 80 000 eggs in each of the 6 egg incubators.

In 2004, 50 000 eggs in each of the 6 egg incubators.

In 2005, about 84 000 eggs in each of the 6 egg incubators.

From 2006 to 2008, 50 000 eggs in each of the 6 egg incubators.

In 2009, 65 000 eggs in 4 egg incubators (1,2,3,4).

From 2010 to 2011, 50 000 eggs in 4 egg incubators (1,2,3,4).

2. Location of egg incubators (since 1996)

The six egg incubators are located on small affluents of the Allier river (Fig. A3.2). Two are located in sector 3 which became a “refuge area” where no stocking is allowed in 2009 (Fig. A3.3 and Fig. A3.4). The four of them are located in sector 4 (arçon, ruisseau du mas, cronce and ruisseau de Peyrusse, Fig. A3.5, A3.6, A3.7 and A3.8).

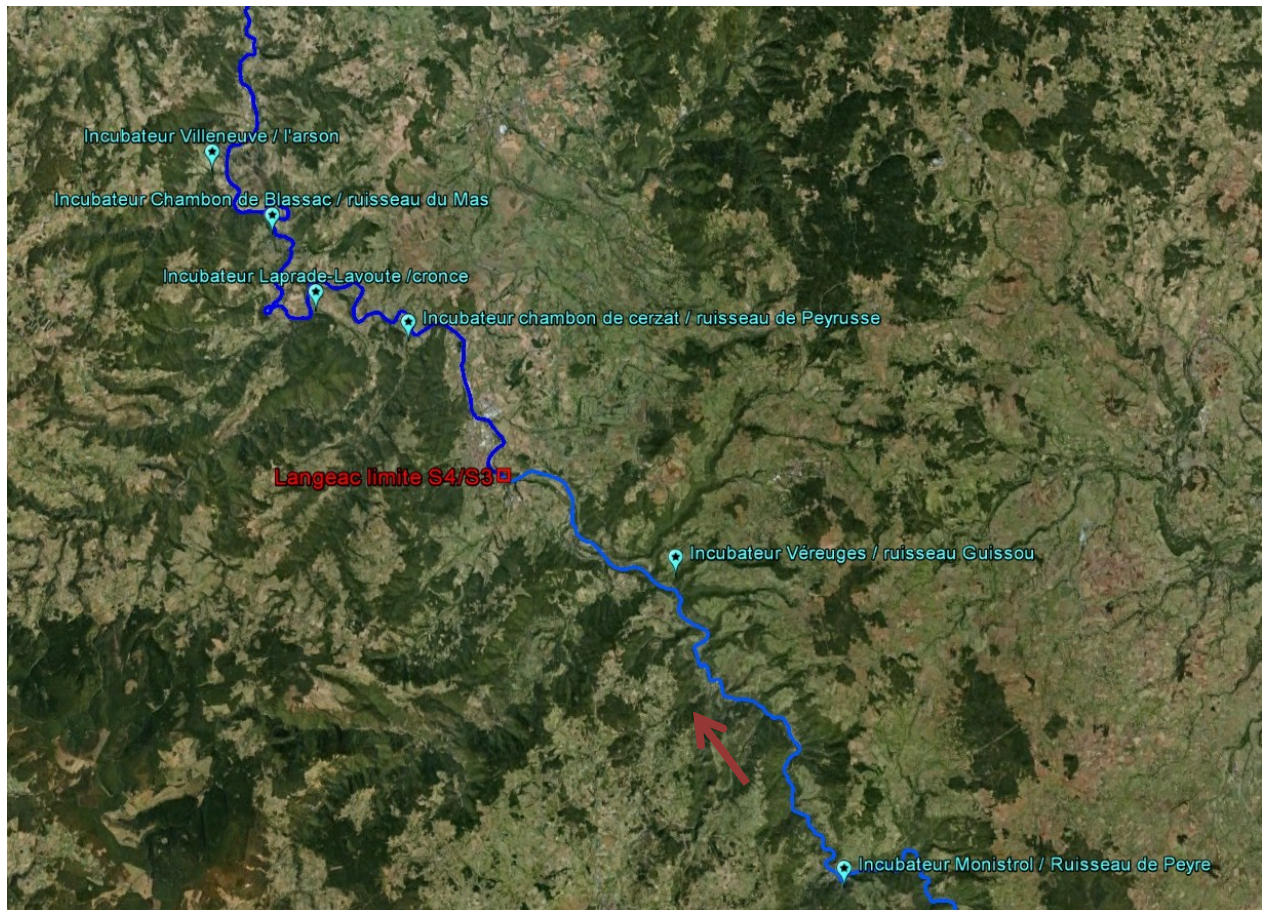


Figure A3.2: Localisation of the six egg incubators. Red arrow indicates upstream/downstream direction.

For each incubators we calculated a surface potentially affected by the incubator. Beall *et al.* (1994) found that 89 % of fry were found as 0+ in october following emergence within 1600m downstream of the egg nest. This study was carried out in a small tributary so transferring this distance in the Allier catchment is fairly conservative. We provide a map for each incubator, with the surface potentially affected by the incubator as well as an indication of the presence of electric fishing sites within this zone.

Sector 3 : Monistrol



Figure A3.3: Potential zone of influence of the egg incubator located in the ruisseau de Peyre and electric fishing site within this zone (1600m from the egg incubator to the furthest point downstream). Red arrows indicate upstream/downstream direction.

The potential zone of influence of this egg incubator is 16411 m². There is one electric fishing site within this zone. Unfortunately, it was only fished before the use of the egg incubator.

Sector 3: Véreuges / ruisseau Guissou

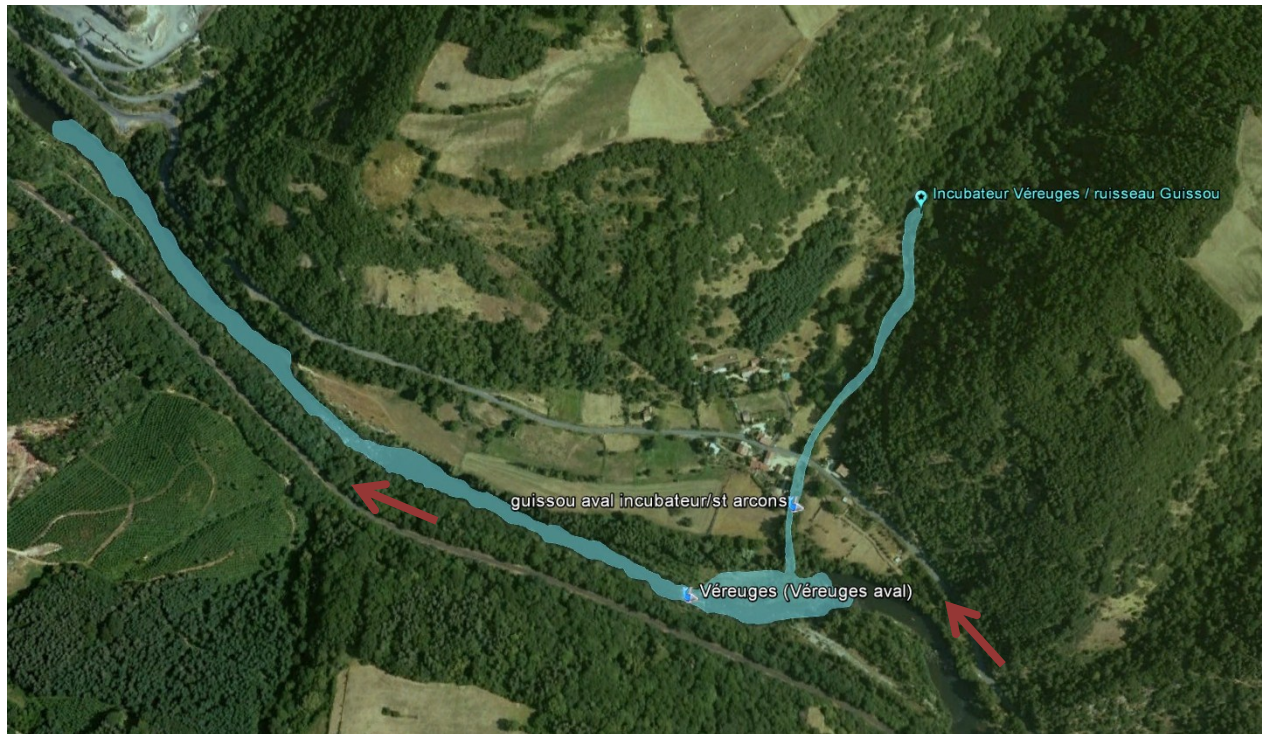


Figure A3.4 : Potential zone of influence of the egg incubator located in the ruisseau de Guissou and electric fishing site within this zone (1600m from the egg incubator to the furthest point downstream). Red arrows indicate upstream/downstream direction.

The potential zone of influence of this egg incubator is 16564 m². There are two electric fishing sites within this zone which were fished only before 2004.

Sector 4: Chambon de Cerzat / ruisseau de Peyrusse:



Figure A3.5: Potential zone of influence of the egg incubator located in the ruisseau de Peyrusse and electric fishing site within this zone (1600m from the egg incubator to the furthest point downstream). Red arrows indicate upstream/downstream direction.

The potential zone of influence of this egg incubator is 9213 m². There is one electric fishing site within this zone. Unfortunately it was fished only once in 2009.

Sector 4: Lavoute / cronce:



Figure A3.6: Potential zone of influence of the egg incubator located in the ruisseau Cronce and electric fishing site within this zone (1600m from the egg incubator to the furthest point downstream). Red arrows indicate upstream/downstream direction.

The potential zone of influence of this egg incubator is 8355 m². There are two electric fishing sites within this zone. The sites stopped being fished in 2000.

Sector 4: Chambon de Blassac / ruisseau du mas:

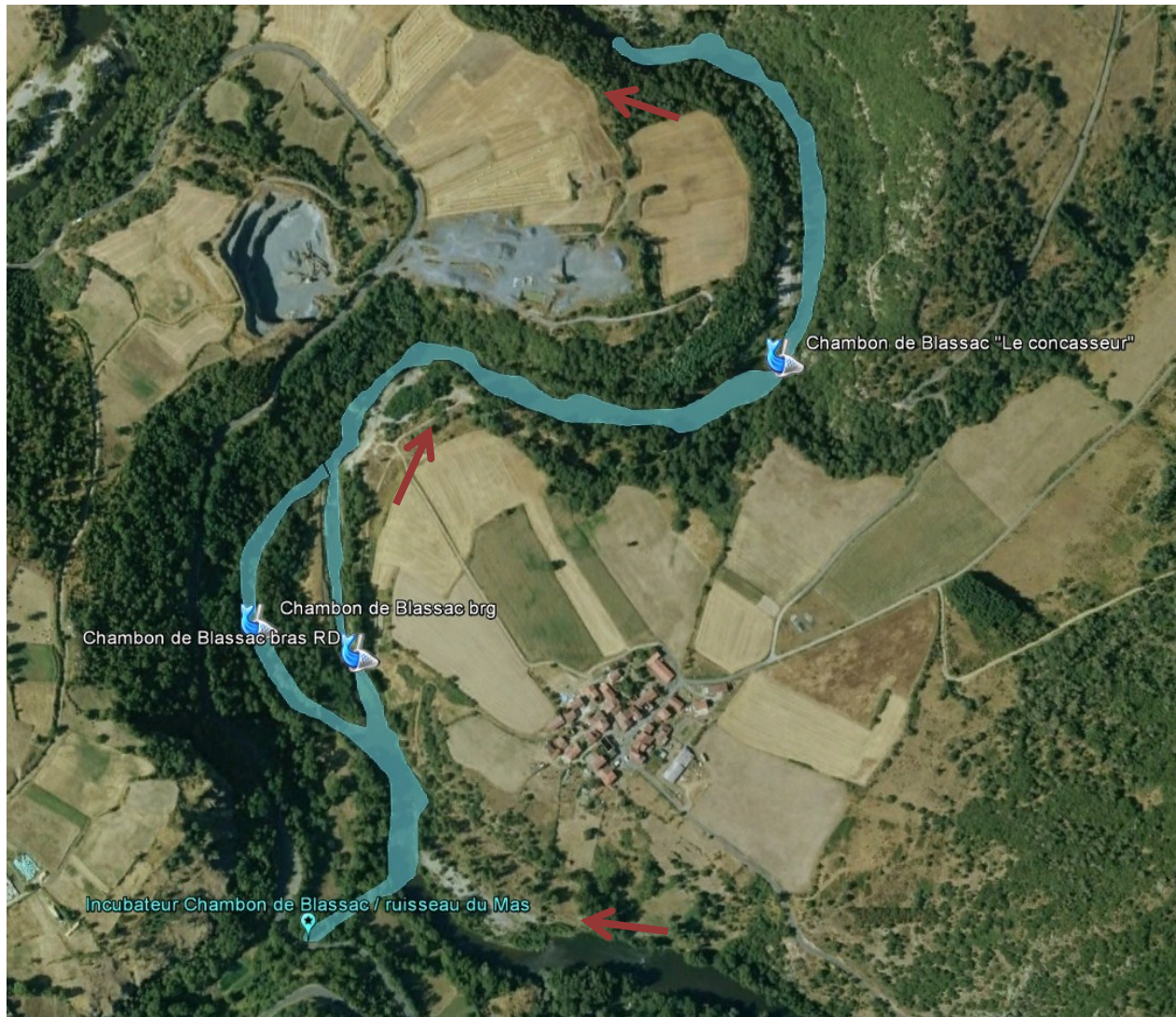


Figure A3.7 : Potential zone of influence of the egg incubator located in the ruisseau du Mas and electric fishing site within this zone (1600m from the egg incubator to the furthest point downstream). Red arrows indicate upstream/downstream direction.

The potential zone of influence of this egg incubator is 10556 m². There are three electric fishing sites within this zone. "Chambon de Blassac bras RD" was fished regularly over the 1994-2011 time period while the two other sites were only fished occasionally.

Sector 4: Villeneuve / l'Arson:



Figure A3.8: Potential zone of influence of the egg incubator located in the ruisseau du Mas and electric fishing site within this zone (1600m from the egg incubator to the furthest point downstream). Red arrows indicate upstream/downstream direction.

The potential zone of influence of this egg incubator is 12754 m². There are no electric fishing sites within this zone.

References:

Beall E., Dumas J., Claireaux D., Barrière L. and Marty C. (1994) Dispersal patterns and survival of Atlantic salmon (*Salmo salar* L.) juveniles in a nursery stream. *ICES J. Mar. Sci.* 51 (1): 1-9.

Appendix A.4:

Potential spawners to redd counts relationship

Estimating spatial distribution of Atlantic salmon escapement using redd counts despite changes over time in counting procedure: application to the Allier River population

Guillaume J.R. Dauphin^{1,2,3}, Catherine Brugel⁴, Marion Hoffmann-Legend⁵, Etienne Prévost^{1,2}

¹INRA, UMR 1224 ECOBIOP, Aquapôle, Ibarron, 64310, Saint-Pée-sur-Nivelle, France

²UPPA, UMR 1224 ECOBIOP, UFR Sciences et Techniques Côte Basque, Campus Montaury, 64600, Anglet, France

³Department of Fisheries and Oceans, Science Branch, Northwest Atlantic Fisheries Center, 80 East White Hills Road, PO Box 5667, St John's, NL, Canada

⁴ONEMA, Délégation interrégionale Massif Central, 9 allée des Eaux et Forêts, 63370, Lempdes, France

⁵Logrami, 8 rue de la Ronde, 03500, Saint-Pouçain sur Sioule, France

Accepted for publication April 16, 2013

Abstract – In salmonid species, such as Atlantic salmon (*Salmo salar* L.), the most frequent type of data set available related to adult escapements are redd counts. When collected over a broad spatio-temporal domain, redd counts data are of great interest for tracking the variation through time of the spatial distribution of the potential spawners. This is important for management purposes when the habitat quality is variable across river sections of a catchment or when the spatial distribution can vary depending on management actions or on environmental factors. However, long-term data sets are prone to changes in data collection methodology. In this article, we present a new hierarchical Bayesian modelling approach that allows both (i) to account for a change in the data collection procedure and (ii) to analyse the variation through time of the potential spawners' spatial distribution. The value of the proposed approach is demonstrated by its application to the Atlantic salmon redd counts data collected in Allier (France) catchment from 1977 to 2011. The Allier can be divided into three main sections according to management and habitat considerations, and an important change occurred in the redd data collection in 1997: counts by foot or by boat were replaced by counts from a helicopter. A significant effect of this change on methodology is detected: less redds counted when using the helicopter counts. However, its explicit consideration in the modelling makes little difference with regard to the estimates of potential spawner abundance and their associated uncertainty.

Key words: Atlantic salmon; Bayesian modelling; population abundance; redd counts; spawner

Introduction

Accurate estimates of fish escapements are important for fisheries management and for conservation to evaluate the status of a population. This is particularly true for emblematic species such as Atlantic salmon (*Salmo salar* L.) for which there is important conservation stakes. However important they are, accurate adult escapement estimates are difficult to obtain, mainly due to the lack of informative long-term data sets for most of the Atlantic salmon populations.

One of the most frequent types of data set available related to adult escapements is redd counts (Hay 1987; Emlen 1995; Isaak et al. 2003; Murdoch et al. 2010). A redd is the nest structure that salmonid female digs to lay their eggs. Redd counts data sets can be affected by various factors related to the sampling process or the observer's experience (Dunham et al. 2001; Muhlfeld et al. 2006). Most often, there is no data available on these factors or it is not possible to distinguish all the factors explicitly. This means that redd counts are noisy measurements of the adult escapement. It has thus been argued that

Correspondence: Guillaume J.R. Dauphin, Department of Fisheries and Oceans, Science Branch, Northwest Atlantic Fisheries Center, 80 East White Hills Road, PO Box 5667, St John's, NL, Canada. E-mail: Guillaume.Dauphin@dfo-mpo.gc.ca

Dauphin et al.

redd counts should not be used to assess salmonid escapement (Parsons & Skalski 2010). Nonetheless, redd counts are often the only data available throughout long time series (ICES 1995; Crozier et al. 2003). Therefore, the issue is not to decide whether redd counts should be discarded or not, but rather how to make the best use of these data sets to estimate adult escapement while appropriately reflecting their associated uncertainty. To do so, Dauphin et al. (2010) proposed a method relying on a hierarchical Bayesian model (HBM).

Redd counts data sets collected over a broad spatio-temporal domain are of great interest for tracking the variation through time of the spatial distribution of the potential spawners. This is important for management purposes when the habitat quality is variable across river sections of a catchment or when the spatial distribution can vary depending on management actions or on environmental factors. However, long-term data sets are also prone to changes in data collection methodology (Brun et al. 2011).

In the present article, we show how Dauphin et al. (2010) modelling approach can be used and expanded to both (i) account for a change in the data collection procedure and (ii) analyse the variation through time of the potential spawners' spatial distribution. The first issue is addressed by the introduction of a data collection procedure effect. The importance of accounting for the change in the data collection methodology is assessed by a formal comparison with another model ignoring the change in the data collection. The second is dealt with by connecting Dauphin et al. (2010) potential spawners to redd model to an explicit representation of the spatial distribution process of the potential spawners. The expanded modelling approach is demonstrated in a case study carried out on the Atlantic salmon population of the Allier River (France). The Atlantic salmon population has been severely declining in this catchment over the last decades and presents crucial conservation interest because of its unique genetic (Perrier et al. 2011) and phenotypic (Cuinat 1988) characteristics. Adults have to migrate at least 700 km to reach the first spawning grounds, and the Allier is the last large river holding Atlantic salmon in the southern range of its distribution.

Redd counts are available from 1977 to 2011 in the Allier catchment. But an important change occurred in the redd data collection in 1997: counts by foot or by boat were replaced by counts from a helicopter. The Allier can be divided into three main sections according to management and habitat considerations. The uppermost section became available to returning Atlantic salmon adults in the middle of the time series. The lowermost section is of poorer habitat quality for reproduction and juvenile rearing.

Three fish counters were installed progressively during the time series along the Allier River at the downstream end of each river section. They provide exhaustive or partial returning adult counts in the different river sections considered. Years for which both redd and adult counts are simultaneously available are used to build a calibration relationship relating the two types of data. Once estimated, the parameters of this relationship are then used to derive potential spawner estimates in years for which only redd counts are available. The model is described and applied to the available data to provide retrospective estimates of the abundance of potential spawners in the three river sections of the Allier catchment from 1977 to 2011.

Materials and methods

Study site and data available

The Allier River (44° 35' 23" N 3° 48' 04" E) is the main tributary of the Loire. It drains a 14,310-km² catchment and flows into the Loire about 421 km from its source. To reach the first spawning grounds in the Allier River, adult salmon have to migrate for at least 700 km from the mouth of the Loire River (Fig. 1). According to the description of the habitat quality in the Allier River made by Cuinat (1988), the area downstream of Langeac is poor for salmon spawning and juvenile rearing. Upstream from Langeac, much better spawning and nursery habitat is found because of steeper gradient and better water quality.

The Allier catchment is divided into three river sections delimited by the adult counting stations (Fig. 1): between Vichy and Langeac, between Langeac and Poutès and upstream from Poutès. They are represented by the index $i = \{1, 2, 3\}$. Data were collected between 1977 and 2011 represented by the index $t = \{1, \dots, 35\}$.

The 4 data sets used for this study are given in Tables S1 and 2. They include the following: annual redd counts $R_{t,i}$ and the associated proportion of spawning areas surveyed $p_{t,i}^R$, annual number of adults moving upstream of the three counting stations at Vichy, Langeac and Poutès (Fig. 1; N^V , N^L , N^P , respectively) and the number of adults removed before spawning to be used as broodstock in a hatchery B_t . Redds are counted around December once most of the females have spawned (Bach et al. 2010). From 1977 to 1996, the counting operations were carried out by foot or by boat. Since 1997, the counts were fulfilled by means of a helicopter (Ros 1997). The efficiency of the counting station at Langeac is dependent on the water conditions: at high flows, the structure is submerged and fish may move upstream without being counted. As a consequence,

Estimating spatial distribution of Atlantic salmon escapement using redd counts

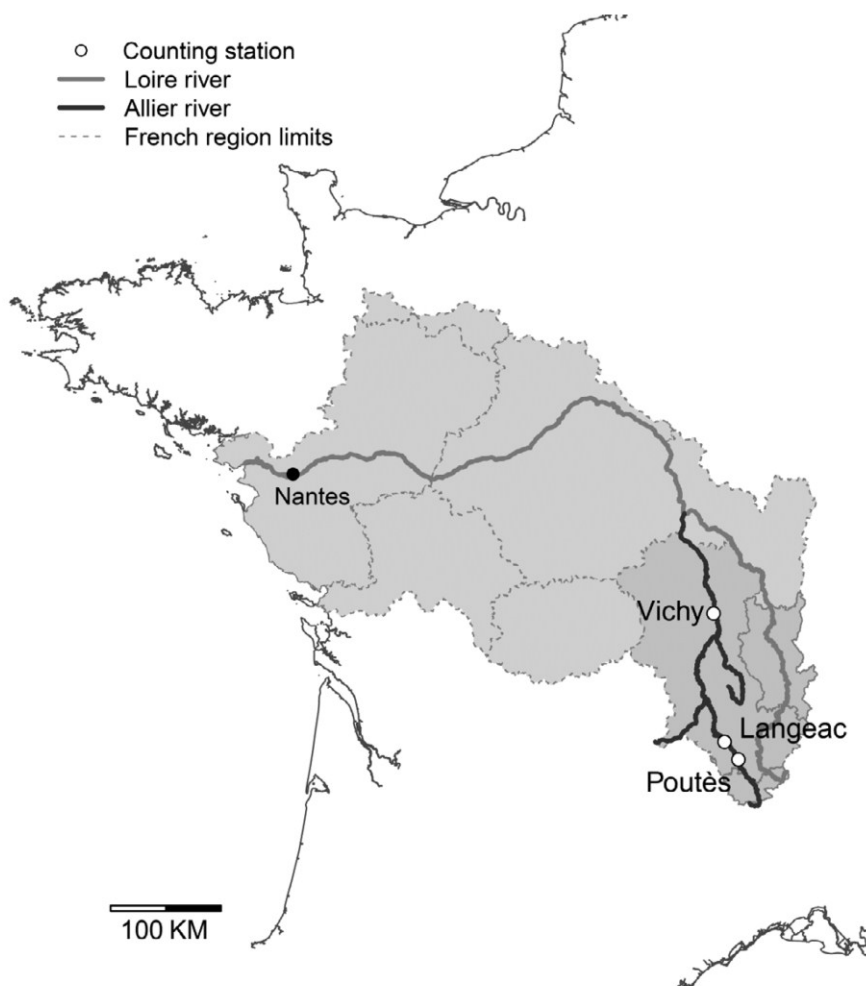


Fig. 1. Location of the Loire river and the Allier river and the three adults counting station in Vichy, Langeac and Poutès.

the count data provided by this station (from 2003 to 2008 only) are used as a minimum number of fish moving upstream of Langeac. The two other adult counting stations were considered to count exhaustively the adults migrating upstream. Fish can only move upstream by going through two fishways at Vichy and a fish lift at Poutès. These facilities are continuously surveyed by means of video-recording. Counting errors, if any, are thus negligible relative to the interannual variations of the escapement numbers. Adult counts are available from 1997 to 2011 at Vichy and from 1986 to 2011 at Poutès.

Modelling

Henceforth, the notation $a|b \sim f(b)$ means the random variable a (whether unobservable or observa-

ble) is distributed according to the probability distribution function (PDF) f conditionally on b . Unobservable quantities are necessarily unknown, but observable quantities may be unknown as well in case of missing data. Numbers of adults moving upstream of Vichy, Langeac and Poutès (N^V , N^L and N^P) are observable quantities, but they have been observed only during part of the full time series covered by this study. At Vichy, data are missing for N^V up to 1996. Partial counts are available at Langeac for a few of the last years only (2003–2008); hence, data are essentially missing for N^L over the entire time series. Although counts at Poutès are not available before 1986, there is no missing data for N^P . Indeed, counts have always been carried out once the fish lift giving access to the upstream of Poutès was built.

Dauphin et al.

Models description

Spatial repartition of potential spawners

The number of adult salmon returning in the Allier River in year t and passing above Vichy N_t^V is assumed to follow a lognormal distribution.

$$N_t^V | \mu^V, \tau^V \sim \text{LogNormal}(\log(\mu^V), \tau^V) \quad (1)$$

with μ^V and τ^V the underlying mean and precision (in log scale) parameters of the number of adult salmon migrating upstream of Vichy's counting station.

Upstream migration is viewed as a random process, and for every year of the time series, salmon adults have a probability p_t^L to reach the area upstream of Langeac counting station. The number of adults reaching the area upstream of Langeac N_t^L is assumed to follow a binomial distribution.

$$N_t^L | N_t^{V-B}, p_t^L \sim \text{Binomial}(N_t^{V-B}, p_t^L) C(N_t^{L-\min}), \quad (2)$$

where N_t^{V-B} is the number of adults returning to Vichy minus the number of fish taken out as broodstock. The term $C(N_t^{L-\min})$ indicates that the distribution is left-censored by the minimum adult counts observed at Langeac counting station $N_t^{L-\min}$.

In the absence of observations for the factors affecting the probability of reaching the upstream area, we rely on the parsimonious hypothesis that all annual probabilities p_t^L are exchangeable and drawn from a normal distribution (logit scale) with common mean and precision parameters, μ^L and τ^L , respectively.

$$\text{Logit}(p_t^L) | \mu^L, \tau^L \sim \text{Normal}(\text{Logit}(\mu^L), \tau^L) \quad (3)$$

As mentioned in the study site section, during the first 9 years of the time series (1977–1985), only the area downstream of Poutès dam is accessible to salmon spawners. From 1986 (for $t = \{10, \dots, 35\}$), after the construction of a fish lift, the adults were allowed to move upstream of Poutès dam. This is modelled in a similar way to that of the fish moving upstream of Langeac. Adult fish reaching the area upstream of Langeac N_t^L have a probability p_t^P of reaching the area upstream of Poutès dam. Adults reaching the area above Poutès dam N_t^P are drawn from a binomial distribution:

$$N_t^P | N_t^L, p_t^P \sim \text{Binomial}(N_t^L, p_t^P) \quad (4)$$

$$\text{Logit}(p_t^P) | \mu^P, \tau^P \sim \text{Normal}(\text{Logit}(\mu^P), \tau^P) \quad (5)$$

The annual probability of moving upstream of Poutès p_t^P is drawn from a normal distribution (logit

scale) with mean and precision parameters, μ^P and τ^P , respectively.

The number of potential spawners is then calculated for each of the three river sections of the Allier catchment. The term 'potential spawner' refers to the number of adults reaching one of the three river sections before spawning. (This does not mean that all these adults will actually breed.) The potential spawners in the river section between Vichy and Langeac counting stations are obtained as follows:

$$S_{t,1} = N_t^V - B_t - N_t^L \quad (6)$$

Before the opening of the river section upstream of Poutès dam (up to 1985), the number of potential spawners in the Langeac–Poutès section $S_{t,2}$ is equal to the number of adults moving upstream of Langeac:

$$S_{t,2} = N_t^L \quad (7a)$$

After the opening of the river section upstream of Poutès dam (from 1986), the number of potential spawners $S_{t,2}$ in the Langeac–Poutès River is as follows:

$$S_{t,2} = N_t^L - N_t^P \quad (7b)$$

Finally, the number of potential spawners in the river section upstream of Poutès is equal to the number of adults moving upstream of Poutès dam:

$$S_{t,3} = N_t^P \quad (8)$$

Potential spawners to redd counts relationship

We used a formulation very similar to the one proposed by Dauphin et al. (2010). For each year t and each river section i , the number of redds $R_{t,i}$ is assumed to follow a Poisson distribution:

$$R_{t,i} | S_{t,i}, k_{t,i}, p_{t,i}^R, \gamma_k \sim \text{Poisson}(S_{t,i} \times k_{t,i} \times p_{t,i}^R \times \gamma_k) \quad (9)$$

The number of redds $R_{t,i}$ is dependent on the product of the number of potential spawners in a given river section $S_{t,i}$, the redd:potential spawner ratio $k_{t,i}$, the proportion of spawning grounds surveyed during the redd counts data collection $p_{t,i}^R$ and the data collection methodology effect γ_k . The index k stands for the counting methodology: $k = 1$ from 1977 to 1996 when the counts are carried out by foot or boat and $k = 2$ from 1997 to 2011 when the counts are carried out by helicopter. For the sake of identifiability, γ_1 is set equal to 1, γ_2 remain unknown and to be estimated (model 2). In this general formulation, the hypothesis that the counting methodology has no effect can be modelled as a special case where

Estimating spatial distribution of Atlantic salmon escapement using redd counts

Table 1. Prior distributions of the main parameters of model 1 (accounting for change in redd data collection methodology) and their associated posterior distribution ($\epsilon = 0.001$).

Parameter's symbols and descriptions	Prior	Posterior							
		Mean	SD	2.5%	25%	50%	75%	97.5%	
μ^V	Mean number of adults migrating upstream of Vichy	Uniform (1,5000)	423	57.95	313	384	422	462	541
τ^V	Precision of adults migrating upstream of Vichy	Gamma (0.01,0.01)	3.764	1.463	1.635	2.704	3.512	4.570	7.219
μ^L	Mean probability of migrating upstream of Langeac	Inv. Logit (Normal (0, ϵ))	0.302	0.038	0.231	0.276	0.300	0.326	0.380
τ^L	Precision of probability of migrating upstream of Langeac	Gamma (0.01,0.01)	17.67	28.91	1.986	5.093	9.194	17.94	88.33
μ^P	Mean probability of migrating upstream of Poutès	Inv. Logit (Normal (0, ϵ))	0.308	0.062	0.193	0.265	0.305	0.349	0.435
τ^P	Precision of probability of migrating upstream of Poutès	Gamma (0.01,0.01)	0.877	0.390	0.363	0.611	0.803	1.051	1.799
$\mu^{k_{down}}$	Mean downstream redd:potential spawner ratio	Gamma (1, ϵ)	0.857	0.219	0.528	0.706	0.825	0.973	1.371
$\mu^{k_{up}}$	Mean upstream redd:potential spawner ratio	Gamma (1, ϵ)	1.782	0.417	1.123	1.487	1.728	2.015	2.770
β	Inverse-scale of redd:potential spawner ratio	Gamma (0.01,0.01)	2.068	0.615	1.069	1.629	1.998	2.422	3.438
γ_2^H	Helicopter effect	Gamma (1,1)	0.667	0.164	0.392	0.549	0.652	0.7651	1.033

$\gamma_1 = \gamma_2 = 1$ (model 1). The redd:potential spawner ratio is drawn from a Gamma distribution:

$$k_{r,i} | \alpha_i, \beta \sim \text{Gamma}(\alpha_i, \beta) \quad (10)$$

$$\alpha_i = \mu_i^k \times \beta \quad (11)$$

The $k_{r,i}$ distribution is thus governed by two hyperparameters: the mean μ_i^k and the inverse scale β . Earlier model versions showed differences in the potential spawners to redds relationship between the river section downstream of Langeac and the two other river sections upstream of Langeac. To reflect these differences, two mean hyperparameters were introduced such as: $\mu_1^k = \mu^{k_{down}}$ and $\mu_2^k = \mu_3^k = \mu^{k_{up}}$.

Bayesian inference

Weakly informative and independent prior probability distributions were assigned to model parameters (Table 1) to make sure the posterior inferences primarily reflect the information brought by the observed data. The joint posterior distribution of all the model unknowns (i.e., unobservable quantities and observables in case of missing data) was approximated using MCMC sampling (Gelman et al. 2003). All computations were carried out with the OpenBUGS[®] software (version 3.2.1; Thomas et al. 2006; Spiegelhalter et al. 2007) and R (version 2.14.0, www.r-project.com).

To test the convergence of the MCMC sampling on the model parameters, three MCMC chains with contrasted starting points were ran in parallel. The Gelman–Rubin (Brooks & Gelman 1998) diagnostics were used as implemented by OpenBUGS[®]. These diagnostics indicated that good mixing of the MCMC chains was obtained after 10^6 iterations. One in every 100 iteration was retained to obtain a sample of 10,000 values, the

first 2000 were discarded to remove the influence of the MCMC starting values. The 8000 values left were then used to approximate posterior distributions of all the model unknowns.

Posterior checking and model comparison

Following the approach proposed by Gelman et al. (1996), the consistency between the assumed model and the data was checked by means of posterior predictive assessment techniques. These techniques extend classical goodness-of-fit tests in the Bayesian setting by averaging over the posterior distribution of unknown quantities of the model. The omnibus chi-square statistic, a measure of discrepancy between the model and the data, was used (see Gelman et al. 2003 for detailed description).

$$\chi^2(X, \theta) = \sum_{t,i} \frac{(X_{t,i} - E(X_{t,i} | \theta_{t,i}))^2}{\text{Var}(X_{t,i} | \theta_{t,i})}, \quad (12)$$

with X being any observable quantity and θ the set of unknown parameters controlling the probability distribution of X . The realised discrepancies $\chi^2(R_{t,i}, \theta^R)$, $\chi^2(N_{t,i}, \theta^N)$ and $\chi^2(N_{t,i}^{Data}, \theta^{N-Data})$, computed with the observed values of $R_{t,i}$, $N_{t,i}$, and $N_{t,i}^{Data}$ (only years when adult counting data are available), were compared with the corresponding posterior predicted chi-square discrepancies $\chi^2(R_{t,i}^{rep}, \theta^R)$, $\chi^2(N_{t,i}^{rep}, \theta^N)$ and $\chi^2(N_{t,i}^{rep-Data}, \theta^{N-Data})$. The later were computed with a posteriori replicated data $(R_{t,i}^{rep}, N_{t,i}^{rep}$ and $N_{t,i}^{rep-Data})$ as simulated by the model.

The deviance information criterion (DIC, Spiegelhalter et al. 2002) was calculated to formally compare the general model accounting for the change in the redd counting methodology (model 2) with its simplified version considering that this change has no effect (model 1).

Results

The chi-square discrepancy statistics did not reveal any inconsistency between the two models and the data (Table 2), but the two models had significantly different DICs: 781.4 for the general model (model 1) and 695.9 for the model accounting for the change in the redd counting methodology (model 2). The methodology effect γ was found to be significant ($P(\gamma < 1) = 0.96$, Table 1), that is, there is on average a third less redd counted per potential spawner when data are collected using a helicopter ($\gamma = 0.667$, Table 1). Given these results, the model incorporating a redd counting method effect is favoured, and its results are presented in the sequel.

All the parameters of the model were significantly updated from their prior distributions (Table 1). The average redd:potential spawner ratio downstream and upstream of Langeac counting station $\mu^{k_{down}}$ and $\mu^{k_{up}}$ was significantly different ($P(\mu^{k_{up}} > \mu^{k_{down}}) = 0.99$). On average, a potential spawner is related to 0.857 counted redd in the section downstream of Langeac, whereas this figure is doubled in the sections upstream of Langeac (1.782 counted redds for one potential spawner, Table 1, Fig. 2). Some strong variations can be found in the annual redd:potential spawner ratio, with $k_{i,i}$ reaching occasionally values around 4 (e.g., upstream of Poutès in 2009, Fig. 2).

While the number of potential spawners reaching the section upstream of Poutès is known for each year, the number of potential spawners settling in the Vichy–Langeac and Langeac–Poutès sections has to be estimated each year. During the last thirty years, the Vichy–Langeac, Langeac–Poutès and upstream of Poutès sections received on average 316, 106 and 55 potential spawners, respectively (Fig. 3a–c). There is no clear trend observed during the period of time considered. These potential spawners are estimated with different levels of uncertainty. When no information about adult counts is available, the CVs of annual potential spawners are fairly high (ranging from 28% to 89%). When adult counts become available at Vichy counting station, the CVs of potential

spawners in the Vichy–Langeac sections are significantly reduced (ranging from 8% to 13%). There is also a reduction in the CVs for potential spawners in the Langeac–Poutès sections, but they remain high (ranging from 27% to 42%). On average, two-third of the potential spawners stay in the lower part of the catchment between Vichy and Langeac, 25% of the total number of potential spawners stay between Langeac and Poutès and <10% of the potential spawners migrate upstream of Poutès (Fig. 3d–f).

The probabilities for potential spawners to move upstream of Langeac and Poutès (p_i^L and p_i^P) follow two different patterns. The probability of moving upstream of Langeac is on average 0.302, with a low variability across years. The probability of moving upstream of Poutès conditionally on the probability of having moved upstream of Langeac is on average 0.308, but is highly variable, with yearly mean probabilities ranging from 0.04 to 0.77 (Table 1, Fig. 4).

Discussion

In this study, the model developed by Dauphin et al. (2010) relating adult counts to redd counts is adapted and combined with a spatial repartition model to provide potential spawner estimates for three river sections of the Allier catchment during a thirty-year period. Two models were tested: the first one ignoring the change in the redd data collection procedure (model 1) and the second one taking it into account (model 2). A significant effect of this change is detected. The two models produce similar estimates of the unknowns of ultimate interest (i.e., potential spawner abundances), although model 2 generally produces estimates slightly more uncertain than model 1 (see Fig. 5c,d). Because of the significant methodology effect, a lower DIC and its more general formulation, the model 2 was retained.

The model relies on a stationarity hypothesis regarding the redd:potential spawner ratio parameter $k_{i,i}$ and the probabilities of moving upstream of Langeac p_i^L and Poutès p_i^P (i.e., their mean and variance do not vary over time). Posterior checking of the model residuals (not reported here) indicates that there

Table 2. Posterior model checking: Bayesian P -values of chi-square statistics based on data replication technique for model 1 and model 2.

	P-values					
	$P(\chi^2(R^{rep}, \theta^R) \geq \chi^2(R, \theta^R))$		$P(\chi^2(N^{rep}, \theta^N) \geq \chi^2(N, \theta^N))$		$P(\chi^2(N^{rep_Data}, \theta^N) \geq \chi^2(N^{Data}, \theta^N))$	
	Model 1	Model 2	Model 1	Model 2	Model 1	Model 2
Vichy–Langeac	0.4981	0.4890	0.5292	0.5075	0.3884	0.3980
Langeac–Poutès	0.5189	0.5149	0.5002	0.5047	0.4954	0.5045
Upstream of Poutès	0.4315	0.6666	0.4953	0.5045	-	-

Estimating spatial distribution of Atlantic salmon escapement using redd counts

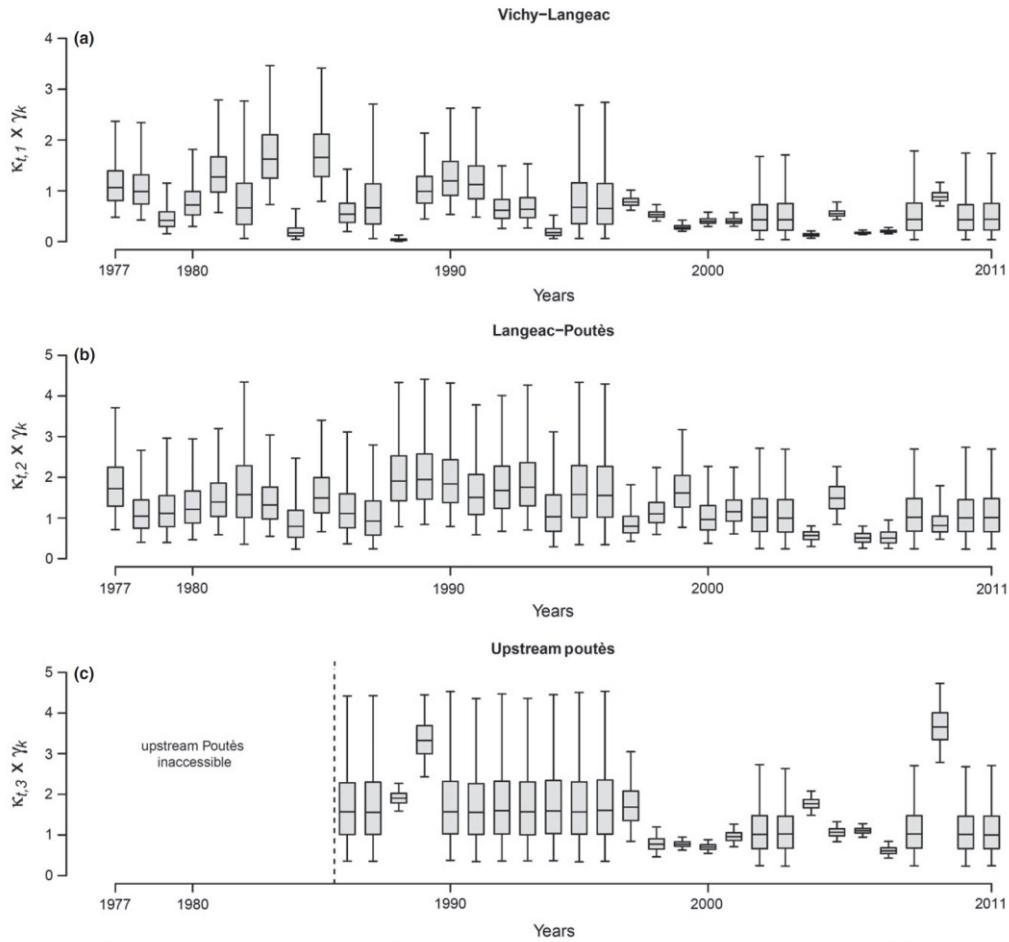


Fig. 2. Model 2's (accounting for change in redd data collection methodology) posterior distribution of the product of the annual redd: potential spawner ratio $k_{t,i}$ and the methodology effect γ_k for each river sections of the river Allier: (a) Vichy-Langeac, (b) Langeac-Poutès and (c) upstream of Poutès. Boxplots indicate the 2.5th, 25th, median, 75th and 97.5th percentiles.

is no reason to suspect that this hypothesis is wrong. The redd:potential spawner ratio $k_{t,i}$ aggregates several processes/factors. It includes mortality of adults returning in each river section before they can spawn (Baisez et al. 2011), the spawners sex ratio, the number of redds dug by each female and the number of redds counted for each redd actually dug. All these processes/factors might be trended over time, but there is no indication of such oriented changes in our case. The model could easily be altered to accommodate nonstationarity by applying time series modelling techniques to the $k_{t,i}$ instead of the full exchangeability approach retained here.

The redd:potential spawner ratios $k_{t,i}$ in the lower part of the catchment are on average two times

lower than in the upper part of the catchment (on average, 0.86 redds per potential spawners downstream of Langeac and 1.78 upstream of Langeac when counts are carried out by foot or boat). Average and annual values of the redd:potential spawner ratio are within the range of what is encountered in Atlantic salmon populations (de Gaudemar et al. 2000) with the only exception of 2009 in the section upstream of Poutès. Higher redd:potential spawner ratios in the upstream part of the catchment could be explained by a sex ratio more biased towards female in the higher part of the catchment. It could be equally well explained by the size of the river that renders redd observation more difficult in the lower part of the river. An additional

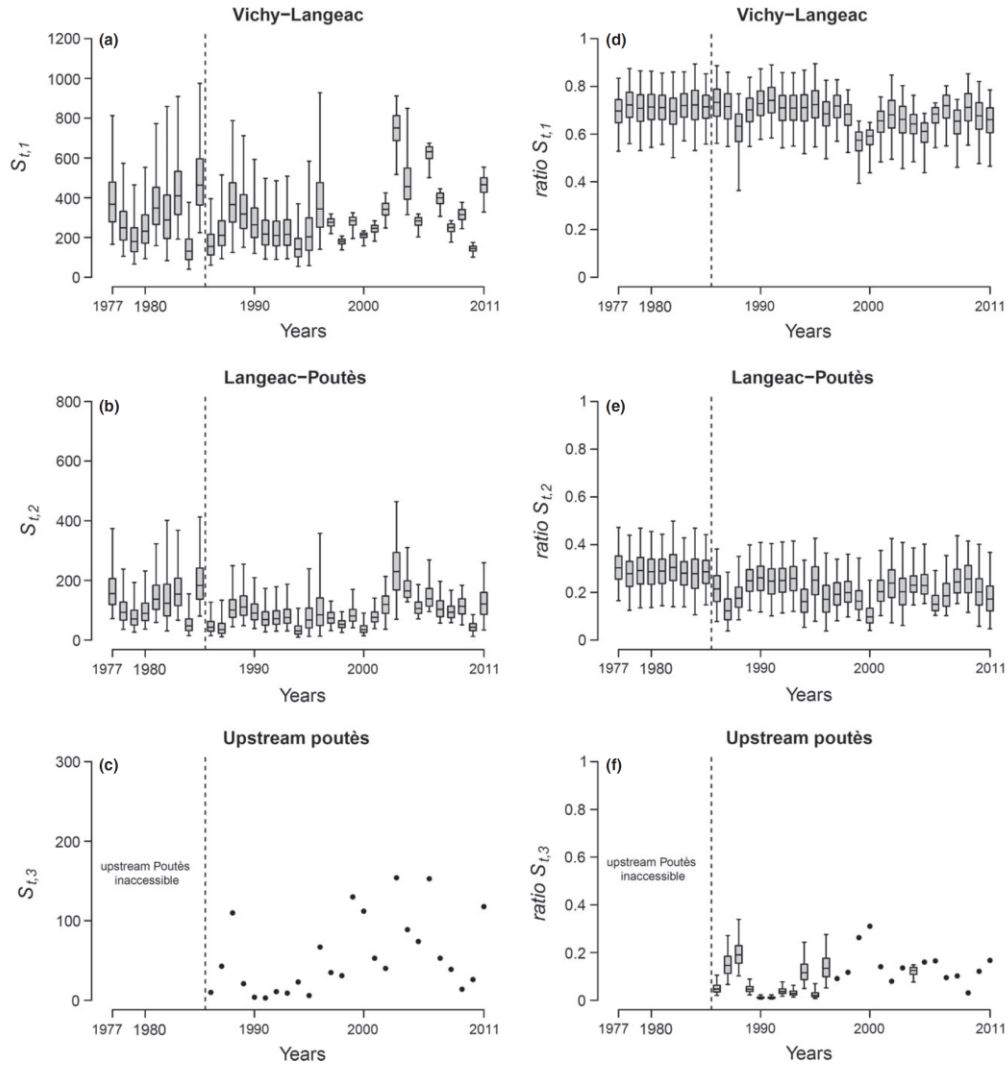


Fig. 3. Model 2's (accounting for change in redd data collection methodology) posterior distributions of the annual absolute and relative potential spawners abundances in each river section of the Allier: (a, d) Vichy-Langeac, (b, e) Langeac-Poutès and (c, f) upstream of Poutès. Boxplots indicate the 2.5th, 25th, median, 75th and 97.5th percentiles. The dashed vertical line indicate the opening of the river section upstream of Poutès to salmon migration.

and most important explanation is the adult mortality prior to spawning occurring mainly in the lower section of the Allier as revealed by radio-tracking studies (Baisez et al. 2011). The redd:potential spawner ratio for the river section upstream of Poutès in 2009 seems to stand out from the range of the habitual values (Fig. 2c). Due to the nature of the counting facility (i.e., a fish lift which is the only way upstream), it is not possible to miss any

migrating adults entering this portion of the catchment. The redd counts are subject to various types of observation errors (Dunham et al. 2001; Muhlfeld et al. 2006). However, for this particular year, it is reported that the observation conditions for the redd counts were particularly good (i.e., low flow and clear weather). Unobserved factors driving female salmon to dig more redds are the most likely, although still elusive, explanation.

Estimating spatial distribution of Atlantic salmon escapement using redd counts

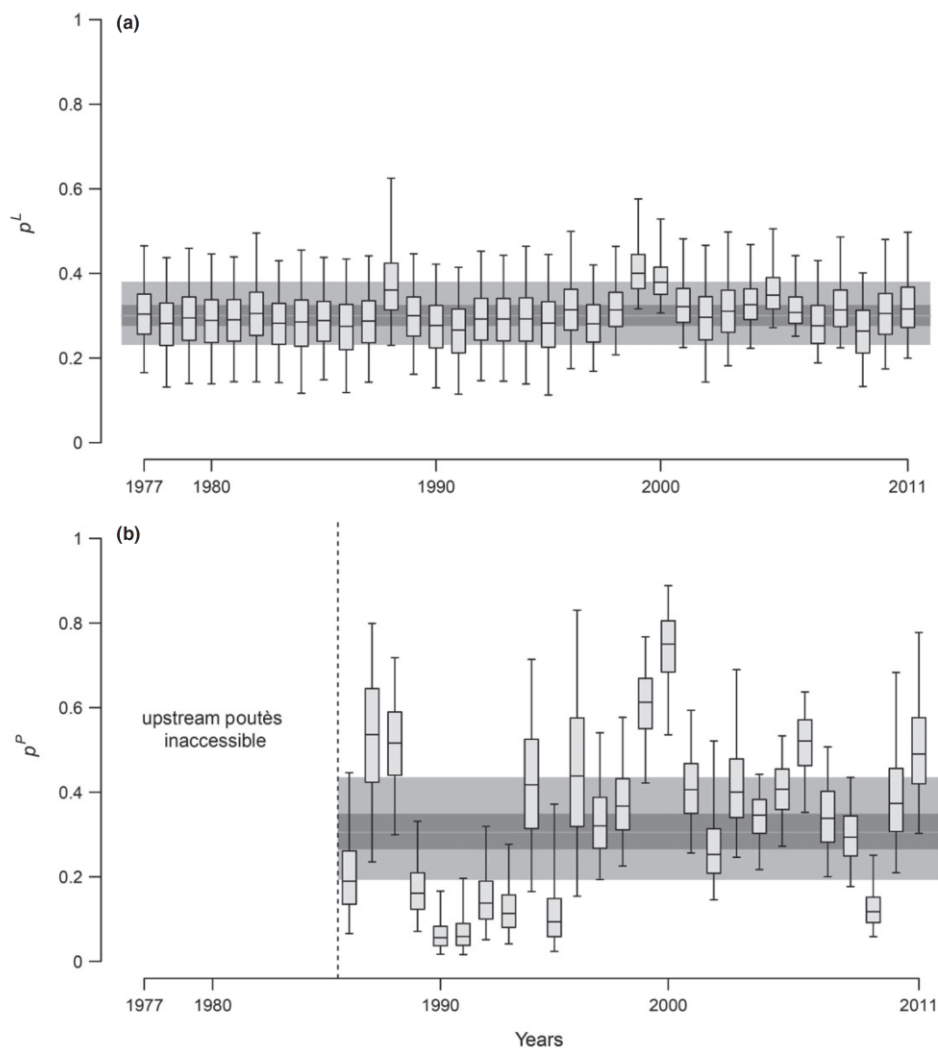


Fig. 4. Model 2's (accounting for change in redd data collection methodology) posterior distributions of the annual proportion of potential spawners moving upstream of (a) Langeac p^L and (b) Poutès p^P (model 1 in black and model 2 in grey). Boxplots indicate the 2.5th, 25th, median, 75th and 97.5th percentiles. The grey bands in the background represent the 2.5th, 25th, median, 75th and 97.5th percentiles of the hyper-parameters μ^L and μ^P . The dashed vertical line indicate the opening of the river section upstream of Poutès to salmon migration.

The model developed in this study provides spatially distributed estimates of potential spawners over a thirty-year time series with varying levels of precision. When the adult counting stations' data are available, the estimates are fairly precise. On average, the CVs are 11.0% and 32.3% for Vichy–Langeac and Langeac–Poutès sections, respectively (Figs 3 and 5). The precision of the potential spawner estimates suffers from the absence of adult counts, especially for the Vichy–Langeac river sections where the average CV goes up to 47.1%. The loss of precision in the Langeac–Poutès river sections is much lower (average CV goes up to 50.4%) and in connection

with the fact that the Langeac counting facility only provides a minimal count value (Fig. 3). Despite their limited precision, the potential spawner estimates allow to detect important variations over time. In contrast to these variations in terms of absolute numbers, the spatial repartition of potential spawners in the three river sections is fairly stable (Fig. 3d–f). The majority of potential spawners stay below Langeac (two-thirds on average). Additionally, it seems like the opening of Poutès dam in 1986 only had a limited impact on the proportion of fish staying in the lowermost river section. This point is of special importance for management purpose as the potential spawners

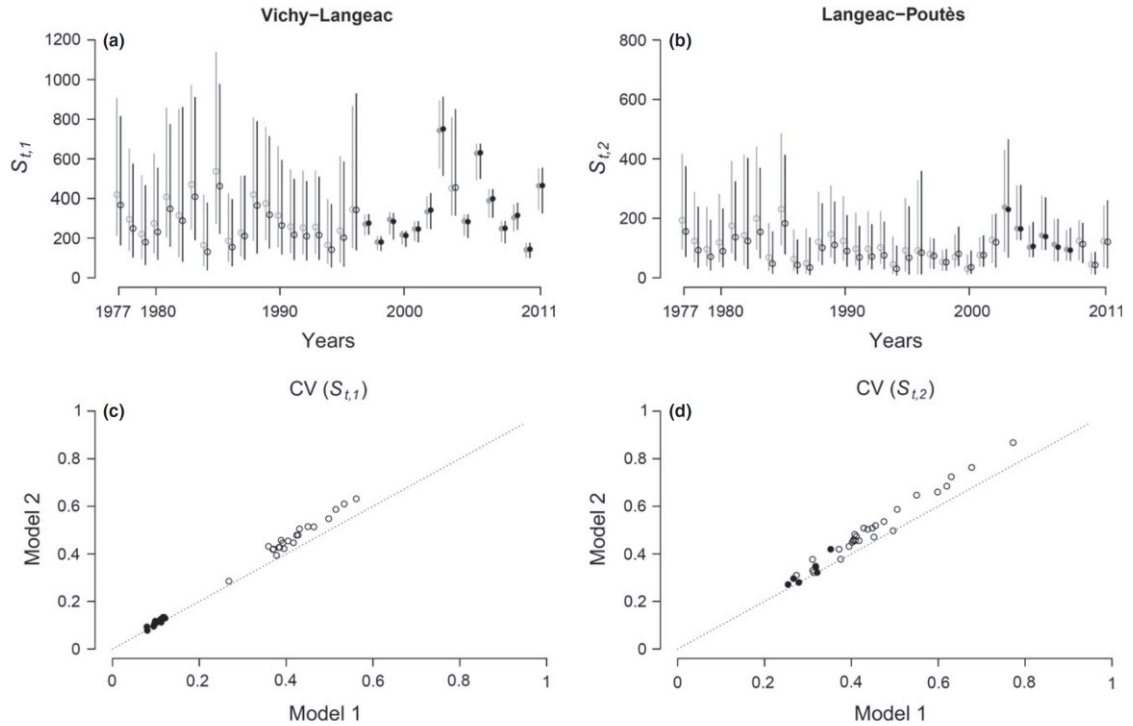


Fig. 5. Model 1 (not accounting for change in redd data collection methodology, grey) and model 2 (accounting for change in redd data collection methodology, black) posterior distributions of the annual potential spawners abundances in Vichy-Langeac (a) and Langeac-Poutès (b) river section of the Allier. Vertical segments indicate the 95% posterior probability interval and the dots indicate the median. Panels c and d compare the coefficient of variations of the posterior distributions of the annual potential spawners abundances in Vichy-Langeac and Langeac-Poutès river sections respectively. Plain dots indicate years for which data relative to potential spawners is available. The dotted line represents the one-to-one line.

suffer higher mortality prior to spawning in this section (Baisez et al. 2011), which is also less suitable for juvenile production (Minster & Bomassi 1999).

The model presented herein is simple enough to run quickly (less than an hour for full MCMC convergence) and is flexible in the sense that additional information regarding covariates or processes can be incorporated as more data become available. In the current situation and due to various logistic constraints, no additional data related to redd counts are likely to become available in a near future. However, one of the next objectives is to incorporate this model in a larger Bayesian state-space model such as the ones developed by Rivot et al. (2004) or Michielsens et al. (2008). This model will use additional available information related to Atlantic salmon in the Allier catchment (e.g., 0+ sampling, juvenile stocking) to provide better estimates of the potential spawners but also estimates of the different parameters related to the life cycle of Atlantic salmon in the Allier catchment. Another potential use of the calibration relationship between redd and adult counts developed in this study would be to build a hierarchi-

cal model that would pool other calibration relationships available for Atlantic salmon in different rivers (such as Dauphin et al. 2010) and using them to provide spawning escapement estimates in rivers where only redd counts are available.

Acknowledgements

This research was part of the Plan Loire Grandeur Nature and financially supported by the European Regional Development Fund (ERDF), the Agence de l'eau Loire Bretagne and the Etablissement public Loire. The authors would like to thank the two anonymous reviewers for their comments and suggestions which greatly improved the content of the manuscript.

References

- Bach, J.-M., Parouty, T., Leon, C., Senecal, A., Cornu, V., Portafaix, P., Juin Tremeur, E., Lelievre, M. & Baisez, A. 2010. Recueil de données biologiques 2009, Saint-Pourçain-sur-Sioule: LOGRAMI. 346 pp.
- Baisez, A., Bach, J.-M., Leon, C., Parouty, C., Terrade, R., Hoffman, M. & Lafaille, P. 2011. Migration delays and

Estimating spatial distribution of Atlantic salmon escapement using redd counts

- mortality of adult Atlantic salmon *Salmo salar* en route to spawning grounds on the River Allier, France. *Endangered Species Research* 15: 265–270.
- Brooks, S.P. & Gelman, A. 1998. General methods for monitoring convergence of iterative simulations. *Journal of Computational and Graphical Statistics* 7: 434–455.
- Brun, M., Abraham, C., Jarry, M., Dumas, J., Lange, F. & Prévost, E. 2011. Estimating an homogeneous series of a population abundance indicator despite changes in data collection procedure: a hierarchical Bayesian modelling approach. *Ecological Modelling* 222: 1069–1079.
- Crozier, W.W., Potter, E.C.E., Prévost, E., Schön, P.J. & O'Maoileidigh, N. 2003. SALMODEL - A Coordinated Approach Towards the Development of a Scientific Basis for Management of Wild Atlantic Salmon in the North-East Atlantic.
- Cuinat, R. 1988. Atlantic salmon in an extensive French river system: the Loire-Allier. In: Mills, D., Piggins, D., eds. *Atlantic salmon: planning for the future*. London: Croom Helm, pp 389–399.
- Dauphin, G., Prévost, E., Adams, C.E. & Boylan, P. 2010. Using redd counts to estimate salmonids spawner abundances: a Bayesian modelling approach. *Fisheries Research* 106: 32–40.
- Dunham, J., Rieman, B. & Davis, K. 2001. Sources and magnitude of sampling error in redd counts for bull trout. *North American Journal of Fisheries Management* 21: 343–352.
- Emlen, J.M. 1995. Population viability of the Snake River Chinook salmon (*Oncorhynchus Tshawytscha*). *Canadian Journal of Fisheries and Aquatic Sciences* 52: 1442–1448.
- de Gaudemar, B., Schroder, S.L. & Beall, E.P. 2000. Nest placement and egg distribution in Atlantic salmon redds. *Environmental Biology of Fishes* 57: 37–47.
- Gelman, A., Meng, X.L. & Stern, H. 1996. Posterior predictive assessment of model fitness via realized discrepancies. *Statistica Sinica* 6: 733–760.
- Gelman, A., Carlin, J.B., Stern, H.S. & Rubin, D.B. 2003. *Bayesian data analysis*, 2nd edn. London; Chapman & Hall/CRC.
- Hay, D.W. 1987. The relationship between redd counts and the numbers of spawning salmon in the Girmock burn, Scotland. *ICES Journal of Marine Science* 43: 146–148.
- ICES 1995. Report of the North Atlantic salmon working group, Copenhagen, 3–12 April 1995. International Council for the Exploration of the Sea CM 1995/Assess: 14, Ref: M. pp. 191.
- Isaak, D.J., Thurow, R.F., Rieman, B.E. & Dunham, J.B. 2003. Temporal variation in synchrony among chinook salmon (*Oncorhynchus tshawytscha*) redd counts from a wilderness area in central Idaho. *Canadian Journal of Fisheries and Aquatic Sciences* 60: 840–848.
- Michielsens, C.G.J., McAllister, M.K., Kuikka, S., Mantyniemi, S., Romakkaniemi, A., Pakarinen, T., Karlsson, L. & Uusitalo, L. 2008. Combining multiple Bayesian data analyses in a sequential framework for quantitative fisheries stock assessment. *Canadian Journal of Fisheries and Aquatic Sciences* 65: 962–974.
- Minster, A.M. & Bomassi, P. 1999. Repérage et évaluation des surfaces potentielles de développement de juvéniles de saumons atlantiques. Proposition d'un modèle de gestion des stocks sur les bassins de l'Allier et de l'Arroux. Rapport LOGRAMI/CSP DR6, 44 p. + annexes.
- Muhlfeld, C.C., Taper, M.L., Staples, D.F. & Shepard, B.B. 2006. Observer error structure in bull trout redd counts in Montana streams: implications for inference on true redd numbers. *Transactions of the American Fisheries Society* 135: 643–654.
- Murdoch, A.R., Pearsons, T.N. & Maitland, T.W. 2010. Estimating the spawning escapement of hatchery- and natural-origin spring Chinook salmon using redd and carcass data. *North American Journal of Fisheries Management* 30: 361–375.
- Parsons, A.L. & Skalski, J.R. 2010. Quantitative assessment of salmonid escapement techniques. *Reviews in Fisheries Science* 18: 301–314.
- Perrier, C., Guyomard, R., Baglinière, J.-L. & Evanno, G. 2011. Determinants of hierarchical genetic structure in Atlantic salmon populations: environmental factors vs. anthropogenic influences. *Molecular Ecology* 20: 4231–4245.
- Rivot, E., Prévost, E., Parent, E. & Baglinière, J.-L. 2004. A Bayesian state-space modelling framework for fitting a salmon stage-structured population dynamic model to multiple time series of field data. *Ecological Modelling* 179: 463–485.
- Ros, O. 1997. Comptage des frayères de Saumon par hélicoptère sur la rivière Allier, de Vieille-Brioude à Langeac. Rapport LOGRAMI/DR6, 9 p.
- Spiegelhalter, D.J., Best, N.G., Carlin, B.P. & Van der Linde, A. 2002. Bayesian measures of model complexity and fit (with discussion). *Journal of the Royal Statistical Society, Series B* 64: 583–616.
- Spiegelhalter, D.J., Thomas, A., Best, N. & Lunn, D. 2007. *WinBUGS: user manual*, version 2.10. Cambridge: Medical research Council Biostatistics Unit.
- Thomas, A., O'Hara, B., Ligges, U. & Sturtz, S. 2006. Making BUGS Open. *R News* 6: 12–17.

Supporting Information

Additional Supporting Information may be found in the online version of this article:

Table S1 Annual redd counts and proportion of potential spawning area surveyed for the 3 sections of the river Allier

Table S2 Adults counted at the 3 counting stations: Vichy, Langeac and, Poutès.

Appendix A : Datasets

Table A.1 : Annual redd counts and proportion of potential spawning area surveyed for the 3 sections of the river Allier. – indicates that the area was not accessible for adult salmon.

Years	Redd counts			Proportion of spawning area surveyed		
	Vichy-Langeac	Langeac-Poutès	Upstream Poutès	Vichy-Langeac	Langeac-Poutès	Upstream Poutès
1977	168	120	-	0.429	0.448	-
1978	166	39	-	0.673	0.414	-
1979	41	32	-	0.551	0.414	-
1980	50	93	-	0.296	0.862	-
1981	399	190	-	0.898	1	-
1982	NA	NA	-	0	0	-
1983	598	202	-	0.898	1	-
1984	6	31	-	0.306	0.862	-
1985	692	273	-	0.898	1	-
1986	22	47	NA	0.265	1	0
1987	NA	31	NA	0	1	0
1988	2	194	116	0.276	1	0.825
1989	136	216	42	0.429	1	0.825
1990	137	144	NA	0.429	0.862	0
1991	105	89	NA	0.429	0.862	0
1992	56	96	NA	0.429	0.793	0
1993	59	92	NA	0.429	0.690	0
1994	10	21	NA	0.429	0.690	0
1995	NA	NA	NA	0	0	0
1996	NA	NA	NA	0	0	0
1997	132	58	7	0.612	1	0.125
1998	86	58	14	0.898	1	0.617
1999	58	132	85	0.745	1	0.850
2000	57	34	66	0.673	1	0.850
2001	69	88	43	0.704	1	0.850
2002	NA	NA	NA	0	0	0
2003	NA	NA	NA	0	0	0
2004	53	93	136	0.889	1	0.850
2005	115	159	67	0.746	1	0.850
2006	92	69	169	0.873	1	1
2007	79	50	31	1	1	1
2008	NA	NA	NA	0	0	0
2009	241	91	57	0.865	1	0.950
2010	NA	NA	NA	0	0	0
2011	NA	NA	NA	0	0	0

Table A.2 : Adults counted at the 3 counting stations: Vichy, Langeac and, Poutès. Note that Langeac station only provides a minimum count and that in 2004 Vichy only provided minimum count (indicated in italic with a *). – indicates that the area was not accessible for adult salmon. And adults taken between Vichy and Langeac for breeding.

Years	Adults counted			Adults taken for breeding between Vichy and Langeac
	Vichy	Langeac	Poutès	
1977	NA	NA	-	14
1978	NA	NA	-	34
1979	NA	NA	-	44
1980	NA	NA	-	52
1981	NA	NA	-	48
1982	NA	NA	-	64
1983	NA	NA	-	38
1984	NA	NA	-	5
1985	NA	NA	-	40
1986	NA	NA	10	10
1987	NA	NA	43	20
1988	NA	NA	110	9
1989	NA	NA	21	5
1990	NA	NA	4	8
1991	NA	NA	3	10
1992	NA	NA	11	16
1993	NA	NA	9	4
1994	NA	NA	23	0
1995	NA	NA	6	0
1996	NA	NA	67	15
1997	393	NA	35	8
1998	267	NA	31	3
1999	515	NA	130	20
2000	380	NA	112	20
2001	400	NA	53	25
2002	541	NA	40	40
2003	1238	189 *	154	103
2004	657 *	216 *	89	63
2005	510	142 *	74	47
2006	950	246 *	153	27
2007	572	107 *	53	17
2008	421	95 *	39	39
2009	491	NA	14	49
2010	227	NA	26	14
2011	755	NA	118	50

Appendix A.5:

Full lifecycle model

1. Introduction

In this section we describe the model used to represent the full lifecycle of Atlantic salmon in the Allier catchment. This model incorporates the two observations models described in App. A.2 (0+ Juvenile densities model) and App. A.4 (Potential spawners to redd counts relationship model).

The aim of this model is to attempt understanding the population dynamics of the Atlantic salmon in the Allier catchment and the role that stocking had in this dynamics over a 35 years time-series. This was done by first doing a review of all the dataset available and then finding a way to relate them to life stages of interests and bring them all together in one single model making the most of the information available on Atlantic salmon in the Allier catchment at this day.

One of the main difficulty relied on the fact that Atlantic salmon has a complex lifecycle and that, there is not necessarily data available on every lifestage of interest (e.g. smolts) and when there is some information available it can be limited (e.g. only a few sites electric fished to estimate densities, limited years of adult counts, etc.). Also, because of the difficulty to obtain such data for salmon population, there is a lack of information regarding some crucial transition parameters such as 0+ to smolt survival, or sea survival.

Moreover, in this particular study, there is an additional challenge: the heavy stocking program carried out in the Allier catchment throughout the time-series. Different lifestages have been stocked and not all of them have been marked to be able to identify these fish from the wild. For instance the eggs and 0+ juveniles were never marked. The situation for the smolts is a bit more complicated: from 1975 to 1994 no smolts were marked, from 1995 to 2002 only a fraction of the stocked were marked (cryomarking or adipose fin clipping) and from 2003 all stocked smolts were adipose fin clipped.

Due to this fragmented information (missing data, differences in spatial or/and tempora scale) it is often necessary to make strong assumptions about the various processes relating the lifestages to each other.

It may seem like the model presented here relies on strong hypotheses and it is sometimes the case (these are discussed in the main report) however, it should be kept in mind that this model was not built straight away in this version. It was started as something simple and complexity or/and data were added step by step, verifying at each step that the outputs were coherent and fitting with the data. Biological hypotheses as well as hypotheses regarding the data collection/quality were discussed with the different persons who had an expertise on or collected them. Additionally to reviewing available literature related to the assumptions made, several meetings were organised during the project to be assured that the different partners were agreeing with them.

2. Model

0+ juvenile cohort

The juvenile production model (see App. A.2) provides each year and for each of the 3 river sections of the Allier catchment, an average 0+ juvenile density $D_{t,i}^{tot}$. For each river section, a form of 0+ juvenile production $J_{t,i}$ is calculated simply by multiplying the average 0+ density by the surface of favourable 0+ juvenile rearing habitat available H_i .

$$(Eq. A5.1) \quad J_{t,i} = D_{t,i}^{tot} \times H_i$$

All habitats are assumed to be used in an average and similar way. For each river section, the cohort of 0+ juveniles (i.e. all the years during which the juvenile production will influence the adult returns of a given year t) can be calculated.

$$(Eq. A5.2) \quad J_{t,i}^{coh} = \frac{1}{3} \times J_{t-3,i} + \frac{1}{3} \times J_{t-4,i} + \frac{1}{3} \times J_{t-5,i}$$

Note that the cohort is made of 3 years of 0+ juvenile production (these 3 years represent more than 90% of the life-histories encountered in the Allier catchment, Cuinat, 1988) and that each of them are assumed to have an equal contribution. It is likely that there are some annual differences in the relative contributions however, this is an average relationship, and the variation around it will be embedded in the overall variance parameter of the adult returns at Vichy τ^V . The total 0+ juvenile production for the whole catchment $J_t^{coh_tot}$ can be calculated as:

$$(Eq. A5.3) \quad J_t^{coh_tot} = \sum_{i=1}^3 J_{t,i}^{coh}$$

Stocked smolts

The adult returns at Vichy of a given year N_t^V will also be conditioned by the number of smolts stocked 2 years Sm_{t-2} and 3 years earlier Sm_{t-3} . Only two years are contributing since this is what is shown from the data that is available from the returning marked adults (for some years a proportion or all smolts are fin clipped, it is then possible to identify these fish when they return as adult at Vichy).

$$(Eq. A5.4) \quad Sm_t^{coh} = \frac{1}{2} \times Sm_{t-2} + \frac{1}{2} \times Sm_{t-3}$$

Every year, the smolts produced by the salmon farm come in two size modes (number in each mode are known). The larger smolts are expected to leave the system the year they are stocked while the smaller are assumed to leave the following year. The total number of smolts of a given year Sm_t is therefore the number of larger smolts of this given year t plus the number of smaller smolts of the precedent year t-1 who which survived. The smaller smolts which are staying an additional year in the river system are likely to have a different mortality compared to the smolts leaving just after being stocked. However, no information on this parameter is available. Therefore, any differences in survival as well as differences in the annual contributions of the different years of smolt stocking will be incorporated in the overall variance parameter of the adult returns at Vichy τ^V .

Returning adults

The average number of adults returning at Vichy can be calculated as follow:

$$(Eq. A5.5) \quad \mu_t^V = (\mu^{s-J} \times J_t^{coh-tot} + \mu^{s-Sm} \times Sm_t^{coh}) \times \gamma_t^S$$

Where μ^{s-J} is the average 0+ to returning adult survival and μ^{s-Sm} the average stocked smolt to returning adult survival. μ^{s-J} is estimated since no information on this survival is available. However μ^{s-Sm} is assumed to be known since some information about the return rate of the marked stocked smolts during a 14 years period available. Since it is not possible to identify precisely the life history of the marked returning adults, an average return rate of smolts stocked was calculates as the sum of the marked returning adult between 1997 and 2011 divided by the total number of marked smolts stocked between 1995 and 2009 ($\mu^{s-Sm} = 5.45 \times 10^{-4}$).

Additionally, in earlier versions of the model, it was found that setting only one average survival level for μ^{s-J} and μ^{s-Sm} across the time-series did not produce the best fit to the data. Therefore it was assumed that both μ^{s-J} and μ^{s-Sm} may have changed during the time-series. Therefore it was assumed that the survivals during the first part of the time series were affected by a multiplicative coefficient γ_t^S , the years during which the switch to the present level of survival occur was estimated as follow:

$$(Eq. A5.6) \quad \gamma_t^S = e^{(s^{level} \times I_t^S)}$$

With

$$(Eq. A5.7a) \quad I_{1:7}^{S'} = 1 \quad (Eq. A5.9) \quad s^{level} \sim Normal(0,1)$$

$$(Eq. A5.8a) \quad I_7^{S'} = 1$$

For $t = \{8, \dots, 37\}$

$$(Eq. A5.7b) \quad I_t^{S'} \sim Bernouilli(0.5)$$

$$(Eq. A5.8b) \quad I_t^S = I_{t-1}^S \times I_t^{S'}$$

The 6 first years of the time series are assumed to have the first level of survival. The reason for this is the lack of information regarding the 0+ juvenile production associated with the adult returns of these first 6 years. During the following years, there is a 0.5 probability $I_t^{S'}$ to switch to the other average level of survival. Note that in this structure, once the switch has occurred, it is not possible to go back to the initial level of survival.

The annual number of returning adults at Vichy N_t^V is drawn from a Log-Normal distribution. During the first 6 years of the time-series, there is no information about the 0+ juvenile cohorts associated with these returns, an informative prior is used so the average returns at Vichy range from 50 to 17300 (95% credibility interval) with a mean of 3300. These values are assumed to be within the range of returns occurring during these years.

For $t = \{1, \dots, 6\}$

$$(Eq. A5.10) \quad N_t^V \sim \text{Log} - \text{Normal}(6.9, 0.0453) I(\min_t^{N-V}, 15000)$$

For the rest of the time-series, the number of returning adults at Vichy is drawn from the following Log-Normal distribution:

For $t = \{7, \dots, 37\}$

$$(Eq. A5.11) \quad N_t^V | \mu_t^{N-V}, \tau^V \sim \text{Log} - \text{Normal}(\text{Log}(\mu_t^{N-V}), \tau^V) I(\min_t^{N-V}, 15000)$$

In order to avoid unrealistic high values of adult returns, a censorship is put on the right side of the distribution (maximum $N_t^V = 15000$). Also, some professional fisheries and angling data as well as the number of fish taken for the salmon farm breeding program is valorised by using them as a minimum boundary of the N_t^V distribution. The minimum number of adults returning at Vichy \min_t^{N-V} is calculated as follow:

$$(Eq. A5.12) \quad \min_t^{N-V} = \max(N_t^P + 2, C_t^{tot} + 2) + B_t$$

With

$$(Eq. A5.13) \quad C_t^{tot} = C_t^{down-V} + C_t^{up-V}$$

$$(Eq. A5.14) \quad C_t^{down-V} = p^{r-V} \times C_t^{down-tot}$$

Where N_t^P is the number of adults counted at Poutès fish lift (when available). C_t^{tot} is the number of fish caught upstream of Vichy C_t^{up-V} plus the proportion p^{r-V} of the total number of adults caught downstream of Vichy $C_t^{down-tot}$ which would have made it upstream of Vichy. At this time, most of the salmon population was originating from the Allier catchment therefore an informative prior was given to p^{r-V} to reflect this belief (table A5.1). B_t is the annual number of adults captured for broodstock purposes (all these fish are captured at or upstream of Vichy).

The returning adults at Vichy N_t^V (minus the ones caught by anglers or for broodstock) will have a probability p_t^L to migrate upstream of Langeac counting station. The returning adults at Langeac N_t^L are drawn from a Binomial distribution with a censorship on the left side of the distribution min_t^{N-L} corresponding to the adults counted at Langeac station. This counting station is affected by heavy water conditions and is therefore assumed to provide only a minimum value of the number of adults moving upstream:

For $t = \{1, \dots, 37\}$

$$(Eq. A5.15) \quad N_t^L | N_t^V, C_t^{tot}, B_t, p_t^L \sim Binomial(N_t^V - C_t^{tot} - B_t, p_t^L) I(min_t^{N-L},)$$

With

$$(Eq. A5.16) \quad Logit(p_t^L) | \mu_t^{p-L}, \tau^{p-L} \sim Normal(\mu_t^{p-L}, \tau^{p-L})$$

The average probability of moving upstream of Langeac μ_t^{p-L} is explicitly conditioned by two main components: 1) the ratio of 0+ juvenile habitat available in the river section upstream of Langeac φ_t^{H-L} in order to reflect the fact that adults may distribute themselves following an ideal free distribution and 2) the ratio of the cohort of 0+ juvenile production in the river section upstream of Langeac φ_t^{J-L} in order to reflect the fact that returning adults may be distributing themselves depending on where they grew up as juveniles (homing). Note that the two ratios

φ_t^{H-L} and φ_t^{J-L} are calculated differently throughout the time-series reflecting the impact of the installation of the fish lift at Poutès in 1986 which opened some new habitat for the adults to migrate in and for the juveniles to grow in (Eq. A5.19a and b). No information about the relative contribution p^φ of these two components is available; therefore this contribution is given a weakly-informative prior (table A5.1) and estimated.

$$(Eq. A5.17) \quad \mu_t^{p-L} = \text{Logit}(\varphi_t^L) + \alpha^L$$

$$(Eq. A5.18) \quad \varphi_t^L = p^\varphi \times \varphi_t^{H-L} + (1 - p^\varphi) \times \varphi_t^{J-L}$$

For $t = \{1, \dots, 11\}$, when the area upstream of Poutès is not available:

$$(Eq. A5.19a) \quad \varphi_t^{H-L} = \frac{H_2}{\sum_{i=1}^2 H_i} \text{ and,}$$

$$(Eq. A5.20a) \quad \varphi_t^{J-L} = \frac{J_{t,2}^{coh}}{\sum_{i=1}^2 J_{t,i}^{coh}}$$

For t in $\{12: 37\}$, when area upstream of Poutès is available:

$$(Eq. A5.19b) \quad \varphi_t^{H-L} = \frac{H_2}{\sum_{i=1}^3 H_i} \text{ and,}$$

$$(Eq. A5.20b) \quad \varphi_t^{J-L} = \frac{J_{t,2}^{coh}}{\sum_{i=1}^3 J_{t,i}^{coh}}$$

Where H_i is the wetted area of habit favourable to juvenile rearing in each river section as described in Minster and Bomassi (1999). Additionally, a discrepancy parameter α^L is incorporated so the average probability of moving upstream of Langeac μ_t^{p-L} can be systematically increased or decreased to represent the facilitation or the interference occurring either during the upstream migration of the adults between Vichy and Langeac or the downstream migration of smolts between Langeac and Vichy. Any discrepancies between the data and the model as well as other factors which might affect μ_t^{p-L} (e.g. flow, temperature ...) which are not explicitly implemented in the model will be embedded in the precision parameter τ^{p-L} .

In 1986 ($t = 12$), a fish lift was installed at Poutès dam allowing adults migrating upstream of Langeac N_t^L to move upstream of Poutès with a probability p_t^P . The process is modelled in a similar fashion than for N_t^L and p_t^L . The adults migrating upstream of Poutès (i.e. the fish counted at the fish lift) are drawn from a Binomial distribution:

For $t = \{12, \dots, 37\}$

$$(Eq. A5.21) \quad N_t^P | N_t^L, p_t^P \sim \text{Binomial}(N_t^L, p_t^P)$$

With

$$(Eq. A5.22) \quad \text{Logit}(p_t^P) | \mu_t^{p-P}, \tau^{p-P} \sim \text{Normal}(\mu_t^{p-P}, \tau^{p-P})$$

The average probability of moving upstream of Poutès μ_t^{p-P} is explicitly conditioned by the same two main components than μ_t^{p-L} : i) the ratio of 0+ juvenile habitat 0+ available in the river section upstream of Poutès φ_t^{H-P} and ii) the ratio of the cohort of 0+ juvenile production in the river section upstream of Poutès φ_t^{J-P} . Note that the relative contribution of these two main components p^φ is assumed to be the same than for the adults migrating upstream of Langeac. Similarly to Langeac, a discrepancy parameter α^P is incorporated so the average probability of moving upstream of Poutès μ_t^{p-P} can be systematically increased or decreased to represent the facilitation or the interference occurring either during the upstream migration of the adults between Langeac and Poutès or the downstream migration of smolts between Poutès and Langeac. Any discrepancies between the data and the model as well as other factors which might affect μ_t^{p-P} which are not explicitly implemented in the model will be embedded in the precision parameter τ^{p-P}

$$(Eq. A5.23) \quad \mu_t^{p-P} = \text{Logit}(\varphi_t^P) + \alpha^P$$

$$(Eq. A5.24) \quad \varphi_t^P = p^\varphi \times \varphi_t^{H-P} + (1 - p^\varphi) \times \varphi_t^{J-P}$$

with

$$(Eq. A5.25) \quad \varphi_t^{H-P} = \frac{H_3}{\sum_{i=1}^3 H_i} \text{ and,}$$

$$(Eq. A5.26) \quad \varphi_t^{J-P} = \frac{J_{t,3}^{coh}}{\sum_{i=1}^3 J_{t,i}^{coh}}$$

The potential spawners in each of the river sections are then calculated for the Vichy-Langeac river section:

$$(Eq. A5.27) \quad S_t^V = N_t^V - N_t^L - C_t^{tot} - B_t$$

For the Langeac- Poutès river section:

For $t = \{1, \dots, 11\}$:

$$(Eq. A5.28a) \quad S_t^L = N_t^L \quad \text{and,}$$

for $t = \{12, \dots, 37\}$:

$$(Eq. A5.28b) \quad S_t^L = N_t^L - N_t^P$$

And for the upstream of Poutès river section:

For $t = \{12, \dots, 37\}$:

$$(Eq. A5.29) \quad S_t^P = N_t^P$$

Potential spawners

In order to keep the formulas concise henceforth the notations exponent letters V, L and P will be replaced by an additional index i . For instance, N_t^V , N_t^L and, N_t^P are equivalent to $N_{t,1}$, $N_{t,2}$ and, $N_{t,3}$

As described in appendix A.4, the redd counts data is related to the potential spawners as follow:

$$(Eq. A5.30) \quad R_{t,i} | \lambda_{t,i} \sim Poisson(\lambda_{t,i})$$

With

$$(Eq. A5.31) \quad \lambda_{t,i} = S_{t,i} \times \kappa_{t,i} \times p_{t,i}^R \times \gamma_k$$

Where $\kappa_{t,i}$ is the spawner:red ratio for each river section and $p_{t,i}^R$ the proportion of spawning grounds surveyed during the redd counts data collection. The spawner:red ratio $\kappa_{t,i}$ is governed by two hyper-parameters: the mean μ_i^k and the inverse-scale β . Earlier version of the models showed some differences in the potential spawners to redds relationship between the river section downstream Langeac and the two other river sections upstream Langeac. To reflect these differences, two mean hyper-parameters were introduced such as: $\mu_1^k = \mu^{k_{down}}$ and $\mu_2^k = \mu_3^k = \mu^{k_{up}}$. Due to the change in the counting technique in 1997 (i.e. foot and boat counting to helicopter counting), a “methodology” effect γ_k was implemented. The index k stands for the counting methodology: $k=1$ from 1977 to 1996 when counts are carried out by foot or boat and $k=2$ from 1997 to 2011 when counts are done by helicopter. For the sake of identifiability, γ_1 is set equal to 1, γ_2 remaining unknown and to be estimated. posterior distribution of the parameters of interest can be found in Table A5.2.

Juvenile densities

Using the electric fishing data available in the Allier catchment it is possible to estimate total average densities $D_{t,i}^{tot}$ in the 3 river sections of the Allier catchment that are considered in this study. These densities can be split in three components:

- 1) “wild” 0+, the descendants of the returning adults

- 2) Stocked 0+, the survivors from the stocked 0+ during spring
- 3) Stocked eggs, the survivors from the stocked eggs (in incubators) during winter

The total average densities can be written as follow:

$$(Eq. A5.32) \quad D_{t,i}^{tot} = D_{t,i}^{wild} + I_{t,i}^{D-juv} \times D_{t,i}^{juv} + I_{t,i}^{D-egg} \times D_{t+1,i}^{egg}$$

Where $I_{t,i}^{D-juv}$ and $I_{t,i}^{D-egg}$ are indicators of presence or absence of 0+ juvenile or egg stocking in the river section i during the year t . The densities $D_{t,i}^{tot}$ are the same densities used to calculate the of 0+ juvenile production $J_{t,i}$ in equation A5.1.

Full details of how these densities are modeled can be found in Appendix A.2 The main processes are reminded in the following:

The wild” 0+ juvenile densities component $D_{t+1,i}^{wild}$ observed in the river sections on a given year $t+1$ is related to the potential spawners in the same river sections the year before $S_{t,i}$. The relationship linking these two lifestages is a Beverton and Holt density-dependence relation.

The stocked 0+ juveniles component $D_{t+1,i}^{juv}$ is related to the number of 0+ stocked $Stock_{t+1,i}^{juv}$ in each river section with its parameters constrained by the parameters of the Beverton and Holt relationship of the wild 0+.

The stocked eggs density $D_{t+1,i}^{egg}$ is considered in a different way due to the very local aspects of how the incubators are going to influence the densities and therefore only a survival parameter s^{egg} is estimated.

Table A5.1: Summary of parameters of interest and their associated prior distribution.

Notation	Parameter description	Prior
p^{r-V}	Proportion of fish caught downstream of Vichy which would have made it upstream of Vichy	$Beta(2,1)$
τ^V	Inter-annual precision (1/variance) parameter for the adult returns at Vichy	$Gamma(10^{-3}, 10^{-3})$
τ^{p-L}	Inter-annual precision (1/variance) parameter for the probability of moving upstream of Langeac	$Gamma(10^{-2}, 10^{-2})$
τ^{p-P}	Inter-annual precision (1/variance) parameter for the probability of moving upstream of Poutès	$Gamma(10^{-2}, 10^{-2})$
γ_2	Redd count methodology effect	$Gamma(1,1)$
p^φ	Relative contribution of the habitatratio to the probability of moving upstream a counting station	$Beta(2,2)$
α^L	Systematic discrepancy parameter affecting Langeac counting station	$Normal(0, 10^{-2})$
α^P	Systematic discrepancy parameter affecting Poutès counting station	$Normal(0, 10^{-2})$
μ^{s-J}	Average survival of the juvenile cohort	$Beta(2,2)$

Table A5.2: Posterior distribution of parameters of interest.

Notation	mean	sd	2.5th	25th	Median	75th	97.5th
p^{r-V}	0.351	0.228	0.0438	0.173	0.304	0.481	0.898
τ^V	3.726	1.449	1.537	2.677	3.507	4.560	7.096
τ^{p-L}	34.90	46.60	3.644	9.746	18.64	40.01	162.2
τ^{p-P}	1.245	0.548	0.497	0.868	1.134	1.511	2.563
γ	0.879	0.221	0.517	0.723	0.857	1.007	1.373
p^φ	0.421	0.165	0.149	0.296	0.405	0.530	0.776
α^L	-0.464	0.250	-0.942	-0.633	-0.467	-0.299	0.035
α^P	-0.369	0.375	-1.101	-0.617	-0.371	-0.116	0.366
μ^{s-J}	0.00177	0.00039	0.0011	0.0015	0.0017	0.0020	0.0026

Appendix A.6:

OpenBUGs code for the full lifecycle model

1: Model

```
model{  
  
#####  
# EF CALIBRATION #  
#####  
  
d_moy~dgamma(1,0.001)  
beta_d~dgamma(0.001,0.001)  
  
inv_kappa ~ dgamma(0.001,0.001)  
kappa <-1/ inv_kappa  
  
eta ~ dgamma(0.001,0.001)  
  
L_sigma_p~dunif(0.0001,10)  
L_tau_p<-pow(L_sigma_p,-2)  
L_var_p<-1/L_tau_p  
  
L_mu_p ~dnorm(0,0.001)  
logit(mu_p)<-L_mu_p  
  
alpha_d<-d_moy * beta_d  
  
for (g in 1:calib){  
  # density part  
  d[g]~dgamma(alpha_d,beta_d)  
  
  #5minute EF part  
  lambda_IA[g]<-kappa*pow(d[g],eta)  
  
  EF_IA[g]~dpois(lambda_IA[g])  
  lambda_N[g]<-d[g]*S[g]  
  
  #Abundance follows a Poisson distribution  
  N_tot[g]~dpois(lambda_N[g]),(2000)  
  
  L_p[g]~dnorm(L_mu_p,L_tau_p)  
  logit(p[g]) <- L_p[g]  
  
  # 2 depletion pass part  
  C_1[g]~dbin(p[g],N_tot[g])  
  N_1[g]<-N_tot[g]-C_1[g]  
  C_2[g]~dbin(p[g],N_1[g])  
  
}
```

```

#####
## parameters of the Redd/spawner relationship mode##
#####

mu_zone[1]~dgamma(1,0.001)
mu_zone[2]~dgamma(1,0.001)

beta_zone~dgamma(0.01,0.01)

alpha_zone[1]<- mu_zone[1]*beta_zone
alpha_zone[2]<- mu_zone[2]*beta_zone

#Methodology effect
hel_effect[1]<-1
hel_effect[2]~dgamma(1,1) #

for (t in 1:T){
  zone_effect[t,1]~dgamma(alpha_zone[1],beta_zone)|(0.001,)
  zone_effect[t,2]~dgamma(alpha_zone[2],beta_zone)|(0.001,)
}
for (t in 12:T){
  zone_effect[t,3]~dgamma(alpha_zone[2],beta_zone)|(0.001,)
}

diff_zone1_2<-mu_zone[1]-mu_zone[2]
p_diff_zone1_2<-step(diff_zone1_2 )

#loops for proportion of area prospected

for (t in 1:T+20){
  for (k in 1:2){
    logit(p_area[t,k])<- L_p_area[t,k]
  }
}

for (t in 12:T+20){
  logit(p_area[t,3])<- L_p_area[t,3]
}

#####
# Annual Juvenile Production #
#####

# cut of all the parameters of the calibration

L_mu_p_cut<-cut(L_mu_p)
L_tau_p_cut<-cut(L_tau_p)

kappa_cut<-cut(kappa)
eta_cut<-cut(eta)

# on suppose que le parametre d'echelle est le meme au fil des années
beta_d_cut<-cut(beta_d)

# BH slope parameter
#not sure about the beta parameters ...

zt~dbeta(0.1,2.18)
a<-zt *8000
alpha_dd<- 1/a

a_juv ~dbeta(2,2)
alpha_dd_juv<- 1/a_juv

```

```

Rmax~dgamma(0.01,0.01)|(,15)      #log(Rmax)<-L_Rmax
beta_dd<- 1 / Rmax

s_juv~dbeta(2,2)
s_egg~dbeta(2,2)#|(0.0001,)

alpha_tau <- mu_tau * beta_tau
mu_tau ~ dgamma(0.01,0.01)
beta_tau ~ dgamma(0.01,0.01)

tau_juv_moy[1]~dgamma(0.01,0.01)
tau_juv_site[1]~dgamma(0.01,0.01)
tau_egg_moy[1]~dgamma(0.01,0.01)|(0.01,)
tau_egg_site[1]~dgamma(0.01,0.01)|(0.01,)
tau_wild_moy~dgamma(alpha_tau,beta_tau)
tau_wild_site~dgamma(alpha_tau,beta_tau)
tau_juv_moy[2]~dgamma(alpha_tau,beta_tau)
tau_juv_site[2]~dgamma(alpha_tau,beta_tau)
tau_egg_moy[2]~dgamma(alpha_tau,beta_tau)#|(,50)
tau_egg_site[2]~dgamma(alpha_tau,beta_tau)

sigma_wild_moy <- sqrt( 1 / tau_wild_moy)
sigma_wild_site <- sqrt( 1 / tau_wild_site)
sigma_juv_moy <- sqrt( 1 / tau_juv_moy[2])
sigma_juv_site <- sqrt( 1 / tau_juv_site[2])
sigma_egg_moy <- sqrt( 1 / tau_egg_moy[2])
sigma_egg_site <- sqrt( 1 / tau_egg_site[2])

nu_wild_dwn~dnorm(0,0.01)
nu_wild_up~dnorm(0,0.01)

nu_wild[1] <- nu_wild_dwn - ( (nu_wild_dwn + nu_wild_up) / 2 )
nu_wild[2] <- nu_wild_up - ( (nu_wild_dwn + nu_wild_up) / 2 )
nu_wild[3] <- nu_wild_up - ( (nu_wild_dwn + nu_wild_up) / 2 )

nu_juv_dwn~dnorm(0,0.001)
nu_juv_up~dnorm(0,0.001)

nu_juv[1] <- nu_juv_dwn - ( (nu_juv_dwn + nu_juv_up) / 2 )
nu_juv[2] <- nu_juv_up - ( (nu_juv_dwn + nu_juv_up) / 2 )
nu_juv[3] <- nu_juv_up - ( (nu_juv_dwn + nu_juv_up) / 2 )

# 0+ Juvenile returning in the Allier for a given year
# and originating from the 3 areas of interest

for (t in 7:57){
  Juv_tot[t,1] <- (1/3) * Juv[t-3,1] + (1/3) * Juv[t-4,1] + (1/3) * Juv[t-5,1]
  Juv_tot[t,2] <- (1/3) * Juv[t-3,2] + (1/3) * Juv[t-4,2] + (1/3) * Juv[t-5,2]
}

for (t in 16:16){
  Juv_tot[t,3] <- (1/3) * Juv[t-3,3]
}
for (t in 17:17){
  Juv_tot[t,3] <- (1/3) * Juv[t-3,3] + (1/3) * Juv[t-4,3]
}
for (t in 18:57){
  Juv_tot[t,3] <- (1/3) * Juv[t-3,3] + (1/3) * Juv[t-4,3] + (1/3) * Juv[t-5,3]
}

for (t in 7:15){
  Juv_tot_system[t] <- Juv_tot[t,1]+Juv_tot[t,2]
}

for (t in 16:57){
  Juv_tot_system[t] <- Juv_tot[t,1]+Juv_tot[t,2] +Juv_tot[t,3]
}

```

```

s_juv2ad~dbeta(2,2)
dd_returns~dnorm(0,0.01)

sigma_Vichy <- sqrt( 1 / tau_vichy)      #~dunif(0.001,5)
tau_vichy~dgamma(0.001,0.001)          #<-pow(sigma_Vichy,-2)

L_mu_vichy~dnorm(0,0.01)

p_reach_V~dbeta(2,1)

for (t in 1:37){
  C_dwn_reach[t] <- p_reach_V * C_dwn[t]
  tot_C[t] <-round( C_dwn_reach[t] + C_up[t])
}
for (t in 1:6){
  min_N_1[t]<- tot_C[t] + S_stocking[t]+2
  N[t,1]~dlnorm(6.9,0.0453)|(min_N_1[t],15000)
}
I_surv[7] <- 1
I_surv_prim[7] <- 1

level_s~dnorm(0,1)

for (t in 8:57){
  I_surv_prim[t] ~ dbern(0.5)
  I_surv[t] <- I_surv[t-1] * I_surv_prim[t]
}

for (t in 7:11){

  min_N_1[t]<-tot_C[t] + S_stocking[t]+2

  pool_juv[t]<-s_juv2ad * Juv_tot_system[t] + s_smolt * (0.5 * smolts_tot[t+1] + 0.5 * smolts_tot[t] )

  L_mu_Vichy_nm[t]<-log( s_juv2ad * Juv_tot_system[t] + s_smolt * (0.5 * smolts_tot[t+1] + 0.5 * smolts_tot[t] )) + level_s *
I_surv[t]

  mean_y_surv[t] <- s_juv2ad * exp(level_s * I_surv[t])

  N[t,1]~dlnorm(L_mu_Vichy_nm[t],tau_vichy)|(min_N_1[t],15000)
  res_Vichy[t] <- log(N[t,1]) - L_mu_Vichy_nm[t]
}

# incorporating the effect that probability of passing at Langeac and Poutes is conditioned by the amount of juvenile produced

sigma_p_langeac<-sqrt(1/tau_p_langeac)
tau_p_langeac~dgamma(0.01,0.01)

sigma_p_poutes<-sqrt(1/tau_p_poutes)
tau_p_poutes~dgamma(0.01,0.01)

# filter:
# if negative fish returning in smaller proportion than what was expected regarding juvenile production
# if positive fish returning in higher proportion than what was expected regarding juvenile production

adjust_p_L ~ dnorm(0,0.01)
adjust_p_P ~ dnorm(0,0.01)

for (i in 1:3){
  ratio_habitat[i] <- S_juv_JP[i] /sum( S_juv_JP[])
}

rho_station~dbeta(2,2)

for (t in 1:4){
  ratio_juv_prod_V[t] <-1 - ratio_juv_prod_L[t]

  ratio_juv_prod_L[t]~dbeta(2,2)
}

```

```

ratio_juv_L[t]<- rho_station * (ratio_habitat[2] / (1 - ratio_habitat[3] )) + (1 - rho_station) * ratio_juv_prod_L[t]

L_ratio_juv_L[t] <- logit(ratio_juv_L[t])
L_mu_p_langeac[t]<-L_ratio_juv_L[t] + adjust_p_L
L_p_langeac[t]~dnorm(L_mu_p_langeac[t],tau_p_langeac)

res_p_langeac[t] <- L_p_langeac[t] - L_mu_p_langeac[t]
}
for (t in 5:5){
ratio_juv_prod_V[t] <-1 - ratio_juv_prod_L[t]

ratio_juv_prod_L[t] <- Juv[t-3,2] / ( Juv[t-3,1] + Juv[t-3,2] )

ratio_juv_L[t]<- rho_station * (ratio_habitat[2] / (1 - ratio_habitat[3] )) + (1 - rho_station) * ratio_juv_prod_L[t]

L_ratio_juv_L[t] <- logit(ratio_juv_L[t])
L_mu_p_langeac[t]<-L_ratio_juv_L[t]+ adjust_p_L
L_p_langeac[t]~dnorm(L_mu_p_langeac[t],tau_p_langeac)

res_p_langeac[t] <- L_p_langeac[t] - L_mu_p_langeac[t]
}
for (t in 6:6){
ratio_juv_prod_V[t] <-1 - ratio_juv_prod_L[t]
ratio_juv_prod_L[t] <- (Juv[t-3,2] + Juv[t-4,2] ) / ( Juv[t-3,1] + Juv[t-4,1] + Juv[t-3,2] +Juv[t-4,2] )

ratio_juv_L[t]<- rho_station * (ratio_habitat[2] / (1 - ratio_habitat[3] )) + (1 - rho_station) * ratio_juv_prod_L[t]

L_ratio_juv_L[t] <- logit(ratio_juv_L[t])
L_mu_p_langeac[t]<-L_ratio_juv_L[t]+ adjust_p_L
L_p_langeac[t]~dnorm(L_mu_p_langeac[t],tau_p_langeac)

res_p_langeac[t] <- L_p_langeac[t] - L_mu_p_langeac[t]
}
for (t in 7:11){
ratio_juv_prod_V[t] <-1 - ratio_juv_prod_L[t]

ratio_juv_prod_L[t] <- Juv_tot[t,2] / ( Juv_tot[t,1] + Juv_tot[t,2] )

ratio_juv_L[t]<- rho_station * (ratio_habitat[2] / (1 - ratio_habitat[3] )) + (1 - rho_station) * ratio_juv_prod_L[t]

L_ratio_juv_L[t] <- logit(ratio_juv_L[t])
L_mu_p_langeac[t]<-L_ratio_juv_L[t]+ adjust_p_L
L_p_langeac[t]~dnorm(L_mu_p_langeac[t],tau_p_langeac)

res_p_langeac[t] <- L_p_langeac[t] - L_mu_p_langeac[t]
}
for (t in 12:15){
ratio_juv_prod_V[t] <-1 - ratio_juv_prod_L[t]

ratio_juv_prod_L[t] <- Juv_tot[t,2] / ( Juv_tot[t,1] + Juv_tot[t,2] )

ratio_juv_L[t]<- rho_station * (ratio_habitat[2]+ratio_habitat[3]) + (1 - rho_station) * ratio_juv_prod_L[t]

L_ratio_juv_L[t] <- logit(ratio_juv_L[t])
L_mu_p_langeac[t]<-L_ratio_juv_L[t]+ adjust_p_L
L_p_langeac[t]~dnorm(L_mu_p_langeac[t],tau_p_langeac)

res_p_langeac[t] <- L_p_langeac[t] - L_mu_p_langeac[t]

ratio_juv_prod_P[t] <- 0
ratio_juv_P[t]<- rho_station * ( S_juv_JP[3] / (S_juv_JP[2] + S_juv_JP[3]) ) + (1 - rho_station) * ratio_juv_prod_P[t]

L_ratio_juv_P[t] <- logit(ratio_juv_P[t])
L_mu_p_poutes[t]<-L_ratio_juv_P[t] + adjust_p_P
L_p_poutes[t]~dnorm(L_mu_p_poutes[t],tau_p_poutes)

res_p_poutes[t] <- L_p_poutes[t] - L_mu_p_poutes[t]
}

```

```

for (t in 16:37){
  ratio_juv_V[t] <-1 - ratio_juv_prod_L[t]
  ratio_juv_prod_L[t] <- (Juv_tot[t,2] + Juv_tot[t,3]) / ( Juv_tot[t,1] + Juv_tot[t,2] + Juv_tot[t,3] )
  ratio_juv_L[t]<- rho_station * (ratio_habitat[2]+ratio_habitat[3]) + (1 - rho_station) * ratio_juv_prod_L[t]

  L_ratio_juv_L[t] <- logit(ratio_juv_L[t])
  L_mu_p_langeac[t]<-L_ratio_juv_L[t]+ adjust_p_L
  L_p_langeac[t]~dnorm(L_mu_p_langeac[t],tau_p_langeac)

  res_p_langeac[t] <- L_p_langeac[t] - L_mu_p_langeac[t]

  ratio_juv_prod_P[t] <- Juv_tot[t,3] / ( Juv_tot[t,1] + Juv_tot[t,2] + Juv_tot[t,3] )
  ratio_juv_P[t]<- rho_station * (S_juv_JP[3] / (S_juv_JP[2] + S_juv_JP[3])) + (1 - rho_station) * ratio_juv_prod_P[t]

  L_ratio_juv_P[t] <- logit(ratio_juv_P[t])

  L_mu_p_poutes[t]<-L_ratio_juv_P[t]+ adjust_p_P
  L_p_poutes[t]~dnorm(L_mu_p_poutes[t],tau_p_poutes)

  res_p_poutes[t] <- L_p_poutes[t] - L_mu_p_poutes[t]
}

rho_station_cut <- cut(rho_station)
adjust_p_L_cut <- cut(adjust_p_L)
adjust_p_P_cut <- cut(adjust_p_P)
tau_p_langeac_cut <- cut(tau_p_langeac)
tau_p_poutes_cut <- cut(tau_p_poutes)

for (t in 38:57){
  ratio_juv_V[t] <-1 - ratio_juv_prod_L[t]

  ratio_juv_prod_L[t] <- (Juv_tot[t,2] + Juv_tot[t,3]) / ( Juv_tot[t,1] + Juv_tot[t,2] + Juv_tot[t,3] )
  ratio_juv_L[t]<- rho_station_cut * (ratio_habitat[2]+ratio_habitat[3]) + (1 - rho_station_cut) * ratio_juv_prod_L[t]

  L_ratio_juv_L[t] <- logit(ratio_juv_L[t])
  L_mu_p_langeac[t]<-L_ratio_juv_L[t]+ adjust_p_L_cut
  L_p_langeac[t]~dnorm(L_mu_p_langeac[t],tau_p_langeac_cut)

  res_p_langeac[t] <- L_p_langeac[t] - L_mu_p_langeac[t]

  ratio_juv_prod_P[t] <- Juv_tot[t,3] / ( Juv_tot[t,1] + Juv_tot[t,2] + Juv_tot[t,3] )
  ratio_juv_P[t]<- rho_station_cut * (S_juv_JP[3] / (S_juv_JP[2]+S_juv_JP[3])) + (1 - rho_station_cut) * ratio_juv_prod_P[t]

  L_ratio_juv_P[t] <- logit(ratio_juv_P[t])

  L_mu_p_poutes[t]<-L_ratio_juv_P[t]+ adjust_p_P_cut
  L_p_poutes[t]~dnorm(L_mu_p_poutes[t],tau_p_poutes_cut)

  res_p_poutes[t] <- L_p_poutes[t] - L_mu_p_poutes[t]
}

# Loop for years (only downstream Poutès)
for (t in 1:11){

  #part redd/spawners
  logit(p_langeac[t])<- L_p_langeac[t]

  mu_N_L[t]<-N[t,1] * p_langeac[t]
  tau_N_L[t]<-1/ (N[t,1] * p_langeac[t] * (1-p_langeac[t]) )

  max_N_langeac[t]<- N_corrected[t] - 1 #N[t,1] - S_stocking[t] - 1

  #without fish caught for breeding or rod catches
  N_corrected[t] <- N[t,1] - tot_C[t] - S_stocking[t]

  N[t,2]~dbin(p_langeac[t],N_corrected[t])

```

```

S_ts[t,1]<- max( N[t,1] - tot_C[t] - S_stocking[t] - N[t,2] , 1)
S_ts[t,2]<- max(N[t,2],1)

ratio_S[t,1] <- S_ts[t,1] / ( S_ts[t,1] + S_ts[t,2] )
ratio_S[t,2] <- S_ts[t,2] / ( S_ts[t,1] + S_ts[t,2] )

# Loop for zones; 1= Vichy-Langeac, 2= Langeac-Poutès, 3= upstream Poutès
for (i in 1:2){

  #estimation of the spawners

  R[t,i] ~dpois(lambda[t,i])
  lambda[t,i] <- S_ts[t,i] *zone_effect[t,i] * hel_effect[1] *p_area[t,i]

  #residus calculés pour êtres centrés sur 0 avec varaince homogene
  res_R[t,i]<-(R[t,i]-lambda[t,i])/sqrt(lambda[t,i])

  lambda_cut[t,i]<-cut(lambda[t,i])

  R_rep[t,i]~dpois(lambda_cut[t,i])

  # I_juv_moy = indicator for stocking of 0+ or not
  # I_egg_moy = indicator for stocking of eggs or not

  d_tot_moy[t+1,i] <- d_wild_moy[t+1,i] + I_juv_moy[t+1,i] * d_juv_moy[t+1,i]

  Juv[t+1,i] <- d_tot_moy[t+1,i]*S_juv_JP[i]

  # wild component
  log(d_wild_moy[t+1,i]) <- L_d_wild_moy[t+1,i]

  L_d_wild_moy[t+1,i] ~ dnorm(L_mu_d_wild[t+1,i],tau_wild_moy)(-6.91,1.09)
  L_mu_d_wild[t+1,i] <- log((S_ts[t,i]/S_juv_JP[i]) / (alpha_dd + beta_dd * (S_ts[t,i]/S_juv_JP[i]))) + nu_wild[i]

  res_wild_moy[t+1,i] <- L_d_wild_moy[t+1,i] - L_mu_d_wild[t+1,i]

  # stocked juvenile component
  log(d_juv_moy[t+1,i]) <- L_d_juv_moy[t+1,i]

  L_d_juv_moy[t+1,i] ~ dnorm(L_mu_d_juv[t+1,i],tau_juv_moy[ I_juv_moy[t+1,i]+1])(-6.91,1.09)

  Rmax_juv[t+1,i] <- Rmax - ((S_ts[t,i]/S_juv_JP[i]) / (alpha_dd + beta_dd * (S_ts[t,i]/S_juv_JP[i])))
  beta_dd_juv[t+1,i] <- 1 / Rmax_juv[t+1,i]

  L_mu_d_juv[t+1,i] <- I_juv_moy[t+1,i] * log( (stock_juv[t+1,i]/S_juv_JP[i]) / ( (1/exp(nu_wild[i]) ) * alpha_dd_juv
+ beta_dd_juv[t+1,i] * (stock_juv[t+1,i]/S_juv_JP[i])) ) + (1 - I_juv_moy[t+1,i]) * 0

  res_juv_moy[t+1,i] <- L_d_juv_moy[t+1,i] - L_mu_d_juv[t+1,i]

  # getting out of the zone loop, one loop for each zones and the local densitie
  # to avoid using 3 dimensions matrix
}

# I_site_juv_V/L/P = indicator for presence/absence of stocking on the site

# loop for sites with successive removal EF

#####
# zone 1 Vichy Langeac #
#####
for (k in 1:J[t+1,1]){

  d_V[t+1,k]<- d_wild_V[t+1,k] + I_site_juv_V[t+1,k] * d_juv_V[t+1,k]

  log(d_wild_V[t+1,k])<-L_d_wild_V[t+1,k]
  L_d_wild_V[t+1,k] ~ dnorm( L_d_wild_moy[t+1,1] , tau_wild_site)(-6.91,1.09)

  log(d_juv_V[t+1,k]) <- L_d_juv_V[t+1,k]

```

```

L_d_juv_V[t+1,k] ~ dnorm( L_d_juv_moy[t+1,1] , tau_juv_site[ l_site_juv_V[t+1,k] + 1])|(-6.91,1.09)

lambda_N_V[t+1,k]<-d_V[t+1,k]*S_depl_V[t+1,k]

#Abundance follows a Poisson distribution
N_tot_V[t+1,k]~dpois(lambda_N_V[t+1,k])

L_p_V[t+1,k]~dnorm(L_mu_p_cut,L_tau_p_cut)
logit(p_V[t+1,k]) <-L_p_V[t+1,k]

C_1_V[t+1,k]~dbin(p_V[t+1,k],N_tot_V[t+1,k])
N_1_V[t+1,k]<-N_tot_V[t+1,k]-C_1_V[t+1,k]

#not all sites have 2 pass, this vector show which sites does
for (h in 1:pass_2_V[t+1,k]){
  C_2_V[t+1,k]~dbin(p_V[t+1,k],N_1_V[t+1,k])
  N_2_V[t+1,k]<-N_1_V[t+1,k]-C_2_V[t+1,k]
}

#####
# zone 2 Langeac Poutes #
#####
for (k in 1:J[t+1,2]){

  d_L[t+1,k]<- d_wild_L[t+1,k] + l_site_juv_L[t+1,k] * d_juv_L[t+1,k]

  log(d_wild_L[t+1,k])<-L_d_wild_L[t+1,k]
  L_d_wild_L[t+1,k] ~ dnorm( L_d_wild_moy[t+1,2] , tau_wild_site)|(-6.91,1.09)

  log(d_juv_L[t+1,k]) <- L_d_juv_L[t+1,k]
  L_d_juv_L[t+1,k] ~ dnorm( L_d_juv_moy[t+1,2] , tau_juv_site[ l_site_juv_L[t+1,k] + 1])|(-6.91,1.09)

  lambda_N_L[t+1,k]<-d_L[t+1,k]*S_depl_L[t+1,k]

  #Abundance follows a Poisson distribution
  N_tot_L[t+1,k]~dpois(lambda_N_L[t+1,k])

  L_p_L[t+1,k]~dnorm(L_mu_p_cut,L_tau_p_cut)
  logit(p_L[t+1,k]) <-L_p_L[t+1,k]

  C_1_L[t+1,k]~dbin(p_L[t+1,k],N_tot_L[t+1,k])
  N_1_L[t+1,k]<-N_tot_L[t+1,k]-C_1_L[t+1,k]

  #not all sites have 2 pass, this vector show which sites does
  for (h in 1:pass_2_L[t+1,k]){
    C_2_L[t+1,k]~dbin(p_L[t+1,k],N_1_L[t+1,k])
    N_2_L[t+1,k]<-N_1_L[t+1,k]-C_2_L[t+1,k]
  }
  #not all sites have 2 pass, this vector show which sites does
  for (m in 1:pass_3_L[t+1,k]){
    C_3_L[t+1,k]~dbin(p_L[t+1,k],N_2_L[t+1,k])
  }
}

}

# Loop for years (all zones)

for (t in 12:22){

  #part redd/spawners
  logit(p_langeac[t])<- L_p_langeac[t]

  logit(p_poutes[t])<- L_p_poutes[t]

  pool_juv[t]<-s_juv2ad * Juv_tot_system[t] + s_smolt * (0.5 * smolts_tot[t+1] + 0.5 * smolts_tot[t] )

  L_mu_Vichy_nm[t]<-log(s_juv2ad * Juv_tot_system[t] + s_smolt * (0.5 * smolts_tot[t+1] + 0.5 * smolts_tot[t] )) + level_s
  *_surv[t]

```

```

mean_y_surv[t] <- s_juv2ad * exp(level_s * l_surv[t])

min_N_1[t] <- max(N[t,3]+2,tot_C[t] +2)+S_stocking[t]
N[t,1] ~ dlnorm(L_mu_Vichy_nm[t],tau_vichy)(min_N_1[t],15000)

#without fish caught for breeding or rod catches
N_corrected[t] <- N[t,1] - tot_C[t] - S_stocking[t]

res_Vichy[t] <- log(N[t,1]) - L_mu_Vichy_nm[t]

#mu_N_L[t] <- N[t,1] * p_langeac[t]
#tau_N_L[t] <- 1/ (N[t,1] * p_langeac[t] * (1-p_langeac[t]) )

max_N_langeac[t] <- N_corrected[t] - 1
min_L_P[t] <- max(min_L[t], N[t,3]+1)

N[t,2] ~ dbin(p_langeac[t],N_corrected[t])l(min_L_P[t],)

max_N_poutes[t] <- N[t,2]-1
N[t,3] ~ dbin(p_poutes[t],N[t,2])

mu_S_ts[t,1] <- N[t,1] - N[t,2] - S_stocking[t]
mu_S_ts[t,2] <- N[t,2]-N[t,3]

test[t] <- mu_S_ts[t,1]-S_ts[t,1]

S_ts[t,1] <- max(N[t,1] - N[t,2] - S_stocking[t] - tot_C[t] , 1)
S_ts[t,2] <- max( N[t,2]-N[t,3],1) #
S_ts[t,3] <- max( N[t,3],1)

ratio_S[t,1] <- S_ts[t,1] / ( S_ts[t,1] + S_ts[t,2] + S_ts[t,3])
ratio_S[t,2] <- S_ts[t,2] / ( S_ts[t,1] + S_ts[t,2] + S_ts[t,3])
ratio_S[t,3] <- S_ts[t,3] / ( S_ts[t,1] + S_ts[t,2] + S_ts[t,3])

# Loop for zones; 1= Vichy-Langeac, 2= Langeac-Poutès, 3= upstream Poutès
for (i in 1:3){

  #estimation of the spawners
  R[t,i] ~ dpois(lambda[t,i])
  lambda[t,i] <- S_ts[t,i] * zone_effect[t,i] * hel_effect[1] * p_area[t,i]

  res_R[t,i] <- (R[t,i]-lambda[t,i])/sqrt(lambda[t,i])

  lambda_cut[t,i] <- cut(lambda[t,i])

  R_rep[t,i] ~ dpois(lambda_cut[t,i])

  #S_counter[t,i] <- R[t,i] / (zone_effect[t,i] * p_area[t,i])

  #chisq_disc_R[t,i] <- (R[t,i]-lambda[t,i]) * (R[t,i]-lambda[t,i]) / (lambda[t,i])
  #chisq_disc_R_rep[t,i] <- (R_rep[t,i]-lambda[t,i]) * (R_rep[t,i]-lambda[t,i]) / (lambda[t,i])

  # I_juv_moy = indicator for stocking of 0+ or not
  # I_egg_moy = indicator for stocking of eggs or not

  d_tot_moy[t+1,i] <- d_wild_moy[t+1,i] + I_juv_moy[t+1,i] * d_juv_moy[t+1,i] + I_egg_moy[t+1,i] *
d_egg_moy_surff[t+1,i]

  Juv[t+1,i] <- d_tot_moy[t+1,i]*S_juv_JP[i]

  d_egg_moy_surff[t+1,i] <- (S_inc_JP[t+1,i]/S_juv_JP[i]) * d_egg_moy[t+1,i]

  # wild component
  log(d_wild_moy[t+1,i]) <- L_d_wild_moy[t+1,i]

  L_d_wild_moy[t+1,i] ~ dnorm(L_mu_d_wild[t+1,i],tau_wild_moy)(-6.91,1.09)
  L_mu_d_wild[t+1,i] <- log((S_ts[t,i]/S_juv_JP[i]) / (alpha_dd + beta_dd * (S_ts[t,i]/S_juv_JP[i]))) + nu_wild[i]

```

```

res_wild_moy[t+1,i] <- L_d_wild_moy[t+1,i] - L_mu_d_wild[t+1,i]

# stocked juvenile component
log(d_juv_moy[t+1,i]) <- L_d_juv_moy[t+1,i]

L_d_juv_moy[t+1,i] ~ dnorm(L_mu_d_juv[t+1,i],tau_juv_moy[ l_juv_moy[t+1,i]+1])|(-6.91,1.09)

# We recalculate the Rmax "available" to stocked 0+ by subtracting wild 0+ density and stocked eggs density
# to the total Rmax of the density dependence relationship
Rmax_juv_temp[t+1,i] <- Rmax - ((S_ts[t,i]/S_juv_JP[i]) / (alpha_dd + beta_dd * (S_ts[t,i]/S_juv_JP[i]))) -
l_egg_moy[t+1,i] * (S_inc_JP[t+1,i]/S_juv_JP[i]) * exp( L_mu_d_egg[t+1,i] )

Rmax_juv[t+1,i]<-max( Rmax_juv_temp[t+1,i] , 0.000001)

beta_dd_juv[t+1,i] <- 1 / Rmax_juv[t+1,i]

L_mu_d_juv[t+1,i] <- l_juv_moy[t+1,i] * log( (stock_juv[t+1,i]/S_juv_JP[i]) / ( (1/exp(nu_wild[i]) ) * alpha_dd_juv
+ beta_dd_juv[t+1,i] * (stock_juv[t+1,i]/S_juv_JP[i])) ) + (1 - l_juv_moy[t+1,i]) * 0

res_juv_moy[t+1,i] <- L_d_juv_moy[t+1,i] - L_mu_d_juv[t+1,i]

# stocked egg component
log(d_egg_moy[t+1,i]) <- L_d_egg_moy[t+1,i]

L_d_egg_moy[t+1,i]~ dnorm(L_mu_d_egg[t+1,i],tau_egg_moy[ l_egg_moy[t+1,i] +1])|(-6.91,1.09)

res_egg_moy[t+1,i] <- L_d_egg_moy[t+1,i] - L_mu_d_egg[t+1,i]

# l_egg_unit = indicator of presence of incubators or not: only zone 1 and 2 concerned
# l_egg_VL = indicator for incubators in zone 1
# l_egg_LP = indicator for incubators in zone 2
# l_list_inc = indicator for each incubators loaded or not

L_mu_d_egg[t+1,i] <- l_egg_moy[t+1,i] * (
  l_egg_VL[t+1,i] * (
    l_list_inc[t+1,1] * log(s_egg * stock_egg[t+1,1] / S_inc[1]) +
    l_list_inc[t+1,2] * log(s_egg * stock_egg[t+1,2] / S_inc[2]) +
    l_list_inc[t+1,3] * log(s_egg * stock_egg[t+1,3] / S_inc[3]) +
    l_list_inc[t+1,4] * log(s_egg * stock_egg[t+1,4] / S_inc[4])
  )
  + l_egg_LP[t+1,i] * (
    l_list_inc[t+1,5] * log(s_egg * stock_egg[t+1,5] / S_inc[5]) +
    l_list_inc[t+1,6] * log(s_egg * stock_egg[t+1,6] / S_inc[6])
  )
) + (1 - l_egg_moy[t+1,i]) * 0

# getting out of the zone loop, one loop for each zones and the local densitie
# to avoid using 3 dimensions matrix
}

# l_site_juv_VL/P = indicator for presence/absence of stocking on the site

# loop for sites with successive removal EF

###
# zone 1 Vichy Langeac
###
for (k in 1:J[t+1,1]){

  d_V[t+1,k]<- d_wild_V[t+1,k] + l_site_juv_V[t+1,k] * d_juv_V[t+1,k]

  log(d_wild_V[t+1,k])<-L_d_wild_V[t+1,k]
  L_d_wild_V[t+1,k] ~ dnorm( L_d_wild_moy[t+1,1] , tau_wild_site)|(-6.91,1.09)

  log(d_juv_V[t+1,k]) <- L_d_juv_V[t+1,k]
  L_d_juv_V[t+1,k] ~ dnorm( L_d_juv_moy[t+1,1] , tau_juv_site[l_site_juv_V[t+1,k] + 1])|(-6.91,1.09)

  lambda_N_V[t+1,k]<-d_V[t+1,k]*S_depl_V[t+1,k]

```

```

#Abundance follows a Poisson distribution
N_tot_V[t+1,k]~dpois(lambda_N_V[t+1,k])
L_p_V[t+1,k]~dnorm(L_mu_p_cut,L_tau_p_cut)
logit(p_V[t+1,k]) <-L_p_V[t+1,k]

C_1_V[t+1,k]~dbin(p_V[t+1,k],N_tot_V[t+1,k])
N_1_V[t+1,k]<-N_tot_V[t+1,k]-C_1_V[t+1,k]

#not all sites have 2 pass, this vector show which sites does
for (h in 1:pass_2_V[t+1,k]){
  C_2_V[t+1,k]~dbin(p_V[t+1,k],N_1_V[t+1,k])
  N_2_V[t+1,k]<-N_1_V[t+1,k]-C_2_V[t+1,k]
}
}

###
# zone 2 Langeac Poutes
###
for (k in 1:J[t+1,2]){

  d_L[t+1,k]<- d_wild_L[t+1,k] + I_site_juv_L[t+1,k] * d_juv_L[t+1,k]

  log(d_wild_L[t+1,k])<-L_d_wild_L[t+1,k]
  L_d_wild_L[t+1,k] ~ dnorm( L_d_wild_moy[t+1,2] , tau_wild_site|(-6.91,3)

  log(d_juv_L[t+1,k]) <- L_d_juv_L[t+1,k]
  L_d_juv_L[t+1,k] ~ dnorm( L_d_juv_moy[t+1,2] , tau_juv_site[ I_site_juv_L[t+1,k] + 1])|(-6.91,1.09)

  lambda_N_L[t+1,k]<-d_L[t+1,k]*S_depl_L[t+1,k]

#Abundance follows a Poisson distribution
N_tot_L[t+1,k]~dpois(lambda_N_L[t+1,k])

L_p_L[t+1,k]~dnorm(L_mu_p_cut,L_tau_p_cut)
logit(p_L[t+1,k]) <-L_p_L[t+1,k]

C_1_L[t+1,k]~dbin(p_L[t+1,k],N_tot_L[t+1,k])
N_1_L[t+1,k]<-N_tot_L[t+1,k]-C_1_L[t+1,k]

#not all sites have 2 pass, this vector show which sites does
for (h in 1:pass_2_L[t+1,k]){
  C_2_L[t+1,k]~dbin(p_L[t+1,k],N_1_L[t+1,k])
  N_2_L[t+1,k]<-N_1_L[t+1,k]-C_2_L[t+1,k]
#not all sites have 2 pass, this vector show which sites does
for (m in 1:pass_3_L[t+1,k]){
  C_3_L[t+1,k]~dbin(p_L[t+1,k],N_2_L[t+1,k])
}
}
}

#####
# zone 3 upstream Poutes #
#####
for (k in 1:J[t+1,3]){
  d_P[t+1,k]<- d_wild_P[t+1,k] + I_site_juv_P[t+1,k] * d_juv_P[t+1,k]

  log(d_wild_P[t+1,k])<-L_d_wild_P[t+1,k]
  L_d_wild_P[t+1,k] ~ dnorm( L_d_wild_moy[t+1,3] , tau_wild_site|(-6.91,1.09)

  log(d_juv_P[t+1,k]) <- L_d_juv_P[t+1,k]
  L_d_juv_P[t+1,k] ~ dnorm( L_d_juv_moy[t+1,3] , tau_juv_site[ I_site_juv_P[t+1,k] + 1])|(-6.91,1.09)

  lambda_N_P[t+1,k]<-d_P[t+1,k]*S_depl_P[t+1,k]

#Abundance follows a Poisson distribution
N_tot_P[t+1,k]~dpois(lambda_N_P[t+1,k])

L_p_P[t+1,k]~dnorm(L_mu_p_cut,L_tau_p_cut)
logit(p_P[t+1,k]) <-L_p_P[t+1,k]

C_1_P[t+1,k]~dbin(p_P[t+1,k],N_tot_P[t+1,k])
N_1_P[t+1,k]<-N_tot_P[t+1,k]-C_1_P[t+1,k]

```

```

#not all sites have 2 pass, this vector show which sites does
for (h in 1:pass_2_P[t+1,k]){
  C_2_P[t+1,k]~dbin(p_P[t+1,k],N_1_P[t+1,k])
  N_2_P[t+1,k]<-N_1_P[t+1,k]-C_2_P[t+1,k]
}

###
# loop for sites with 5 min IA EF
###
# zone 1 Vichy Langeac
###
for (k in 1:K[t+1,1]){

d_egg_V[t+1,k]      d_V[t+1,k]<- d_wild_V[t+1,k] + I_site_juv_V[t+1,k] * d_juv_V[t+1,k] + I_site_egg_V[t+1,k] *

log(d_wild_V[t+1,k])<-L_d_wild_V[t+1,k]
L_d_wild_V[t+1,k] ~ dnorm( L_d_wild_moy[t+1,1] , tau_wild_site)l(-6.91,3)

log(d_juv_V[t+1,k]) <- L_d_juv_V[t+1,k]
L_d_juv_V[t+1,k] ~ dnorm( L_d_juv_moy[t+1,1] , tau_juv_site[ I_site_juv_V[t+1,k] + 1])l(-6.91,1.09)

log(d_egg_V[t+1,k]) <- L_d_egg_V[t+1,k]
L_d_egg_moy_V_inc[t+1,k]<- L_d_egg_moy[t+1,1]/nb_inc[t+1,1]
L_d_egg_V[t+1,k] ~ dnorm( L_d_egg_moy_V_inc[t+1,k] , tau_egg_site[l_site_egg_V[t+1,k] + 1])l(-
6.91,1.09)

#5minute EF part
lambda_IA_V[t+1,k]<-kappa_cut*pow(d_V[t+1,k],eta_cut)

EF_IA_V[t+1,k]~dpois(lambda_IA_V[t+1,k])
}

###
# zone 2 Langeac Poutes
###
for (k in 1:K[t+1,2]){

d_egg_L[t+1,k]      d_L[t+1,k]<- d_wild_L[t+1,k] + I_site_juv_L[t+1,k] * d_juv_L[t+1,k] + I_site_egg_L[t+1,k] *

log(d_wild_L[t+1,k])<-L_d_wild_L[t+1,k]
L_d_wild_L[t+1,k] ~ dnorm( L_d_wild_moy[t+1,2] , tau_wild_site)l(-6.91,1.09)

log(d_juv_L[t+1,k]) <- L_d_juv_L[t+1,k]
L_d_juv_L[t+1,k] ~ dnorm( L_d_juv_moy[t+1,2] , tau_juv_site[ I_site_juv_L[t+1,k] + 1])l(-6.91,1.09)

log(d_egg_L[t+1,k]) <- L_d_egg_L[t+1,k]
L_d_egg_moy_L_inc[t+1,k]<- L_d_egg_moy[t+1,2]/nb_inc[t+1,2]
L_d_egg_L[t+1,k] ~ dnorm( L_d_egg_moy_L_inc[t+1,k] , tau_egg_site[l_site_egg_L[t+1,k] + 1])l(-
6.91,1.09)

#5minute EF part
lambda_IA_L[t+1,k]<-kappa_cut*pow(d_L[t+1,k],eta_cut)

EF_IA_L[t+1,k]~dpois(lambda_IA_L[t+1,k])
}

###
# zone 3 upstream Poutes
###
for (k in 1:K[t+1,3]){

d_P[t+1,k]<- d_wild_P[t+1,k] + I_site_juv_P[t+1,k] * d_juv_P[t+1,k]

log(d_wild_P[t+1,k])<-L_d_wild_P[t+1,k]
L_d_wild_P[t+1,k] ~ dnorm( L_d_wild_moy[t+1,3] , tau_wild_site)l(-6.91,1.09)

log(d_juv_P[t+1,k]) <- L_d_juv_P[t+1,k]
L_d_juv_P[t+1,k] ~ dnorm( L_d_juv_moy[t+1,3] , tau_juv_site[ I_site_juv_P[t+1,k] + 1])l(-6.91,1.09)

```

```

#5minute EF part
lambda_IA_P[t+1,k]<-kappa_cut*pow(d_P[t+1,k],eta_cut)

EF_IA_P[t+1,k]~dpois(lambda_IA_P[t+1,k])
}

}

#####
# change in redd count methodology
#####

for (t in 23:36){
  #part redd/spawners
  logit(p_langeac[t])<- L_p_langeac[t]

  logit(p_poutes[t])<- L_p_poutes[t]

  pool_juv[t]<-s_juv2ad * Juv_tot_system[t] + s_smolt * (0.5 * smolts_tot[t+1] + 0.5 * smolts_tot[t] )

  L_mu_Vichy_nm[t]<-log(s_juv2ad * Juv_tot_system[t] + s_smolt * (0.5 * smolts_tot[t+1] + 0.5 * smolts_tot[t] )) + level_s
  *I_surv[t]

  mean_y_surv[t] <- s_juv2ad * exp(level_s * I_surv[t])

  #min_N_1[t]<-max(N[t,3]+2 , min_L[t]) + S_stocking[t] + 2

  # max is only added for the year we only have a minimum figure at vichy
  temp[t]<-max(tot_C[t] + S_stocking[t]+2,min_N_V[t])

  min_N_1[t]<-max(N[t,3]+2,temp[t] +2)+S_stocking[t]
  N[t,1]~dlnorm(L_mu_Vichy_nm[t],tau_vichy)|(min_N_1[t],15000)

  #without fish caught for breeding or rod catches
  N_corrected[t] <- N[t,1] - tot_C[t] - S_stocking[t]

  res_Vichy[t] <- log(N[t,1]) - L_mu_Vichy_nm[t]

  #mu_N_L[t]<-N[t,1] * p_langeac[t]
  #tau_N_L[t]<-1/ (N[t,1] * p_langeac[t] * (1-p_langeac[t]) )

  max_N_langeac[t]<- N_corrected[t] - 1 #N[t,1] - S_stocking[t]-1
  min_L_P[t]<-max(min_L[t], N[t,3]+1) # max(N[t,3]+1 , min_L[t])

  N[t,2]~dbin(p_langeac[t],N_corrected[t])|(min_L_P[t],) #
  #~dnorm(mu_N_L[t],tau_N_L[t])|(min_L_P[t],max_N_langeac[t])

  #mu_N_P[t]<-N[t,2] * p_poutes[t]
  #tau_N_P[t]<-1/ (N[t,2] * p_poutes[t] * (1-p_poutes[t]) )

  max_N_poutes[t]<-N[t,2]-1
  N[t,3]~dbin(p_poutes[t],N[t,2]) ##~dnorm(mu_N_P[t],tau_N_P[t])|(1,max_N_poutes[t])

  mu_S_ts[t,1]<- N[t,1] - N[t,2] - S_stocking[t]
  mu_S_ts[t,2]<- N[t,2]-N[t,3]

  test[t]<-mu_S_ts[t,1]-S_ts[t,1]

  S_ts[t,1]<- max(N[t,1] - N[t,2] - S_stocking[t] - tot_C[t] , 1) #~dnorm(mu_S_ts[t,1],1)|(0.001,) #
  S_ts[t,2]<- max( N[t,2]-N[t,3],1) #~dnorm(mu_S_ts[t,2],1) #
  S_ts[t,3]<-max( N[t,3],1)

```

```

ratio_S[t,1] <- S_ts[t,1] / ( S_ts[t,1] + S_ts[t,2] + S_ts[t,3])
ratio_S[t,2] <- S_ts[t,2] / ( S_ts[t,1] + S_ts[t,2] + S_ts[t,3])
ratio_S[t,3] <- S_ts[t,3] / ( S_ts[t,1] + S_ts[t,2] + S_ts[t,3])

# Loop for zones; 1= Vichy-Langeac, 2= Langeac-Poutès, 3= upstream Poutès
for (i in 1:3){

  #estimation of the spawners
  R[t,i]~dpois(lambda[t,i])
  lambda[t,i] <- S_ts[t,i] *zone_effect[t,i]* hel_effect[2] *p_area[t,i]

  res_R[t,i]<-(R[t,i]-lambda[t,i])/sqrt(lambda[t,i])

  lambda_cut[t,i]<-cut(lambda[t,i])

  R_rep[t,i]~dpois(lambda_cut[t,i])

  #S_counter[t,i]<-R[t,i] / (zone_effect[t,i] *p_area[t,i])

  #chisq_disc_R[t,i]<- (R[t,i]-lambda[t,i]) * (R[t,i]-lambda[t,i]) / (lambda[t,i])
  #chisq_disc_R_rep[t,i]<- (R_rep[t,i]-lambda[t,i]) * (R_rep[t,i]-lambda[t,i]) / (lambda[t,i])

  # I_juv_moy = indicator for stocking of 0+ or not
  # I_egg_moy = indicator for stocking of eggs or not

  d_tot_moy[t+1,i] <- d_wild_moy[t+1,i] + I_juv_moy[t+1,i] * d_juv_moy[t+1,i] + I_egg_moy[t+1,i] *
d_egg_moy_surff[t+1,i]

  Juv[t+1,i] <- d_tot_moy[t+1,i]*S_juv_JP[i]

  d_egg_moy_surff[t+1,i] <- (S_inc_JP[t+1,i]/S_juv_JP[i]) * d_egg_moy[t+1,i]

  # wild component
  log(d_wild_moy[t+1,i]) <- L_d_wild_moy[t+1,i]

  #
  L_d_wild_moy[t+1,i] ~ dnorm(L_mu_d_wild[t+1,i],tau_wild_moy)/(-6.91,1.09)    #<- L_mu_d_wild[t+1,i]
  L_mu_d_wild[t+1,i] <- log((S_ts[t,i]/S_juv_JP[i]) / (alpha_dd + beta_dd * (S_ts[t,i]/S_juv_JP[i]))) + nu_wild[i]

  res_wild_moy[t+1,i] <- L_d_wild_moy[t+1,i] - L_mu_d_wild[t+1,i]

  # stocked juvenile component
  log(d_juv_moy[t+1,i]) <- L_d_juv_moy[t+1,i]

  L_d_juv_moy[t+1,i] ~ dnorm(L_mu_d_juv[t+1,i],tau_juv_moy[ I_juv_moy[t+1,i]+1])/(-6.91,1.09)

  # We recalculate the Rmax "available" to stocked 0+ by subtracting wild 0+ density and stocked eggs density
  # to the total Rmax of the density dependence relationship
  Rmax_juv_temp[t+1,i] <- Rmax - ((S_ts[t,i]/S_juv_JP[i]) / (alpha_dd + beta_dd * (S_ts[t,i]/S_juv_JP[i]))) -
I_egg_moy[t+1,i] * (S_inc_JP[t+1,i]/S_juv_JP[i]) * exp( L_mu_d_egg[t+1,i] )

  Rmax_juv[t+1,i]<-max( Rmax_juv_temp[t+1,i] , 0.000001)

  beta_dd_juv[t+1,i] <- 1 / Rmax_juv[t+1,i]

  L_mu_d_juv[t+1,i] <- I_juv_moy[t+1,i] * log( (stock_juv[t+1,i]/S_juv_JP[i]) / ( (1/exp(nu_wild[i]) ) * alpha_dd_juv
+ beta_dd_juv[t+1,i] * (stock_juv[t+1,i]/S_juv_JP[i]) ) ) + (1 - I_juv_moy[t+1,i]) * 0

  res_juv_moy[t+1,i] <- L_d_juv_moy[t+1,i] - L_mu_d_juv[t+1,i]

  # stocked egg component
  log(d_egg_moy[t+1,i]) <- L_d_egg_moy[t+1,i]

  L_d_egg_moy[t+1,i]~ dnorm(L_mu_d_egg[t+1,i],tau_egg_moy[ I_egg_moy[t+1,i] +1])/(-6.91,1.09)    #
  res_egg_moy[t+1,i] <- L_d_egg_moy[t+1,i] - L_mu_d_egg[t+1,i]

```

```

# l_egg_unit = indicator of presence of incubators or not: only zone 1 and 2 concerned
# l_egg_VL = indicator for incubators in zone 1
# l_egg_LP = indicator for incubators in zone 2
# l_list_inc = indicator for each incubators loaded or not

L_mu_d_egg[t+1,i] <- l_egg_moy[t+1,i] * (
  l_egg_VL[t+1,i] * (
    l_list_inc[t+1,1] * log(s_egg * stock_egg[t+1,1] / S_inc[1]) +
    l_list_inc[t+1,2] * log(s_egg * stock_egg[t+1,2] / S_inc[2]) +
    l_list_inc[t+1,3] * log(s_egg * stock_egg[t+1,3] / S_inc[3]) +
    l_list_inc[t+1,4] * log(s_egg * stock_egg[t+1,4] / S_inc[4])
  )
  + l_egg_LP[t+1,i] * (
    l_list_inc[t+1,5] * log(s_egg * stock_egg[t+1,5] / S_inc[5]) +
    l_list_inc[t+1,6] * log(s_egg * stock_egg[t+1,6] / S_inc[6])
  )
) + (1 - l_egg_moy[t+1,i]) * 0
# getting out of the zone loop, one loop for each zones and the local densitie
# to avoid using 3 dimensions matrix
}

# l_site_juv_V/L/P = indicator for presence/absence of stocking on the site

# loop for sites with successive removal EF

###
# zone 1 Vichy Langeac
###
for (k in 1:J[t+1,1]){
  d_V[t+1,k] <- d_wild_V[t+1,k] + l_site_juv_V[t+1,k] * d_juv_V[t+1,k]

  log(d_wild_V[t+1,k]) <- L_d_wild_V[t+1,k]
  L_d_wild_V[t+1,k] ~ dnorm( L_d_wild_moy[t+1,1] , tau_wild_site) | (-6.91, 1.09)

  log(d_juv_V[t+1,k]) <- L_d_juv_V[t+1,k]
  L_d_juv_V[t+1,k] ~ dnorm( L_d_juv_moy[t+1,1] , tau_juv_site[l_site_juv_V[t+1,k] + 1]) | (-6.91, 1.09)

  lambda_N_V[t+1,k] <- d_V[t+1,k] * S_depl_V[t+1,k]

  #Abundance follows a Poisson distribution
  N_tot_V[t+1,k] ~ dpois(lambda_N_V[t+1,k])

  L_p_V[t+1,k] ~ dnorm(L_mu_p_cut, L_tau_p_cut)
  logit(p_V[t+1,k]) <- L_p_V[t+1,k]

  C_1_V[t+1,k] ~ dbin(p_V[t+1,k], N_tot_V[t+1,k])
  N_1_V[t+1,k] <- N_tot_V[t+1,k] - C_1_V[t+1,k]

  #not all sites have 2 pass, this vector show which sites does
  for (h in 1:pass_2_V[t+1,k]){
    C_2_V[t+1,k] ~ dbin(p_V[t+1,k], N_1_V[t+1,k])
    N_2_V[t+1,k] <- N_1_V[t+1,k] - C_2_V[t+1,k]
  }
}

###
# zone 2 Langeac Poutes
###
for (k in 1:J[t+1,2]){
  d_L[t+1,k] <- d_wild_L[t+1,k] + l_site_juv_L[t+1,k] * d_juv_L[t+1,k]

  log(d_wild_L[t+1,k]) <- L_d_wild_L[t+1,k]
  L_d_wild_L[t+1,k] ~ dnorm( L_d_wild_moy[t+1,2] , tau_wild_site) | (-6.91, 3)

  log(d_juv_L[t+1,k]) <- L_d_juv_L[t+1,k]
  L_d_juv_L[t+1,k] ~ dnorm( L_d_juv_moy[t+1,2] , tau_juv_site[ l_site_juv_L[t+1,k] + 1]) | (-6.91, 1.09)

  lambda_N_L[t+1,k] <- d_L[t+1,k] * S_depl_L[t+1,k]

```

```

#Abundance follows a Poisson distribution
N_tot_L[t+1,k]~dpois(lambda_N_L[t+1,k])

L_p_L[t+1,k]~dnorm(L_mu_p_cut,L_tau_p_cut)
logit(p_L[t+1,k]) <-L_p_L[t+1,k]

C_1_L[t+1,k]~dbin(p_L[t+1,k],N_tot_L[t+1,k])
N_1_L[t+1,k]<-N_tot_L[t+1,k]-C_1_L[t+1,k]

#not all sites have 2 pass, this vector show which sites does
for (h in 1:pass_2_L[t+1,k]){
  C_2_L[t+1,k]~dbin(p_L[t+1,k],N_1_L[t+1,k])
  N_2_L[t+1,k]<-N_1_L[t+1,k]-C_2_L[t+1,k]
#not all sites have 2 pass, this vector show which sites does
for (m in 1:pass_3_L[t+1,k]){
  C_3_L[t+1,k]~dbin(p_L[t+1,k],N_2_L[t+1,k])
}
}

###
# zone 3 upstream Poutes
###
for (k in 1:J[t+1,3]){
  d_P[t+1,k]<- d_wild_P[t+1,k] + I_site_juv_P[t+1,k] * d_juv_P[t+1,k]

  log(d_wild_P[t+1,k])<-L_d_wild_P[t+1,k]
  L_d_wild_P[t+1,k] ~ dnorm( L_d_wild_moy[t+1,3] , tau_wild_site)l(-6.91,1.09)

  log(d_juv_P[t+1,k]) <- L_d_juv_P[t+1,k]
  L_d_juv_P[t+1,k] ~ dnorm( L_d_juv_moy[t+1,3] , tau_juv_site[ I_site_juv_P[t+1,k] + 1])l(-6.91,1.09)

  lambda_N_P[t+1,k]<-d_P[t+1,k]*S_depl_P[t+1,k]

#Abundance follows a Poisson distribution
N_tot_P[t+1,k]~dpois(lambda_N_P[t+1,k])

L_p_P[t+1,k]~dnorm(L_mu_p_cut,L_tau_p_cut)
logit(p_P[t+1,k]) <-L_p_P[t+1,k]

C_1_P[t+1,k]~dbin(p_P[t+1,k],N_tot_P[t+1,k])
N_1_P[t+1,k]<-N_tot_P[t+1,k]-C_1_P[t+1,k]

#not all sites have 2 pass, this vector show which sites does
for (h in 1:pass_2_P[t+1,k]){
  C_2_P[t+1,k]~dbin(p_P[t+1,k],N_1_P[t+1,k])
  N_2_P[t+1,k]<-N_1_P[t+1,k]-C_2_P[t+1,k]
}
}

###
# loop for sites with 5 min IA EF
###
# zone 1 Vichy Langeac
###
for (k in 1:K[t+1,1]){

  d_V[t+1,k]<- d_wild_V[t+1,k] + I_site_juv_V[t+1,k] * d_juv_V[t+1,k] + I_site_egg_V[t+1,k] *
d_egg_V[t+1,k]

  log(d_wild_V[t+1,k])<-L_d_wild_V[t+1,k]
  L_d_wild_V[t+1,k] ~ dnorm( L_d_wild_moy[t+1,1] , tau_wild_site)l(-6.91,3)

  log(d_juv_V[t+1,k]) <- L_d_juv_V[t+1,k]
  L_d_juv_V[t+1,k] ~ dnorm( L_d_juv_moy[t+1,1] , tau_juv_site[ I_site_juv_V[t+1,k] + 1])l(-6.91,1.09)

  log(d_egg_V[t+1,k]) <- L_d_egg_V[t+1,k]
  L_d_egg_moy_V_inc[t+1,k]<- L_d_egg_moy[t+1,1]/nb_inc[t+1,1]
  L_d_egg_V[t+1,k] ~ dnorm( L_d_egg_moy_V_inc[t+1,k] , tau_egg_site[l_site_egg_V[t+1,k] + 1])l(-
6.91,1.09)

```

```

#5minute EF part
lambda_IA_V[t+1,k]<-kappa_cut*pow(d_V[t+1,k],eta_cut)

EF_IA_V[t+1,k]~dpois(lambda_IA_V[t+1,k])
}

###
# zone 2 Langeac Poutes
###
for (k in 1:K[t+1,2]){
d_egg_L[t+1,k]
d_L[t+1,k]<- d_wild_L[t+1,k] + I_site_juv_L[t+1,k] * d_juv_L[t+1,k] + I_site_egg_L[t+1,k] *

log(d_wild_L[t+1,k])<-L_d_wild_L[t+1,k]
L_d_wild_L[t+1,k] ~ dnorm( L_d_wild_moy[t+1,2] , tau_wild_site)(-6.91,1.09)

log(d_juv_L[t+1,k]) <- L_d_juv_L[t+1,k]
L_d_juv_L[t+1,k] ~ dnorm( L_d_juv_moy[t+1,2] , tau_juv_site[ I_site_juv_L[t+1,k] + 1])(-6.91,1.09)

log(d_egg_L[t+1,k]) <- L_d_egg_L[t+1,k]
L_d_egg_moy_L_inc[t+1,k]<- L_d_egg_moy[t+1,2]/nb_inc[t+1,2]
L_d_egg_L[t+1,k] ~ dnorm( L_d_egg_moy_L_inc[t+1,k] , tau_egg_site[I_site_egg_L[t+1,k] + 1])(-
6.91,1.09)

#5minute EF part
lambda_IA_L[t+1,k]<-kappa_cut*pow(d_L[t+1,k],eta_cut)

EF_IA_L[t+1,k]~dpois(lambda_IA_L[t+1,k])
}

###
# zone 3 upstream Poutes
###
for (k in 1:K[t+1,3]){
d_P[t+1,k]<- d_wild_P[t+1,k] + I_site_juv_P[t+1,k] * d_juv_P[t+1,k]

log(d_wild_P[t+1,k])<-L_d_wild_P[t+1,k]
L_d_wild_P[t+1,k] ~ dnorm( L_d_wild_moy[t+1,3] , tau_wild_site)(-6.91,1.09)

log(d_juv_P[t+1,k]) <- L_d_juv_P[t+1,k]
L_d_juv_P[t+1,k] ~ dnorm( L_d_juv_moy[t+1,3] , tau_juv_site[ I_site_juv_P[t+1,k] + 1])(-6.91,1.09)

#5minute EF part
lambda_IA_P[t+1,k]<-kappa_cut*pow(d_P[t+1,k],eta_cut)

EF_IA_P[t+1,k]~dpois(lambda_IA_P[t+1,k])

}
}

#Just the last year to estimate spawners
for (t in T:T){

logit(p_langeac[t])<- L_p_langeac[t]

logit(p_poutes[t])<- L_p_poutes[t]

pool_juv[t]<-s_juv2ad * Juv_tot_system[t] + s_smolt * (0.5 * smolts_tot[t+1] + 0.5 * smolts_tot[t] )

L_mu_Vichy_nm[t]<-log(s_juv2ad * Juv_tot_system[t] + s_smolt * (0.5 * smolts_tot[t+1] + 0.5 * smolts_tot[t] )) + level_s
*I_surv[t]

min_N_1[t]<-max(N[t,3]+2,tot_C[t] +2)+S_stocking[t]
N[t,1]~dlnorm(L_mu_Vichy_nm[t],tau_vichy)(min_N_1[t],15000)

res_Vichy[t] <- log(N[t,1]) - L_mu_Vichy_nm[t]

```

```

N_corrected[t]<-N[t,1]-S_stocking[t]

max_N_langeac[t]<- N_corrected[t] -1 #N[t,1] - S_stocking[t]-1
min_L_P[t]<-N[t,3]+1 #max(N[t,3]+2 , min_L[t])

N[t,2]~dbin(p_langeac[t],N_corrected[t])/(min_L_P[t,]) #
#~dnorm(mu_N_L[t],tau_N_L[t])/(min_L_P[t],max_N_langeac[t])

mu_N_P[t]<-N[t,2] * p_poutes[t]
tau_N_P[t]<-1/ (N[t,2] * p_poutes[t] * (1-p_poutes[t]) )

max_N_poutes[t]<-N[t,2]-1

N[t,3]~dnorm(mu_N_P[t],tau_N_P[t]) #~dbin(p_poutes[t],N[t,2])
#~dnorm(mu_N_P[t],tau_N_P[t])/(1,max_N_poutes[t])

S_ts[t,1]<- max( N[t,1] - S_stocking[t] -tot_C[t]-N[t,2],1)
S_ts[t,2]<- max( N[t,2]-N[t,3],1)
S_ts[t,3]<-max( N[t,3],1)

ratio_S[t,1] <- S_ts[t,1] / ( S_ts[t,1] + S_ts[t,2] + S_ts[t,3])
ratio_S[t,2] <- S_ts[t,2] / ( S_ts[t,1] + S_ts[t,2] + S_ts[t,3])
ratio_S[t,3] <- S_ts[t,3] / ( S_ts[t,1] + S_ts[t,2] + S_ts[t,3])

for (i in 1:3){
  R[t,i]~dpois(lambda[t,i])
  lambda[t,i] <- S_ts[t,i] *zone_effect[t,i] * hel_effect[2]*p_area[t,i]

  res_R[t,i]<-(R[t,i]-lambda[t,i])/sqrt(lambda[t,i])

  lambda_cut[t,i]<-cut(lambda[t,i])

  R_rep[t,i]~dpois(lambda_cut[t,i])

  #S_counter[t,i]<-R[t,i] / (zone_effect[t,i] *p_area[t,i])

  #chisq_disc_R[t,i]<- (R[t,i]-lambda[t,i]) * (R[t,i]-lambda[t,i]) / (lambda[t,i])
  #chisq_disc_R_rep[t,i]<- (R_rep[t,i]-lambda[t,i]) * (R_rep[t,i]-lambda[t,i]) / (lambda[t,i])

  # juvenile production (only wild)
  d_tot_moy[t+1,i] <- d_wild_moy[t+1,i]
  Juv[t+1,i] <- d_tot_moy[t+1,i]*S_juv_JP[i]

  # wild component
  log(d_wild_moy[t+1,i]) <- L_d_wild_moy[t+1,i]

  L_d_wild_moy[t+1,i] ~ dnorm(L_mu_d_wild[t+1,i],tau_wild_moy)/(-6.91,1.09)
  L_mu_d_wild[t+1,i] <- log((S_ts[t,i]/S_juv_JP[i]) / (alpha_dd + beta_dd * (S_ts[t,i]/S_juv_JP[i]))) + nu_wild[i]

  res_wild_moy[t+1,i] <- L_d_wild_moy[t+1,i] - L_mu_d_wild[t+1,i]
}
}

tau_vichy_cut <- cut(tau_vichy)
s_juv2ad_cut <- cut(s_juv2ad)

alpha_dd_cut <-cut(alpha_dd)
beta_dd_cut <-cut(beta_dd)

tau_wild_moy_cut <- cut(tau_wild_moy)
for (i in 1:3){
  #tau_wild_moy_cut[i] <- cut(tau_wild_moy[i])
  nu_wild_cut[i] <- cut(nu_wild[i])
}

```

projections for the next 15 years

```
for (t in 38:57){
  logit(p_langeac[t])<- L_p_langeac[t]

  logit(p_poutes[t])<- L_p_poutes[t]

  pool_juv[t]<-s_juv2ad * Juv_tot_system[t] + s_smolt * (0.5 * smolts_tot[t+1] + 0.5 * smolts_tot[t] )

  L_mu_Vichy_nm[t]<-log( s_juv2ad_cut *Juv_tot_system[t] + s_smolt * (0.5 * smolts_tot[t+1] + 0.5 * smolts_tot[t] ))

  min_N_1[t]<-N[t,3]+2+ S_stocking[t] #max(N[t,3]+2 , min_L[t]) + S_stocking[t] + 2
  N[t,1]~dlnorm(L_mu_Vichy_nm[t],tau_vichy_cut)l(3,30000) #l(min_N_1[t],8000)

  res_Vichy[t] <- log(N[t,1]) - L_mu_Vichy_nm[t]

  mu_N_L[t]<-N[t,1] * p_langeac[t]
  tau_N_L[t]<-1/ (N[t,1] * p_langeac[t] * (1-p_langeac[t]) )

  max_N_langeac[t]<-N[t,1] - S_stocking[t]-1
  min_L_P[t]<-N[t,3]+1 #max(N[t,3]+2 , min_L[t])

  N[t,2]~dbin(p_langeac[t],N[t,1])l(min_L_P[t],) #
  #~dnorm(mu_N_L[t],tau_N_L[t])l(min_L_P[t],max_N_langeac[t])

  mu_N_P[t]<-N[t,2] * p_poutes[t]
  tau_N_P[t]<-1/ (N[t,2] * p_poutes[t] * (1-p_poutes[t]) )

  max_N_poutes[t]<-N[t,2]-1

  N[t,3]~dbin(p_poutes[t],N[t,2]) # #~dnorm(mu_N_P[t],tau_N_P[t])l(1,max_N_poutes[t])

  S_ts[t,1] <-max( N[t,1] - S_stocking[t] -N[t,2],1)
  S_ts[t,2]<-max( N[t,2]-N[t,3],1)
  S_ts[t,3]<-max( N[t,3],1)

  ratio_S[t,1] <- S_ts[t,1] / ( S_ts[t,1] + S_ts[t,2] + S_ts[t,3])
  ratio_S[t,2] <- S_ts[t,2] / ( S_ts[t,1] + S_ts[t,2] + S_ts[t,3])
  ratio_S[t,3] <- S_ts[t,3] / ( S_ts[t,1] + S_ts[t,2] + S_ts[t,3])

  for (i in 1:3){

    # juvenile production (only wild)
    d_tot_moy[t+1,i] <- d_wild_moy[t+1,i]

    Juv[t+1,i] <- d_tot_moy[t+1,i]*S_juv_JP[i]

    # wild component
    log(d_wild_moy[t+1,i]) <- L_d_wild_moy[t+1,i]

    L_d_wild_moy[t+1,i] ~ dnorm(L_mu_d_wild[t+1,i],tau_wild_moy_cut)#l(-6.91,1.09)
    L_mu_d_wild[t+1,i] <- log((S_ts[t,i]/S_juv_JP[i]) / (alpha_dd_cut + beta_dd_cut * (S_ts[t,i]/S_juv_JP[i]))) +
nu_wild_cut[i]

    res_wild_moy[t+1,i] <- L_d_wild_moy[t+1,i] - L_mu_d_wild[t+1,i]

  }

}

### end model bracket
}}
```

2. Data

```
list(  
  
# index for Rmax/beta_dd  
  
# data smolt stocking  
# + adult counts at Vichy  
  
T=37,  
  
# marked smolts  
# note: for a given year t  
# stocked smolts have usual two size modes  
# the bigger smolts are expected to migrate on year t  
# smaller smolts are expected to migrate on year t+1  
# therefore stocked smolts are composed of two components:  
# 1. smolts of larger  
  
#first 3 years correspond to 1972,1973,1974,  
# we assume that there isn't any smolt stocking during these years  
  
#smolts_m=c(  
#0,0,0,  
#0,0,0,0,0,  
#0,0,0,0,0,  
#0,0,0,0,0,  
#0,0,0,0,0,  
#24200,20000,0,0,0,  
#0,10985,25925,118649,185654,  
#211824,213501,277593,176473,247906,  
#254932,251408),  
  
#smolts_nm=c(  
#0,0,0,  
#7624,14545,30676,16482,52110,  
#9534,8306,23273,34105,37464,  
#39279,47307,39403,28010,59814,  
#48165,22000,66310,35767,33870,  
#10800,800,6300,3180,8750,  
#11630,1980,124160,47416,0,  
#0,0,0,0,0,  
#0,0),  
  
smolts_tot=c(  
0,0,0,  
7624,14545,30676,16482,52110,  
9534,8306,23273,34105,37464,  
39279,47307,39403,28010,59814,  
48165,22000,66310,35767,33870,  
35000,20800,6300,3180,8750,  
11630,12965,150085,166065,185654,  
211824,213501,277593,176473,247906,  
254932,251408, 0, 0, 0,  
  
0,0,0,0,0,  
0,0,0,0,0,  
0,0,0,0,0,  
0,0,  
).  
  
s_smolt=0.000545,
```


Adult marked and non marked seen at Vichy

```
#Vichy_m=c(  
#0,0,0,0,0,  
#0,0,0,0,0,  
#0,0,0,0,0,  
#0,0,0,0,0,  
#0,0,6,9,11,  
#0,0,3,66,22,  
#121,227,125,85,69,  
#39,42),
```

```
#Vichy_nm=c(  
#NA,NA,NA,NA,NA,  
#NA,NA,NA,NA,NA,  
#NA,NA,NA,NA,NA,  
#NA,NA,NA,NA,NA,  
#NA,NA,387,258,504,  
#380,400,538,1172,635,  
#389,723,447,336,422,  
#188,713),
```

avant 1986 on suppose que les poissons ne peuvent pas remonter
pas de passe a poisson sur le barrage Poutès
N[,1] = passage à vichy

```
min_N_V=c(  
2,2,  
2,2,2,2,2,  
2,2,2,2,2,  
2,2,2,2,2,  
2,2,2,2,2,  
2,2,2,2,2,  
2,2,657,2,2,  
2,2,2,2,2),
```

```
N=structure(.Data = c(  
NA, NA, 0,  
  
NA, NA, 0,  
NA, NA, 0,  
NA, NA, 0,  
NA, NA, 0,  
NA, NA, 0,  
  
NA, NA, 0,  
NA, NA, 10,  
NA, NA, 43,  
NA, NA, 110,  
NA, NA, 21,  
  
NA, NA, 4,  
NA, NA, 3,  
NA, NA, 11,  
NA, NA, 9,  
NA, NA, 23,  
  
NA, NA, 6,  
NA, NA, 67,  
393, NA, 35,  
267, NA, 31,  
515, NA, 130,  
  
380, NA, 112,  
400, NA, 53,  
541, NA, 40,
```

```

1238, NA, 154,
NA, NA, 89,

510, NA, 74,
950, NA, 153,
572, NA, 53,
421, NA, 39,
491, NA, 14,

227, NA, 26,
755, NA, 118,

NA, NA, NA,
), .Dim=c(57,3)),

```

```

C_dwn=c(
420,439,77,124,190,
318,819,388,169,286,
438,614,385,731,260,
196,0,0,0,0,
0,0,0,0,0,
0,0,0,0,0,
0,0,0,0,0,
0,0),

```

```

C_up=c(
1190,700,315,220,200,
1280,514,1163,410,314,
807,72,91,425,140,
88,135,110,112,0,
0,0,0,0,0,
0,0,0,0,0,
0,0,0,0,0,
0,0),

```

#Spawners taken at Brioude or Vichy for stocking production

```

S_stocking=c(
0,0,14,34,44,
52,48,64,38,5,
40,10,20,9,5,
8,10,16,4,0,
0,15,8,3,20,
20,25,40,103,63,
47,27,17,39,49,
14,50,
0,0,0,0,0,
0,0,0,0,0,
0,0,0,0,0,
0,0,0,0,0
),

```

```

min_L=c(
1,1,1,1,1,
1,1,1,1,1,
1,1,1,1,1,
1,1,1,1,1,
1,1,1,1,1,
1,1,1,1,1,
1,1,1,189,216,
142,246,107,95,1,
1,1,
1,1,1,1,1,
1,1,1,1,1,
1,1,1,1,1,
1,1,1,1,1

```

),

calib=9,

Index of abundance 5 minutes 0+

```

EF_IA=c(
52,82,131,120,159,15,21,21,61),

```

#prospected area in m2

```

S=c(
1210,2880,464,1134.3,751.2,1854,1192.5,752,828),

```

#year

#1=1997; 2=2000; 3=2001

#Y=c(

```

#1,3,2,2,2,2,3,3,2),

```

#Day of the IA EF fishing

#D=c(

```

#239,256,269,270,270,271,289,289,271),

```

Duration of the first depletion pass

#T_1=c(

```

#2628,NA,828,1296,1044,2232,1692,1080,1368),

```

Duration of the second depletion pass

#T_2=c(

```

#2196,NA,684,1512,720,1584,1044,972,1080),

```

0+ fish caught during the first depletion pass

C_1=c(

```

222,136,83,221,296,50,46,21,140),

```

0+ fish caught during the second depletion pass

C_2=c(

```

68,121,34,132,60,21,31,14,45),

```

#number of years with stocking

#s1=25

#s2=18

#s3=14

```

#s_1=c(0,1,    0,    2,    0,    3,    4,    5,    0,    6,    7,    0,    0,
      0,    0,    0,    0,    8,    0,    0,    9,    10,   11,   12,   #13,
      14,   15,   16,   17,   18,   19,   20,   21,   22,   23),
#s_2=c(0,0,    0,    0,    0,    1,    0,    0,    0,    0,    0,    0,    0,
      0,    0,    0,    2,    0,    0,    0,    3,    4,    5,    6,    7,
      #8,    9,    10,   11,   12,   13,   14,   15,   16,   0),
#s_3=c(0,0,    0,    0,    0,    0,    0,    0,    0,    0,    0,    0,    0,
      0,    0,    0,    0,    1,    2,    3,    4,    5,    6,    7,    8,
      #0,    9,   10,   11,    0,   12,   13,   14,    0,    0),

```

```
#Wetted area available for juveniles for each sections
# 1. V_L, 2. L_P, 3. amont poutes
```

```
S_juv_JP=c(2522116,489436,655661),
```

```
# surface habitat 0+ incubateur en m²
# arson ruisseau du mas cronce gourdon vereuges monistrol
```

```
S_inc=c(12754, 10556, 8355, 9213, 15564, 16411),
```

```
#####
# Time series depletion 1975 to 1990 #
#####
```

```
# rows years from 1975 to 1990
```

```
# columns, geographic area: 1= V->L, 2=L->P,3=P->
```

```
J=structure(.Data = c(
```

```
0, 3, 0,
```

```
0, 0, 0,
```

```
0, 0, 0,
```

```
2, 5, 0,
```

```
1, 5, 0,
```

```
0, 0, 0,
```

```
0, 1, 0,
```

```
0, 4, 0,
```

```
1, 4, 0,
```

```
1, 3, 0,
```

```
#pour L->P: 1 site supplementaire sans surface non incorporé
```

```
#pour L->P :1 site supplementaire sans surface non incorporé
```

```
3, 5, 1,
```

```
1, 2, 0,
```

```
1, 3, 0,
```

```
1, 2, 1,
```

```
1, 3, 3,
```

```
#pour P->: 1 site supplementaire sans surface non incorporé
```

```
2, 3, 4,
```

```
0, 0, 0,
```

```
0, 0, 0,
```

```
0, 0, 0,
```

```
0, 0, 0,
```

```
0, 0, 0,
```

```
0, 0, 0,
```

```
0, 0, 0,
```

```
0, 0, 0,
```

```
0, 0, 0,
```

```
0, 0, 0,
```

```
0, 0, 0,
```

```
0, 0, 0,
```

```
0, 0, 0,
```

```
0, 0, 0,
```

```
0, 0, 0,
```

```
0, 0, 0,
```

```
0, 0, 0,
```

```
0, 0, 0,
```

```
0, 0, 0
```

```
),
```

```
.Dim=c(37,3)),
```

```
# surface for depletion sites between Vichy and Langeac
# columns: years 1975 to 1990
```

```
# rows: sites
```

```
S_depl_V=structure(.Data = c(
```

```
NA, NA, NA,
NA, NA, NA,
NA, NA, NA,
4000, 3860, NA,
2880, NA, NA,
NA, NA, NA,
NA, NA, NA,
NA, NA, NA,
4200, NA, NA,
4200, NA, NA,
1378, 870, 2178,
640, NA, NA,
480, NA, NA,
750, NA, NA,
1398, NA, NA,
512, 1398, NA
```

```
),
```

```
.Dim=c(16,3)),
```

```
# 1st depletion pass for sites between Vichy and Langeac
```

```
# columns: years 1975 to 1990
```

```
# rows: sites
```

```
C_1_V=structure(.Data = c(
```

```
NA, NA, NA,
NA, NA, NA,
NA, NA, NA,
247, 808, NA,
44, NA, NA,
NA, NA, NA,
NA, NA, NA,
NA, NA, NA,
133, NA, NA,
197, NA, NA,
41, 19, 21,
26, NA, NA,
53, NA, NA,
49, NA, NA,
134, NA, NA,
14, 54, NA
```

```
),
```

```
.Dim=c(16,3)),
```

```
# 2nd depletion pass for sites between Vichy and Langeac
```

```
# columns: years 1975 to 1990
```

```
# rows: sites
```

```
#vecteur deuxieme passage
```

```
pass_2_V=structure(.Data = c(
```

```
0, 0, 0,
0, 0, 0,
0, 0, 0,
0, 0, 0,
1, 0, 0,
0, 0, 0,
0, 0, 0,
0, 0, 0,
1, 0, 0,
0, 0, 0,
1, 0, 0,
1, 0, 0,
1, 0, 0,
0, 0, 0,
1, 0, 0,
1, 1, 0
```

```
),
```

```
.Dim=c(16,3)),
```

```

C_2_V=structure(.Data = c(
NA,      NA,      NA,
NA,      NA,      NA,
NA,      NA,      NA,
NA,      NA,      NA,
18,      NA,      NA,
NA,      NA,      NA,
NA,      NA,      NA,
NA,      NA,      NA,
55,      NA,      NA,
NA,      NA,      NA,
22,      NA,      NA,
4,        NA,      NA,
26,      NA,      NA,
NA,      NA,      NA,
63,      NA,      NA,
2,        7,      NA
),
.Dim=c(16,3)),

```

```

# surface for depletion sites between Langeac and Poutes
# columns: years 1975 to 1990
# rows: sites

```

```

S_depl_L=structure(.Data = c(
840,    1500,    3700,    NA,      NA,
NA,     NA,     NA,     NA,     NA,
NA,     NA,     NA,     NA,     NA,
1360,   600,    2830,   5880,   3000,
1560,   2830,   5321,   3200,   4845,
NA,     NA,     NA,     NA,     NA,
520,    NA,     NA,     NA,     NA,
4000,   1820,   2535,   1257,   NA,
948,    1258,   3599,   2600,   NA,
948,    1400,   1000,   NA,     NA,
847,    1166,   770,    2178,   1018,
759,    500,    NA,     NA,     NA,
212,    720,    588,    NA,     NA,
638,    630,    NA,     NA,     NA,
1663,   649,    1352,   NA,     NA,
1663,   648,    1350,   NA,     NA
),
.Dim=c(16,5)),

```

```

# 1st depletion pass for sites between Langeac and Poutes
# columns: years 1975 to 1990
# rows: sites

```

```

C_1_L=structure(.Data = c(
11,     13,     44,     NA,     NA,
NA,     NA,     NA,     NA,     NA,
NA,     NA,     NA,     NA,     NA,
136,    61,     411,    112,    196,
205,    144,    122,    87,     5,
NA,     NA,     NA,     NA,     NA,
76,     NA,     NA,     NA,     NA,
155,    296,    214,    178,    NA,
158,    288,    779,    174,    NA,
11,     418,    100,    204,    NA,
36,     75,     104,    21,     91,
72,     90,     NA,     NA,     NA,
130,    170,    101,    NA,     NA,
130,    168,    NA,     NA,     NA,
40,     81,     120,    NA,     NA,
42,     33,     25,     NA,     NA
),
.Dim=c(16,5)),
#no area for 5th site
#no area for 4th site

```

```
# 2nd depletion pass for sites between Langeac and Poutes
# columns: years 1975 to 1990
# rows: sites
```

```
#vecteur deuxieme passage
```

```
pass_2_L=structure(.Data = c(
1,1,1,0,0,
0,0,0,0,0,
0,0,0,0,0,
0,1,0,1,0,
1,1,1,1,1,
0,0,0,0,0,
1,0,0,0,0,
1,0,1,1,0,
1,1,1,1,0, #no area for 5th site
1,0,1,0,0, #no area for 4th site
1,1,1,0,1,
1,1,0,0,0,
1,1,1,0,0,
1,1,0,0,0,
1,1,1,0,0,
1,1,1,0,0
),
.Dim=c(16,5)),
```

```
C_2_L=structure(.Data = c(
2, 4, 10, NA, NA,
NA, NA, NA, NA, NA,
NA, NA, NA, NA, NA,
NA, 25, NA, 59, NA,
96, 49, 141, 35, 2,
NA, NA, NA, NA, NA,
17, NA, NA, NA, NA,
0, NA, 1, 0, NA,
86, 62, 149, 276, NA, #no area for 5th site
11, NA, 41, 118, NA, #no area for 4th site
13, 23, 48, NA, 49,
27, 44, NA, NA, NA,
44, 65, 33, NA, NA,
23, 134, NA, NA, NA,
18, 12, 32, NA, NA,
15, 4, 11, NA, NA
),
.Dim=c(16,5)),
```

```
# 3rd depletion pass for sites between Langeac and Poutes
# columns: years 1975 to 1990
# rows: sites
```

```
#vecteur troisieme passage
```

```
pass_3_L=structure(.Data = c(
1,0,1,0,0,
0,0,0,0,0,
0,0,0,0,0,
0,0,0,0,0,
0,0,0,0,0,
0,0,0,0,0,
0,0,0,0,0,
0,0,0,0,0,
0,0,0,0,0, #no area for 5th site
1,0,0,0,0, #no area for 4th site
0,0,0,0,0,
0,0,0,0,0,
0,0,0,0,0,
0,1,0,0,0,
0,0,0,0,0,
0,0,0,0,0
),
.Dim=c(16,5)),
```

```

C_3_L=structure(.Data = c(
2,      NA,      6,      NA,      NA,
NA,     NA,     NA,     NA,     NA,
NA,     NA,     NA,     NA,     NA,
NA,     NA,     NA,     NA,     NA,
NA,     NA,     NA,     NA,     NA,
NA,     NA,     NA,     NA,     NA,
NA,     NA,     NA,     NA,     NA,
NA,     NA,     NA,     NA,     NA,
1,      NA,     NA,     NA,     NA,
NA,     48,     NA,     NA,     NA,
NA,     NA,     NA,     NA,     NA,
NA,     NA,     NA,     NA,     NA
),
.Dim=c(16,5)),

```

```

# surface for depletion sites upstream Poutes
# columns: years 1975 to 1990
# rows: sites

```

```

S_depl_P=structure(.Data = c(
NA,     NA,     NA,     NA,
847,    NA,     NA,     NA,
NA,     NA,     NA,     NA,
NA,     NA,     NA,     NA,
520,    NA,     NA,     NA,
1715,   1088,   896,    NA,
1600,   400,   1232,   2400
),
.Dim=c(16,4)),

```

```

# 1st depletion pass for sites upstream Poutes
# columns: years 1975 to 1990
# rows: sites

```

```

C_1_P=structure(.Data = c(
NA,     NA,     NA,     NA,
36,     NA,     NA,     NA,
NA,     NA,     NA,     NA,
NA,     NA,     NA,     NA,
81,     60,     NA,     NA,
77,     33,     194,   NA,
32,     45,     148,    4
),
.Dim=c(16,4)),
#no area for second site

```

```
# 2nd depletion pass for sites upstream Poutes
# columns: years 1975 to 1990
# rows: sites
#vecteur deuxieme passage
```

```
pass_2_P=structure(.Data = c(
0, 0, 0, 0,
0, 0, 0, 0,
0, 0, 0, 0,
0, 0, 0, 0,
0, 0, 0, 0,
0, 0, 0, 0,
0, 0, 0, 0,
0, 0, 0, 0,
0, 0, 0, 0,
0, 0, 0, 0,
1, 0, 0, 0,
0, 0, 0, 0,
0, 0, 0, 0,
1, 0, 0, 0,
1, 1, 1, 0,
1, 1, 1, 1
),
.Dim=c(16,4)),
#no area for second site
```

```
C_2_P=structure(.Data = c(
NA, NA, NA, NA,
13, NA, NA, NA,
NA, NA, NA, NA,
NA, NA, NA, NA,
23, 16, NA, NA,
30, 6, 64, NA,
7, 7, 23, 0
),
.Dim=c(16,4)),
#no area for second site
```

```
#####
# Time series IA 1994 to 2009 #
#####
```

```
# rows years from 1994 to 2009
#for Poutes 1995 to 2009
# columns, geographic area: 1= V->L, 2=L->P,3=P->
```

```
K=structure(.Data = c(
0, 0, 0,
0, 0, 0,
0, 0, 0,
0, 0, 0,
0, 0, 0,

0, 0, 0,
0, 0, 0,
0, 0, 0,
0, 0, 0,
0, 0, 0,

0, 0, 0,
0, 0, 0,
0, 0, 0,
0, 0, 0,
0, 0, 0,
```


NA,	NA, NA, NA,	NA, NA,										
NA,	NA, NA, NA, NA,	NA, NA, NA,										
NA,	NA, NA, NA, NA,	NA, NA, NA,										
NA,	NA, NA, NA, NA,	NA, NA, NA,										
NA,	NA, NA, NA, NA,	NA, NA, NA,										
NA,	NA, NA, NA, NA, NA,	NA, NA, NA,										
17,	3, NA, NA, NA,	4, NA,	3, NA,	3, NA,	1, NA,	1, NA,	1, NA,	2, NA,	2, NA,	NA, NA,	NA, NA,	NA, NA,
5,	2, 1, NA,	3, 1,	3, 3,	4, 10,	4, 2,	3, 2,	1, NA,	1, NA,	2, NA,	1, NA,	3, NA,	1, NA,
7,	9, NA, NA, NA,	2, NA,	8, NA,	18, NA,	13, NA,	4, NA,	1, NA,	3, NA,	2, NA,	NA, NA,	NA, NA,	NA, NA,
47,	16, NA, NA, NA,	72, NA,	109, NA,	4, NA,	31, NA,	12, NA,	3, NA,	3, NA,	6, NA,	9, NA,	NA, NA,	NA, NA,
16,	10, 21, NA,	5, 6,	11, 4,	29, 36,	13, 10,	31, 3,	15, 14,	12, NA,	2, NA,	4, NA,	18, NA,	6, NA,
9,	4, 7, 2,	10, 1,	6, 7,	18, 6,	8, 8,	2, 2,	6, 5,	7, 17,	4, 12,	1, 12,	5, 11,	9, 1,
19,	38, 50, NA,	16, 14,	9, 21,	72, NA,	35, NA,	37, NA,	61, NA,	6, NA,	1, NA,	4, NA,	25, NA,	47, NA,
42,	5, 28, NA, NA,	19, 42,	21, 8,	21, 12,	23, 10,	11, 2,	10, 223,	13, NA,	23, NA,	23, NA,	7, NA,	8, NA,
32,	8, NA, NA, NA,	21, NA,	13, NA,	12, NA,	10, NA,	3, NA,	2, NA,	12, NA,	6, NA,	3, NA,	4, NA,	5, NA,
23,	14, NA, NA,	7, NA,	15, NA,	20, NA,	32, NA,	8, NA,	15, NA,	20, NA,	5, NA,	0, NA,	NA, NA,	NA, NA,
13,	27, 32, NA,	12, 10,	7, 54,	8, NA,	5, NA,	2, NA,	2, NA,	2, NA,	0, NA,	37, NA,	52, NA,	41, NA,
17,	13, 34, NA,	12, 45,	59, 3,	23, NA,	10, NA,	9, NA,	16, NA,	18, NA,	5, NA,	2, NA,	1, NA,	7, NA,
15,	26, 3, NA,	27, 1,	37, 0,	9, 0,	6, 233,	21, 100,	24, 197,	12, NA,	13, NA,	3, NA,	0, NA,	8, NA,
1,	5, 13, NA,	4, 10,	10, NA,	0, NA,	1, NA,	8, NA,	2, NA,	18, NA,	5, NA,	0, NA,	5, NA,	42, NA,
58,	25, 36, 16,	66, 18,	116, 34,	70, 8,	4, 5,	17, 5,	23, 2,	42, 0,	37, 42,	4, 35,	10, 37,	13, 8,
67,	25, 29, NA,	57, 54,	28, 32,	55, 1,	30, 0,	62, 38,	30, 51,	46, 161,	15, 39,	19, 16,	52, 96,	0, NA,

1,	1, NA, NA,	1, NA,	NA, NA,	NA, NA,								
#2004												
1,	1, 1, NA,	1, 1,	1, 1,	1, NA,	0, NA,	0, NA,	0, NA,	0, NA,	0, NA,	1, NA,	1, NA,	1, NA,
#2005												
0,	0, 0, NA,	0, 0,	0, 0,	0, NA,	0, NA,							
#2006												
1,	1, 1, NA,	1, 1,	1, 1,	1, 1,	1, 1,	1, 1,	1, 1,	1, NA,	1, NA,	1, NA,	1, NA,	1, NA,
#2007												
1,	1, 1, NA,	1, 1,	1, NA,	1, NA,								
#2008												
1,	1, 1, 1,	1, 1,	1, 1,									
#2009												
1,	1, 1, NA,	1, 1,	1, NA,									
#2010												
1,	1, 1, 1,	1, 1,	1, 1,									
#2011												
1,	1, 1, NA	1, 1,	1, NA,	1, NA,								

),
.Dim=c(37,26)),

```
l_site_juv_L=structure(.Data = c(
0, 0, 0, NA, NA, NA, NA, NA, NA, NA,
NA, NA, NA, NA, NA, NA, NA, NA, NA, NA,
NA, NA, NA, NA, NA, NA, NA, NA, NA, NA,
0, 0, 0, 0, 0, NA, NA, NA, NA, NA,
0, 0, 0, 0, 0, NA, NA, NA, NA, NA,
NA, NA, NA, NA, NA, NA, NA, NA, NA, NA,
0, NA, NA, NA, NA, NA, NA, NA, NA, NA,
0, 0, 0, 0, NA, NA, NA, NA, NA, NA,
0, 0, 0, 0, NA, NA, NA, NA, NA, NA,
0, 0, 0, 0, NA, NA, NA, NA, NA, NA,
0, 0, NA, NA, NA, NA, NA, NA, NA, NA,
0, 0, 0, NA, NA, NA, NA, NA, NA, NA,
0, 0, 0, NA, NA, NA, NA, NA, NA, NA,
0, 0, 0, NA, NA, NA, NA, NA, NA, NA,
NA, NA, NA, NA, NA, NA, NA, NA, NA, NA,
NA, NA, NA, NA, NA, NA, NA, NA, NA, NA,
NA, NA, NA, NA, NA, NA, NA, NA, NA, NA,
NA, NA, NA, NA, NA, NA, NA, NA, NA, NA,
1, 1, 1, 1, 1, 1, 1, 1, 1, 1,
1, 1, 1, 1, 1, 1, 1, NA, NA, NA,
1, 1, 1, 1, 1, 1, NA, NA, NA, NA,
1, 1, 1, 1, 1, 1, NA, NA, NA, NA,
0, 0, 0, 0, 0, 0, NA, NA, NA, NA,
1, 1, 1, 1, 1, 1, NA, NA, NA, NA,
1, 1, 1, 1, 1, NA, NA, NA, NA, NA,
1, 1, 1, 1, NA, NA, NA, NA, NA, NA,
1, 1, 1, 1, 1, NA, NA, NA, NA, NA,
```



```

0,    0,    0,    1,    0,    0,    0,    0,    0,    0,    0,    NA,    NA,
    NA,    NA,    NA,    NA,    NA,    NA,    NA,    NA,    NA,    NA,    NA,    NA,    NA,
0,    0,    0,    1,    0,    0,    0,    0,    0,    0,    0,    0,    0,
    0,    0,    0,    0,    NA,    NA,    NA,    NA,    NA,    NA,    NA,    NA,    NA,
0,    0,    0,    1,    0,    0,    0,    0,    0,    0,    0,    0,    0,
    0,    0,    0,    0,    NA,    NA,    NA,    NA,    NA,    NA,    NA,    NA,    NA,
0,    0,    0,    1,    0,    0,    0,    0,    0,    0,    0,    0,    0,
    0,    0,    0,    NA,    NA,    NA,    NA,    NA,    NA,    NA,    NA,    NA,    NA,
0,    0,    0,    1,    0,    0,    0,    0,    0,    0,    0,    0,    0,
    0,    0,    0,    0,    0,    0,    0,    0,    0,    0,    0,    0,    0,
0,    0,    1,    0,    0,    1,    0,    0,    0,    0,    0,    0,    0,
    0,    0,    0,    0,    0,    0,    0,    0,    0,    0,    0,    0,    NA,
0,    0,    0,    0,    0,    0,    1,    0,    0,    0,    0,    0,    0,
    0,    0,    0,    0,    0,    0,    0,    0,    0,    0,    0,    0,    0,
0,    0,    0,    0,    1,    0,    0,    0,    0,    0,    0,    0,    0,
    0,    0,    0,    0,    0,    0,    0,    0,    0,    0,    0,    NA,    NA,
    NA

```

```

),
.Dim=c(37,26)),

```

```

l_site_egg_L=structure(.Data = c(

```

```

NA,    NA,    NA,    NA,    NA,    NA,    NA,    NA,    NA,    NA,
NA,    NA,    NA,    NA,    NA,    NA,    NA,    NA,    NA,    NA,
NA,    NA,    NA,    NA,    NA,    NA,    NA,    NA,    NA,    NA,
NA,    NA,    NA,    NA,    NA,    NA,    NA,    NA,    NA,    NA,
NA,    NA,    NA,    NA,    NA,    NA,    NA,    NA,    NA,    NA,
NA,    NA,    NA,    NA,    NA,    NA,    NA,    NA,    NA,    NA,
NA,    NA,    NA,    NA,    NA,    NA,    NA,    NA,    NA,    NA,
NA,    NA,    NA,    NA,    NA,    NA,    NA,    NA,    NA,    NA,
NA,    NA,    NA,    NA,    NA,    NA,    NA,    NA,    NA,    NA,
NA,    NA,    NA,    NA,    NA,    NA,    NA,    NA,    NA,    NA,
0,    0,    0,    0,    0,    0,    0,    0,    0,    0,
0,    0,    0,    0,    0,    0,    0,    NA,    NA,    NA,
0,    0,    0,    0,    0,    0,    0,    NA,    NA,    NA,
0,    0,    0,    0,    1,    1,    0,    NA,    NA,    NA,
0,    0,    0,    0,    0,    0,    0,    NA,    NA,    NA,
0,    0,    0,    0,    0,    NA,    NA,    NA,    NA,    NA,
0,    0,    0,    0,    NA,    NA,    NA,    NA,    NA,    NA,
0,    0,    0,    0,    0,    NA,    NA,    NA,    NA,    NA,
0,    0,    0,    0,    0,    NA,    NA,    NA,    NA,    NA,
0,    0,    0,    0,    0,    NA,    NA,    NA,    NA,    NA,
0,    0,    0,    0,    0,    NA,    NA,    NA,    NA,    NA,
0,    0,    0,    0,    0,    NA,    NA,    NA,    NA,    NA,
0,    0,    0,    0,    0,    0,    NA,    NA,    NA,    NA,
0,    0,    0,    0,    0,    0,    NA,    NA,    NA,    NA,
0,    0,    0,    0,    0,    0,    NA,    NA,    NA,    NA,
0,    0,    0,    0,    0,    0,    NA,    NA,    NA,    NA

```

```

),.Dim=c(37,10)),

```

```
#####  
# Stocking 0+ 1975->2010 #  
#####
```

```
#indicatrice 0+ stocking
```

```
l_juv_moy=structure(.Data = c(  
1, 0, 1,  
1, 0, 0,  
0, 0, 0,  
1, 0, 0,  
0, 0, 0,  
  
1, 1, 0,  
1, 0, 0,  
1, 0, 0,  
0, 0, 1,  
1, 0, 1,  
  
1, 0, 0,  
0, 0, 0,  
0, 0, 0,  
0, 0, 0,  
0, 0, 0,  
  
0, 0, 0,  
0, 1, 0,  
1, 0, 1,  
0, 0, 1,  
0, 0, 1,  
  
1, 1, 1,  
1, 1, 1,  
1, 1, 1,  
1, 1, 1,  
1, 0, 1,  
  
1, 1, 0,  
1, 1, 1,  
1, 1, 1,  
1, 1, 1,  
1, 0, 0,  
  
0, 1, 1,  
1, 1, 1,  
1, 0, 1,  
1, 0, 0,  
1, 0, 0,  
  
1, 0, 0,  
1, 0, 0  
) , .Dim=c(37,3)),
```

```
l_egg_moy=structure(.Data = c(  
0, 0, 0,  
0, 0, 0,  
0, 0, 0, #1, 1, 0,  
0, 0, 0, #1, 0, 0,  
0, 0, 0,  
0, 0, 0,  
0, 0, 0,  
0, 0, 0,  
0, 0, 0, #1, 0, 0,  
  
0, 0, 0,  
0, 0, 0,  
0, 0, 0,  
0, 0, 0,
```

```

0,      0,      0,
0,      0,      0,
0,      0,      0,
0,      0,      0,
0,      0,      0,
0,      0,      0,

0,      0,      0,
1,      0,      0,
1,      0,      0,
1,      1,      0,
1,      1,      0,
1,      1,      0,
1,      1,      0,
1,      1,      0,
1,      1,      0,
1,      1,      0,
1,      1,      0,

1,      1,      0,
1,      1,      0,
1,      1,      0,
1,      1,      0,
1,      0,      0,
1,      0,      0,
1,      0,      0
), .Dim=c(37,3)),

```

```

nb_inc=structure(.Data = c(
0.01,0.01,
0.01,0.01,
0.01,0.01,
0.01,0.01,
0.01,0.01,
0.01,0.01,
0.01,0.01,
0.01,0.01,
0.01,0.01,
0.01,0.01,
0.01,0.01,
0.01,0.01,
0.01,0.01,

0.01,0.01,
0.01,0.01,
0.01,0.01,
0.01,0.01,
0.01,0.01,
0.01,0.01,
0.01,0.01,
0.01,0.01,
0.01,0.01,
0.01,0.01,

0.01,0.01,
1,0.01,
1,0.01,
2,1,
3,2,
4,2,
4,2,
4,2,
4,2,
4,2,
4,2,

4,2,
4,2,
4,2,
4,2,
4,0.01,
4,0.01,
4,0.01
), .Dim=c(37,2)),

```



```

1,      1,      1,      1,      1,      1,
1,      1,      1,      1,      1,      1,
1,      1,      1,      1,      1,      1,
1,      1,      1,      1,      1,      1,
1,      1,      1,      1,      1,      1,
1,      1,      1,      1,      0,      0,
1,      1,      1,      1,      0,      0,
1,      1,      1,      1,      0,      0,
1,      1,      1,      1,      0,      0
),
.Dim=c(37,6)),

```

```

S_inc_JP=structure(.Data=c(
0,      0,      0,
0,      0,      0,
0,      0,      0,
0,      0,      0,
0,      0,      0,
0,      0,      0,
0,      0,      0,
0,      0,      0,
0,      0,      0,
0,      0,      0,
0,      0,      0,
0,      0,      0,
0,      0,      0,
0,      0,      0,
0,      0,      0,
0,      0,      0,
0,      0,      0,
0,      0,      0,
0,      0,      0,
0,      0,      0,
8355,   0,      0,
8355,   0,      0,
17568,  15564,  0,
40878,  31975,  0,
40878,  31975,  0,
40878,  31975,  0,
40878,  31975,  0,
40878,  31975,  0,
40878,  31975,  0,
40878,  31975,  0,
40878,  31975,  0,
40878,  0,      0,
40878,  0,      0,
40878,  0,      0
),
.Dim=c(37,3))

```

```

)
```

3: Initialisation

```
list(  
#Inits Redds/spawners
```

```
L_mu_vichy=6.5,  
dd_returns=0.9,
```

```
level_s = 0.2,  
l_surv_prim=c(  
NA,NA,NA,NA,NA,  
NA,NA,0,0,0,  
0,0,0,0,0,  
0,0,0,1,1,  
1,1,1,1,1,  
1,1,1,1,1,  
1,1,1,1,1,  
1,1,  
  
1,1,1,1,1,  
1,1,1,1,1,  
1,1,1,1,1,  
1,1,1,1,1,  
),
```

```
hel_effect=c(NA,0.8),
```

```
p_reach_V=0.4,
```

```
a_juv=0.5,
```

```
rho_station=0.5,
```

```
adjust_p_L=0.1,  
adjust_p_P=0.1,
```

```
ratio_juv_prod_L=c(  
0.4,0.4,0.4,0.4,NA,  
NA,NA,NA,NA,NA,  
NA,NA,NA,NA,NA,  
NA,NA,NA,NA,NA,  
NA,NA,NA,NA,NA,  
NA,NA,NA,NA,NA,  
NA,NA,NA,NA,NA,  
NA,NA,NA,NA,NA,  
NA,NA,  
NA,NA,NA,NA,NA,  
NA,NA,NA,NA,NA,  
NA,NA,NA,NA,NA,  
NA,NA,NA,NA,NA,  
),
```

```
#ratio_juv_prod_P=c(  
#NA,NA,NA,NA,NA,  
#NA,NA,NA,NA,NA,  
#NA,0.3,0.3,0.3,0.3,  
#NA,NA,NA,NA,NA,  
#NA,NA,NA,NA,NA,  
#NA,NA,NA,NA,NA,  
#NA,NA,NA,NA,NA,  
#NA,NA,  
#NA,NA,NA,NA,NA,  
#NA,NA,NA,NA,NA,  
#NA,NA,NA,NA,NA,  
#NA,NA,NA,NA,NA),
```

```
tau_p_langeac=0.9,  
tau_p_poutes=0.9,  
L_p_langeac=c(
```



```
R=structure(.Data = c(
2,      2,      NA,
2,      2,      NA,
NA,     NA,     NA,
```

```
100,    20,     NA,
NA,     NA,     NA,
NA,     NA,     NA,
NA,     NA,     NA,
NA,     NA,     9,
```

```
300,    NA,     40,
NA,     NA,     NA,
NA,     NA,     NA,
NA,     NA,     4,
NA,     NA,     3,
```

```
NA,     NA,     10,
NA,     NA,     8,
NA,     NA,     21,
300,    40,     6,
300,    40,     62,
```

```
NA,     NA,     NA,
```

```
300,    40,     40,
300,    40,     40,
NA,     NA,     NA,
NA,     NA,     NA,
NA,     NA,     NA,
```

```
NA,     NA,     NA,
300,    40,     40,
NA,     NA,     NA,
300,    40,     40,
300,    40,     40,
```

```
NA,NA,NA, #300, 40, 40,
```

```
), .Dim=c(57,3)),
```



```
R_rep=structure(.Data = c(
```

```
2,      2,      NA,  
2,      2,      NA,  
168,    120,    NA,  
166,    39,     NA,  
41,     32,     NA,  
50,     93,     NA,  
399,    190,    NA,  
300,    100,    NA,  
598,    202,    NA,  
6,      31,     NA,  
692,    273,    NA,  
22,     47,     20,  
100,    31,     15,  
2,      194,    116,  
136,    216,    42,  
137,    144,    20,  
105,    89,     20,  
56,     96,     20,  
59,     92,     20,  
10,     21,     20,  
100,    50,     20,  
100,    50,     20,  
132,    58,     7,  
86,     58,     14,  
58,     132,    85,  
57,     34,     66,  
69,     88,     43,  
100,    50,     20,  
100,    50,     20,  
53,     93,     136,  
115,    159,    67,  
92,     69,     169,  
79,     50,     31,  
100,    50,     20,  
241,    91,     57,  
241,    91,     57,  
241,    91,     57
```

```
#241,    91,     57,  
#241,    91,     57,  
#241,    91,     57,  
#241,    91,     57,  
#241,    91,     57,  
#241,    91,     57,  
#241,    91,     57,  
#241,    91,     57,  
#241,    91,     57,  
#241,    91,     57,  
#241,    91,     57,  
#241,    91,     57,  
#241,    91,     57,  
#241,    91,     57,  
#241,    91,     57
```

```
), .Dim=c(37,3)),
```

```
#####
```

```
s_juv2ad=0.1,
```

```
L_d_egg_L = structure(.Data = c(
```

```
NA,      NA,      NA,      NA,      NA,  
NA,      NA,      NA,      NA,      NA,
```


-4.513,-4.708,-4.764, NA, NA,
 NA, NA, NA, NA, NA, NA,
 NA, NA, NA, NA, NA, NA,
 NA, NA, NA,-0.7595,-0.9576,
 -1.358,-1.05,-1.027,-0.9738,-2.175,
 -0.7284,-1.212,-5.031,-3.837,-0.8742,
 -1.011,-0.7829,-1.082,-0.8167,-0.7912,
 -0.7848,-0.6458,-0.6745, NA, NA,
 NA, NA, NA, NA,-1.825,
 -2.045,-2.413,-2.008,-3.748,-2.31,
 -4.764,-9.546,-1.748,-2.268,-2.324,
 -2.322,-2.135,-2.181,-2.319,-2.026,
 -2.045,-2.239,-2.024,-2.451,-2.152,
 -2.19,-2.509,-2.172,-1.9,-2.164,
 -1.438,-1.509,-1.322,-1.202,-1.371,
 -1.338,-2.83,-1.656,-1.658,-1.582,
 -1.614,-1.786,-1.831,-1.406,-1.617,
 -1.501, NA, NA, NA, NA, NA, NA,
 NA, NA, NA, NA, NA, NA, NA,
 NA,-0.1518,-0.2355,-0.1823,0.009519,
 -5.584,-0.1968,-0.3337,-0.2795,-0.2054,
 -0.06442,-0.1319,-0.359,-0.1659,-0.1099,
 -0.1673,0.2141,-0.01379,0.1389,-0.2165,
 -0.08792, NA, NA, NA, NA, NA,
 NA, NA,-1.526,-1.581,-1.862,
 -1.666,-2.855,-1.496,-1.432,-1.552,
 -1.82,-1.566,-1.589,-1.394,-1.489,
 NA, NA, NA, NA, NA,
 NA, NA, NA, NA, NA,
 NA, NA, NA,-1.304,-1.461,
 -1.807,-3.079,-1.394,-1.576,-1.251,
 -1.665,-1.517,-1.485,-1.456, NA,
 NA, NA, NA, NA, NA, NA,
 NA, NA, NA, NA, NA, NA,
 NA, NA, NA, NA,-1.399,
 -1.427,-1.503,-6.193,-1.149,-1.349,
 -1.474,-1.535,-0.9662,-1.391,-1.457,
 -1.013,-1.076,-1.434,-1.378,-1.181,
 NA, NA, NA, NA, NA,
 NA, NA, NA, NA, NA,
 -1.029,-1.679,-1.814,-1.304,-1.618,
 -1.856,-1.62,-1.653,-1.516,-1.976,
 -1.781,-1.78,-1.771,-1.458,-1.643,
 -1.774, NA, NA, NA, NA, NA,
 NA, NA, NA, NA, NA, NA,
 NA,-1.406,-1.442,-1.662,-6.613,
 -1.282,-1.575,-1.563,-1.4,-1.628,
 -1.469,-1.735,-1.382,-1.484,-1.576,
 -1.55,-1.668,-1.381,-1.505,-1.441,
 -1.549, NA, NA, NA, NA, NA,
 NA, NA,-1.539,-1.505,-1.614,
 -2.765,-1.453,-1.53,-1.244,-1.679,
 -1.352,-1.582,-1.341,-1.389,-1.577,
 -1.452,-1.558, NA, NA, NA, NA,
 NA, NA, NA, NA, NA, NA,
 NA, NA, NA,-0.9353,-0.8758,
 -1.115,-4.975,-1.078,-1.119,-0.8529,
 -1.23,-1.1,-1.199,-1.468,-1.087,
 -1.22,-1.067,-1.037,-0.9666,-1.246,
 -0.8945,-1.049,-0.8191,-0.8939,-0.8554,
 -1.134,-0.8482,-1.022,-0.7408,-1.32,
 -1.53,-1.54,-1.422,-1.548,-5.549,

```

-1.728,-1.062,-1.507,-1.702,-1.361,
-1.362,-1.758,-1.47,-1.46,-1.426,
-1.267,-1.473,-1.469,-1.244,-1.485,
-1.521,-1.574,-1.644,      NA,      NA,
-1.385,-1.28,-1.427,-1.134,-1.326,
-1.384,-1.032,-1.016,-1.424,-1.022,
-1.386,-1.234,-1.439,-1.473,-1.656,
-1.684,-1.468,-1.442,-1.559,-1.35,
-1.498,-1.588,-1.228,-1.717,-1.127,
-1.344,-0.6965,-0.7931,-0.6069,-0.596,
-3.346,-0.7656,-0.7492,-0.5163,-0.792,
-0.9078,-0.9814,-1.071,-0.5967,-1.104,
-0.7013,-0.8111,-0.9865,-0.7835,-0.8143,
-1.155,-0.9297,-1.055,-0.7542,      NA,
      NA,      NA),
.Dim = c(37,26)),

```

```

L_d_egg_moy = structure(.Data = c(
      NA,      NA,      NA,      NA,      NA,
      NA,-0.1087,0.003013,-0.04268,-0.02881,
0.02139,0.03365,-0.002018,0.03992,0.01065,
-0.1011,-0.02793,-0.02382,-0.02467,0.03216,
-0.1001,0.003002,0.0862,-0.01488,0.03543,
-0.09822,-0.06402,-0.03631,0.07821,0.08401,
0.003339,-0.01611,0.05505,-3.077,-0.02766,
-0.06737,-4.776,-5.455E-4,0.1382,-1.751,
-2.341,-0.03073,-6.557,-6.493,0.01572,
-5.909,-6.078,-0.06149,-0.3317,1.06,
-0.1042,-6.753,-6.696,-0.09477,-5.731,
-5.637,0.07738,-5.127,-4.992,0.02665,
-6.623,-5.77,-0.04636,-6.028,-5.167,
-0.02277,-5.99,-5.461,-0.001411,-3.984,
-3.74,0.04797,-5.65,-0.0429,0.04374,
-5.519,-0.01368,-0.09316,-3.239,0.007022,
0.02725),
.Dim = c(37,3)),

```

```

L_d_juv_L = structure(.Data = c(
      NA,      NA,      NA,      NA,      NA,
      NA,      NA,      NA,      NA,      NA,
0.1583,-0.3769,-0.06065,0.0826,0.6496,
      NA,      NA,      NA,      NA,      NA,
-0.09673,0.04531,-0.1952,0.3897,0.04427,
      NA,      NA,      NA,      NA,      NA,
      NA,      NA,      NA,      NA,      NA,
      NA,      NA,      NA,      NA,      NA,
-0.2154,      NA,      NA,      NA,      NA,
      NA,      NA,      NA,      NA,      NA,
-0.4864,0.3311,-0.02702,0.3256,      NA,
      NA,      NA,      NA,      NA,      NA,
0.4004,0.5051,0.7602,0.333,      NA,
      NA,      NA,      NA,      NA,      NA,

```

0.5148,0.3536,0.1724, NA, NA,
 NA, NA, NA, NA, NA, NA,
 -0.4257,0.5547,-0.2944,-0.2515,0.3494,
 NA, NA, NA, NA, NA, NA,
 -0.2073,-0.2324, NA, NA, NA, NA,
 NA, NA, NA, NA, NA, NA,
 -0.06329,-0.3385,-0.02166, NA, NA,
 NA, NA, NA, NA, NA, NA,
 -0.05513,-0.1891, NA, NA, NA,
 NA, NA, NA, NA, NA, NA,
 0.1848,0.13,-0.01202, NA, NA,
 NA, NA, NA, NA, NA, NA,
 -0.04117,0.06007,-0.1035, NA, NA,
 NA, NA, NA, NA, NA, NA,
 -6.901,-4.306,-3.197,-4.079,-5.794,
 -3.418,-4.214,-3.849,-3.807,-4.682,
 -5.914,-1.636,-5.074,-5.505,-3.115,
 -4.068,-2.92, NA, NA, NA,
 -5.902,-1.504,-1.286,-1.365,-4.064,
 -4.246, NA, NA, NA, NA,
 -2.621,-1.267,-4.032,-2.759,-1.696,
 -5.156, NA, NA, NA, NA,
 0.07847,0.03587,-0.7359,0.2587,0.5623,
 -0.09455,0.4868, NA, NA, NA,
 -1.477,-0.6886,-1.395,-0.9023,-0.5606,
 -2.401, NA, NA, NA, NA,
 -1.543,-1.798,-6.188,-5.135,-4.347,
 NA, NA, NA, NA, NA,
 -2.06,-1.626,-0.9039,-1.455, NA,
 NA, NA, NA, NA, NA,
 -4.582,-1.146,-1.257,-1.243,-5.468,
 NA, NA, NA, NA, NA,
 0.1532,0.026,0.4552,-0.01967,-3.785E-4,
 NA, NA, NA, NA, NA,
 -1.114,-0.9295,-6.553,-2.522,-3.378,
 NA, NA, NA, NA, NA,
 -2.421,-1.076,-2.313,-1.573, NA,
 NA, NA, NA, NA, NA,
 0.6898,0.1533,0.2506,-0.3799,0.0656,
 NA, NA, NA, NA, NA,
 0.4022,0.04871,0.2573,-0.008991,0.5451,
 NA, NA, NA, NA, NA,
 0.2678,0.3544,0.1616,0.2884,0.2357,
 0.231, NA, NA, NA, NA,
 -0.5646,-0.008172,-0.6358,-0.0483,-0.4697,
 0.1189, NA, NA, NA, NA,
 0.1971,-0.1053,-0.1086,-0.07311,0.01295,
 0.4231, NA, NA, NA, NA),
 .Dim = c(37,10)),

NA, NA, NA, NA, NA,
 NA,-4.379,-6.716,-5.228,-6.711,
 -3.751,-4.57,-5.175,-5.515,-6.525,
 -5.897, NA, NA, NA, NA, NA,
 NA, NA, NA, NA, NA, NA,
 NA, NA,-1.727,-4.439,-6.608,
 -0.8278,-5.014,-5.864,-2.707,-6.412,
 -6.292,-6.452,-6.205, NA, NA,
 NA, NA, NA, NA, NA,
 NA, NA, NA, NA, NA,
 NA, NA, NA,-2.353,-3.134,
 -3.517,-2.866,-6.332,-3.275,-3.304,
 -3.79,-3.078,-5.103,-6.811,-2.618,
 -3.716,-2.39,-4.095,-4.125,-2.096,
 -6.478,-5.141,-2.923, NA, NA,
 NA, NA, NA, NA,-3.953,
 -3.898,-3.039,-3.774,-6.23,-5.056,
 -6.562,-3.744,-3.658,-4.57,-5.208,
 -5.088,-6.617,-4.812,-6.465,-4.078,
 -5.007,-3.143,-4.774,-5.813,-2.347,
 -3.18,-5.087,-2.898,-6.21,-6.348,
 -3.005,-1.749,-4.876,-4.092,-1.394,
 -1.966,-2.011,-1.862,-4.917,-5.043,
 -4.194,-2.273,-2.587,-4.331,-2.529,
 -6.084, NA, NA, NA, NA, NA,
 NA, NA, NA, NA, NA, NA,
 NA,-1.633,-4.773,-2.45,-2.268,
 -2.579,-5.615,-3.296,-4.499,-4.568,
 -2.615,-3.641,-3.218,-5.429,-4.536,
 -1.751,-3.181,-3.922,-4.125,-4.59,
 -0.1087, NA, NA, NA, NA, NA,
 NA, NA,-2.364,-3.688,-2.198,
 -3.119,-4.391,-2.885,-6.133,-4.331,
 -3.791,-5.609,-4.929,-6.879,-6.726,
 NA, NA, NA, NA, NA,
 NA, NA, NA, NA, NA,
 NA, NA, NA,-2.284,-2.994,
 -4.827,-6.628,-2.583,-2.26,-5.446,
 -6.522,-2.532,-4.815,-6.572, NA,
 NA, NA, NA, NA, NA,
 NA, NA, NA, NA, NA,
 NA, NA, NA, NA,-3.287,
 -2.036,-6.711,-5.0,-3.736,-6.678,
 -6.905,-6.663,-6.601,-6.517,-2.629,
 -1.53,-2.39,-2.316,-2.79,-1.482,
 NA, NA, NA, NA, NA,
 NA, NA, NA, NA, NA,
 -0.004654,-0.5426,0.1057,-0.1686,0.1901,
 -0.5419,0.006196,0.2747,-0.49,-0.3155,
 0.2476,-0.005572,-0.3459,-0.00448,0.1241,
 0.05704, NA, NA, NA, NA,
 NA, NA, NA, NA, NA,
 NA,-3.342,-6.417,-2.232,-2.17,
 -3.395,-5.714,-2.436,-2.308,-5.935,
 -4.681,-4.632,-5.99,-4.199,-4.59,
 -4.21,-6.388,-5.588,-2.157,-0.8342,
 -0.2635, NA, NA, NA, NA,
 NA, NA,-6.35,-4.212,-5.401,
 -5.268,-6.372,-5.13,-3.368,-5.401,
 -2.697,-3.287,-6.398,-6.761,-1.691,
 -6.759,-6.52, NA, NA, NA,

```

        NA,      NA,      NA,      NA,      NA,
        NA,      NA,      NA,-5.509,-5.048,
-1.32,-4.837,-2.818,-5.816,-2.709,
-3.189,-1.787,-5.353,-3.89,-3.119,
-3.181,-5.674,-4.973,-4.461,-5.887,
-6.229,-3.695,-3.343,-6.492,-1.725,
-6.828,-3.114,-3.843,-3.052,-1.366,
-3.696,-3.089,-3.42,-2.643,-4.452,
-4.603,-4.21,-2.799,-3.516,-2.766,
-1.855,-5.711,-2.498,-1.581,-3.374,
-4.618,-5.026,-4.076,-6.704,-0.8016,
-2.667,-4.325,-1.272,      NA,      NA,
-3.349,-5.103,-3.409,-2.439,-2.341,
-6.196,-5.101,-1.971,-5.594,-4.378,
-5.178,-6.705,-4.649,-1.631,-5.785,
-2.857,-4.381,-3.699,-5.93,-1.649,
-3.163,-0.4222,-2.514,-1.064,-3.955,
-1.578,-4.501,-6.438,-2.577,-1.146,
-1.815,-5.431,-2.566,-2.505,-4.902,
-4.6,-2.79,-3.446,-1.481,-2.24,
-4.427,-4.113,-5.975,-0.8637,-2.784,
-1.815,-3.494,-2.319,-4.476,      NA,
      NA,      NA),
.Dim = c(37,26)),
L_d_juv_moy = structure(.Data = c(
      NA,      NA,      NA,-2.582,-0.0431,
      NA,0.04291,0.1387,      NA,-2.138,
0.021,      NA,-0.1633,-0.1457,      NA,
-4.184,-2.518,      NA,-5.417,0.08707,
      NA,-2.28,0.06505,      NA,-0.05415,
0.2492,      NA,-2.331,0.274,      NA,
-6.744,0.006845,      NA,-0.1747,0.03703,
      NA,-0.2383,-0.1881,0.09862,-0.1871,
-0.04373,0.07322,-0.02151,0.1958,0.1377,
-0.004251,-0.06714,0.001825,0.01797,-8.71,
0.08109,-5.724,-0.07391,-6.906,0.03156,
0.06144,-6.595,0.1217,-0.1602,-3.219,
-6.102,-5.932,-5.7,-9.036,-8.452,
-6.815,-6.397,-5.636,-5.53,-7.539,
-8.588,-6.804,-10.41,0.124,-9.828,
-7.864,-7.034,-0.07424,-2.733,-3.257,
-3.929,-9.966,-8.414,-8.224,-7.961,
-6.861,-6.076,-6.818,0.05348,-0.28,
-0.1098,-8.17,-9.462,-3.102,-4.549,
-4.613,-4.185,0.1854,-5.18,-3.049,
0.1428,-0.05218,-3.094,0.2292,0.08728,
-2.229,-0.1499,0.06829,-3.538,0.05781,
0.04643),
.Dim = c(37,3)),
L_d_wild_L = structure(.Data = c(
      NA,      NA,      NA,      NA,      NA,
      NA,      NA,      NA,      NA,      NA,
-1.112,-1.568,-1.413,-3.061,-2.004,
      NA,      NA,      NA,      NA,      NA,
-1.479,-2.497,-1.488,-3.05,-6.187,
      NA,      NA,      NA,      NA,      NA,
      NA,      NA,      NA,      NA,      NA,
      NA,      NA,      NA,      NA,      NA,

```

-1.764, NA, NA, NA, NA,
 NA, NA, NA, NA, NA,
 -3.278,-1.311,-2.421,-1.954, NA, NA,
 NA, NA, NA, NA, NA,
 -0.9575,-1.286,-1.31,0.6317, NA, NA,
 NA, NA, NA, NA, NA,
 -3.735,-1.005,-1.523, NA, NA,
 NA, NA, NA, NA, NA,
 -2.6,-2.242,-1.123,-3.784,-1.589,
 NA, NA, NA, NA, NA,
 -1.806,-1.139, NA, NA, NA,
 NA, NA, NA, NA, NA,
 -0.114,-0.9711,-1.396, NA, NA,
 NA, NA, NA, NA, NA,
 -1.267,-0.4913, NA, NA, NA,
 NA, NA, NA, NA, NA,
 -3.027,-1.86,-2.083, NA, NA,
 NA, NA, NA, NA, NA,
 -2.951,-2.939,-3.064, NA, NA,
 NA, NA, NA, NA, NA,
 -2.875,-4.331,-5.018,-5.665,-3.467,
 -4.209,-3.857,-6.89,-4.517,-4.355,
 -4.813,-5.223,-5.386,-6.183,-4.442,
 -3.746,-2.649, NA, NA, NA,
 -1.449,-3.699,-2.228,-4.373,-1.989,
 -1.843, NA, NA, NA, NA,
 -3.843,-5.528,-5.163,-4.348,-5.944,
 -4.13, NA, NA, NA, NA,
 -3.134,-2.138,-2.51,-4.633,-6.097,
 -6.676,-1.819, NA, NA, NA,
 -5.98,-5.915,-6.759,-5.116,-4.351,
 -5.324, NA, NA, NA, NA,
 -1.898,-2.348,-1.677,-1.229,-1.415,
 NA, NA, NA, NA, NA,
 -6.825,-2.709,-6.588,-5.551, NA, NA,
 NA, NA, NA, NA, NA,
 -1.588,-6.658,-4.889,-4.988,-1.53,
 NA, NA, NA, NA, NA,
 -0.7044,-0.9803,-1.28,-2.869,-2.032,
 NA, NA, NA, NA, NA,
 -5.216,-1.63,-1.092,-6.477,-1.988,
 NA, NA, NA, NA, NA,
 -4.91,-4.699,-2.807,-4.309, NA, NA,
 NA, NA, NA, NA, NA,
 -1.284,-1.687,-4.23,-3.663,-2.461,
 NA, NA, NA, NA, NA,
 -1.451,-1.122,-1.499,-2.402,-3.548,
 NA, NA, NA, NA, NA,
 -1.169,-0.8889,-1.523,-1.697,-1.959,
 -0.7334, NA, NA, NA, NA,
 -0.8534,-1.259,-1.451,-1.883,-2.814,
 -4.512, NA, NA, NA, NA,
 -1.144,-0.7978,-3.93,-3.534,-3.491,
 -3.611, NA, NA, NA, NA),.Dim = c(37,10)),

NA, NA, NA, NA, NA,
 NA,-3.883,-3.191,-6.385,-3.269,
 -2.919,-3.096,-4.512,-5.783,-3.318,
 -6.158, NA, NA, NA, NA, NA,
 NA, NA, NA, NA, NA, NA,
 NA, NA,-3.077,-3.051,-1.093,
 -5.923,-4.384,-1.992,-6.079,-4.97,
 -4.526,-3.717,-3.264, NA, NA,
 NA, NA, NA, NA, NA,
 NA, NA, NA, NA, NA,
 NA, NA, NA,-6.825,-5.583,
 -4.207,-6.427,-2.326,-4.726,-3.586,
 -3.7,-5.441,-5.377,-5.685,-3.463,
 -6.409,-6.454,-4.264,-5.831,-5.697,
 -3.251,-4.631,-6.269, NA, NA,
 NA, NA, NA, NA,-5.134,
 -4.69,-5.796,-5.951,-3.131,-3.846,
 -6.557,-5.05,-3.586,-5.531,-6.115,
 -3.568,-3.125,-3.515,-6.055,-4.78,
 -4.462,-5.502,-5.697,-3.971,-5.339,
 -3.764,-3.053,-6.103,-6.551,-5.004,
 -3.302,-5.188,-2.627,-3.331,-3.836,
 -6.328,-5.0,-2.596,-3.379,-5.654,
 -4.608,-3.284,-2.175,-1.523,-5.21,
 -2.814, NA, NA, NA, NA, NA,
 NA, NA, NA, NA, NA, NA,
 NA,-4.009,-4.121,-4.743,-5.402,
 -5.631,-2.466,-5.646,-3.422,-2.63,
 -6.191,-2.41,-6.02,-3.535,-2.097,
 -3.951,-6.676,-4.222,-3.877,-5.228,
 -3.402, NA, NA, NA, NA, NA,
 NA, NA,-3.885,-5.461,-6.191,
 -6.891,-6.21,-5.82,-6.112,-6.165,
 -3.613,-4.133,-5.511,-3.76,-3.912,
 NA, NA, NA, NA, NA,
 NA, NA, NA, NA, NA,
 NA, NA, NA,-6.595,-6.55,
 -4.085,-3.92,-6.755,-2.724,-3.084,
 -3.031,-5.988,-4.76,-5.105, NA,
 NA, NA, NA, NA, NA,
 NA, NA, NA, NA, NA,
 NA, NA, NA, NA,-3.867,
 -4.956,-2.847,-4.075,-4.888,-3.873,
 -3.829,-3.771,-4.494,-6.725,-2.609,
 -4.471,-2.524,-3.455,-6.33,-6.539,
 NA, NA, NA, NA, NA,
 NA, NA, NA, NA, NA,
 -2.715,-3.175,-2.582,-5.073,-2.541,
 -2.808,-3.692,-2.664,-2.893,-3.235,
 -3.717,-5.303,-3.742,-1.893,-1.594,
 -4.505, NA, NA, NA, NA, NA,
 NA, NA, NA, NA, NA,
 NA,-3.652,-2.061,-3.877,-2.607,
 -4.035,-3.535,-3.876,-6.257,-3.173,
 -2.338,-5.62,-6.705,-3.667,-6.365,
 -6.705,-4.911,-6.682,-0.3278,-5.404,
 -3.708, NA, NA, NA, NA,
 NA, NA,-6.498,-5.307,-4.957,
 -6.647,-6.513,-4.149,-4.467,-6.204,
 -5.926,-4.067,-5.477,-3.233,-4.502,
 -2.758,-2.951, NA, NA, NA,

```

      NA,      NA,      NA,      NA,      NA,
      NA,      NA,      NA,-1.388,-2.229,
-6.167,-0.7969,-1.761,-4.184,-6.199,
-3.441,-6.014,-1.897,-5.435,-5.237,
-6.034,-1.913,-2.849,-2.264,-3.524,
-4.06,-6.119,-5.998,-5.07,-4.926,
-1.816,-2.769,-5.113,-2.732,-6.267,
-2.232,-6.723,-2.384,-1.52,-2.005,
-1.471,-2.495,-2.059,-3.563,-3.276,
-2.538,-5.92,-3.217,-2.76,-1.925,
-6.029,-4.961,-1.86,-1.609,-1.723,
-2.275,-2.947,-2.215,      NA,      NA,
-1.958,-2.57,-2.783,-4.452,-2.135,
-1.461,-2.582,-6.078,-4.717,-3.411,
-2.512,-3.596,-2.841,-6.744,-3.995,
-3.22,-2.599,-3.172,-2.242,-4.753,
-1.618,-5.757,-2.061,-3.72,-3.96,
-5.09,-1.429,-1.538,-2.798,-4.61,
-4.29,-2.069,-6.407,-3.339,-3.869,
-2.083,-2.655,-4.309,-5.004,-2.193,
-1.797,-4.087,-1.322,-4.653,-0.7288,
-3.701,-5.393,-6.735,-2.322,      NA,
      NA,      NA),
.Dim = c(37,26)),

```

```

L_d_wild_moy = structure(.Data = c(

```

```

      NA,      NA,      NA,
-3.453,-2.746,      NA,
-5.045,-3.656,      NA,
-2.791,-2.165,      NA,
-5.665,-3.526,      NA,
-5.664,-2.204,      NA,
-5.324,-1.855,      NA,
-6.495,-2.194,      NA,
-3.567,-1.572,      NA,
-5.851,-1.945,      NA,

-4.373,-2.044,      NA,
-5.028,-2.387,      NA,
-3.421,-1.899,-6.695,
-1.926,-2.641,-4.263,
-4.508,-3.342,-4.106,
-2.491,-3.406,-5.103,
-5.978,-3.88,-4.744,
-6.202,-5.407,-6.438,
-6.313,-5.363,-6.607,
-3.371,-2.351,-6.405,

-5.4,-4.714,-5.989,
-6.868,-6.393,-6.344,
-5.583,-4.676,-5.91,
-6.837,-6.634,-6.466,
-6.897,-6.882,-6.893,
-6.868,-6.858,-6.532,
-4.877,-2.409,-5.341,
-6.878,-6.839,-6.904,
-6.904,-6.211,-6.757,
-6.79,-6.439,-6.294,

-6.906,-6.907,-6.834,
-4.457,-5.881,-2.41,
-5.617,-2.519,-4.505,

```

```
-4.16,-1.807,-4.743,  
-3.07,-1.215,-4.741,  
-3.569,-2.806,-4.279,  
-3.012,-2.88,-3.929,
```

```
-3.012,-2.88,-3.929,  
-3.012,-2.88,-3.929,  
-3.012,-2.88,-3.929,
```

```
-3.012,-2.88,-3.929,  
-3.012,-2.88,-3.929,  
-3.012,-2.88,-3.929,  
-3.012,-2.88,-3.929,  
-3.012,-2.88,-3.929,  
-3.012,-2.88,-3.929,  
-3.012,-2.88,-3.929,  
-3.012,-2.88,-3.929,  
-3.012,-2.88,-3.929,  
-3.012,-2.88,-3.929,  
-3.012,-2.88,-3.929,  
-3.012,-2.88,-3.929,  
-3.012,-2.88,-3.929,  
-3.012,-2.88,-3.929,  
-3.012,-2.88,-3.929,  
-3.012,-2.88,-3.929,
```

```
-3.012,-2.88,-3.929,  
-3.012,-2.88,-3.929,  
-3.012,-2.88,-3.929  
)  
.Dim = c(58,3)),
```

```
L_mu_p = -0.1058,  
L_p = c(  
0.8415,-1.805,-0.7957,-0.159,1.195,  
-0.2437,0.2641,-0.3813,0.8715),  
L_p_L = structure(.Data = c(  
NA, NA, NA, NA, NA,  
NA, NA, NA, NA, NA,  
NA, NA, NA, NA, NA,  
-0.6992,-0.2651,0.2975,-0.4511,0.4035,  
0.4843,0.1808,-2.03,0.3207,-0.9022,  
NA, NA, NA, NA, NA,  
0.6709, NA, NA, NA, NA,  
4.17,0.4924,5.599,7.812, NA,  
-0.2888,1.477,1.33,-3.007, NA,  
0.1047,2.06,-0.5091, NA, NA,  
0.08707,0.3588,-0.6969,-0.3065,-0.1805,  
0.5348,0.4308, NA, NA, NA,  
0.734,0.4375,0.4736, NA, NA,  
1.747,-0.2638, NA, NA, NA,  
0.5386,1.395,0.8967, NA, NA,  
-0.2779,1.415,-1.031, NA, NA),  
.Dim = c(16,5)),  
L_p_P = structure(.Data = c(  
NA, NA, NA, NA, NA,  
NA, NA, NA, NA, NA,
```

```

NA,      NA,      NA,      NA,      NA,
NA,      NA,      NA,      NA,      NA,
NA,      NA,      NA,      NA,      NA,
NA,      NA,0.9446, NA,      NA,      NA,
NA,0.5098,0.4243,0.864, NA,      NA,
1.652,0.9126,1.653,1.96),
.Dim = c(16,4)),
L_p_V = structure(.Data = c(
NA,      NA,      NA,      NA,      NA,
NA,      NA,      NA,      NA,-0.01616,
1.335,    NA,-0.3119, NA,      NA,
NA,      NA,      NA,      NA,      NA,
NA,      NA,      NA,      NA,0.3847,
NA,      NA,0.03955, NA,      NA,
-0.9759,-0.5749,-1.458,2.376, NA,
NA,-0.1638, NA,      NA,-1.11,
NA,      NA,-0.4847, NA,      NA,
1.124,1.445, NA),
.Dim = c(16,3)),
L_sigma_p = 1.417,
N_tot = c(
320.0,978.0,242.0,513.0,375.0,
93.0,97.0,59.0,202.0),
N_tot_L = structure(.Data = c(
NA,      NA,      NA,      NA,      NA,
NA,      NA,      NA,      NA,      NA,
NA,      NA,      NA,      NA,      NA,
437.0,134.0,684.0,277.0,351.0,
355.0,240.0,1291.0,142.0,13.0,
NA,      NA,      NA,      NA,      NA,      NA,
104.0,    NA,      NA,      NA,      NA,
156.0,492.0,215.0,178.0,    NA,
360.0,362.0,981.0,4897.0,    NA,
23.0,475.0,210.0,    NA,      NA,
63.0,115.0,263.0,47.0,211.0,
108.0,149.0,    NA,      NA,      NA,
193.0,275.0,160.0,    NA,      NA,
156.0,424.0,    NA,      NA,      NA,
67.0,97.0,167.0,    NA,      NA,
85.0,39.0,76.0,    NA,      NA),
.Dim = c(16,5)),
N_tot_P = structure(.Data = c(
NA,      NA,      NA,      NA,      NA,
NA,      NA,114.0,    NA,      NA,
NA,131.0,47.0,279.0,    NA,
40.0,55.0,181.0,4.0),
.Dim = c(16,4)),
N_tot_V = structure(.Data = c(
NA,      NA,      NA,      NA,      NA,
NA,      NA,      NA,      NA,506.0,
1019.0,    NA,95.0,    NA,      NA,
NA,      NA,      NA,      NA,      NA,
NA,      NA,      NA,      NA,221.0,

```

```

      NA,      NA,406.0,      NA,      NA,
161.0,53.0,69.0,30.0,      NA,
      NA,117.0,      NA,      NA,207.0,
      NA,      NA,332.0,      NA,      NA,
18.0,65.0,      NA),
.Dim = c(16,3)),

```

```

beta_tau = 31.26,
mu_tau = 0.1532,

```

```

Rmax = 0.1,
beta_d = 7.153,

```

```

d = c(
0.2708,0.3292,0.5003,0.4575,0.5031,
0.06149,0.08001,0.07957,0.2559),
d_moy = 0.3221,
eta = 1.097,
inv_kappa = 0.003667,

```

```

nu_juv_dwn = -57.17,
nu_juv_up = -0.2706,
nu_wild_dwn = 5.109,
nu_wild_up = 64.3,

```

```

#p_lh = c(
#0.33,0.34,0.33),
#p_lh_smolt = c(
#0.2345,      NA),

```

```

rep_C_1 = c(
242.0,144.0,70.0,243.0,287.0,
36.0,49.0,25.0,140.0),
rep_C_2 = c(
62.0,119.0,52.0,130.0,58.0,
27.0,32.0,15.0,40.0),
rep_EF_IA = c(
71.0,73.0,115.0,105.0,107.0,
14.0,16.0,15.0,57.0),
s_egg = 0.03984,
s_juv = 0.04614,
#sigma_Vichy = 2,
tau_vichy=2,

```

```

tau_egg_moy = c(
275.7,0.2062),
tau_egg_site = c(
36.19,0.07903),
tau_juv_moy = c(
60.57,0.12),
tau_juv_site = c(
12.2,0.07651),

```

```

tau_wild_moy=0.5,      # =c( 0.2857,0.35,NA),
tau_wild_site = 0.1712,
zt = 0.004182)

```